GEORG CHARLES DE HEVESY: THE FATHER OF NUCLEAR MEDICINE

GEORG CHARLES DE HEVESY
1 August 1885–5 July 1966

It is especially timely and fitting at the end of the first quarter of a century of the existence of The Society of Nuclear Medicine to realize that the commemorative presentation at our annual meeting will be designated henceforth as The Hevesy Nuclear Medicine Pioneer Lecture. In this manner we will be reminded each year of "the one who started it all" and thereby acknowledge our gratitude and indebtedness to him for the immense impact of his intuition on our lore. Much of the basic origins of Nuclear Medicine stemmed from the insights and the seminal contributions of Professor Hevesy. The consuming drive of his scientific curiosity and his indefatigable enterprise made of him the towering intellectual genius that he was.

Manifestations of Hevesy's manifold and vividly imaginative pioneering investigations, which spanned more than a half century, were chronicled fittingly in the 1047 pages of two monumental volumes published in 1962 (*1*) and aptly titled, "Adventures in Radioisotope Research." Here are reprinted, in translation into English from as many as four other languages, a selection of 100 of his nearly 400 publications, together with intercalations of numerous commentaries of invaluable historical content.

Although Hevesy's training lay principally in the field of physical chemistry, his interests were highly diverse and his prodigious endeavors penetrated into many areas of science. Specifically important to us in Nuclear Medicine was his discovery of the indicator tracer method of analysis and the initiation of applications of it in biomedicine.

It was Hevesy who, in 1923, first used a naturally radioactive isotope, 10.6-hour Lead-212 (ThB), to study the uptakes of labeled lead ions from dilute solutions by the roots, stem, leaves and fruit of *Vicia faba* (horse-bean). He used an electroscope to assay the relative amounts of radioactivity present in ashed samples of parts of the plants. Because of the extreme sensitivity of physical radioassay methods, he carried out these experiments with such minuscule concentrations of lead as to avoid the toxic properties of it. He proved also that the lead taken up by the plants was present in them in ionizable form (*1* pp 876–883, *2*).

The following year Hevesy published with Christiansen and Lomholt (*1* pp 143–145) the results of the first experiments in animals in which radiochemical methods were employed. They used 5.0-day Bismuth-210 (RaE) to label and to follow the circulation of bismuth in the bodies of rabbits after intramuscular injections of antisyphilitic medicaments containing bismuth. Similarly, they used 22.3-year Lead-210 (RaD) as a radioindicator to follow the excretion and the distribution of lead in

* For reprints contact: William G. Myers, Department of Radiology, The Ohio State University Hospital, 410 West Tenth Avenue, Columbus, Ohio 43210

several organs after injection of labeled lead hydroxide mixed with olive oil (*1* pp 146–147). The measurements were made at The Institute of Theoretical Physics (now The Bohr Institute) at The University of Copenhagen, where Hevesy pursued many of his investigations. There he enjoyed the appreciative interest of his cherished friend, Niels Bohr.

While Hevesy was in Manchester a dozen years previously, Professor Ernest Rutherford importuned the young chemist to separate radioactive Lead-210 from its admixture with the large amounts of nonradioactive lead in the laboratory there by saying to him (*1* p 14), "If you are worth your salt, you separate radium D from all that nuisance of lead." For two years, Hevesy tried in vain to carry out the separation by chemical methods. Failing in this, he concluded the great sensitivity of physical methods for measuring radioactivity would make imponderable amounts of Pb-210 an excellent radioindicator tracer to "represent" nonradioactive lead atoms in qualitative and quantitative processes. Thus, Hevesy's fertile imagination converted adversity into advantage and the concept of radioindicator chemistry was born! Frustration from his failure serendipitously had led to triumph and to the discovery of the most sensitive method of analysis.

When Hevesy went to The Vienna Radium Institute early in 1913, he found Doctor Fritz Paneth had been working quite independently there on the same problem, and with the same fruitless results. The two young chemists then decided to publish jointly their findings on the chemical inseparability of Lead-210 (RaD) from nonradioactive lead. They also published together the use of Pb-210 as a radioindicator tracer to analyze quantitatively the slight solubilities of lead sulfide and lead chromate (*1* pp 31–35, *3*, *4*). In these papers they introduced the method and the technical terminology, "radioelements as indicators." These two publications in 1913 constituted the first in which radioindicator tracers played a unique role in chemical analysis. Twenty five years later in their book (*5*), "A Manual of Radioactivity," these two pioneers clearly defined their term, 'indicator.' . . ." In problems of this kind, in which the radio-element is not the object but the agent of the investigation, we say that the radio-elements serve as 'indicators,' (*5* p 166). . . . "An *indicated element* is an element containing a small amount of an isotopic element which serves as an indicator for the purpose of detection or measurement." (*5* p 168).

While with Rutherford in Manchester in 1911, Hevesy performed a delightfully imaginative and practical experiment to demonstrate that the landlady in his boarding house was recycling food. It seems she had been serving freshly-prepared meat only on Sunday and then disguised it in servings of hash, goulash, and other forms the rest of the week. When Hevesy cautiously suggested it would be tasty to have freshly-cooked meat served more frequently than once a week, she retorted indignantly that she served it every day. Hevesy was a sparse eater; and so, to prove her assertion was not true, he "spiked" a scrap of leftover meat on his plate one day with a tiny amount of a radioactive material. A few days later he brought an electroscope to the table to demonstrate to her that the hash served that day was radioactive. "This is magic," she exclaimed! This labeling of food, under such piquant circumstances, may have been the first tagging experiment in the life sciences, although, unfortunately, it was of course not published formally.

Hevesy used radioindicator methods during the decade between 1913 and 1923 in several radiochemical determinations; and many of his publications were coauthored with Paneth. Some of his papers involved colloid chemistry or electrochemistry, and others were concerned with self-diffusion in metals (*1*). Also, partial separations of isotopes of mercury and of chlorine were effected with Bronsted.

In 1923, Hevesy and Coster found the missing element 72 and named it Hafnium, after the Latin name for Copenhagen, in honor of the city where the discovery was made, and of which Hevesy was particularly fond.

Hevesy and Hofer, in 1934, first used in medicine an enriched stable isotope to determine the rate of elimination of water from the human body (*1* pp 536–538). They drank dilute deuterated water, HOD, discovered by Urey only two years previously, and assayed the further isotopic dilution of the deuterium in their urine. From their results they concluded the average time a water molecule spent in their bodies was 13 ± 1.5 days.

"Chance only favors the prepared mind," wrote Pasteur. Hevesy's brilliant mind and previous pioneering experiences with applications in biomedicine of natural radionuclides, and with a stable one, had prepared him fully and well to embrace immediately new opportunities to exploit the discoveries of radioindicators of "biochemical/physiological" elements similarly. Frederic Joliot and Irene Curie discovered artificial radioactivity early in 1934 by creating in their laboratory in Paris positron emitters of two "biological" elements, 2.5-minute Phosphorus-30 and 10-minute Nitrogen-13 (*6*). Within several months, Fermi and his students used a Radon–Beryllium neutron source in Rome in their discoveries of a large number of radionuclides of

many elements. Among them was 14.3-day Phosphorus-32.

Hevesy recognized immediately the potential applicability of this convenient radioactive form of a "vital" element to extend his radioindicator method to studies of diverse natural metabolic processes. Within a year after P-32 was discovered he published with Chievitz (chief of surgery at The Finsen Hospital in Copenhagen) the first radioindicator study in the life sciences with a man-made radionuclide (*1* pp 149–151). "Radioactive Indicators in the Study of Phosphorus Metabolism in Rats" appeared in *Nature* in 1935 (*7*). This landmark contribution was reprinted in *The Journal of Nuclear Medicine* in 1975 (*8*), along with my commentary and with a picture I made of Hevesy in 1950. Phosphorus-32 . . . "can be utilized as an indicator of inactive phosphorus in the same way that the radioactive isotopes of lead, bismuth and so on were formerly used as indicators of these elements." . . .

A strong neutron source was immersed in ten liters of carbon disulfide for some weeks to generate about a microcurie of P-32 in the $^{32}S(n,p)^{32}P$ transmutation (*1* pp 152–167). The P-32 thus obtained was converted into ^{32}P-phosphate before placing it on bits of bread to feed to rats. Geiger-Müller detectors were used to assay the amounts of P-32 found in various organs and excreta as a function of time. Among interesting findings was that the average time spent by a phosphorus atom in the rat was about two months. This first biomedical study with artificial radioactivity led to the conclusion there is a rapid turnover of phosphorus atoms in bone. *Thus emerged the concept of the dynamic state of the body constituents.*

Hevesy now hit his stride in applying radioindicators in biomedicine. As radionuclides of additional "biochemical" elements (Na-24, K-42, etc.) soon were discovered and became available, chiefly by generating them with cyclotrons, he devoted his time increasingly to applying them in studies of a large variety of metabolic and physiological processes. The results found in most of these were reprinted in 1962 (*1*), as noted previously.

His interests remained broad, however. In 1936, only four years after Chadwick discovered the neutron in England, Hevesy and Hilde Levi used it in Copenhagen in their discovery of neutron radioactivation analysis. This sprang from studies of the rare earth elements (*1* pp 47–62) and of several other elements (*1* pp 63–73).

"Radioactive Indicators" was the title of Hevesy's 556-page book, published in 1948 (*9*). It is a landmark contribution in which he succinctly summarized in quite complete review the basic concepts and the experimental findings in our subject to that time. Hevesy did not function in isolation but kept abreast of developments in applications of indicator tracer methodology in biomedical laboratories throughout the world. This book constituted also a turning point in the history of Nuclear Medicine; for, almost all of the myriads of measurements made by the numerous investigators had depended on assays made *in vitro*, chiefly of β-particles, by means of Geiger-Müller detectors or electroscopes.

Hevesy himself seems to have used methods of assay *in vivo* by means of penetrating γ-rays little, if at all. In 1948, also, a new era dawned with the discovery of the NaI(Tl) scintillation detector by Hofstadter (*10*). Its much greater efficiency of interaction with γ-rays and other advantages soon led to the "inside-out" assays and imaging that now dominate the explosive expansion of Hevesy's concepts into clinical nuclear medicine.

Hevesy received The Nobel Prize for Chemistry in 1943 . . . "for his work on the use of isotopes as tracer elements in researches on chemical processes." In his Nobel Lecture on "Some Applications of Isotopic Indicators" (*1* pp 928–960, *11*), he stated . . . "The most remarkable result obtained in the study of the application of isotopic indicators is perhaps the discovery of the dynamic state of the body constituents. The molecules building up the plant or animal organism are incessantly renewed." . . .

Near the end of his Faraday Lecture in 1950 (*1* pp 961–996, *12*) on "The Applications of Radioactive Indicators in Biochemistry," Hevesy said . . . "The application of isotopic indicators opened the only way to determine the rate, place and sequence of formation of many molecular constituents of the living organism. The very existence of such methods was instrumental in opening new trains of thought . . . in concentrating our interest on the problem of the velocity of the fundamental biological processes. . . . The indicator chemist is to some extent an historian, highly interested in the past of atoms, molecules, and molecular aggregates. He has a great concern in the distinction of how far molecules present in the tissue are "old" or "new." . . . He wishes to know when the potassium atoms present in the tissue cells left the circulation" . . .

Another instance of Hevesy's keen sense of history was illustrated in his handwritten letter to Ernest Lawrence on 14 January 1938 when he thanked Lawrence for mailing sufficient Phosphorus-32 to carry out investigations about milk formation. . . . "It is always a sign of appreciation to keep letters, but it is a sign of utmost appreciation to treat letters

as we did treat yours. A trace of phosphorus penetrated the envelope . . . and this induced us to dissolve your letter and to recover the trace of phosphorus it contained. When historians will once describe your life history I hope they won't omit this incident, showing how precious your letters were." . . . In those days radioisotopes simply were airmailed in ordinary envelopes! Hevesy was highly appreciative of Lawrence's generosity, for the cyclotron in Berkeley was the only major source of the radionuclides he needed to pursue the numerous ideas overflowing from his mind.

I first met Hevesy at The Symposium on Radiobiology held at Oberlin College in 1950. There he presented an extensive paper on "Ionizing Radiation and Cellular Metabolism" (*13*). Hevesy always was ahead of his time! He was among the first to apply radioactive indicators in studies of the effects of ionizing radiations (*1* pp 692–875). Also, he and his colleagues first used indicator tracer methods to study cancerous tumors.

My Doctor of Medicine thesis on "Applications of The Cyclotron and Its Products in Biomedicine" was written early in 1941, only seven years after artificial radioactivity was described (*6*). I appreciated the role this epoch-making discovery already had had on Hevesy's insights and increased productivity by noting that 16 of the 87 references cited in the review were authored by Hevesy and coworkers (*14*).

Hevesy's firsthand acquaintanceships with Niels Bohr, Marie and Irene Curie, Frederic Joliot, Albert Einstein, Fritz Paneth, Ernest Rutherford, and many other of the "greats" in basic nuclear science made of him an eyewitness historian of many momentous events. That he was an able reporter of these was reflected in his giving of our second Nuclear Pioneer Lecture on 15 June 1961 in Pittsburgh at the eighth annual meeting of The Society of Nuclear Medicine, "Marie Curie and Her Contemporaries: The Becquerel–Curie Memorial Lecture" (*15*). Hevesy already had been made an honorary member of The Society of Nuclear Medicine, in 1959.

The Gesellschaft für Nuklearmedizin began to honor Hevesy a decade ago by awarding The Hevesy Prize and by the giving of The Hevesy Lecture annually. This prize first was given to Doctor H. Saul Winchell at the meeting in Zürich in 1969, and he gave the lecture the first time then also. At the Gesellschaft meeting in 1976 in Berlin, Doctor Henry Wagner gave The Hevesy Lecture; and his appreciation of the scientist led him later to coin the aphorism (*16*), "Biochemical motion—What Hevesy conceived, we now perceive." How true! Doctor Rosalyn Yalow gave The Hevesy Lecture and received The Hevesy Medal in Madrid in 1978 at the 16th annual meeting of The Gesellschaft für Nuklearmedizin. In her essay on "Radioimmunoassay: Past, Present and Potential," she expressed regret for not having met Hevesy, but regarded him through his book in 1948 (*9*) almost as having been her teacher. In her lecture when she received The Nobel Prize for Medicine in 1977, she acknowledged Hevesy as a scientific progenitor of her career (*17*).

Hilde Levi worked closely with Hevesy as an assistant and knew him so well as to become his principal biographer. She published in 1976 a delightful portrayal of him and his methods in the laboratory, as well as of some of his warm and kindly interpersonal relationships (*18*), "George Hevesy and His Concept of Radioactive Indicators—In Retrospect." . . . "He was possessed by his scientific ideas which dominated his thinking so much he did not have time for other activities." . . . Her historical essay was the first paper to be published in the new European Journal of Nuclear Medicine (*18*).

A decade earlier, Levi published a shorter sketch about Hevesy (*19*). His . . . "inexhaustible stream of new ideas, his dynamic personality, his incredible memory for everything done or read, and his apparently effortless endurance—he never could sleep more than a few hours each night—brought about his ever-presence at all odd hours of the day in different laboratories scattered all over the city of Copenhagen." . . .

Her obituary concerning Hevesy in 1967 (*20*) sketched his lifework in summary outline. It includes a photograph of him and a reliable source of reference to serve as a complete and correct bibliography of his 397 publications.

"Hevesy wrote practically everything by hand (*18*)." The treasured longhand letters I received from him reflect the warmth, humility, modesty, and considerateness of the man. His extensive correspondence resulted in his stating a point laconically. . . . "Radioiodine-123 is a most useful substance" . . . appeared in his letter to me in July 1962.

One finds much in McCagg's documentary book in 1972 (*21*) about the origins of five scientists in modern Hungary whom he considered to be geniuses, and Hevesy was one of them.

Hevesy was born 1 August 1885 in Budapest, Hungary and completed his secondary school education at The Piarist Grammar School. His academic studies began at The University of Budapest, continued in Berlin, and he received his Ph.D. degree in chemistry and physics from The University of Freiburg in 1908. After appointments in many

laboratories in several countries, he became professor of physical chemistry at Freiburg, 1926–1935. He left there to go to The Bohr Institute in Copenhagen, where he stayed during the occupation until 1943 when he settled down in The Institute for Organic Chemistry of The University of Stockholm. He died in a clinic in Freiburg on 5 July 1966.

Numerous honors were bestowed on Hevesy in addition to The Nobel Prize in 1943 and The Atoms for Peace Award in 1959. He regarded especially highly his election to be a foreign member of The Royal Society of London and his being awarded The Copley Medal by it in 1949. He received more than a dozen honorary degrees: and he may have been unique insofar as four of them were honorary Doctor of Medicine degrees. Four Faculties of Medicine thus indicated the esteem in which they held Hevesy for his basic contributions to medicine.

Nuclear Medicine is endowed with an especially rich and variegated heritage. Paraphrasing Newton, "We stand on the shoulders of giants:" and our activities stem from an integration of some of the insights of no less than three dozen Nobel Laureates and the sagacity of many other gifted scientists. Distinctly notable among our forebears was Georg Charles de Hevesy. At the end of the first 25 years of The Society of Nuclear Medicine, we opportunely and appropriately demonstrate our maturity when we acknowledge our cognizance and appreciation of the magnificent scientific legacy we derive from Hevesy and recognize him to have been our inspirational leader and our principal intellectual forefather.

WILLIAM G. MYERS, Historian
The Society of Nuclear Medicine
College of Medicine
The Ohio State University
Columbus, Ohio

REFERENCES

1. HEVESY G: *Adventures in Radioisotope Research*, New York, Pergamon Press, 1962
2. HEVESY G: The absorption and translocation of lead by plants. A contribution to the application of the method of radioactive indicators in the investigation of the change of substance in plants. *Biochem J* 17: 439–445, 1923
3. HEVESY G, PANETH F: Die Löslichkeit des Bleisulfids und Bleichromats. *Z anorg Chem* 82: 323–328, 1913
4. PANETH F, HEVESY G: Über Radioelemente als Indikatoren in der analytischen Chemie. *Monatsh Chem* 34: 1401–1407, 1913
5. HEVESY G, PANETH F: *A Manual of Radioactivity*, Second Edition, London, Oxford University Press, 1938
6. JOLIOT F, CURIE I: Artificial production of a new kind of radio-element. *Nature* 133: 201–202, 10 February 1934
7. CHIEVITZ O, HEVESY G: Radioactive indicators in the study of phosphorus metabolism in rats. *Nature* 136: 754–755, 1935
8. MYERS WG: The first radioindicator study in the life sciences with a man-made radionuclide. *J Nucl Med* 16: 1106–1108, 1975
9. HEVESY G: *Radioactive Indicators*, 556 pages, New York, Interscience Publishers, 1948
10. HINE GJ: The inception of photoelectric scintillation detection commemorated after three decades. *J Nucl Med* 18: 867–871, 1977
11. HEVESY G: Some applications of isotopic indicators. *In Les Prix Nobel en* 1940–1944, Stockholm, Norstedt & Söner, 1946, pp 95–127
12. HEVESY GC: The application of radioactive indicators in biochemistry. *J Chem Soc:* June, 1951, pp 1618–1639
13. HEVESY G: Ionizing radiation and cellular metabolism. Chap. 11. In *Symposium on Radiobiology*, New York, Wiley, 1952, pp 189–215
14. MYERS WG: Applications of the cyclotron and its products in biomedicine. Unpublished MD thesis, 1941
15. HEVESY G: Marie Curie and Her Contemporaries: The Becquerel-Curie Memorial Lecture. *J Nucl Med* 2: 169–182, 1961
16. WAGNER HN, JR: Personal communication, 1977
17. YALOW RS: Radioimmunoassay: A Probe for the fine structure of biological systems. *Science* 200: 1236–1245, 16 June 1978
18. LEVI H: George Hevesy and his concept of radioactive indicators—In retrospect. *Eur J Nucl Med* 1: 3–10, 1976
19. LEVI H: The development of the tracer method, 1935–1945. *Int J Appl Rad & Isotopes* 16: 511–513, 1965
20. LEVI H: George de Hevesy. *Nuclear Physics* A98: 1–24, 1967
21. MCCAGG WO, JR: *Jewish Nobles and Geniuses In Modern Hungary*, New York, Columbia University Press, 1972

Atlanta 1979

Over the past 25 years, the general format of the Annual Meeting of the Society of Nuclear Medicine has remained essentially unchanged. This year, several fundamental changes in the Annual Meeting program will be evident.

Many attendees at recent meetings have expressed the opinion that the meetings are too long and too congested: that there are too many days filled with too much occurring, giving no opportunity to digest the material presented or to renew professional and social acquaintances. Another frequent observation is the apparent isolation and inaccessibility of the Board of Trustees and Committee meetings to the interested membership.

With these critical observations in mind, and with suggestions from the Education and Training Committee, Trustees, officers, and members, the Scientific Program Committee has developed an entirely new meeting format for the 26th Annual Meeting in Atlanta.

On Monday, June 25, at the Hyatt Regency Hotel, the various committees of the Society will conduct their deliberations in meetings that will be open to the membership. The times and places of these meetings will be circulated beforehand and will be displayed prominently in Atlanta.

Another major change will be the separation of continuing education sessions from direct competition with scientific papers. On Monday, June 25—the day preceding the official meeting—two symposia will be presented concurrently with the committee meetings. The subjects of these symposia will be bone scanning and cardiovascular nuclear medicine. They will consist of an update of these, prepared by the Education and Training Committee, and will be presented as separate courses, offering AMA Category I credit and for which a separate fee will be charged.

The Annual Meeting proper will begin Tuesday, June 26. At the opening Plenary Session, the subjects discussed will be directed toward defining the role of nuclear medicine in the diagnosis and management of clinical cardiovascular and neuropsychiatric diseases. The exhibits will open following the Plenary Session, the scientific papers will begin in the afternoon, and both will continue through the final day, Friday, June 29. Tuesday will be utilized by the SNM staff and Trustees to prepare and distribute committee reports, giving the Board time to consider and discuss proposals before taking action.

On Wednesday, June 27, there will be no formal scientific presentations. The Board of Trustees will meet, and this meeting will be open to the membership and to meeting registrants. Simultaneously, there will be three Continuing Education sessions, two concerned with clinical subjects and one with basic science. Admission to these sessions will be open to all meeting registrants.

Thursday and Friday, June 28 and 29, will be devoted to presentations of scientific papers and poster sessions. In the hope of encouraging interaction among the various subdisciplines within nuclear medicine, the Scientific Program Committee attempted to maintain minimum competition between clinical and basic science presentations.

The Scientific Program Committee Vice-Chairmen have identified special topics that they believe to be of interest to the membership and these subjects are emphasized in topic symposia. Some of these target symposia will be highly focused and of interest to special groups (for example, pharmacokinetic modeling sponsored by the Radiopharmaceutical Chemistry section). Other symposia will be on topics of wider interest, for example, a receptor symposium, cosponsored by the radiopharmaceutical chemistry and in vitro sections, which should appeal as well to many clinicians and lead to a stimulating exchange between interested groups. These mini-symposia will be complemented by presented papers and the liberal use of poster sessions.

This year, the Scientific Program Committee was

gratified to receive the largest number of abstracts ever submitted to a SNM meeting—almost 800. The Committee worked to identify those papers with the highest scientific merit and broadest interest for what will be the 26th Annual Meeting and the 25th Anniversary of the founding of our Society. Despite a compressed meeting structure—only three days for scientific presentations—we worked to accomplish a 50% acceptance rate because of the high quality of the submitted abstracts. The Vice-Chairmen and all the reviewers who gave time and talent are to be congratulated for our final program, which is the result of their efforts. This meeting has much to offer, and I urge all of you to take full advantage of the opportunities to learn and to enjoy.

RICHARD C. REBA
Chairman, 1979 Scientific Program Committee
The Society of Nuclear Medicine

TABLES OF SCIENTIFIC SESSIONS

TUESDAY, JUNE 26 • SNM 1979 ANNUAL MEETING

REGISTRATION 7:30 to **5:30** (Congress Center) — *EXHIBIT HALL OPEN* 11:30 to **5:30**

8:30 to 11:30	**Opening Remarks** Awards Presentations Hevesy Nuclear Medicine Pioneer Lecture			**PLENARY SESSION** "Defining the Role of Nuclear Medicine in the Diagnosis and Management of Cardiovascular and Neuropsychiatric Disorders"			
11:30 to **12:00**	**Grand Opening of the Exhibits**						
12:00 to **1:30**	**VISIT THE EXHIBITS**						
	CLINICAL SCIENCE/APPLICATIONS			**RADIOPHARMACEUTICAL CHEMISTRY**	**IN-VITRO**	**INSTRUMENTATION, COMPUTERS, AND DATA ANALYSIS**	**RIA (Workshops)**
1:30 to **3:30**	**CS** **Image Correlation** Room 210	**CA** **Bone/Joint** Room 211	**CS** **Cardiovascular I** Room 300/301	**Symposium I** **Pharmaco-Kinetic Modeling** **Berson-Yalow Paper** Room 201		**Poster Session:** **A. Dosimetry** **B. Image Processing** **C. Instrumentation Hardware** Room 204	
	BREAK						**Workshop A** **3:30-5:30** Room 212
4:00 to **5:30**	**CS** **Neurology** Room 210	**CS** **Pulmonary** Room 211		**Symposium II** **Pharmaco-Kinetic Modeling** Room 201	**Poster Session** Room 206		
	Technologists' Georgia Country Bash 6:30 p.m. to 1:00 a.m.						

Times in lightface are a.m., those in **boldface are p.m.**

WEDNESDAY, JUNE 27 • SNM 1979 ANNUAL MEETING

REGISTRATION 7:30 to **5:30** (Congress Center)

	CONTINUING EDUCATION			**EXECUTIVE AND ADMINISTRATION**	**SPECIAL PROGRAMS**	**RIA**	**EXHIBITS**
8:30 to 10:00	**Gastroenterology** Room 300/301	**Pediatrics** Room 208/209	**Radioassay** Room 201		**Nuclear Magnetic Resonance** 900-11:00		**Exhibit Hall** open 8:30 to **5:30**
	BREAK			**BOARD OF TRUSTEES**		**Workshop B** 10:00-12:00 Room 212	
10:30 to **12:00**	**Pulmonary** Room 300/301	**Tumor** Room 208/209	**Radiopharmaceutical** Room 201	Room 305/306	Room 307		
	LUNCH						
1:30 to **3:00**	**Thyroid Cancer** Room 300/301	**Brain** Room 208/209	**Instrumentation** Room 201	**Board of Trustees** Room 305/306	**Nurses and Clinical Specialists in Nuclear Medicine** 1:00-3:00	**Workshop A** 2:00-4:00 Room 212	
	BREAK						
3:15 to **4:15**	**Renal** Room 300/301	**Hematology** Room 208/209	**Computer Science** Room 201		Room 307		
	BREAK						
	SNM BUSINESS MEETING Room 305/306						

TABLES OF SCIENTIFIC SESSIONS (continued)

THURSDAY, JUNE 28 • SNM 1979 ANNUAL MEETING

REGISTRATION 8:00-5:30 (Congress Center) — EXHIBIT HALL OPEN 8:30 to 5:30

	CLINICAL SCIENCE/APPLICATIONS			RADIOPHARMACEUTICAL CHEMISTRY	IN-VITRO	INSTRUMENTATION, COMPUTERS, AND DATA ANALYSIS	RIA
8:30 to 10:00	**Mixed Posters I** Renal/Pulmonary/ Brain/Endocrine/ GI/H-A Exhibit Hall	**CA** Renal/Endocrine Room 211	**CS** Cardiovascular II Room 300/301		Measurement of Free Thyroxine Room 206	Instrumentation Room 204	
	BREAK						
10:30 to 12:00	**CS** Renal/Electrolyte/ Hypertension Room 210	**CS** Gastroenterology I Room 211	Peripheral Vascular Room 300/301	Mechanism of Reaction and Epidemiology of Peptide and Steroid Hormone Receptors Room 201		Physics Room 204	
	LUNCH & VISIT THE EXHIBITS						Workshop C 1:30-3:30 Room 212
2:00 to 3:30	**CS** Pediatrics Room 210	**CA** Pulmonary Room 211	**CS** Cardiovascular III Room 300/301	Technetium Chemistry Room 201		Mini Symposium: Edge Detection and Pinhole Tomography Room 204	
	BREAK						Workshop D 3:30-5:30 Room 212
4:00 to 5:30	**CS** Oncology Room 210	**CS** Bone/Joint Room 211	**CS** Cardiovascular IV Poster Session I Room 300/301	Poster Session I Room 201		Mathematics Room 204	
	Evening: Dinner Theatre Party						

FRIDAY, JUNE 29 • SNM 1979 ANNUAL MEETING

REGISTRATION 8:00 to 2:00 (Congress Center) — EXHIBIT HALL OPEN 8:30-2:00

	CLINICAL SCIENCE/APPLICATIONS			RADIOPHARMACEUTICAL CHEMISTRY	IN-VITRO	INSTRUMENTATION, COMPUTERS, AND DATA ANALYSIS	RIA
8:30 to 10:00	**CS** Hematology and Infectious Disease Room 210		**CA** Cardiovascular Room 300/301	Cyclotron Produced Radiotracers Room 201	Recent Advances in Cardiology and Tumor Markers Room 206	Image Processing Room 204	
	BREAK						
10:30 to 12:00	**CS** Radiation Effects Symposium Room 210	**Mixed Poster II** Bone/Oncology Exhibit Hall	**CS** Cardiovascular V Poster Session II Room 300/301	Receptor Binding Radiotracers Room 201	Hepatobiliary Disease Room 206		**Workshop E** 10:30-12:00 Room 212
	LUNCH & VISIT THE EXHIBITS (Exhibits Close)						
2:00 to 3:30	**CS** Endocrine Room 210	**CA** Gastroenterology/ Pediatrics Room 211		Poster Session II Room 201		Scientific Meeting Highlights Henry N. Wagner, Jr. Room 204	
	BREAK						
3:45 to 5:00	**CS** Gastroenterology II Room 210		**CS** Cardiovascular Room 300/301				
	MEETING ADJOURNS						

Proceedings of the 26th Annual Meeting

Atlanta—1979

SCIENTIFIC PROGRAM

TUESDAY, JUNE 26, 1979

8:30 a.m.-11:30 a.m. Auditorium

FORMAL OPENING

8:30-8:45 **CALL TO ORDER AND REMARKS.** Richard C Reba, Chairman, Scientific Program Committee

REMARKS AND INTRODUCTIONS. C Douglas Maynard, President, Society of Nuclear Medicine

PRESENTATION OF THE PAUL C. AEBERSOLD AWARD to JOHN McAFEE

PRESENTATION OF THE SOCIETY OF NUCLEAR MEDICINE EDUCATION AND RESEARCH FOUNDATION BERSON-YALOW AWARD to H. WACHSLICHT-RODBARD and J. ROTH

8:45-9:15 **HEVESY NUCLEAR MEDICINE PIONEER LECTURE.** William C Myers, Historian, Society of Nuclear Medicine, "Georg Charles de Hevesy — The Father of Nuclear Medicine"

Plenary Session

9:30-11:30 **DEFINING THE ROLE OF NUCLEAR MEDICINE IN THE DIAGNOSIS AND MANAGEMENT OF CARDIOVASCULAR AND NEUROPSYCHIATRIC DISORDERS**

Moderator: Thomas F. Budinger, Donner Laboratory, University of California.

Problems in Brain Research and Psychiatric Disorders. Daniel X. Freedman, Professor and Chairman, Dept. of Psychiatry, University of Chicago. *

What Nuclear Medicine Can Accomplish for Neuropsychiatry. David E Kuhl, Professor and Director, Division of Radiological Sciences and Nuclear Medicine, UCLA *

*At time of publication abstracts were not available.

Assessing the Current Needs of Cardiology. Burton E Sobel, Professor and Director, Cardiovascular Division, Washington University

Regional quantitation of myocardial metabolism is needed for detection of myocardial ischemia and necrosis, and characterization of cryptogenic cardiomyopathies with as yet unidentified metabolic etiologies. Its importance for objective evaluation of potential therapy cannot be overemphasized. Procedures employing single photon emitters suffer intrinsic limitations regarding quantification, despite providing valuable semi-quantitative information. Positron-emitting tracers of physiological substrates preferred by the heart, such as ^{11}C-palmitate, are particularly promising. When ^{11}C-palmitate was administered to isolated rabbit hearts at constant flow (n = 38) metabolic consequences of ischemia were detectable quantitatively. In dogs given ^{11}C-palmitate i.v., morphological infarct size correlated with tomographic estimates obtained with PETT III (r = .93) as did the distributions of ^{14}C- and ^{11}C-palmitate (r = .92). In patients studied with PETT IV infarction locus and extent was readily defined with ^{11}C-palmitate, particularly when the cardiac blood pool was delineated with ^{11}CO-hemoglobin. Definitive assessment of myocardial metabolism tomographically with ^{11}C-palmitate requires independent characterization of circulating FFA levels, intracardiac lipid pools, and metabolic pathways of deposition of tracer in normal and abnormal zones. However, contrary to non-physiological analogs (such as iodinated fatty acids), ^{11}C-palmitate is metabolized identically to its physiological counterpart. Thus, tomographic results can be interpreted on the basis of extensive information already available characterizing fatty acid metabolism in normal, ischemic, and cardiomyopathic tissue.

The Role of Nuclear Medicine in Assessing the Needs of Cardiology. William L Ashburn, Professor and Director, Division of Nuclear Medicine, University of California-San Diego *

DISCUSSION TO FOLLOW

11:30-12:00 **GRAND OPENING OF THE EXHIBIT HALL**

1:30 p.m.-3:30 p.m. Room 210

CLINICAL SCIENCE

IMAGE CORRELATION

Chairman: David A. Turner
Co-Chairman: Gerald R. Berg

COMPLEMENTARY ROLE OF SONOGRAPHY AND SCINTIGRAPHY IN HEPATOBILIARY DISEASE. N.R. Zusmer, V. Maturo, M. Stern, W.M. Smouk, W.R. Janowitz, A.J. Gilson. Mt. Sinai Medical Center, Miami Beach, FL.

A plethora of techniques exist at the present time for evaluating patients with suspected gallbladder disease. Grey scale ultrasonography and hepatobiliary imaging with Technetium^{99m} Pipida are both relatively new methods for evaluating these patients. The purpose of this study was to assess the relative roles of the two complementary techniques. 120 Patients presenting with signs and symptoms referrable to the gallbladder were evaluated by both grey scale ultrasonography and Technetium^{99m} Pipida scintigraphy over a period of one year. This report concerns itself with 30 patients with surgically proven gallbladder disease.

Scintigraphic evidence of gallbladder disease was either nonvisualization or delayed visualization of the gallbladder.

Pipida biliary scintigraphy diagnosed 100% of the 24 surgical proven cases of acute cholecystitis with a cystic duct obstruction.

29% Of patients with proven acute cholecystitis demonstrated no definite evidence of gallstones, gallbladder wall edema or distention of the gallbladder on ultrasound examination.

Of the 6 patients with surgical proven chronic cholecystitis with stones, 50% of the patients had normal Pipidas. These patients all had ultrasonic evidence of gallstones.

In conclusion, Pipida is the procedure of choice in patients with acute cholecystitis. A normal Pipida study does not exclude gallbladder disease and the complementary role of ultrasonography is necessary for detection of patients with chronic cholecystitis.

TECHNETIUM-99m PIPIDA AND TECHNETIUM-99m SULFUR COLLOID LIVER SCANNING COMBINED WITH ULTRASOUND IN THE EVALUATION OF PATIENTS WITH JAUNDICE. Edward K. Prokop. Hospital of St. Raphael, New Haven, CT

Ultrasound imaging is the accepted procedure for evaluating patients with jaundice to determine if the etiology is an intrahepatic or an extrahepatic process. However, satisfactory ultrasound images cannot be obtained on all patients. A possible alternative method for evaluating jaundiced patients is described below.

Seven patients with jaundice were studied with Tc-99m sulfur colloid scans, hepatobiliary scans, and ultrasound. Ultrasound demonstrated intrahepatic bile duct dilatation in 5 patients and was technically inadequate in one patient. One patient was not studied with ultrasound. In all patients studied with hepatobiliary imaging, there was poor concentration of Tc-99m PIPIDA in the liver and no activity was seen in the gastrointestinal tract after 4 hours. These patients had no evidence of significant diffuse liver disease by Tc-99m sulfur colloid scanning.

Thus, if the Tc-99m sulfur colloid liver scan is relatively normal and the hepatobiliary scan is abnormal without any activity in the gastrointestinal tract, the cause of the jaundice is probably extrahepatic. Anatomical imaging with ultrasound can frequently determine the cause of the extrahepatic obstruction.

EFFICACY OF A COMBINED DIAGNOSTIC APPROACH TO JAUNDICE: Tc-99m HIDA AND ULTRASOUND. J.W. Ryan, M. Hill, M. Isikoff, and G.S. Johnston. The University of Maryland Hospital, Baltimore, MD.

59 clinically jaundiced patients (bilirubin < 2 to 42 mg/dl) were imaged by both gray scale ultrasound (GSUS) and Tc-99m HIDA. Tc-HIDA showed biliary flow patterns and GSUS evaluated biliary anatomy. Obstruction in both studies (8 cases) was caused by a focal blockage of the main biliary ducts. Absence of obstruction in either study (30 cases) represented hepatocellular dysfunction (25), cholelithiasis with recent transient common duct obstruction (4), or metastatic disease (1). Divergent results occurred in 21 cases. Dilated ducts but patent flow (12 cases) represented incomplete extrahepatic obstruction from focal lesions (11) or cirrhosis (1). Totally obstructed flow without dilated ducts (9 cases) resulted from both cancer of the pancreas (4) and diffuse intrahepatic obstruction due to cholestasis (2), cholangiocarcinoma (1), or biliary atresia (2).

From these data the initial recommended imaging approach to the adult jaundiced patient is GSUS. If dilated ducts are present, future surgical management does not require biliary flow patterns. If GSUS shows no evidence of obstruction, Tc-HIDA will separate patients with totally obstructed biliary flow, who require additional testing to define the correct therapy, from those with patent biliary flow for whom medical management is indicated initially. In this latter group, patients with cholecystitis may also be identified from additional diagnostic features contained in the images.

Thus, the sequential use of these two complementary imaging modalities in jaundiced patients provides a rapid, accurate, non-invasive approach for the initial determination of appropriate therapeutic categories.

BRAIN IMAGING WITH RADIONUCLIDE (RN) AND COMPUTERIZED TOMOGRAPHIC (CT) TECHNIQUES E.B. Silberstein, J.H. Kim. The University of Cincinnati Medical Center, Cincinnati, OH.

No study relating RN and CT has employed the optimum brain scan techniques available: technetium chelate, two hour delayed scan, routine flow study, and vertex view. We used all these to compare the results to CT (with frequent contrast infusion and a 160 x 160 matrix). 197 consecutive patients with tumor, C.V.A., subdural hematoma (SDH), abscess, or without demonstrable intracranial disease were identified who had been imaged with both modalities. Documentation of disease was provided by autopsy (5%), at surgery (21%), by angiography (24%), skull film (1%). The other half of the cases had a minimum eighteen month clinical follow-up, frequently with EEG correlation, and final diagnosis agreed upon by two physicians other than the authors of this study.

The sensitivities for RN and CT respectively were: tumor 86% and 90%; C.V.A. 87% and 79%; SDH 93% and 93%; abscess 100% and 100%. For normals specificity for RN was 94%, CT 88%. CT provided 7 false positives (FP) while the RN provided 4. All FP readings occurred in patients with non-focal symptoms or signs.

A comparison of incorrect readings in 1975 versus 1977 showed no significant difference, suggesting that the extra experience in using RN and CT did not alter results.

Metastatic tumor detection was equal for RN and CT, but two more primary brain tumors, out of 26 total, were detected by CT than RN. CT appeared better than RN in detecting tumors of the posterior fossa.

RN accuracy was 90%, and CT accuracy 87%, not significantly different. RN detected more intracranial cerebrovascular disease. CT provided more FP results than RN. CT appeared better than RN in detecting posterior fossa tumors.

NONINVASIVE ASSESSMENT OF REGIONAL ASYNERGY IN ACUTE MYOCARDIAL INFARCTION BY RADIONUCLIDE VENTRICULOGRAPHY AND TWO-DIMENSIONAL ECHOCARDIOGRAPHY. J. Wynne, J.C. Birnholz, B.L. Holman, H. Finberg, J.S. Alpert. Peter Bent Brigham Hospital and Harvard Medical School, Boston, MA.

Radionuclide ventriculography (RVG) and two-dimensional echocardiography (2DE) were performed at the bedside with-

in 24 hours of each other in 30 patients (pts) with suspected acute myocardial infarction (MI). Regional wall motion (RWM) was assessed in anteroseptal, apical and inferoposterior regions by each technique. RVG ejection fraction (EF) and a 2DE semiquantitative estimate (SE) of global left ventricular function (LVF) based on visual assessment of RWM exhibited a linear correlation (r=0.76). RWM assessment by each technique was in agreement in 82% (74/90) of regions. Dyskinesis was detected in 9 pts (RVG 3 pts; 2DE 6 pts), although only 4 pts (13%) demonstrated paradox by both techniques. Of 18 pts with documented MI 29 regions demonstrated pathologic Q waves on electrocardiogram. RWM was abnormal in 25/29 (86%) regions by RVG and 24/29 (83%) regions by 2DE; 4/5 discordant regions were normal by both techniques. In pts with MI there was a correlation between LVF as assessed by RVG and 2DE and peak creatine kinase (CK) levels. Patients could be grouped according to CK and LVF:

*p<0.025	EF(mean±SEM)(%)		SE(mean±SEM)		
CK<1000IU/L	58.3±6.9	*	7.00±0.44	NS	*
CK>1000IU/L	44.2±6.3	*	9.67±0.85	NS	
CK>2500IU/L	26.0±4.5		12.30±0.51		

Thus, both 2DE and RVG consistently demonstrate RWM abnormalities in pts with MI, and both techniques generally agree as to the location and severity of asynergy.

TRANSMISSION COMPUTED TOMOGRAPHIC FINDINGS AFTER EXPERIMENTALLY-PRODUCED ACUTE PULMONARY ARTERIAL OCCLUSION IN THE DOG. Z.D. Grossman, G.M. Gagne, A. Zens, F.D. Thomas, C.C. Chamberlain, A. Singh, W.N. Cohen, and E.R. Heitzman. The Upstate Medical Center, Syracuse, N.Y.

CT of the chest in the supine dog reveals an increasing anterior-to-posterior density gradient which reverses when the animal's position changes from supine to prone. This gradient probably results from blood flow distribution, and thus the less dense non-dependent lung is somewhat oligemic compared to dependent lung. Since CT identifies the relative oligemia based upon gravity effects, we investigated CT's value for identification of supposed oligemia distal to acute pulmonary arterial occlusion.

We occluded pulmonary arteries in the dog by Swan-Ganz balloon catheter or intravenous injection of autologous clot and studied the chest with CT, Tc-99m-MAA gamma imaging, and plain radiographs. The arterial occlusions were between one and five hours old.

Radiographs revealed no lesions. Tc-99m-MAA scans revealed 10 of 11 lesions. CT identified 2 of 11 lesions (when the animal was imaged prior to peripheral intravenous injection of Renografin-60) and 4 of 10 lesions (after peripheral intravenous injection of Renografin-60). The appearance of lesions on CT was highly variable.

Tc-99m-MAA gamma imaging, therefore, is far more accurate then CT in the identification of experimentally-produced acute pulmonary arterial occlusion in the dog, and our study fails to suggest a secure place for CT in the diagnosis of clinical human pulmonary emboli. Moreover, the assumption that such lesions are oligemic is questioned.

SCINTIGRAPHYCALLY GUIDED ULTRASONIC STUDIES IN THE DETECTION OF INTRA-ABDOMINAL ABSCESSES. T. Stanton, W. Bohlman, M. Schreyer, K. Vanags, B. Kovaleski, and J. Franco, O'Connor Hospital, San Jose, CA.

Indium-111 oxine labelled leucocytes have been recently reported to be useful in the detection of intra-abdominal abscesses. However, the procedure is costly, time consuming and may not be readily available at the community hospital level.

A useful alternative has been Ga-67 scanning and scintigraphically directed ultrasonic studies. Twenty-six patients were studied as follows: 1) abdominal scintigraphy 5 hours after the administration of 3-6 mCi of Ga-67 citrate, and 2) quick, real time ultrasonic scanning of any areas of scintigraphic abnormality.

Twelve cases of intra-abdominal abscesses were correctly identified by this combined approach.

Three patients had Ga-67 uptake associated with variably distended urinary bladder. Five patients had questionable gallium uptake, but there was no abnormality in the ultrasonic study. These 8 studies and the remaining 6 cases were interpreted as negative for abscesses. There were no false negatives.

At the community hospital level, this combined approach appears adequate for the detection of intra-abdominal abscesses.

DO CLINICIANS VIEW RADIONUCLIDE AND ULTRASOUND LIVER IMAGING AS SUBSTITUTES OR COMPLEMENTS? B.D. Collier and D.E. Drum. Joint Program in Nuclear Medicine, Department of Radiology, Peter Bent Brigham Hospital and Harvard Medical School, Boston, MA.

The decision to examine the liver by radionuclide (RN) or by ultrasound (US) imaging or by both is generally made by clinicians. To discern whether their choice of indication and of imaging sequence may affect diagnostic accuracy and utility, we have reviewed the records of 144 patients for whom both US and RN exams were obtained during a single disease episode.

There was no preference in image sequence for the 39 patients referred for independent indications (different disease states or areas) and for 50 referred with different indications (same disease). In contrast, when done for identical indications (55 patients), US was ordered before RN in 27%. This was undesirable, since the sensitivity for detection of metastases (proven present in 14 of 50 patients with primary cancers referred for that indication) by US alone or as a first exam was 0.57 or 0.20, respectively. When US followed RN, their joint sensitivity, specificity and accuracy were 0.71, 1.0 and 0.92, respectively. Thus, directed US following RN acted as a complementary exam which markedly improved specificity and moderately raised accuracy, in accord with studies on record.

These data suggest that clinicians often view the two studies as substitutes rather than as complements. However, for liver metastases, RN and directed US are complementary exams. These disparate viewpoints of referral and radiologic physicians need to be reconciled if maximal efficacy is to be realized.

1:30 p.m.-3:30 p.m. Room 211

CLINICAL APPLICATIONS

BONE/JOINT

Chairman: Albert S. Hale
Co-Chairman: Robert L. Mecklenberg

GALLIUM SCINTIGRAPHY FOR DISC SPACE INFECTIONS. D. A. Bruschwein, M. L. Brown, and R. A. McLeod. Mayo Clinic and Mayo Foundation, Rochester, MN.

Disc space infection may present a difficult diagnostic problem. We studied 100 consecutive patients with suspected disc space infection in whom a Gallium scan was obtained. The usefulness and accuracy of the Gallium scan was evaluated and compared to other modalities such as standard radiographs and computed tomography.

Of the 100 cases, 19 had a disc space infection. The Gallium scan was positive in 17. In three of these, the Gallium scan was positive while the initial radiographs and other tests were normal. In four others, the Gallium scan was considered to be instrumental in establishing the diagnosis even though there was other evidence to support disc space infection.

Disc space infection was not present in 72 of these patients, and this was accurately reflected by a normal Gallium scan in 61. There were 11 false positive. These erroneously positive scans were caused by other spinal or

paraspinal abnormalities (metastasis (2), degenerative disc disease (2), pancreatic carcinoma, pancreatic abscess, vertebral lymphoma, epidural abscess, compression fracture, spondylolisthesis).

Nine cases were excluded from the study because of inadequate workup at our institution.

Gallium scanning is a useful adjunct in the evaluation of a patient with a suspected disc space infection. In this study, the scan had a sensitivity of 90 percent, a specificity of 85 percent, and an accuracy of 86 percent.

HYPERTROPHIC PULMONARY OSTEOARTHROPATHY: AN OVERVIEW. M. Tetalman, E. Fordham, A. Ali, J. Chiles, S. Patel, K. Schmidt, and D. Turner. The Ohio State University Hospitals, Columbus, OH; Rush-Presbyterian-St. Luke's Medical Center, Chicago, IL; and Holy Family Hospital, Des Plaines, IL.

The bone scans of 54 confirmed cases of hypertrophic pulmonary osteoarthropathy (HPO) were analyzed in a bone-by-bone fashion. Several new observations, some of which have not been reported earlier about the distribution pattern of HPO were made. The tibia is the most commonly involved bone followed by femora, forearm, hands, and feet. In any extremity, distal long bones are more commonly and/or more strikingly involved, with the exception of the radium and ulna where proximal involvement is sometimes more striking. Asymmetric involvement is not uncommon and is seen more commonly in lower extremities than upper extremities. Isolated involvement of lower extremities alone occurs with regularity; isolated involvement of upper extremities was not found in this series. Facial, clavicular, scapular, and patellar involvement is very common. Involvement of tubular bones of hands and feet is more common at the metaphysis, often limited to one side of the joint. Additionally, the bone scan is often an indicator of the status of the disease, becoming negative with approoriate treatment but converting to positive with recurrence or progression of the primary disease. Finally, the bone scan is more sensitive in demonstrating the presence and extent of disease rather than roentgenography as the degree of abnormality of the radionuclide image tends to be related more to the rate of pathophysiologic change; the degree of roentgenographic abnormality is often related more to the duration of the disease process.

COMPARISON OF BONE SCANNING AND RADIOLOGY IN METABOLIC BONE DISEASE. I. Fogelman, D. E. Carr. Department of Nuclear Medicine, Royal Infirmary, Glasgow, Scotland.

Bone scans and x-rays from 113 patients with metabolic bone disease were evaluated independently by 2 observers.

In 25 patients with Paget's disease there were 129 sites of involvement, 123 (95.4%) were recognised on the bone scan as compared to 93 (72.1%) on x-ray. In primary hyperparathyroidism the bone scan was suggestive of a metabolic bone disorder in 7 of 14 (50%) patients, while x-rays were reported as showing evidence of hyperparathyroidism in 3 (21%) cases. The bone scan suggested the presence of a metabolic bone disorder in all 24 patients with renal osteodystrophy and 15 patients with osteomalacia while the correct diagnosis was obtained in 14 (58%) and 9 (60%) of those patients on x-ray. The bone scan was not suggestive of a metabolic bone disorder in any of 37 patients with histologicall proven osteoporosis. In 22 (61%) cases the x-rays were reported as showing osteoporosis. In 19 (70%) patients vertebral fractures were seen on x-ray while these were noted in 12 (44%) patients on the bone scan. Vertebral fractures were usually visualised on the bone scan when these had occurred less than one year from the time of study.

It is concluded that the bone scan is the more sensitive investigation in patients with osteomalacia, primary hyperparathyroidism, renal osteodystrophy and Paget's disease, and should be performed prior to routine radiology. For osteoporosis radiology is the investigation of choice but the bone scan may be of value in assessing the duration of vertebral collapse.

IMPACT OF BONE MARROW IMAGING ON BONE AND GALLIUM SCAN INTERPRETATIONS. N. Bidani, P.T. Kirchner, J.W. Ryan, and M. Cooper. University of Chicago, Chicago, IL.

Focal marrow hyperplasia has been observed by us to masquerade as metastasis on bone or gallium scans. To evaluate this finding and the overall contribution of bone marrow imaging to the diagnostic accuracy of bone and gallium scans, we selected 23 patients with unexplained symptoms or focal abnormalities on bone or gallium scans for additional bone marrow imaging with Tc-99m sulfur colloid.

In 13 patients with underlying malignancies (26 bone scan abnormalities), marrow scans changed the initial interpretation of 7 abnormalities: 6 from malignant to benign and 1 from benign to malignant. For 9 abnormalities the probability of metastasis was increased; in 10 others metastasis was confirmed. In 4 children recognition of bilateral symmetric metaphyseal lesions (metastases in 3) depended on the marrow scan. In 2 patients with abnormal bone scans, normal marrow scans reduced the likelihood of malignancy in one. In 8 patients with sickle cell (SS) disease (11 bone scan abnormalities) marrow imaging increased the diagnostic certainty of infarction in 7 while uncovering 4 old infarcts.

These findings confirm that marrow imaging often clarifies selected focal bone or Ga-67 scan abnormalities. In SS disease it increases detection of both acute and old infarcts. In children it significantly facilitates the diagnosis of symmetrically located metaphyseal metastases. Most important, we have established a new application for bone marrow imaging: non-invasive differentiation of focal marrow proliferation from metastasis as a cause for abnormal bone and gallium scans. This may avoid false positive diagnoses, particularly in patients whose bone marrow has been irradiated or who have anemia from other causes.

BONE SCANNING IN THE PAINFUL TOTAL HIP PROSTHESIS WITH PARTICULAR EMPHASIS ON SEPARATING LOOSENING FROM INFECTION. B.R.J. Williamson, R.E. McLaughlin, C.D. Teates, S.T. Bray, B.Y. Croft. University of Virginia Medical School, Charlottesville, VA. 22908.

Total hip replacement is successful though still subject to complications, mainly loosening and infection. Over a two year period, we evaluated 21 patients with 23 painful total hip replacements. All the patients had a bone scan, on average 42 months post surgery, range 6-81 months. Eleven patients had arthrograms, 9 had preoperative needle aspirations and 19 underwent surgery.

Bone scanning was the most sensitive in judging normal versus abnormal. We therefore assessed the patterns to see if specificity could be improved. Three main patterns emerged:- 1) ectopic calcification. 2) focal activity at the upper and lower ends of the femoral prosthesis. 3) diffuse increased activity around the femoral prosthesis, or diffuse increased activity around the femoral and acetabular components.

There were 9 focal patterns of which 7 were loose, 1 was false positive for loosening and 1 had moderate synovial inflammation; none had demonstrable infection at surgery. There were 4 diffuse femoral component results: 3 were loose and 1 had severe synovial inflammation but no infection could be demonstrated at surgery. There were 3 diffuse femoral and acetabular patterns: 2 were infected and 1 had both components loose. Four further cases with diffuse femoral and acetabular type activity were found in the literature; 3 were infected and 1 had both components loose. From these early results it appears that infection is unlikely with a focal pattern but should be strongly considered if there is a diffuse femoral and acetabular pattern.

THREE PHASE BONE SCAN IN DIABETIC FOOT. H.Park, J.Wheat, A.Siddiqui, R.Burt, J.Robb, H.N.Wellman. Indiana University Medical Center, Indianapolis, IN.

To evaluate difficult foot problems in diabetics, 3-phase Tc-99m MDP bone scans were obtained and evaluated in 3 groups of patients; (A) Nondiabetics without foot problems (n=11), (B) Diabetics without foot problems (n=

10), (C) Diabetics with foot problems (n=22). In all patients, plantar feet scans were obtained in 3 phases, i.e., I(dynamic study-3 sec/frame x 12), II("blood pool" image-5 min postinj.) and III(bone image-2 hr).

Open biopsy confirmed osteomyelitis (Om) in 8 and excluded in 4 other patients. Scan abnormalities were graded as -1, 0, 1, 2 and 3 compared to the background activity by 3 nuclear physicians.

	Group A	Group B	Group C
age(mean)	56.4	51.7	55.3
male/female	4/7	1/9	15/7
% abnl feet	23%	55%	73%
# abnl foci/pt.	0.45	1.4	2.3

The scan scores in all 3 phases were significantly higher in proven Om sites than in areas with degenerative changes.

	Phase I	Phase II	Phase III
Om (n=8)	1.03±.92	1.75±.72	2.28±.74
Deg.(n=17)	0.09±.19	0.32±.36	1.21±.53
p	<0.01	<0.001	<0.01

Ischemic ulcers scored lower in phases I and II than in III. Cellulitis without Om scored high in I and II but low in III. X-rays were helpful when scan was abnormal. Diabetics without symptoms or signs had 3 times more foot abnormalities than nondiabetics.

Three phase bone scan is a very useful tool in management of diabetic foot problems.

DIAGNOSIS OF TEMPOROMANDIBULAR JOINT DISEASE. H.A. Goldstein, C.Y. Bloom, and J.R. Hansell. Veterans Administration Medical Center and the University of Pennsylvania, Philadelphia, PA.

The covert causes of diffuse facial pain are a diagnostic challenge. The purpose of this study is to unravel the enigma of perifacial pain as it relates to temporomandibular joint (TMJ) disorders.

Eight patients with significant lateral facial pain are evaluated. Routine radiographic studies (facial bone and TMJ series, and tomography) and histologic preparations are correlated with bone scintigraphy and clinical symptomatology.

Patients are classified by radiographic, scintigraphic, and histologic findings. The four patients in Class I had abnormal radiographic, scintigraphic, and histologic results. The three patients in Class II had negative radiographic studies with abnormal bone scintigraphy and histology. The one patient in Class III had normal radiographs, bone scintigraphs and histology.

Bone scintigraphy in all eight patients correlated with histologic findings. Three patients in which there were normal radiographic studies demonstrated abnormal histology.

In patients with perifacial pain this series suggests that the bone scintigraph is useful when the radiograph is normal in detecting early degenerative TMJ changes, and in ruling out pain of psychogenic origin.

EVALUATION OF APLASTIC ANEMIA WITH INDIUM-111 CHLORIDE SCANNING. N.L. Horn, L.R. Bennett, and D. Marciano. UCLA Medical Center, Los Angeles, CA.

Aplastic anemia is a serious disease with diverse causes and high morbidity and mortality. The eventual outcome in an individual patient is notoriously difficult to predict. A non-invasive procedure which could moniter a patient's course would be of substantial clinical utility.

We performed a retrospective analysis of all patients with a diagnosis of aplastic anemia who underwent Indium-111 chloride bone marrow scintigraphy between July, 1974 and June, 1978 in the section of Nuclear Medicine at the UCLA Medical Center. Twenty-four patients (14 males, 10 females) with multiple causes of aplastic anemia had Indium-111 chloride bone marrow scintigraphy. Nineteen whole body studies were performed with the 12 plane Pho/Con instrument and 10 whole body scans with the 5" dual probe rectilinear scanner. Good correlation of the scan interpretation with other clinical parameters including the peripheral blood count and bone marrow biopsy was found in 28 of the 29 studies.

These encouraging results with a non-invasive procedure which permits evaluation of the entire bone marrow organ in addition to extramedullary sites of hematopoieses suggest a broader use for Indium-111 chloride bone marrow scintigraphy in aplastic anemia and other hematologic diseases. Moreover, as shown in this study, clinically useful scans can be made with conventional instrumentation as well as with more sophisticated equipment.

1:30 p.m.-3:30 p.m. Room 300/301

CLINICAL SCIENCE

CARDIOVASCULAR I

Chairman: Bertram Pitt
Co-Chairman: James Caldwell

MYOCARDIAL UPTAKE OF RUBIDIUM-82 USING POSITRON EMISSION TOMOGRAPHY. T.F. Budinger, Y. Yano, S.E. Derenzo, R.H. Huesman, J.L. Cahoon, B.R. Moyer, W.L. Greenberg, and H.A. O'Brien, Jr.* Donner and Los Alamos* Scientific Laboratories, University of California, CA.

Rubidium-82 ($T_{\frac{1}{2}}$=1.25 min) is a positron emitter obtained from Sr-82 ($T_{\frac{1}{2}}$=25 d) using a table-top generator comprised of an ion exchange column. The short half-life, low whole body dose of 1.9 mrad/mCi and immediate availability independent of cyclotron location give this radionuclide unique potentials for physiological and clinical studies. The Donner 280-crystal positron emission tomograph has been employed in imaging studies with animals and patients with and without myocardial infarcts using Rb-82 and N-13-ammonia. The overall resolution of this system in the stationary mode for these studies was 9.8 mm FWHM and infarcts as small as 1.5 cc are detected. Rb-82 images were similar to ammonia.

For patient studies 20 mCi or more can be injected in an infusion of 20 cc, 2% NaCl over a minimum period of 7 sec. Patient studies (4) show uptake defects commensurate with correlative EKG and catheterization findings. Constant infusion of Rb-82 at approx. 2 mCi/min gives equilibrium images from which specific volume flow can be estimated from the ratio of myocardial to ventricular activity.

Although Rb-82 gives images of myocardial perfusion under low and normal flow conditions with similar diagnostic value to N-13-ammonia and K-38, the unique potential of Rb-82 is for sequential evaluation of perfusion during pharmacological maneuvers and intervention therapy in acute myocardial infarction.

This is the first report of Rb-82 transverse section tomography in animals and humans.

N-13 AMMONIA FOR THE NON-INVASIVE MEASUREMENT OF MYOCARDIAL BLOOD FLOW. H. Schelbert, M. Phelps, G. Robinson, S. Huang, E. Hoffman, C. Selin. UCLA School of Medicine, Los Angeles, CA.

The possibility of measuring myocardial blood flow (MBF) by IV N-13 ammonia was studied in 15 open chest dogs. Myocardial extraction fraction (E) and half-times of N-13 ammonia were determined by monitoring myocardial activity following intracoronary (ic) N-13 ammonia at control, during papaverine (ic) induced hyperemia and IV infusion of isoproterenol (I) or propranolol (P). At the end of each experiment, N-13 ammonia was injected IV and radioactive microspheres into the left atrium during anterior descending coronary artery occlusion and circumflex hyperemia while arterial blood was withdrawn. The animals were sacrificed and myocardial tissue activities determined. E averaged 0.81 ± 0.06 SD at flows of 100 ml/min/100 gm and was not significantly altered by I or P. Control half-times averaged 220 min and were not affected by I or P (160 and 320 min; NS). Employing the arterial reference technique, N-13 ammonia underestimated MBF determined by microspheres,

but correlated in a non-linear manner. However, during I and P, MBF by N-13 ammonia varied. HPLC of the reference blood samples showed that only 66% of the total activity was free N-13 ammonia in 4 control dogs and only 56% during I and 83% during P. Using only free N-13 ammonia activity as arterial input function consistently over-estimated MBF but reduced the deviation of MBF measurements during I or P from the predicted MBF by 59.2%. The results indicate that E and half-times of N-13 ammonia are relatively stable and unaffected by I and P induced metabolic and hemodymic changes. Correction of the arterial input function for metabolized N-13 permits reproduceable MBF measurements and should allow non-invasive MBF measurement with iv N-13 ammonia and positron emission tomography.

N-13 AMMONIA AND POSITRON EMISSION COMPUTERIZED AXIAL TOMOGRAPHY FOR THE ASSESSMENT OF CORONARY ARTERY DISEASE IN MAN. H. Schelbert, L. Gould, G. Wisenberg, R. Marshall, M. Phelps, E. Hoffman. UCLA School of Medicine, Los Angeles, CA and VA Hospital, Seattle, WA.

The potential of positron emission computerized axial tomography (PCT) and IV N-13 ammonia for detecting 47% diameter coronary stenosis has been demonstrated in awake animals in our laboratory. To examine this diagnostic possibility in man, four normal subjects (mean age 26.5 yrs) and 9 pts (mean age 54.9 yrs) with arteriographically proven coronary artery stenosis (>50%) were studied. Following IV injection of N-13 ammonia at control up to 6 cross-sectional PCT images spaced 1.2 cm apart were obtained. After 1 hr, while coronary dilatation was induced by IV dipyridamole (10 mg/min) N-13 ammonia injection and PCT imaging was repeated. N-13 ammonia distribution in myocardium was uniform (12.5% mean SD) in normals. Hyperemia increased myocardial N-13 ammonia activity by 40.6% without significantly altering uniform distribution. By contrast, in 2 of the 9 CAD pts defects were present at control and hyperemia induced new or more extensive defects in 6 CAD pts. Regional myocardial N-13 ammonia activity at rest varied by 13.8%. In 8 of CAD pts. hyperemia caused inhomogeneity of N-13 ammonia distribution significantly different from normals. N-13 ammonia activity during hyperemia increased by 29.9% (range 17.6 to 39.0%; $p<.02$ vs. normals) in myocardium supplied by normal vessels and by 9.7% +13.6% in segments supplied by vessels with >50% diameter stenosis ($p<.02$). In 2 pts with 65% and 100% stenoses regional N-13 ammonia activity fell by 3.1 and 19.1% resp. We conclude that N-13 ammonia and PCT may be useful for detecting coronary stenosis and assessing its significance in man.

FEASIBILITY OF 19-F AS AN AGENT FOR NMR IMAGING OF MYOCARDIAL INFARCTION: AN IN VITRO STUDY. M.R. Goldman, E.T. Fossel, J. Ingwall, and G.M. Pohost. Massachusetts General Hospital, Boston, MA.

Nuclear magnetic resonance (NMR) proton imaging has been used to make thin section tomograms of intact animals and humans. Fluoride (F), because of its sensitivity to NMR is a possible imaging agent. To determine whether F could be used to distinguish between injured and normal myocardium, ^{19}F NMR was used to measure F levels in 1 gram biopsies from normal, infarcted (<10% nl blood flow), and hypoperfused (10% - 70% nl blood flow) regions of 6 dog hearts. Analysis was performed 48 hours after infarction, produced by ligation of the left anterior descending artery; blood flow was determined using ^{46}Sc microspheres. A broad (FWHM = 7KHz) ^{19}F resonance was observed in all samples. The area of this resonance/g tissue was decreased in regions of hypoperfused areas (50% of normal, $P<.01$) but not in infarcted regions (118% of normal, NS). Fluoride electrode analysis of myocardial extracts demonstrated a substantial concentration of ^{19}F in canine heart (1-2 mM). In myocardial samples of infarcted and minimally perfused (10% - 40% nl flow) regions from dog hearts receiving infusions of NaF prior to sacrifice, a narrow resonance (FWHM = 0.3KHz) was also present. This resonance was absent in control regions. These data suggest that the ^{19}F NMR of endogenous F distinguishes ischemic from infarcted and normal regions of canine myocardium and that resonances from administered F^- distinguishes injured from normal myocardium. This may provide the basis for ^{19}F NMR imaging of myocardial injury.

GALLIUM (Ga-67) MYOCARDIAL SCINTIGRAPHY IN CARDIOMYOPATHY. J. O'Connell, R. Henkin, J. Robinson, R. Gunnar. Loyola Univ. Med. Ctr., Maywood, IL.

The purpose of this investigation was to determine whether Ga-67 imaging could aid in selecting a subgroup of patients (pts) with idiopathic congestive cardiomyopathy (ICCM) in whom ongoing myocardial inflammation could be demonstrated.

Imaging was performed 72 hours after I.V. administration of Ga-67 citrate in the anterior, 45 degrees and 60 degrees LAO and left lateral projections.

22 pts with ICCM and 20 pts in a control group (C) undergoing Ga-67 scans for reasons other than chest pathology, had the above studies performed. Among the patients with ICCM, 9 had myocardial localization of gallium and 13 had no abnormal gallium concentration in the chest. None of the 20 pts in the C group had Ga-67 localization in the chest. In the pts with ICCM there were no differences in the clinical, electrocardiographic, radiologic, or angiographic findings between the Ga-67+ and Ga-67- pts. No other tests including ESR, antinuclear and antimyocardial antibodies or lymphocyte subpopulations could differentiate these two groups.

6 of the Ga-67+ pts were treated with immunosuppressive agents which have not been previously used in this entity. 5 of these pts had significant clinical improvement on immunosuppressive therapy. 1 of the Ga-67- patients treated with immunosuppressive therapy showed no clinical improvement.

This study demonstrates the feasibility of Ga-67 imaging in identifying pts with ICCM in whom persistent myocardial inflammation may be present and who may be responsive to immunosuppressive therapy.

NONINVASIVE RADIOISOTOPIC TECHNIQUE FOR DETECTION OF PLATELET DEPOSITION IN CORONARY ARTERY BYPASS GRAFTS IN DOGS AND ITS REDUCTION WITH PLATELET-INHIBITORS. M. K. Dewanjee, V. Fuster, M. P. Kaye, and M. Josa. Mayo Clinic and Mayo Foundation, Rochester, MN.

At 8 and 30 hours after saphenous vein bypass graft surgery in dogs, in vivo images (174 and 247 keV) were obtained with a gamma camera after I.V. injection, 2 hours postoperatively of autologous Indium-111-labeled platelets (0.25-0.50 mCi) and Iodine-125-labeled fibrinogen (0.08-0.1 mCi). Under identical conditions, in dogs treated with Dipyridamole (2.5 mg/kg/day) plus Aspirin (15 mg/kg/day), (D + ASA), the grafts and hemorrhagic cardiac muscle had significantly less platelet deposition as estimated by imaging. The radioactivity ratio of In-111 in isolated graft sections to non-target tissues of blood, lung, and cardiac muscle in control and treated animals, sacrificed at 32 hours after administration, demonstrated a threefold reduction in platelet deposition as shown below:

	Section	Graft/Blood	Graft/Lung	Graft/Myocardium
Control (n = 7)	Proximal	14.0 ± 8.8	28.4 ± 25.1	37.8 ± 30.1
	Distal	18.5 ± 13.6	31.5 ± 25.7	36.4 ± 28.7
Treated (D+ASA) (n = 12)	Proximal	4.3 ± 2.4	6.5 ± 5.4	29.8 ± 27.5
	Distal	4.5 ± 4.0	7.1 ± 6.2	30.7 ± 28.5

On the other hand, fibrinogen uptake in the graft was not reduced by platelet-inhibitors and graft to blood, lung, and myocardium ratios of 10.5 ± 3.4, 21.9 ± 9.3, and 85.6 ± 34.9 respectively were obtained in both control and treated animals. This technique may be a promising tool for a better understanding of the role played by platelets and fibrinogen in the process of occlusion of saphenous vein bypass grafts and arteriosclerosis and its reduction with platelet-inhibitors.

I-123-FIBRINOGEN SCINTIGRAPHIC DETECTION OF INTRACARDIAC THROMBI. S.J. DeNardo, A.R. Twardock, G.L. DeNardo and S. M. Steffen. Department of Nuclear Medicine, University of California, Davis, CA Supported by ACS PDT-94A

Intracardiac thrombi have been reported in 40% of patients with MI or ventricular aneurysm, but often were undiagnosed. The use of highly iodinated (35-50 I/F) I-123-fibrinogen (HIF) to detect intracardiac thrombus was investigated in 10 dogs. Following thoracotomy the left atrial appendage was clamped and filled with 5% Na morrhuate (9 dogs) or saline (1 dog). After 1 minute the solution was removed, clamp released and chest closed. 7 dogs were injected IV with 2.0 mCi HIF and 0.1 mCi normally iodinated (2 I/F) I-125-fibrinogen (NIF) and 3 dogs with 2.0 mCi moderately iodinated (20 I/F) I-123-fibrinogen (MIF) and NIF 30-60 min post morrhuate. The thorax was imaged and blood samples obtained serially for 2-3 hrs in 5 dogs and 14-18 hrs in another 5 dogs after fibrinogen injection; then the dogs were sacrificed to obtain samples of thrombus, atria, left ventricle and post mortem clot. Thrombi were easily visualized with I-123 in 8 of the 9 morrhuate dogs in whom the clots weighed 0.29-1.09g and contained with adjacent atrial wall 0.4-0.85% of the injected dose. 1 thrombus which weighed 0.13g and contained 0.21% of the dose was not visualized. Clot concentrations of HIF and NIF were similar at both time intervals. However, HIF cleared more rapidly from the blood so that thrombus-blood ratios at 3 and 18 hrs respectively for HIF were 5.3 and 22.0, compared to 4.6 and 15.9 for NIF, and 5.3 and 6.5 for MIF. The $T_{\frac{1}{2}}$ of the second ("catabolic") phase of the blood clearances in the 18-hour dogs were 9.8±1.3 hrs for HIF, 15.5±4.6 hrs for NIF, and 21.7±8.8 for MIF. These results suggest HIF scintigraphy to be promising for the detection of intracardiac thrombi.

INDIUM-111 DIETHYLENETRIAMINE PENTAACETIC ACID-ANTIMYOSIN FAB FRAGMENTS LOCALIZATION AND IMAGING IN EXPERIMENTAL MYOCARDIAL INFARCTION. B.A.Khaw, J.T. Fallon, W. Strauss, H.K. Gold, H.A. Katus, B. Essington, and E. Haber, Massachusetts General Hospital, Boston, Massachusetts

Cardiac specific anti-myosin antibody (Ab) labeled with radioiodine will localize in experimental myocardial infarction and permits visualization of the infarct with a gamma camera. We now report the use of a bifunctional chelating agent, diethylenetriamine pentaacetic acid (DTPA) to label Ab-Fab fragments with Indium-111 (In-111-Ab) to image experimental MI following intracoronary (IC) or intravenous administration of In-111-Ab. Ab was purified by myosin sepharose affinity chromatography and Fab fragments were obtained by papain digestion of whole Ab. Experimental MI was produced in 10 dogs by ligation of the left anterior descending coronary artery for 4 hr after which the occlusive ligature was removed. 3 of the dogs (Group A) received IC injection of 1mCi of In-111-Ab into the left main coronary artery under fluoroscopy. 3 dogs (Group B) received 2mCi In-111-Ab intravenously. All injections were given 15 minutes after reperfusion. Group A dogs were imaged within 1 hr of Ab injection. Reimaging was performed at 24 and 48 hr. Group B dogs were imaged 24 hr after Ab administration. All experimental MI confirmed by Triphenyltetrazolium chloride (TTC) histochemical staining showed discreet localization of In-111-Ab in gamma images. Ratios of radioactivity in MI to normal posterior left ventricular myocardium were greater than 10:1. Four sham operated dogs in Group C with IC injection did not show localization of In-111-Ab. Utilization of a bifunctional chelating agent to label a biologically active macromolecule with In-111 without loss of the biological activity should proved a useful imaging marker of acutely infarcted myocardium.

1:30 p.m.-3:30 p.m. Room 201

RADIOPHARMACEUTICAL CHEMISTRY SYMPOSIUM: I

PHARMACOKINETIC MODELING BERSON-YALOW PAPER

Chairman: William C. Eckelman
Co-Chairman: James Bassingthwaighte

KINETICS OF BLOOD-TO-CELL UPTAKE OF TRACERS DURING TRANSORGAN PASSAGE. J.B. Bassingthwaighte M.D., Ph.D., Center for Bioengineering, Seattle, WA.

In an organ with heterogeneity of regional perfusion, one can use multicapillary models to interpret experimental data on the time course of tissue uptake or transport into the venous outflow following an injection into the outflow. Experimentally, by using appropriate sets of tracer molecules of somewhat differing characteristics, one can obtain usefully accurate estimates of values for parameters of particular interest, for example, cellular uptake rates for glucose or thallium in the heart. Such types of analyses are also useful for defining the ability to make estimates of regional flows from the profiles of deposition of a tracer or for correcting or refining such estimates.

A NEW METHOD FOR MEASURING THE WHOLE-BODY INSULIN RECEPTOR COMPARTMENT IN VIVO IN MAN: COMPARISON WITH IN VITRO METHODS. H. Wachslicht-Rodbard, and J. Roth. National Institutes of Health, Bethesda, Md.

We have developed a new method for measurement of the fraction of insulin bound to receptors on target tissues in vivo in man. We inject I-125-labeled insulin and I-131-labeled proinsulin tracers, and study the kinetics of distribution and degradation of both compounds with measurement of total plasma radioactivity, and that precipitable with anti-insulin antibodies or trichloroacetic acid. Proinsulin has low affinity for the insulin receptor, and is passively distributed in the circulation. In contrast, approximately 50% of the insulin tracer is sequestered from the freely exchangeable plasma pool and is protected from degradation, apparently by binding to insulin receptors. In 3 normal subjects and two with massive obesity (>200% ideal body weight), the apparent initial distribution volume was 3.22±0,35(SEM) times larger than that for proinsulin, corresponding to a fractional binding of insulin of 44-72%, with a mean of 66.8±5.0%. Results of this procedure were compared with in vitro radioligand assays employing monocytes, and with a newly developed procedure for measurement of insulin receptors on erythrocytes. This in vivo method provides a good means to validate the in vitro procedures in man under physiological conditions, and should be widely applicable to other hormones which have specific receptor compartments.

PHYSIOLOGIC TOMOGRAPHY MEASURE OF CEREBRAL AND MYOCARDIAL METABOLIC RATE FOR GLUCOSE (MRGlc): MODELS AND MEASUREMENT OPTIMIZATION. M.E. Phelps, S.C. Huang, H.S. Schelbert, E.J. Hoffman, D.E. Kuhl. UCLA School of Medicine, Los Angeles, CA.

Pharmacokinetic and physiologic studies require compartmental tracer kinetic models as a framework for development, evaluation and application of physiologically active labeled compounds. These models provide i) description of process, ii) method for evaluating physiologic integrity of compound and iii) operational eqs. for calculation of rate constants (k's), metabolism, binding affinity, etc.

We derived a 3 compartment model for FDG in brain and heart as an extension of Sokoloff's model. K's of model are measured for brain in man and heart in dogs. Measured range of k's are used to determine error limits in measure of MRGlc with average k's and to optimize study protocol. Initially after injection, model is sensitive to errors in k's and dependent on blood flow (BF). After 40 min, near steady state conditions are reached, sensitivity to exact k's and BF are reduced. Precision of repeated tomographic MRGlc studies in 13 subjects (brain) and 6 dogs (heart) is ±5%. Dog studies were performed to determine BF sensitivity of model. Papaverine, in left cercumflex artery (LCX), was used to produce high BF (450cc/min/100gm) and normal MRGlc. MRGlc with FDG was normal and equaled LAD region. A 15 min occlusion and release of LCX produced hyperemic

BF of 500cc/min/100gms and blockage of glucose metabolism (tissue acidosis). FDG MRClc in LCX was 10% of LAD region even though BF was 6 times higher. This model reflects metabolism and not BF. Emission tomography (ECT) provides in vivo measurements not previously possible. Combining labeled physiologic compds that behave in predictable manner with physiologic models allow ECT to be developed into PT

EMISSION TOMOGRAPHIC IMAGES OF THE CANINE HEAD AND HEART WITH ^{18}F-3-DEOXY-3-FLUORO-D-GLUCOSE. M.M. Goodman, D.R. Elmaleh, H.W. Strauss, R.H. Ackerman, and G.L. Brownell, Massachusetts General Hospital, Boston, MA 02114

^{18}F-3-Deoxy-3-Fluoro-D-Glucose (3-^{18}FDG) was prepared by the nucleophilic substitution of 1,2:5,6-di-O-isopropylidene-O-trifluoromethane sulfonyl-2-O-allofuranose with Cs ^{18}F in HMPA followed by treatment with boron trichloride and hydrolysis (according to Tewson, et al). The fluorine-18 was produced by ^{20}Ne(d,α) ^{18}F reaction on the MGH compact medical cyclotron. The ^{18}F cesium fluoride (Cs^{18}F) was prepared by recirculating the bombarded Neon through silver wool impregnated with anhydrous cesium hydroxide.

2.5mCi of 3-^{18}FDG was administered intravenously to anesthetized dogs after positioning the animals in the MGH positron camera. A set of emission images were collected at 15 equally spaced angles in a half a circle about the animal. A total of 90 2-dimensional images were collected in 20 min. These data were sufficient to reconstruct 24 transverse section images corrected for random coincidences photon absorption and radioactive decay. The sections are spaced 1.4 cm apart and exhibit a spacial resolution of approximately 1 cm. The activity distribution in the head is displayed in a few sections; the images clearly show the activity distribution within the brain.

In a similar fashion a set of emission images were collected about the animals chest. The images clearly show the heart. This data compares favorably with images previously taken by us using ^{18}F-2-Deoxy-2-fluoro-D-Glucose (supplied by Brookhaven National Laboratory).

COMPARTMENTAL ANALYSIS OF THE STEADY-STATE DISTRIBUTION OF OXYGEN-15 LABELED OXYGEN AND WATER. R.E. Bigler, J.A. Kostick, J.S. Laughlin, Memorial Sloan-Kettering Cancer Center, New York, NY, J.R. Gillespie. City University of New York, Lehman College, New York, NY

The possibility of making quantitative regional measurements of oxygen metabolism by analysis of the steady-state distribution of O-15 ($T_{\frac{1}{2}}$=123 s) administered by inhalation as molecular oxygen has received considerable interest. If water of metabolism produced by oxygen utilization were retained at the site of production for a time long in comparison to the half-life of O-15, converting O-15 activity concentrations to oxygen utilization rates would require simple multiplication by the O-15 decay constant. Since this condition is not met throughout the body, corrections for water of metabolism redistribution are needed. The purpose of this work is to develop a compartmental model suitable for this purpose. Deuterium oxide data of Edelman (Am J Physiol 171,1952) were used to establish a three compartmental model which lumps the rapid and slowly exchanging tissues into separate compartments. Berman's SAAM27 computer program was used. This model allowed us to evaluate the magnitude of biological metabolic water loss and uptake at the steady-state. The slow and rapid compartments lose, respectively, about 10 and 30% and gain from recirculation by 16 and 4 %. We expanded our model to include cerebral grey and white matter using data from Ter-Pogossian (J Clin Invest 49, 1970). Metabolic water loss by biological clearance for grey and white matter amount to 75 and 45%, respectively. Our analysis supports the assumption that water exchange corrections are needed for all body regions. The magnitude of the corrections for the rapidly exchanging tissues may make such corrections impractical.

ERROR PROPAGATION IN THE DETERMINATION OF CEREBRAL BLOOD FLOW WITH THE INHALATION OF $C^{15}O_2$. S.C. Jones, M. Reivich, J.H. Greenberg. University of Pennsylvania, Philadelphia PA

The inhalation of $C^{15}O_2$ can be used for determining local cerebral blood flow[2] (LCBF) using the quantitative model of Subramanyam et al. The determination of LCBF in three dimensions using positron emission tomography, (PET), involves errors due to counting statistics and data manipulation. This work examines the error propagation and its relation to the radiation dose to the subject's lungs.

An expression has been derived for the root mean square uncertainty in LCBF as a function of LCBF, the spatial resolution and the sensitivity of PET instrument, and absorbed radiation dose to the subject's lungs. The error in LCBF increases as CBF increases. At a normal cortical LCBF of 80ml/100g-min and a PET instrument with a 1.5cm FWHM resolution, and a 37,000 cps per μCi/g sensitivity per slice, an error of 4.4% results from an inhaled activity of 200mCi, resulting in a lung dose of 5 rads, the maximum permissible dose allowed. For a more reasonable dose of 1.2 rads the error increases to 9%. At a higher resolution (0.7cm FWHM) and lower sensitivity (5220 cps per μCi/g per slice), errors become of the order of 100% for a lung dose of 1.2 rads.

This consideration of error and its relation to radiation dose is necessary if this inhalation technique is to be used effectivity for the quantification of LCBF.

Subramanyam, R., Alpert, N.M., Hoop, B., Jr., Brownell, G.L Taveras, J.M. J. Nucl. Med. 19:48-53 (1978)

A MODEL FOR THE GASTROINTESTINAL TRANSPORT OF TECHNETIUM IN THE MOUSE. K.A. Lathrop, B.M.W. Tsui, and P.V. Harper. The University of Chicago, Chicago, IL.

Using the SAAM-27 program and data collected after intraluminal (I.L.) and intravenous (I.V.) administration of NaTc(99m)O$_4$, transfer-rate constants (k) have been calculated for the transport of Tc-99m to and from the wall and content of each of 12 isolated intestinal segments. The biologic model assumed for the analysis was a linear four compartment closed system consisting of blood, intestinal wall, intestinal content, and all other tissues grouped together. The data were collected using CFI mice at 5, 10, and 20 min after administration, the interval during which most of the redistribution of Tc occurs. In such a compartmental model introduction of pertechnetate into any compartment does not change the values of the k's if the chemical form of the pertechnetate remains unchanged. Our finding of significantly different k values (as much as 10^3 or 10^4) between the I.L. and I.V. routes, indicates that such a change is taking place. For instance in the colon I.L. pertechnetate is transferred from the intestinal content to the intestinal wall much faster (10^2 X) than after I.V. administration suggesting that Tc secreted into the colon is in a form other than pertechnetate and is thus absorbed much slower. This approach appears to have provided new insights into the metabolism of pertechnetate. Further efforts appear to be needed both in the collection of more detailed distribution data and in the definition of the chemical form of the technetium in the tissues in order to perfect and extend the model, and to confirm the preliminary conclusions.

KINETICS OF PHAGOCYTOSIS AND PROTEOLYTIC METABOLISM IN LIVER MACROPHAGES IN NORMAL PERSONS AND TUMOR PATIENTS. S.N. Reske, K. Vyska, and L.E. Feinendegen. Institute for Medicine, Nuclear Research Center Jülich, F.R. Germany

The in vivo evaluation of macrophage functions is expected to yield useful clinical information concerning the immune status of patients. A new method for the in vivo measurement of phagocytosis and proteolysis of an Tc-99m labelled albumin microparticle (TMP, diameter 0.5-2.0 μm) in Kupffer cells [KC] was developed. After injection of 2.0 mCi TMP the liver was sequentially scanned over 90 minutes at a frame rate of 15/s. The time activity curve over a ROI liver was computer-fitted with three exponential functions. 7 normal persons (nls) and 8 patients (pts) with different carcinomas were examined. Based on the principal characteristics of the interaction of particular material with macrophages (i.e. attachment-phagocy-

tosis-digestion) a three compartment model was proposed for the pharmacokinetics of TMP. The turnover curves in all compartments (particle distribution pool [A]-KC membrane receptor sites [B]-intracellular KC pool [C]) were calculated. The turnover curves in pool C in 7 nls were practically identical to curves of phagocytosis determined in macrophage monolayers described by Karnovsky, whereas these curves in 8 pts demonstrated a significantly retarded accumulation phase. The rate constants were found to be in 7 nls: k_{ba} = 0.38 ± 0.083, k_{cb} = 0.11 ± 0.023, k_{ob} = 0.024 ± 0.011, k_{oc} = 0.0028 ± 0.0011 and in 8 pts: k_{ba} = 0.53 ± 0.12, k_{cb} = 0.055 ± 0.046, k_{ob} = 0.012 ± 0.0081, k_{oc} = 0.0014 ± 0.00092. These results indicate a significant retardation of phagocytosis and a normal to delayed proteolysis of the radiopharmaceutical in liver macrophages in tumor patients.

1:30 p.m.-3:30 p.m. Room 204

INSTRUMENTATION, COMPUTERS, AND DATA ANALYSIS

POSTER SESSION: A; DOSIMETRY, *Chairman:* Vincent J. Sodd, *Co-Chairman:* Lewis R. Carroll; **B; INSTRUMENTATION AND IMAGE PROCESSING,** *Chairman:* Edward J. Hoffman, *Co-Chairman:* Alan B. Ashare; **C; INSTRUMENTATION HARDWARE,** *Chairman:* Gerd Muehllehner, *Co-Chairman:* John A. Correia

CONTRIBUTION OF CONTAMINANTS TO THE RADIATION DOSE FROM THALLIUM-201. E. E. Watson and J. L. Coffey. Oak Ridge Associated Universities, Oak Ridge, TN.

During the past few years thallium-201 has become widely used for myocardial imaging. The Tl-201 preparation contains varying quantities of two other thallium isotopes, Tl-200 (half-life=26.1 hr.) and Tl-202 (half-life=12.2 days), as contaminants. Although at the designated calibration time these contaminants constitute less than 3% of the total activity, the proportion of Tl-202 activity in relation to that of Tl-201 (half-life=3.04 days) increases if the administration of the radiopharmaceutical occurs several days after the calibration time because of the longer half-life of Tl-202. Using still unpublished decay scheme data for Tl-200 and Tl-202, we have calculated S factors and estimated the radiation dose from Tl-201 plus contaminants administered 24 hrs. before calibration, at calibration, and 168 hrs. after calibration (expiration date). The contaminants may increase the radiation dose to some organs by one-third if the administration is delayed until the expiration date.

ESTIMATES OF SPECIFIC ABSORBED FRACTIONS FOR PHOTON SOURCES IN THE HEART WALL AND HEART CONTENTS OF A HETEROGENEOUS PHANTOM. J.L. Coffey, M. Cristy, and G.G. Warner. Oak Ridge Associated Universities and Oak Ridge National Laboratory, Oak Ridge, TN.

The generalized heart model of the Medical Internal Radiation Dose (MIRD) Committee's heterogeneous phantom has no separation of heart wall from heart contents. Dose estimates based on this model are therefore only a first approximation because it is unlikely that a radionuclide would be uniformly distributed throughout the heart wall and contents. The MIRD Committee did not include the heart as either a source or target organ in MIRD Pamphlet No. 5, Revised. We have developed a more detailed model of the heart that has a separation of wall from contents for each of the four chambers. Since the lungs of the phantom were to be modified to make room for the revised heart, they were also modified to make them more anatomically correct by making the right lung 16% larger than the left. The new heart and the modified lungs were incorporated into the phantom and the Monte Carlo technique was employed to calculate specific absorbed fractions to 21 target organs. As a start, the entire heart wall and the entire heart contents were taken as the source organs. These specific absorbed fractions allow the calculation of dose to the heart wall which has not previously been possible with the MIRD technique. Specific absorbed fractions for the modified lungs as a source organ were not calculated because these should not be significantly different from those of MIRD Pamphlet No. 5, Revised.

The results of this study will be published as a MIRD Pamphlet.

A COMPUTER DATA BASE OF BIBLIOGRAPHIC ENTRIES ON RADIOPHARMACEUTICALS. E. E. Watson, J. L. Coffey, A. T. Schlafke, and R. J. Cloutier. Oak Ridge Associated Universities, Oak Ridge, TN.

The major problem today in calculating radiation dose from radiopharmaceuticals is the lack of information on the numerous factors that influence the dose, such as organ uptake, residence times, clearance rates, chemical and physical properties of the radionuclide, and effects of disease and age. The Radiopharmaceutical Internal Dosimetry Information Center at Oak Ridge Associated Universities has established a computer data bank of bibliographic references relating to radiopharmaceuticals. The data bank now contains more than 12,000 entries on papers dealing with the use of radiopharmaceuticals as well as those dealing with other pertinent topics such as decay scheme data, calculation techniques, physiologic behavior, and distribution patterns in human subjects. Twelve different journals are reviewed routinely along with current reports and proceedings of symposia. Although the data base is designed to provide references to material needed for dose estimation, many references provide data useful to researchers developing new radiopharmaceuticals, comparing radiopharmaceuticals used for similar procedures, or analyzing results from nuclear medicine procedures. The Center will make information from the data base available to researchers upon request.

HUMAN DOSIMETRY OF TC-99M PIPIDA. L.E. Williams, R.A. Ponto, L.A. Forstrom, M.K. Loken, and D.R. Hoogland. University of Minnesota Hospitals, Minneapolis, MN.

The human dosimetry of Tc-99m-PIPIDA (Diagnostic Isotopes) was calculated using data obtained from six normal adult male volunteers. Gut (88%) and renal (12%) clearance fractions were obtained using excreta sampling over a 36h interval. Time-activity curves for blood, liver and gall bladder and the two excretory routes were used to determine biological half times for absorbed fraction dosimetry calculations. Source organs included blood, kidney, bladder, liver and gall bladder and the various segments of the intestine. The following Table indicates the target organ dose per millicurie of injected agent.

PIPIDA Dosimetry Table

Target Organ	Dose/mCi PIPIDA
Liver and Gall Bladder	200 mrem
Upper Large Intestine	420
Lower Large Intestine	220
Small Intestine	110
Kidney	80
Marrow, Spleen, Testes	12
Whole Body	20
Ovary	45

All intestinal organs were assumed to include contents. The small splenic dose reflects the lack of demonstrable uptake by that organ. Published MIRD computations for I-131-Rose Bengal yield liver and small intestine doses of 800 and 3500 mrem/mCi respectively. Thus Tc-99m-PIPIDA offer a significant reduction in dose/mCi of injected material.

PRECISION COMPUTER DISPLAY TECHNIQUES IN NUCLEAR MEDICINE IMAGING. B.S. Baxter, P.E. Christian, and R.E. Coleman. University of Utah Medical Center, Salt Lake City, UT.

This investigation was undertaken to evaluate the poten-

tial for improved interpretation of scintillation camera images using precision computer display techniques.

Providing the clinician with a viewable image that is an accurate representation of computer scintillation camera data requires 1) correction for grayscale nonlinearities of the display and film, 2) interpolation to fill in the intensity field between grid points, and 3) sufficiently fine graylevel resolution to avoid generating artificial contours. Transparencies made on a specially constructed computer display/film system were compared with corresponding analog scintigrams to determine whether the linearity and stability of digital recording might be exploited effectively.

Results of these experiments were encouraging, indicating: a) a wider range of count rate data was visible in the digital images, giving better identification of low count rate areas, b) display artifacts, due to regularly spaced patterns of data samples, were completely eliminated as were contour artifacts caused by too few graylevels, and c) anatomical and pathological entities of interest were frequently demonstrated with improved clarity.

Conclusions to be drawn from these results are, first, the poor regard accorded to computer recording and display of nuclear medicine images is due to poor display performance, and, second, by overcoming these display limitations, transparencies can be produced which are as effective as analog scintigrams in providing a basis for accurate image interpretation. In many cases the digital images are superior.

A Spatial Distortion Correction Method for Gamma Cameras
E. W. Stoub, J. G. Colsher, P. C. Lee, and G. Muehllehner
Searle Diagnostics, Des Plaines, IL

A method to correct for the spatial distortions of gamma cameras has been developed. The method consists of two parts: measuring spatial distortions and repositioning events during accumulation. Distortions are measured using a pattern consisting of parallel slits on 15mm centers with slit pattern images obtained in two orthogonal orientations. Slit locations are used to determine x and y displacements, which are then interpolated to obtain a 64 x 64 array of distortion coefficients. The coefficients are refined by using the gradient of the field flood intensity as an indicator of the direction and strength of the residual distortion at each point. In repositioning camera events, x and y event coordinates are digitized and correction displacements added. Interpolation is used to obtain these correction displacements from the array of x and y distortion coefficients. The procedure is implemented in hardware which repositions each event in real time without introducing additional dead time.

Distortion correction offers considerable advantage over other uniformity improvement schemes since it correctly compensates for the major cause of nonuniformity, spatial distortion. The method may be used for quantitative studies, because it does not change the number of detected events. In addition, cameras can be designed for improved intrinsic resolution with less attention given to spatial distortions since these can now be corrected.

SIMPLE OPTICAL BACK-PROJECTION OF KIRCH COLLIMATOR (7-PINHOLE) IMAGES FOR TOMOGRAPHIC RECONSTRUCTION.
B. Brunsden, P. Kirchner, D. Charleston, and P.V. Harper
The University of Chicago, Chicago, IL.

Computer reconstruction of Kirch collimator images permits tomographic imaging of the myocardium on a semi-quantitative basis. We have developed a simple, rapid technique for optical back-projection of the 7-pinhole images that yields similar quality tomographic images in any number of planes.

Optical back-projection requires only a camera with bellows and a lens replaced by an opaque plate containing 6 pinholes (7th center hole is optional) in a scaled optical version of the Kirch collimator. Transparency film (e.g., from microdot) bearing the 7 images seen by the collimator is viewed by the camera so that the 6 pinholes of the camera are in coincidence with the 6 peripheral images on the film. With the pinhole plate fixed, a change in the film-to-plate distance changes the image plane in the 3-dimensional reconstruction. Tilting the film relative to the plate permits oblique tomographic cuts (currently not possible with the computer).

Phantom studies in air and in scatter and background media showed optical reconstruction to be better in the Z axis and comparable to computer images in X&Y. Patient studies with N-13-ammonia produced good myocardial images.

Optical back-projection of 7-pinhole-collimator images permits tomographic reconstruction without online computers. Its low cost, simplicity, speed and variable planing make it attractive for preliminary technical or clinical evaluation before computer reconstructions are available for detailed analysis.

THE EFFECT OF COMPTON SCATTERING ON EMISSION TRANSAXIAL TOMOGRAPHY.
S.C. Pang and S. Genna. VA Medical Center and Boston University School of Medicine, Boston, MA.

Scattered photons generated by point sources in a cylindrical medium are computer simulated using Klein Nishina cross sections. These scattered photons are selectively projected in parallel paths to a collimated line detector which accepts only photons within a prescribed energy window. Transaxial reconstruction from these projections by standard means are generated to examine point spread functions generated by the scattered photons. The method is first formulated for the single scattering process and is then extended to include double scattering by modifying the Compton differential cross sections. Studies with point sources located on and off the detector plane provides an understanding of the artifacts in reconstruction due to scattering. For example, in the vicinity of a source point, the reconstructed scattered photons behave similar to the reconstructed primary point source, and cause negligible degradation through its incorporation into the reconstructions. The problems arise from spread function tails and off-plane scatter which are broadly and nonisotropically distributed. One application of this work is to derive methods of correcting for scatter in single photon ECT. For example, the method can be used to delineate a scatter energy window such that filtered subtraction of the images obtained thereby from photopeak window images optimally reduce scatter and its reconstruction artifacts.

ANALYSIS OF THE SCATTER RESPONSE FUNCTION OF COLLIMATED IMAGING SYSTEMS.
F.B. Atkins and R.N. Beck.
Walter Reed Army Medical Center, Washington, D.C. and
The Franklin McLean Memorial Research Institute, The University of Chicago, Chicago, Il.

The scattered component of the response of an imaging system can be a significant factor affecting the overall determination of image quality, as well as the quantitative aspects of the recorded data, especially when using low energy sources. We have evaluated this component with the intent of eliminating unnecessary factors, such as the collimator, and of formulating a model of the scattered component which can be applied over the range of photon energies useful for imaging (i.e., 80-511 keV). To permit detailed investigations of the many parameters that are involved, e.g., source energy, depth, baseline setting, and collimator, we chose to use Monte Carlo techniques for the analysis. Some of the results of the various simulations corroborate the observations that:

1. The scatter fraction, or the ratio of scattered to unscattered photons is essentially independent of the collimator for all baseline settings, source energies, and source depths (>1cm.).
2. A series equivalent formulation of the scattered component of the transfer function is likewise independent of the collimator design for these same parameters.

From these observations we have generalized the scatter response function in terms of an equivalent scattering angle, which is then applicable for all source energies. These simulations were performed for both scanner and camera collimators with comparable results.

SAMPLING REQUIREMENTS OF EMISSION COMPUTED TOMOGRAPHIC (ECT) SCANNERS. S.C. Huang, E.J. Hoffman, M.E. Phelps, D.E. Kuhl. UCLA School of Medicine, Los Angeles, CA.

Sampling distance is an important consideration in ECT scanner design. Insufficient sampling can create aliasing artifacts on images. By computer simulation of equally spaced parallel lines, reconstruction of various frequency components in images can be examined separately. Various line spacings (ΔL=1.0 to 1.6cm), FWHM's (W=0.4 to 1.2cm), and sampling distances (ΔT=0.3 to 1.0cm) have been used in simulations to study the inter-relationships that would give reconstructions free of aliasing artifacts. Point sources have also been simulated to examine aliasing effects on isolated point sources. Line spread functions have been assumed to have a Gaussian shape and standard filtered back-projection with ramp filter functions have been used for image reconstruction.

It was found that, for $\Delta T > \Delta L/2$, parallel lines are not reconstructed correctly. Some parallel lines are seen on images, but line locations are incorrect and total number of lines seen is smaller than true number. For $W/3 < \Delta T < \Delta L/2$, total number of lines is correct, but line spacing and line widths are not uniform on image. Only for $\Delta T < W/3$ can lines be reconstructed uniformly and consistently. Contrast of reconstructed lines decreases as W increases. For $W > 0.92\Delta L$, reconstructed contrast is smaller than 5% of original. For point sources, insufficient sampling is reflected in variability of reconstructed activity depending on location. For $\Delta T > 2W/3$ variability is larger than 10% of correct value. It is concluded from this study that 1) FWHM should be smaller than 0.92 times desirable image resolution to obtain reasonable recovery and sampling distance should be smaller than 1/3 of FWHM to prevent aliasing and 2) equally spaced line patterns could be used as a sensitive and convenient phantom for checking sampling adequacy of ECT scanners.

EMISSION AND TRANSMISSION NOISE PROPAGATION IN POSITRON EMISSION COMPUTED TOMOGRAPHY. G.T. Gullberg and R.H. Huesman. Donner Laboratory, Univ. of Calif., Berkeley. CA.

Errors in positron emission computed tomograms are the result of noise propagated from three sources: 1) the statistical fluctuation in the positron coincidence events; 2) the statistical fluctuation in the incident transmission beam; and 3) the statistical fluctuation in the transmitted beam. The data for the transmission study in 2) and 3) are used to compensate for internal absorption of the distributed positron source. For the reconstruction of a circular phantom using the convolution algorithm, the percent root-mean-square uncertainty (RMS) is related to the total measured positron events C and the incident photon flux per ray I_0. Our derivation of the RMS uncertainty based on the propagation of errors yields a simple expression: RMS = $\sqrt{K_1/C + K_2/I_0}$ where K_1 and K_2 are constants dependent on the size of the object and the type of convolver.

The constants $K_1 = 4.45 \times 10^8$ and $K_2 = 3.97 \times 10^5$ were determined for a 20 cm diameter disc based on computer simulation with various emission and transmission statistics. The projection data were analytically calculated with an attenuation coefficient $\mu = 0.0958$ cm^{-1} for 140 angles between 0 and π. Poisson noise was added to the positron coincidence events, the incident transmission events I_0, and the transmitted events. These results indicate that for incident transmission data of 1000 events per ray (which for 140 angles is equivalent to 8.4×10^6 total incident photons and 2.1×10^6 transmitted photons), the contrast resolution for a fixed spatial resolution is limited to 20% even with an infinite number of emission events. For a total of 10^6 emission events the contrast resolution is 29%.

ADRENAL SCINTIGRAPHY: COMPARISON OF THE ANGER TOMOGRAPHIC SCANNER AND LARGE FIELD GAMMA CAMERA. M. L. Brown, I. D. Hay, H. W. Wahner, and T. C. Hammell. Mayo Clinic and Mayo Foundation, Rochester, MN.

Adrenal scintigraphy using 6-iodomethyl-19-norcholesterol (NP-59) has proved to be clinically useful in the investigation of adrenocortical function. In order to evaluate observer performance with two different imaging instruments and to assess the requirement for computer processing in routine adrenal imaging, 120 gamma camera images (55 with and 65 without computer processing) and 47 Anger tomoscanner studies have been interpreted independently by three observers.

Of the 30 patients studied, four had normal adrenal function and 26 had adrenocortical disease, either bilateral (14) or unilateral (12). Thirty-eight pairs of images were used in the study comparing the tomoscanner with the large field gamma camera; 44 pairs of images were used to compare the gamma camera with and without computer processing. Receiver operating characteristic curve analysis demonstrated that the tomographic images were superior for adrenal detection. When each patient was individually considered, the tomoscanner was preferred in 37%, and in 50% of the cases both instruments were considered equally valuable. The computer-processed images with background subtraction and smoothing did not aid in adrenal detection.

In this study, the tomoscanner increased the diagnostic accuracy of imaging and resulted in an improved rate of adrenal detection. The Anger tomoscanner is therefore a superior imaging device for adrenal scanning and for this purpose represents an advance over conventional and large field gamma cameras. Although essential for the quantitation of adrenal uptakes, computer processing does not improve the diagnostic yield from adrenal scintigraphy when a gamma camera is employed.

AUTOMATED ROC CURVES FOR TEACHING, TESTING, AND TRAINING. A.B. Ashare. Wright State University, Dayton, OH.

A computer algorithm (Autoroc) has been developed to automatically produce receiver operational characteristic (ROC) curves. This program is used to teach ROC analysis as well as for the teaching, testing, and training of scintigraphic interpretation. The program uses two computer display screens, one for alphanumeric information and the other for display of images. Images are stored in a 128 by 128 matrix, called to the display screen on a random basis, and displayed in a 512 x 512 matrix. Up to sixty images can be evaluated for the production of an ROC curve. After the user types in his/her name or other identification, the images appear on the display screen with instructions to respond to each image on a five level rating scale with 1 indicating a normal image and 5 an abnormal image. When a response is given, either the next image is displayed or the correct answer (normal or abnormal) may be shown just before the next image. If a response is not given within thirty seconds, then an answer of unsure (category 3) is provided for the image and the next image is displayed. After all the images are interpreted, the resultant decision matrix appears on the display screen and is output by the line printer. The ROC points are plotted and a curve is generated. A computer analysis of the individual's curve is produced by the line printer. All data is stored for later retrieval; this includes the decision matrix for each user and the interpretations for each image from all readers. Autoroc offers the user the opportunity to visualize changes in his/her ROC curves when reading criteria are changed.

CALCULATING THE AMOUNT OF INFORMATION TRANSMITTED BY MEDICAL IMAGES. A.B. Ashare. Wright State University, Dayton, OH.

Classical information theory can be used to calculate the amount of information transmitted by medical images. The communication channel for this information is the imaging device and the resultant image, the sender is the patient, and the receiver is the physician who will interpret the image. An information transmission measure (ITM) can be calculated for a physician who has interpreted a group of images. In order to obtain the ITM, a decision matrix must be formed with the known diagnoses on the abscissa and the physician's interpretations on the ordinate. Binary decision matrices (BDM) have four entries in a 2 x 2 matrix which represent the true positive (TP) readings, the false positive (FP) readings, the false negative (FN) readings, and the true negative (TN) readings. The BDM provides the physician with the opportunity of categorizing images into normal and abnormal interpretations. However, it is often possible for the physician to provide

a more definitive interpretation for the abnormal images; a specific diagnosis or disease pattern can frequently be suggested. The BDM can be expanded with specific diagnoses or disease patterns on the abscissa and ordinate. The ITM can be calculated for this expanded decision matrix (EDM); also, measures of accuracy, sensitivity, and predictive value can be calculated as in the BDM. Advantages of one imaging technique over another can be hidden in the BDM, and can be well illustrated by using the EDM. ITM and EDM provide a method for comparing the efficacy of different imaging techniques to convey specific diagnoses or disease patterns.

A FLOW BASED DYNAMIC PHANTOM FOR QUALITY CONTROL OF NUCLEAR CARDIOLOGY STUDIES. J.R. Halama, D.J. Simpkin, and R.[illegible]. University of Wisconsin, Radiology Department, Madison, WI.

Computerized nuclear cardiological studies are only as good as the operator responsible for analysis of the image data. A flow based dynamic phantom has been developed that simulates cardiac kinetics in both normal and pathological states. The physiologic compartments of right ventricle, lung, and peripheral circulation are mimicked by hydraulic mixing and contracting components. Various nuclear cardiology procedures can be assessed, such as first-pass and equilibrium measurements of ejection fraction and cardiac output. Ventricular volumes, shunts, and valvular insufficiencies may be selected to simulate pathologic conditions. The various phantom compartments are spatially separated for ease of imaging, allowing the operator to outline regions of interest uncontaminated by activity from neighboring chambers. This idealized data is then used to exercise the cardiac routines. Any substantial deviation between the derived parameter and its preset value can signal either a breakdown in the assumptions underlying the commercial algorithms or operator inexperience. Experience is rapidly gained as the ventricular region is enlarged to incorporate a successively more realistic background. Thus the phantom serves not only as a quality control device for cardiology computer algorithms, but also as a teaching aid for physicians, technologists, and computer programmers.

PROPERTIES OF A ROTATING PARALLEL SLIT COLLIMATOR. I. Metal and S. Lapidus. Raytheon Medical Electronics. Stamford, CT.

Standard multihole collimators for an Anger Camera have geometric efficiences of ≈ .1%. We have investigated, both theoretically and by computer simulation, the efficiency, resolution, local and global noise characteristics of a rotating parallel slit collimator. This yields a set of projections. The source distribution is reconstructed by convolution-back-projection with a Hanning filter on 128x128 and 256x256 matrices.

We compare a multihole collimator (hole size = 1.27mm, length = 25.4mm) to a slit collimator (slit size = .82mm, length = 25.4mm) for the worst case - a flood field. The efficiency gain is 24. For a 128x128 matrix, we can achieve the same S/N with a Dose-Time Product gain of 3.8. The resolution for the slit system (assuming 5mm FWHM for the camera) is worse at the surface (6.38 vs 5.16mm), equal at 3" (7.13mm) and better at greater depth (8.54 vs 10.2mm at 6"). For a 256x256 matrix, the D-T product gain is 2.4 with slightly worse resolution at the surface (5.36 vs 5.16mm), equal at 1" (5.65mm) and much better with depth (6.29 vs 7.13mm at 3"; 7.9 vs 10.2 at 6").

In the best case, a point source, the D-T product gain is ≈ 20 for equivalent S/N at the source. Nevertheless, the noise is shifted outside the source and the "global noise", the noise summed over the full field of view, is almost independent of the source distribution.

Similar analysis can also be applied to emission and transmission tomographic systems and rotating strip solid state detector systems.

GEOMETRIC RESPONSE OF A GAMMA CAMERA COLLIMATOR WITH PARALLEL HOLES. C.E. Metz, F.B. Atkins*, and R.N. Beck. Dept. Radiology and the Franklin McLean Memorial Research Institute, The University of Chicago, Chicago, IL, and *Walter Reed Army Medical Center, Washington, D.C.

Previous studies of gamma camera collimators have been restricted largely to empirical measurements of the combined collimator-camera system. We have developed a theoretical approach that allows the geometric component of camera collimator response to be predicted independent of other system characteristics, and which thus provides a powerful tool for collimator design and camera system analysis. To deal with the positional dependence of a point source image due to the collimator hole array, we define an effective or average point spread function as the normalized image of a point source that would result if the collimator were randomly translated (but not rotated) during image formation, with the source and camera fixed. We have shown that the corresponding geometric component of the collimator transfer function is given by a general expression of the form

$$OTF_G(\vec{\nu}) = \left|A\{[1+(Z+B)/L]\vec{\nu}\}\right|^2$$

where $A(\vec{\nu})$ is the normalized two-dimensional Fourier transform of the aperture of a single hole, L is the collimator thickness, Z is the collimator-source distance, and B is the distance from the collimator to the effective image plane of the camera crystal. Closed-form expressions have been obtained for the common hole shapes: round, hexagonal, square and triangular. Monte Carlo simulations and experimental measurements of collimator geometrical response have shown this approach to be highly accurate, with disagreement typically less than 0.005 at all spatial frequencies.

A GATED PROBE SYSTEM FOR REAL-TIME CREATION OF PRESSURE-VOLUME LOOPS. H.G. Ostrow, S.I. Allen, S.L. Bacharach, M.V. Green, and J.S. Borer. National Institutes of Health, Bethesda, MD.

A non-imaging ECG-gated scintillation probe system has been developed which in conjunction with left ventricular (LV) heart catheterization permits simultaneous quantification of the variation of LV volume and pressure. The system combines a new high efficiency scintillation probe with computerized data acquisition, processing, and display. The probe system produces a time-activity curve in real-time. When the probe is properly positioned over the left ventricle, this time-activity curve is a measure of change of left venticle volume. By simultaneously measuring LV pressure and LV activity, parameters such as LV compliance can be continuously monitored.

The system is configured around a microcomputer programmed to automatically 1) acquire scintillation data from the probe and pressure data from a transducer, 2) organize these data into single or multiple beat time-activity and pressure curves which span a complete cardiac cycle, 3) construct curves from heartbeats having user selected intervals, 4) correct the time-activity curve for background and calibrates the curves, 5) calculate various parameters from the curves, 6) store the data and calculated values on floppy disk, 7) plot and display all calculated values and curves as a function of time for both beat-to-beat and trend analysis and produce pressure-volume loops.

The system is flexible, user-oriented, and suited for experimental evaluation of drug intervention where measurements of pressure-volume relationships are desired.

HALF-INCH VS. QUARTER-INCH ANGER CAMERA TECHNOLOGY: RESOLUTION AND SENSITIVITY DIFFERENCES AT LOW PHOTOPEAK ENERGIES. D. Chapman, K. Newcomer, D. Berman, and A. Waxman. Cedars-Sinai Medical Center, Los Angeles, California.

The purpose of this study was to compare the performance differences between a ½" and ¼" thick crystal detector.

Measurements were performed using an Ohio Nuclear 420 mobile camera. The initial study employed a ½" crystal detector and was repeated immediately following a change to the ¼" detector with the remainder of the system unchanged.

Parameters were quantitated for energies in the range of thallium-201 and technetium-99m, including: full width half maximum of the linespread functions, modulation transfer, function, sensitivity, paralyzable deadtime, and energy resolution. In addition, subjective analysis of clinical studies was performed. Results are summarized below:

	ON½"	ON½"
FWHM		
Tl-201 Intrinsic	4.3mm	5.7mm
Tc-99m Intrinsic	3.4mm	4.2mm
Tc-99m 2" Scatter	6.0mm	6.9mm
Sensitivity:		
Au-195	3640 cps/mCi	3397 cps/mCi
Co-57	3835 cps/mCi	4036 cps/mCi
Paralyzable Deadtime	6.9 u/sec	7.7 u/sec

The results clearly show a superior performance record for the ½" detector, especially for thallium-201, with almost no difference seen in sensitivity measurements. Preliminary clinical tests show a significant subjective improvement in image quality.

We recommend the use of ½" technology for Anger cameras which are used for low energy radionuclide scintigraphy.

4:00 p.m.-5:30 p.m. Room 210

CLINICAL SCIENCE

NEUROLOGY

Chairman: Kenneth A. McKusick
Co-Chairman: Abass Alavi

ASSESSMENT OF REGIONAL CEREBRAL BLOOD FLOW BY CONTINUOUS CAROTID INFUSION OF KRYPTON-81m AND EMISSION COMPUTERIZED TOMOGRAPHY. F. Fazio, C. Fieschi, M. Nardini, M. Collice, M. Possa and F. Spinelli. Ospedale Niguarda, Milano, Italy; University of Roma, Italy; University of Siena, Italy; Hammersmith Hospital, London, U.K.

Emission computerized tomography is a new technical development which provides more detailed information on the in vivo distribution of radioactive isotopes by removing superimposition of information with depth. The aim of this study is to assess the feasibility of obtaining tomographic images of brain perfusion using continuous carotid infusion of short-lived Kr-81m (1).

Eleven patients with various brain diseases were studied. During carotid infusion of Kr-81m in solution, the activity over the brain was recorded on a γ camera equipped with a mechanical gantry suitable to allow a 360° rotation of the detector around the patient. Data were recorded on a digital computer, sorted out in angular projections, corrected for attenuation, and subsequently reconstructed in both transaxial and longitudinal sections.

Tomographic images showed the following advantages over conventional views: (a) visualization of blood flow distribution within brain structures (grey and white matter, basal ganglia); (b) more accurate localization and evaluation of areas of relatively reduced or increased perfusion; (c) better definition of patterns of collateral circulation; (d) greater sensitivity and specificity in detecting and defining blood flow changes during physiological activation studies.

(1) Fazio, F., Nardini, M., Fieschi, C., et al (1977) Assessment of regional cerebral blood flow by continuous carotid infusion of krypton-81m. J.Nucl.Med., 18: 962-966.

CAN N-13 AMMONIA BE USED AS A CEREBRAL BLOOD FLOW TRACER? M.E. Phelps, S.C. Huang, D.E. Kuhl, C. Selin, E.J. Hoffman. UCLA School of Medicine, Los Angeles, CA.

N-13 ammonia was originally proposed by Hunter-Monohan and Harper et al for imaging heart, brain and liver. Phelps et al proposed that uptake in brain and heart was proportional to capillary perfusion via a unidirection Renkin-Crone Model with metabolic trapping. Studies in brain by Phelps et al and Schelbert et al in heart provided support to this concept. Since $^{13}NH_3$ is not a flow limited tracer in brain and heart, response of $^{13}NH_3$ uptake will be nonlinear with flow and dependent on capillary permeability-surface area product (PS) and rate of metabolic trapping and release.

Relationship between $^{13}NH_3$ uptake in brain was studied in 16 dogs. Cerebral blood flow (CBF) variations were produced by i) embolization of left hemisphere/elevated $PaCO_2$ and ii) local compression in left hemisphere/elevated $PaCO_2$ and iii) local penicillin induced seizure with a wide CBF range (0 to 250 cc/min/100 gms). $^{13}NH_3$ was injected I.V. and CBF measured with μ spheres. Relative local tissue $^{13}NH_3$ and ammonia flow index (i.e. using μ sphere model) had a near linear response from 0 to 80 cc/min/100 gms, but above 80 response became progressively nonlinear. Response was very similar for animal models i, ii, and iii, and for different cerebral structures, except grey matter was more responsive. Renkin-Crone Model, although crude, provides a basis for interpretation of data.

$^{13}NH_3$ is a good flow tracer in heart due to its high PS product. Lower PS of brain makes it a good flow tracer at medium to low flow but not very high flow. $^{13}NH_3$ appears to be a good flow tracer for cerebral ischemia.

SERIAL ASSESSMENT OF MEAN TRANSIT TIME DIFFERENCE FOLLOWING SUPERFICIAL TEMPORAL-MIDDLE CEREBRAL ARTERY ANASTOMOSIS. S.H. Yeh, R.S. Liu, and L.C. Wu. Veterans General Hospital, Taipei, Taiwan

This study assessed the value of serial determinations of mean transit time difference (MTTD) in evaluating the patients following superficial temporal artery-middle cerebral artery (STA-MCA) anastomosis.

MTTD for MCA area was determined after I.V. injection of Tc-99m pertechnetate by using a computer routine for calculating a vascular mean transit time by the width of the time-activity curve at 1/e of its peak value. In 6 patients undergoing STA-MCA anastomosis, MTTD's were determined preoperatively and postoperatively at 1 wk as well as at 1, 3, and 6 mo. Clinical response was recorded at the same intervals. Angiography was performed at 1 wk and 6 mo. MTTD was also determined in 192 normal individuals to get the normal range (mean ± 1 S.D. = 0.70 ± 0.51 sec).

Preoperatively, these 6 patients had increased MTTD's (range 3.52-16.38 sec). In 2 cases with asymptomatic result and 1 with improvement at 6 mo after operation, MTTD's gradually decreased with time from abnormal to normal or near normal values (0.29-1.40 sec for asymptomatic cases and 1.90 sec for improved one at 6 mo), whereas angiograms showed good filling of MCA at 1 wk and 6 mo. In 3 cases with unchanged result, MTTD's remained increased and angiograms showed partial filling of MCA throughout the study.

Our preliminary results indicate that serial MTTD's provide indexes reflecting changes in brain perfusion parallel to the clinical response after STA-MCA anastomosis. Perfusion improvement is a slow process in spite of good filling of MCA. Thus, serial assessment of MTTD would be a useful, non-invasive, and objective adjunct to angiography for evaluating patients following cerebral revascularization.

THE ROLE OF CEREBRAL PERFUSION SCINTIGRAPHY IN PATIENTS WITH RUPTURED INTRACRANIAL ANEURYSMS. R.J. Gorten and P.J. Kelly. University of Texas Medical Branch, Galveston, TX.

Intracranial surgery for ruptured cerebral aneurysm (RCA) must be properly timed to optimize the chances for a favorable outcome. Aneurysmal neck clipping too early after bleeding is often complicated by infarction with permanent disability or demise. A longer waiting period is sometimes interrupted by repeat subarachnoid hemorrhage.

Retrospective analysis of a previous group of 44 RCA patients revealed that those patients with prompt and symmetrical perfusion preoperatively, as determined by dynamic cerebral imaging (DCI), had a better clinical response after operative intervention. Patients with unilateral delayed perfusion had a higher incidence of intraoperative or postoperative complications, particularly cerebral infarction, with an operative mortality of 22%.

In a prospective study of 45 patients with RCA, DCI was used to help select the optimum time for surgery. Opera-

tions were not delayed in clinically stable patients with normal DCI. If abnormal, the test was repeated until prompt and symmetrical, after which intracranial surgery was undertaken. Operative mortality in this group was only 3.4% with satisfactory or better outcome in all survivors. Preoperative rebleeding occurred in 3 patients but on each occasion normal DCI had already been obtained. The hemorrhages were relatively minor and all 3 recovered well and underwent successful surgery.

The use of DCI for assessment of cerebral perfusion serves an extremely important role in selecting the optimum time for surgical intervention of RCA and has significantly improved operative results.

CORRELATION OF PERTECHNETATE UPTAKE AND CAPILLARY ULTRASTRUCTURE IN HUMAN BRAIN TUMORS.
D. Front, P. Bar-Sella, R. Hardoff, I. Nir.
Rambam Medical Center and the Technion Faculty of Medicine, Haifa, Israel.

This study was undertaken to investigate the ultrastructural basis for the different pertechnetate uptakes by various human brain tumors. Radionuclide angiography, and early and late scintigrams, with Tc-99m pertechnetate and Tc-99m labeled red blood cells, were performed in 14 patients with brain tumors to evaluate pertechnetate uptake and tumor vascularity. The capillaries of these tumors were studied by electron microscopy for the nature of their intercellular gaps and the presence of fenestrations in the endothelial wall.

It was found that tumors with open endothelial junctions (width 75-200A°) showed rapid and intense uptake of pertechnetate. Intercellular tight junctions were associated with little uptake or no uptake at all. The presence of fenestration and high vascularity were not essential for increased pertechnetate uptake.

The correlation of pertechnetate uptake as determined by scintigraphy, with the patency of the intercellular junctions, might be of importance in planning chemotherapy of brain tumor in the individual patient.

MAPPING OF FUNCTIONAL ACTIVITY IN THE HUMAN BRAIN WITH F-18-FLUORODEOXYGLUCOSE. A. Alavi, M. Reivich, J. Greenberg, D. Christman, J. Fowler, P. Hand, A. Rosenquist, W. Rintelmann, and A. Wolf. University of Pennsylvania, Philadelphia, PA and Brookhaven National Laboratory, Upton, NY.

The F-18-fluorodeoxyglucose technique for measuring local cerebral glucose consumption has made it possible for the first time to examine the connectivity of the human brain. A region of the brain which is functionally activated has a corresponding increase in its metabolic rate. Thus if we can detect those regions whose metabolic rates increase in response to a stimulus, it is possible to map those areas which are functionally activated.

In all 6 subjects examined during stimulation of one visual field (3 right and 3 left), with the other field dark, glucose utilization of the calcarine cortex was asymmetrical, with the side contralateral to the stimulated field having the higher metabolic rate.

In all 3 subjects with somatosensory stimulation consisting of brush stroking of the fingers and hand (2 right, 1 left) an increase in glucose utilization was observed in the dorsal portion of the contralateral postcentral gyrus.

In all 6 subjects hearing connected discourse monaurally (3 right ear, 3 left) the glucose consumption of the right temporal cortex was higher than the left.

Thus, the F-18-FDG technique can be used to map functional neural pathways in the brain.

4:00 p.m.-5:30 p.m. Room 211

CLINICAL SCIENCE

PULMONARY

Chairman: Philip O. Alderson
Co-Chairman: Bruce Line

VENTILATION-PERFUSION LUNG IMAGING IN EARLY DETECTION OF LUNG CANCER. Robert D. Katz, Philip O. Alderson, Melvin S. Tochman, Julia W. Buchanan, and Henry N. Wagner, Jr. Johns Hopkins Medical Institutions, Baltimore, Md.

To evaluate the role of ventilation-perfusion lung imaging in the Johns Hopkins Project for Early Detection of Lung Cancer, the Tc-99m microsphere perfusion scans (P) of 87 patients (pts) with lung cancer were reviewed. Xe-133 ventilation studies (V) were obtained in 83 of the pts. Seventy V-P studies from pts without lung cancer were included in the review and chest radiographs were withheld to reduce observer bias. The diagnosis and site of tumor were established by thoracotomy, bronchoscopy or biopsy. The tumor was accompanied by a P defect in 59 of 75 pts (79%) with positive radiographs and in 6 of 12 pts with radiographically occult tumors. Only 31 of the 65 P defects (48%) were segmental or lobar; the others were nonsegmental. Both V and P abnormalities were present in the tumor region in 46 pts, but the pattern of a segmental or lobar P defect accompanied by decreased Xe-133 entry and delayed clearance occurred in only 17 pts. V abnormalities were present at one or more sites remote from the tumor in 47 cancer pts (57%), and 46 had P scan defects unrelated to the tumor. This high frequency of co-existent lung disease made an accurate diagnosis of lung cancer difficult. Similar V-P abnormalities occurred in 14 of 15 pts in the Lung Project who had tissue confirmation of benign lung disease other than cancer. In one pt with lung cancer and negative radiographs the lung scan helped localize the tumor. In the other pts it was useful for quantification of regional lung function prior to tumor resection.

NUCLEAR MEDICINE IN THE INTENSIVE CARE UNIT: ASSESSMENT OF ALVEOLOCAPILLARY PERMEABILITY IN SEPTIC PULMONARY EDEMA (RDS). A.A. Driedger, W.J. Sibbald, J. Moffat, J. Calvin, B.D. Reid, and R.L. Holliday. Victoria Hospital, London, Ontario, Canada.

Pulmonary edema of RDS may be due to increased permeability of the alveolocapillary structures. The objective of this study was to compare the leak of small and large molecules in RDS using cardiac edema patients (CE) for reference.

The appearance of I-125 human serum albumin (HSA) and In-111-DTPA in tracheobronchial aspirate (TBA) was measured and averaged over 4 hours following intravenous injection in 17 patients, 9 having RDS and 8 having CE. Pulmonary wedge pressure (WP) was measured by an indwelling flow-positioned catheter and serum oncotic pressure (OP) was calculated from serum protein concentrations.

Clearances of DTPA (RDS: .40 ± .08; CE: .04 ± .01; $p < .01$) (mean ± SEM) and HSA (RDS: .18 ± .01; CE: .01 ± .001; $p < .01$) were greater in patients with RDS. Clearance of DTPA varied inversely with (OP-WP) gradient in cardiac edema ($r = -.91$; $p < .01$) while the clearance of HSA varied inversely with (OP-WP) in RDS ($r = -.98$; $p < .01$).

We conclude that 1) small molecules leak across the alveolocapillary membrane at a slow rate under the influence of pressure alone, 2) the permeability of the alveolocapillary membrane to both small and large molecules is increased in RDS and 3) the magnitude of the alveolocapillary albumin leak in RDS may be influenced by alteration of the (OP-WP) pressure gradient.

THE DIAGNOSTIC VALUE OF A FULLY AUTOMATED THRESHOLDING ALGORITHM FOR VENTILATION-PERFUSION MISMATCHES. J.E. Baumert, R.L. Lantieri, H.D. Fawcett and M.L. Goris, Stanford University School of Medicine, Stanford, CA.

The controversy surrounding the use of ventilation-perfusion scintigraphy is based in part on the question of the categorical significance of mismatch. The hypothesis to be tested is that primary vascular disease (i.e., thromboembolism) is uniquely characterized by a decrease in regional perfusion above and beyond that which can be explained as secondary to parenchymal dysfunction.

We have developed a fully automated algorithm to analyze the ventilation ($\dot{V}$) and perfusion ($\dot{Q}$) distribution images obtained with Krypton-81m and Tc-99m-microspheres respectively. The algorithm normalizes the images and corrects for the higher background in the ventilation image. The predicted difference between $\dot{Q}$ and $\dot{V}$ is computed on the basis of the standard error of the estimate (linear regression) and Poisson error. To obtain a clear threshold, a ratio image is constructed in which the actual difference in $\dot{Q}$ and $\dot{V}$ was compared with the weighted predicted difference and represented in a non-linear scale with a sharp difference between normal and abnormal. With a weighting factor varying from 1.4 to 1.8, sensitivity decreased from 94% to 81% and specificity increased from 83% to 100% when pulmonary arteriography was used as a standard (N=28).

From our results, we could not document a single quantitative limit which unequivocally separates pulmonary embolism from other pulmonary disease. However, the ability to quantitate the degree of $\dot{V}/\dot{Q}$ mismatch allows us to objectively and consistently select the levels of sensitivity and specificity required.

SMALLER LUNG PARTICLES FOR SAFER PERFUSION EXAMINATIONS (CAPILLARY VS. ARTERIOLAR BLOCKADE). G.V. Taplin, D. Elam. UCLA School of Medicine, Los Angeles, CA.

Macroaggregates of human serum albumin (MAA) and human albumin microspheres (HAM) used for lung perfusion imaging have average mean sizes ranging between 20 and 30 μm. The optimum number of particles or spheres is about 300,000 and the total amount of albumin is usually less than 1 mgm. These agents produce temporary arteriolar blockade. With 300 million arterioles in the human lung there is a 1,000 fold margin of safety. Only a few instances of sudden death from hemodynamic reactions have been reported from the millions of patients examined. This hazard may be decreased another 1,000 fold by reducing the size of test agents to produce capillary rather than arteriolar blockade. Only 1 in 1 million of the 280 billion capillary units are occluded following injection of 200,000 to 300,000 small spheres. In dogs, lung images made with equal numbers of 15-40 μm and 7-10 μm spheres are nearly identical. The only difference in image quality is that those obtained with the small spheres appear to have higher resolution. The lung retention of radioactivity at 24 hours is nearly 100% with spheres of both sizes. The optimum sphere size for rapid camera imaging is no larger than the maximum dimension of red blood cells (6-9 μm) because rigid spheres are not reduced in size as are red cells while they traverse the capillary network. Furthermore, lung aggregates and spheres should be made softer to reduce lung removal half times to no more than 1 hour.

It is concluded that smaller and softer particles and spheres are needed to eliminate hemodynamic reactions, while simultaneously reducing radiation exposure and maintaining excellent image quality and resolution.

PERFORMANCE OF XENON-133 VENTILATION STUDIES IN SUBJECTS ON ARTIFICIAL VENTILATION. F. Vieras, L.M. Fraser, and J. R. Bridgeman. Armed Forces Radiobiology Research Institute, Bethesda, MD.

This study was undertaken to design a system for performance of Xe-133 studies in comatose subjects maintained with respirator-driven ventilation. The system involves a standard respirator and a simple Xe-133 delivery box. The washin-equilibrium phase of the study is based on the transfer of volume between two independent closed gas circuits. In one circuit, a mixture of oxygen and Xe-133 is recirculted between a bag (within the Xe-133 delivery box) and the subject, and in the other, air is recirculated between the respirator and the Xe-133 delivery box to collapse and expand the bag. Xenon is kept within the bag-subject circuit without entering the other circuit (respirator-delivery box), thereby preventing contamination of the respirator. This was proven by taking multiple air samples from the rubber hose connecting the respirator to the delivery box. The washout phase is accomplished using a tube fitting that allows passage of exhaled Xe-133 into an exhaust. The system was tested using either a spirometer or deeply anesthetized dogs as subjects. A complete ventilation study can be performed at various tidal volumes and respiratory rates. Pulmonary time-activity curves obtained with the system described here are similar to those obtained in spontaneously breathing subjects. The system should be applicable to the performance of Xe-133 studies in human subjects on artificial ventilation.

ALTERED CLEARANCE OF INHALED SMALL SOLUTES FROM THE LUNGS. J. M. Uszler, R. M. Effros, L. Shapiro. Divisions of Nuclear Medicine and Respiratory Medicine, LAC Harbor-UCLA Medical Center, Torrance, CA.

Current lung imaging procedures do not directly evaluate for interstitial lung disease (ILD) changes. We developed a procedure for this. Subjects inhaled aerosolized solutions of Tc-99m-DTPA and Tc-99m-pertechnetate for 2 minutes while seated with their back against a scintillation camera. Radioactivity was subsequently monitored for 20 minutes over 3 regions of each lung. Percentage clearance per minute in each region was calculated from the best exponential fit of data from the first 7 minutes after the peak of each curve.

Tc-99m-pertechnetate (mw 163) clearance ($\bar{k}$=5.12±0.21%/min, SEM) exceed that of Tc-99m-DTPA (mw 492) ($\bar{k}$=1.56±0.20 %/min. $p<.001$) in both normal and abnormals. Upper lobe clearance of both radionuclides was greater than lower lobe clearance in normal subjects, but this gradient was abolished when exhaling against 7 cm positive end-expiratory pressure (PEEP). 21 patients with diminished CO diffusion and with clinical and x-ray evidence for ILD were studied with DTPA. Although DTPA cleared more slowly in normals, its clearance was increased (4.17±0.28%/min., $p<.005$) in 5 idiopathic pulmonary fibrosis, 4 of 8 sarcoid, 2 of 5 pneumoconioses and 2 of 3 other ILD. No increase was found in 5 with COPD.

These studies suggest that initial clearance of aerosolized hydrophilic radionuclides is accomplished in part by diffusion through epithelium of alveoli and respiratory bronchioles. Clearances are accelerated in ILD. This may indicate increased epithelial permeability related to injury and increased retractile forces, and in this way provide assessment of ILD.

CONTINUOUS RECORDING OF MUCOCILIARY CLEARANCE IN HEALTH AND IN CHRONIC AIRWAYS OBSTRUCTION (CAO). F. Fazio, M. Miniati, A.P. Greening and M.M. Clay. Hammersmith Hospital, London, U.K.

Mucociliary clearance is currently assessed by serial measurements of external activity following inhalation of radioactive aerosols. This method is open to errors due to repositioning and uncertainties on events between measurements: using this technique, conflicting results have been reported on the behavior of mucociliary clearance in patients with CAO relative to normals. We investigated this problem using a new technique which consists in the continuous recording of regional mucociliary clearance.

Seven normal subjects and thirteen patients with CAO were studied. They inhaled over 5 min of normal tidal breathing a nebulization of Tc-99m-labeled albumin microspheres (range 0.2-2.5μ). Activity over the chest was then continuously recorded for two hours with the subject lying supine under a large field gamma camera linked to a digital computer. The continuous computer recording can then be played back at increased speed (2 min = 1 sec) as a cine-film of mucociliary clearance. Areas of interest can be

selected and time activity curves representing regional clearance can be obtained. The 2-hour retention indices calculated from both the hilar and the peripheral regions showed no significant differences between normals and patients with CAO. In this latter group, however, most of the clearance from the hilar region was merely due to cough (recognized as a sudden fall of radioactivity corresponding to a cough event). No significant cough effect was detected at the periphery. Our data indicate that in patients with CAO mucociliary clearance is normal at the lung periphery but impaired in large airways, where secretions would accumulate if not cleared by coughs.

4:00 p.m.-5:30 p.m. Room 201

RADIOPHARMACEUTICAL CHEMISTRY: SYMPOSIUM II

PHARMACOKINETIC MODELING

Chairman: Michael J. Welch
Co-Chairman: Robert J. Lutz

PHYSIOLOGIC PHARMACOKINETIC MODELS FOR SIMULATING DRUG DISTRIBUTION IN VIVO. R.J. Lutz. Biomedical Engineering and Instrumentation Branch, DRG, NIH, Bethesda, MD.

A physiologic pharmacokinetic model provides a means of simulating or predicting the concentration of drugs or other chemicals in various regions of the body as a function of time. It is comprised of a set of compartments which represent specific organs or anatomical regions of the body where the drug distributes. Differential mass balance equations are written to describe the exchange of drug from one compartment to another. This exchange procedure can occur by a variety of physiologic mechanisms such as membrane diffusion and blood flow. Numerous parameters may be required by the model. These are physiological, anatomical, thermodynamic, or transport related e.g., organ sizes, blood flow rates, metabolism constants, clearances, binding coefficients, and membrane permeabilities, to name a few. These parameters can be obtained from known data or can be estimated from properly constructed in vitro or in vivo experiments. A priori predictions of drug concentration is possible, as well as simulation of data occuring to a postulated mechanism of disposition.

OPTIMIZING BONE SCAN TIMING BY COMPARTMENTAL ANALYSIS OF SKELETAL TRACER KINETICS. N.D.Charkes, P.T. Makler, Jr., L.S. Malmud, S. Dessel, and J. Reilley. Temple University Hospital, Philadelphia, PA.

Determination of optimal scanning times has generally been based upon tissue data studies in normal animals and subjective analysis of clinical images. We demonstrate in this investigation that the optimal scanning time can be predicted from knowledge of the kinetics of the radiopharmaceutical obtained by compartmental analysis in patients with disease. We studied the kinetic behavior of fluoride ion (F-18) in 12 patients with bone disease (metastases or Paget's disease). With the patient positioned under a gamma camera for 1 hour, multiple blood samples were obtained and external counts collected in an on-line digital computer. Urine was collected at the end of the study,and a total body scan obtained to estimate the extent of disease. Having shown that F-18 kinetics can be closely approximated by a 5-compartment model in humans without significant bone disease (J.Nucl.Med. 19:1301,1978) we added abnormal-bone-ECF and abnormal-bone-compartments in a catenary arrangement with blood for these patients. The model was solved by the SAAM program for each patient and verified by comparing the predicted curves over bone (plus its ECF) with the actual data (obtained by setting regions of interest over normal and abnormal bone,and background). We then generated time dependent functions for Beck's figure-of-merit (Q) and for abnormal-bone (plus its ECF)-to-normal bone (plus its ECF) contrast for each patient. Q is optimal at about 1 hour post-dose, when bone scans are generally made with F-18 based upon subjective criteria. Contrast continues to rise for several hours. Conclusion: The optimal time for F-18 bone scans can be accurately predicted,objectively, by compartmental analysis of tracer kinetics.

AN EFFICIENT BIEXPONENTIAL CURVE FITTING ALGORITHM. C.R. Appledorn and B.E. Oppenheim. Indiana University School of Medicine, Indianapolis, IN.

The fitting of a sum of exponential curves to experimental data obtained from numerous quantitative procedures (eg., xenon washout, hippurate clearance, and biological half-life determinations) is a frequently encountered problem. Two methods are currently used: (1) "curve stripping" in which the slow phase is first identified and peeled away from the data before the fast phase can be fit, and (2) iterative nonlinear least-squares in which initial estimates for the parameters are iteratively improved until some convergence criteria are satisfied. Both methods are slow and suffer from computational inefficiency.

We present a noniterative technique which yields least-squares estimates for the parameters A_1, A_2, c_1, c_2 when the data is of the form:

$$r_n=r(nT)=A_1\exp(-c_1nT)+A_2\exp(-c_2nT),\ n=0,1,\ldots,N-1.$$

The improved computational efficiency is realized by first identifying the values of the coefficients in the difference equation for the above given by:

$$r_n=p_1r_{n-1}+p_2r_{n-2},\ n=2,3,\ldots,N-1 \text{ where}$$

$$p_1=\exp(-c_1T)+\exp(-c_2T) \text{ and } p_2=-\exp(-(c_1+c_2)T).$$

Once values for p_1 and p_2 have been estimated, the parameter values for c_1 and c_2 quickly follow. The amplitudes A_1, A_2 are then easily found.

This new algorithm has been tested using Monte Carlo simulation of a Poisson process for hippurate clearance using the conventional two compartment model for blood clearance. When the data is length N=128 and has initial activity r_0=2048 counts the error associated with the estimate for the hippurate clearance is typically 3.3% (σ/μ) and the correlation coefficient between the true clearance fraction and estimated fraction is r=0.995.

GALLIUM PHARMACOKINETIC IMAGING FOR EARLY DETECTION OF TUMORS. R. Beihn and M. Vannier. Veterans Administration Medical Center and University of Kentucky Medical Center, Lexington, Ky.

Pharmacokinetic images from ^{67}Ga citrate distribution kinetics have been produced using a pseudo-color rate constant display scale. Immediately following intravenous injection of ^{67}Ga citrate, data was collected at 0.5 min per frame for 30 min using a Searle LFOV scintillation camera interfaced to a Gamma-11 computer system. The anatomical region under observation included heart, liver and abdomen. Thirty minutes of data collection resolved two components of the polyexponential kinetics of ^{67}Ga citrate blood clearance. A monoexponential analysis of each component was performed. Exponential least squares coefficients from each pixel of a 64x64 frame were scaled and mapped into a 16-color image over the observed range of rate constant values. The model chosen had the form:

$$[r]_k = [K]\ (\exp t_k) + [C]$$

where, t_k=time elapsed at frame k, $[r]_k$=64x64 matrix of accumulated counts at frame k, [K]=64x64 matrix of clearance rate constants, [C]=64x64 matrix of additive constant terms, and k=frame number. This resulted in images for [K] and[C], the exponential clearance rate coefficient and constant term calculated at each pixel respectively. The monoexponential analysis of either component, followed by interpolation and 9-point smoothing, resulted in lesion delineation with results in lesion detection appearing 10-30 min after injection.

RADIOPHARMACOKINETICS, OR THE USE OF NUCLEAR MEDICINE TECHNIQUES FOR THE IN VIVO STUDY OF KINETICS AND METABOLISM OF

DRUGS IN HUMANS. W. Wolf, R.C. Manaka, D. Young, and A. Schumitzky. Radiopharmacy Program, University of Southern California, Los Angeles, CA.

Classical pharmacokinetics measures blood levels of the administered drug and of its metabolites, and from these data it intends to infer information on effective drug levels. It has been apparent for some time that it is not the blood levels alone, but rather the organ levels that may provide the most valuable set of parameters. Drug levels in such organs cannot be determined invasively as in blood, and a non-invasive measurement of radioactive concentrations following administration of a labeled drug gives a sum of all the products present, both of the drug and of its metabolites carrying the label. Through the use of identification theory, we have developed mathematical models that allow us, based on preliminary knowledge of the biotransformation pattern of the drug, and a minimum number of invasive measurements in accessible tissues and organs, to resolve the sum curve into its individual components. These studies are currently being tested with 2 drugs, F-18-5-fluorouracil and Pt-195m-cis-platin, where drug response and/or drug toxicity can be evaluated during treatment with a pharmacological dose of the agent, additioned with a small amount of the radioactive tracer. Cis-Pt is bound (apparently irreversibly) to RBC's and proteins, rapidly taken up by tissues and excreted. The total Pt-195m activity detected in blood is hence determined by a six term equation, involving an input function (rate of administration), 3 unidirectional and 2 reversible components. A mathematical treatment is expected to relate these functions, hence modulating and controlling drug response.

4:00 p.m.-5:30 p.m. Room 206

IN VITRO RADIOASSAY

POSTER SESSION

Chairman: John Hansell
Co-Chairman: Eileen L. Nickoloff

DIRECT DETERMINATION OF FREE THYROXINE IN A SINGLE TUBE RADIOIMMUNOASSAY. E.K. Mincey and M.P. McTaggart. Metropolitan Clinical Laboratories, Vancouver, B.C., Canada.

This work was undertaken to develop a direct radioimmunoassay for measurement of free thyroxine in serum.

Because of the need to measure free T-4 with minimal disturbance of the T-4-TBG system, a two-phase sequential incubation method was devised, in which diluted serum is first incubated with the anti-T-4 antibody and then serum components removed before the second incubation phase with the radioactive T-4 tracer solution. Standard serums or test serums (0.05 ml) are incubated in test tubes with phosphate buffered saline, pH 7.4, for 15 min. at room temperature. Incubation is continued for another 15 min. after adding 0.1 ml of previously titered T-4 antibody solution. Polyethylene Glycol (PEG) is added and the precipitated gamma globulins recovered by centrifugation and aspiration of supernatant. The T-4-antibody complex is resuspended in 0.05 ml of barbital buffer, pH 8.6, containing about 5 pg of I-125 T-4 and sodium salicylate and ANS. After another 15 min. incubation, the PEG step is repeated and the radioactivity in the precipitate counted.

The free T-4 levels in a group of 50 euthyroid, 20 hyperthyroid, 20 hypothyroid, 10 pregnant patients, and 2 patients with partial deficiency of TBG were determined and results show complete separation of each category. Pregnant patients and patients with partial TBG deficiency had free T-4 values in the calculated normal range of 1.2-3.2 ng/dl.

We conclude that this single tube procedure represents a simple and rapid method for free T-4 determination which correlates with the clinical findings. It should supercede methods for indirect estimation of free T-4.

SEARCH FOR PROBLEM SAMPLES IN THE KINETIC ANALYSIS OF FREE T4 CONCENTRATION. C. M. Heise, Nuclear Medicine, Bowman Gray School of Medicine, Winston Salem, N. C.

In order to identify potential problem samples in the measurement of FT4 by the kinetic technique of determining the fraction of complex formed by T4 & its antibody, free T4 index (FT4I) was also determined in 296 of 803 samples submitted for testing. Only 57/296 samples differed diagnostically by the 2 parameters and divided into the following classes:

A -NORMAL FT4I & LOW FT4 28/296=9.5% or 3.5% out of 803
B -NORMAL FT4I & HIGH FT4 8/296=2.7% or 1.0% out of 803
C -NORMAL FT4 & LOW FT4I 14/296=4.7% or 1.7% out of 803
D -NORMAL FT4 & HIGH FT4I 4/296=1.4% or 0.4% out Of 803
E -HIGH FT4 & LOW FT4I 3/296=1.0% or 0.4% out of 803

As every effort was made to include as many as possible of potential "problem" samples in the 296 studied, the true incidence of discordance is probably closer to the second figure in each case. The selected 296 samples included more elderly, critically ill patients and subjects with abnormal TBG concentration as these are known to cause problems with the FT4I and T3 Uptake test.

Five additional thyroid tests performed on discordant samples served to assign each sample into a clinical class. By this criterion, FT4 was correct in half of samples in Groups A&B, in 8/11 & 3/4 in Groups C&D. Neither FT4 nor FT4I were thought correct for samples in Group E from patients critically ill with nonthryoidal diseases.

We suggest that the incidence of artefactual results with the kinetic approach to measuring FT4 is small, certainly less than that of T3Uptake and approximately equal to that of FT4I. Simultaneous measurement of total T4 will serve to call attention to most of the artefactual values and patients can then be further evaluated.

THYROID SCREENING IN THE PREMATURE INFANT. R.S. Procianoy, L.A. Monroe, J.A. Garcia-Prats, A.J. Rudolph, J.A. Burdine. Baylor College of Medicine, Texas Children's Hospital, Houston, TX.

Premature infants are known to have lower serum T-4 levels than term infants, and a different pattern of postnatal thyroid development. Infants with hyaline membrane disease (HMD) also have decreased serum T-4. It is thus possible that the normative data obtained from term babies in neonatal thyroid screening may not be appropriate for the evaluation of low birth-weight infants.

We studied the influence of gestational age (GA) and HMD on thyroid screening in premature babies. Micro T-4 analyses were performed using a commercial RIA kit on filter paper specimens obtained during the first 10 days of life from 116 preterm infants, all appropriate for GA as determined by maternal dates and physical examination. Euthyroid status was confirmed by TSH analysis in infants with micro T-4 levels <6 ug/dl. Thirty-three patients had HMD (Group A) confirmed by clinical and radiologic findings, and 83 infants had no distress (Group B). The mean GA for the 2 groups was similar (32.8 $\pm$ 2.9 and 33.2 $\pm$ 2.7 weeks, respectively).

There is a significant correlation between GA and micro T-4 levels. This is independent of the presence or absence of HMD (correlation coefficients: Group A=0.43, $p<0.002$, Group B=0.39, $p<0.001$). Preterm infants with HMD have significantly decreased micro T-4 values (Group A=6.6 $\pm$ 2.8 ug/dl, Group B=7.9 $\pm$ 2.9, $p<0.05$). It is concluded that thyroid screening in preterm infants should be based on consideration of GA and presence or absence of HMD.

DEVELOPMENT OF A HIGHLY SENSITIVE RADIOIMMUNOASSAY FOR HUMAN THYROID-STIMULATING HORMONE (hTSH) AND ITS APPLICATION TO MASS SCREENING FOR NEONATAL HYPOTHYROIDISM. M. Ito K. Ishibashi, R. Ohsawa, and S. Nagataki*. Eiken Immunochemical Laboratory and University of Tokyo*, Tokyo, Japan.

A high-affinity anti-hTSH serum (Keg: 7.8×10^{11} M^{-1}) generated in our laboratory was employed to develop a highly sensitive radioimmunoassay for hTSH in which the detectable minimum amount of hTSH was 0.015 μU/tube. This assay

could measure serum TSH levels in small amounts of serum and was used in mass screening for neonatal hypothyroidism. With this method, TSH concentrations can be measured using a single 3 mm disc of dried blood on filter papers (1.5 µl of plasma). The minimum detectable concentrations are 10 µU/ml, and hence, the method can distinguish neonatal hypothyroidism from normal newborns. Intra-assay coefficients of variation (CV) for dnalyses of 10 samples with serum TSH levels of 56.3 and 129 µU/ml were 10.8% and 5.7%, and inter-assay CV were 16.6% and 14.8%, respectively. Values in blood obtained from 32 patients with mild to moderate hypothyroidism measured by this method correlated significantly with those obtained by standard measurement methods of serum TSH (r:0.94, $p<0.01$). Determinations of serum TSH concentrations in newborns with the present method was carried out in 749 dried blood filter paper specimens. The majority (617) showed values less than 10 µU/ml, 131 cases had values between 10 and 20 µU/ml, and only one showed values greater than 20 µU/ml. These results agree well with previous reports using 9 mm, 6 mm or two 3 mm discs of filter paper. The present method is more sensitive than any other reported method, simple and reliable, and is suitable for use in a screening program.

A COMBINED CORD BLOOD THYROXINE AND THYROTROPIN SCREENING PROGRAM FOR NEONATAL HYPOTHYROIDISM. L. Reese, F.S. Prato, G.J.M. Tevaarwerk, C. Hurst. St. Joseph's Hospital and University of Western Ontario, London, Ont., Canada.

A cord blood screening program for primary neonatal hypothyroidism (PNH) has been implemented in a general hospital using conventional radioimmunoassay techniques. From June 1, 1977 to June 30, 1978, 3456 newborns were screened. Cord blood thyroxine (T4) and triiodothyronine (T3) concentrations were measured. Where T4 values fell below 8.0 ug/dl the concentration of thyrotropin (thyroid stimulating hormone - TSH) was assayed. One PNH was identified (T4 = 5.0 ug/dl; TSH = 158 mU/l) and treated. A greater percentage of males (9.7%) than females (4.7%) had low T4 values (< 8.0 ug/dl). In males but not in females, birth weight (prematurity) correlated with T4 values (e.g. below 6.0 ug/dl the correlation coefficient was 0.7), and the relationship became stronger for lower values of T4. Serum T3 levels were not found to be of value. The predictive value of cord serum T4 was low ($< 1\%$) because of the high number (254) of false positives. The addition of TSH analysis to the latter resulted in an effective and relatively inexpensive screening program for PNH.

LOCAL EFFECTS IN LABELED MOLECULES FOLLOWING IODINE-125 DECAY. M. Berridge, V.W. Jiang, and M.J. Welch. Department of Radiology, Washington University School of Medicine, St. Louis, MO.

Radioiodination of proteins at the specific activity commonly used in radioimmunoassay leads to levels of iodination of greater than one molecule of iodine per protein molecule. Following the decay of one atom of radioiodine the protein is still labeled, but the molecule may have been altered by the first decay. To investigate this effect in a model compound we have studied the results of iodine-125 decay in iodo-tyrosine doubly labeled with iodine-125 and carbon-14. Doubly labeled 3-iodotyrosine was prepared by the chloramine-T iodination of high specific activity universally labeled carbon-14 tyrosine. The iodo-tyrosine was stored at 4°C and aliquots analyzed by cation exchange chromatography and high pressure reverse-phase liquid chromatography at intervals over a three year period. After this time the iodine-125 activity was negligible compared to the carbon-14 activity and the samples were counted in a liquid scintillation counter. The products formed following the iodine decay were small polar molecules which have not been completely identified. No aromatic products were observed. The results contrast dramatically with a previous study using iodine-131 in which the aromatic ring was maintained after decay. The study demonstrates that the coulombic explosion resulting from the Auger cascade accompanying iodine-125 decay destroys the aromatic ring and can be expected to cause breaks in a peptide chain. The labeled fragments produced from multiple-labeled proteins can be expected to result in elevated and irregular assay values.

CRITICAL PARAMETERS OF THE LACTOPEROXIDASE/HYDROGEN PEROXIDE SYSTEM FOR PROTEIN IODINATION. I.D. Miller, M.J. Freeman and S.M. Shaw. Purdue University, West Lafayette, IN.

The lactoperoxidase/hydrogen peroxide method for the iodination of proteins has been accepted as a gentle, non-denaturing method for the incorporation of radioiodine onto the tyrosine molecules of proteins. The reaction yields associated with this method have been quite variable between laboratories and researchers. This research was conducted to pinpoint those elements of the reaction which might be responsible for the variability.

Iodide and hydrogen peroxide, although essential to the reaction, where found to limit the yield at certain concentrations. Hydrogen peroxide proved to be inhibitory at a concentration as low as 0.28mM. Increasing the amounts of iodide raised the threshold of peroxide inhibition; however, iodide became inhibitory at 0.04mM. Dilution of the reactants, an apparent solution to these problems, also resulted in a decrease in labeling efficiency.

A technique was developed which circumvented these problems. The hydrogen peroxide was added in several aliquots at 10 minute intervals, the time found necessary for complete utilization. The amount added in each aliquot was limited so as not to exceed a total concentration of 0.14 mM. The minimal total added was found to be three molecules of peroxide per iodide atom. This method allows one to label as few as 50 ug of protein with efficiencies approaching 100% and to control the specific activity of the labeled protein through a deliberate balance of iodide and hydrogen peroxide molar ratios.

RAPID RADIOMETRIC SERUM TEST FOR ANTIBIOTIC ACTIVITY. R. D'Antonio, P. Charache, H.N. Wagner, Jr., and T. Gedra. Johns Hopkins Medical Institutions, Baltimore, MD.

Serum dilution tests for bacteriostatic activity are used for guiding antibiotic therapy in life threatening infections. The Schlichter tube dilution method (STDM) requires 18 hrs. We have developed a radiometric method which can be completed in 4 hrs.

Normal human serum (NHS) was divided into several lots. One lot was unaltered and served as control. High and low concentrations of either Penicillin-G or Gentamicin were added to the other lots. The sera were serially diluted into vials containing 0.5 ml Mueller-Hinton broth (MHB). The vials were capped and 0.05 ml of H_2O containing radiolabeled (C-14) arginine, glycine, and glucose were injected. ATCC *Pseudomonas aeruginosa*, ATCC *Staph. aureus*, and ATCC *E coli* were grown in MHB for 1 hr. All were adjusted to 3×10^8 org./ml. One-twentieth milliliter of these adjusted cultures was added to each vial except for *E. coli* which was first diluted 1:10. All vials were incubated for 3 hrs. The C-14 O_2 release was then quantitated on a Bactec R301 and recorded as metabolic index units (MIU). Percent inhibition was calculated as follows: 100 - [MIU for test vials/MIU for control vials]. The STDM was run in parallel and recorded as minimal inhibitory concentration (MIC).

Reproducibility was assessed by testing the same serum on 3 different days. Preliminary results suggest both reproducibility and good correlation between the STDM and radiometric method. The clinical application required the development of methods to inactivate antibiotics in patient sera. The radiometric method is now being tested in clinical infections. If further data are collected to confirm the good correlation with the STDM it may be possible to further develop the technique.

RADIOMETRIC ASSAYS OF ESSENTIAL NUTRIENTS IN FOODS. M.F. Chen, J.M. Whipple, and P.A. McIntyre. The Johns Hopkins Medical Institutions, Baltimore, MD.

There is a need for information on the nutrient value of vitamin B12 and folate content in foods. The standard official microbiological method for these vitamins is tedious and requires 3 days to complete. Radiometric microbiological assays have been developed for measuring the level of vitamin B12, folate and niacin in human serum, plasma and red blood cells. The assays are simple, sensitive and less tedious. In the presence of a suitable C-14 labeled substrate, the test organisms produced significant amounts of C-14 CO2 within 16-18 hrs. The C-14 CO2 evolved was quantitated in an ionization chamber and was proportional to the amount of the vitamin present.

Comparison of vitamin B12 content of a variety of foods, such as milk, liverwurst, chicken, pork, lamb, beef, fish, canned fish, oatmeal, and baby foods, showed that the radiometric assay gave B12 values comparable to the standard method ($r = 0.96$), and to published available values. Values obtained with the radiometric assay ranged from 13.4±1.5 µg of vitamin B12/100g of liverwurst to none detectable in baby food carrots. Recovery experiments using cyanocobalamin gave good results with foods of animal origin (106%) but were significantly lower (66%) from foods of vegetable or grain origin. Reproducibility on a variety of foods and replicate samples of the same foods by the radiometric technique was good. Since colored or turbid materials do not interfere with this technique, radiometric microbiological assays may prove to be most suitable for measuring the nutrient value of B12 and folate in foods, especially foods that are low in these essential nutrients.

(ABSTRACT WITHDRAWN)

A CLINICAL EVALUATION OF SERUM FERRITIN LEVELS AS AN INDICATOR OF MALIGNANCIES. K.Torizuka, R.Morita, M.Yoshii, K.Nakajima, and T.Kousaka
Kyoto University Hospital, Kyoto, Japan

To evaluate the usefulness of an assay of serum ferritin levels, we have measured serum ferritin levels in 35 normals and in 203 patients with various diseases by an immunoradiometric assay.

Elevated serum ferritin was seen in most cases with iron excess and acute hepatitis. In malignancies, the levels were markedly high in many cases. However, the range overlapped with that of non-malignancies.

There was no correlation between CEA and ferritin levels in benign or malignant cases. In hepatoma, all cases with negative AFP had markedly increased serum ferritin suggesting the assay is useful for hepatoma.

Serum ferritin significantly correlated with serum iron in normals and in iron deficiency anemia. In most non-malignant cases, the serum ferritin and iron levels distributed on a regression line obtained from normals and iron deficiency anemia. On the other hand, the ferritin levels were abnormally elevated relative to the iron levels in most malignant cases, and 92 % of the cases showed serum ferritin-iron ratio higher than normals. The estimation of the serum ferritin-iron ratio was thought to be an useful means for screening patients or in the differential diagnosis of a suspicious lesion.

CHANGES IN LEVELS OF PRECISION OF COMMON LIGAND ASSAYS DURING SEVEN YEAR INTERVAL. J.R. Hansell and G.T. Haven. Veterans Administration Hospital, Philadelphia, PA and University of Nebraska Medical Center, Omaha, NB.

Data obtained from as many as 970 laboratories subscribing to the Ligand Assay Interlaboratory Survey Programs of the College of American Pathologists were used to define changes in levels of analytic performance. Assays for serum thyroxine, triiodothyroxine, T3 uptake, TSH, cortisol, insulin, digoxin, folate and vitamin B12 were reviewed for periods of four to seven years. Documentation of change in the levels of performance was done by an intercomparison of the average of the coefficients of variation of all methods reported by subscribers. Varying degrees of improvement were demonstrated for each assay when certain biases were removed. These biases resulted when pool specifications were designed to study specific problems of sensitivity, crossreactivity and aberration of matrical protein concentration.

Assays for cortisol, folic acid, insulin and TSH showed the greatest rates of improvement; whereas, thyroxine and T3 uptake, which initially had the best precision at the commencement of the program, experienced smaller incremental improvements.

COMMERCIAL RIA KITS FOR HUMAN GASTRIN ANALYSIS: WHAT ARE THEY MEASURING? P. O. Reece and C. M. Heise. N. C. Baptist Hospital & Bowman Gray School of Medicine, Winston-Salem, N. C.

Of the 20 fractions with gastrin activity identified in human peripheral serum the most abundant, by far, have been designated as G-17-I, G-17-II, G-34-I and G-34-II. Ideally, an antibody used in clinical assays should measure each of these multimolecular forms with equal efficiency in order to be used as a diagnostic indicator of hypergastrinemia.

Two major commercial kits available were compared as to their reagent components and for their ability to measure gastrin in stimulated and in unstimulated human samples. Although the precision and the fasting normal ranges of the 2 kits were comparable, values for elevated gastrin samples were very different. In normal subjects following ingestion of food and in patients following secretin challenge, one assay resulted in changes in gastrin from baseline values several fold greater than the other. Both kits claim to use G-17 as standards and antigen and yet when standards of one kit were analyzed in the other kit very different concentrations of gastrin were measured. Cross-over studies with the kit standards resulted in non-parallel curves indicating both sets of standards could not have been the same molecular species. Elevated patient samples analyzed parallel in one kit but not the other.

Although it may be concluded that one of these kits is clearly superior to the other, neither kit provides sufficient information about antibody specificity for the user to know which species of gastrin is being measured in patient samples or what magnitude of response to challenge testing is considered "normal".

WEDNESDAY, JUNE 27, 1979

CONTINUING EDUCATION

8:30 a.m.-10:00 a.m.

I. RADIONUCLIDE EVALUATION OF THE GASTROINTESTINAL SYSTEM

Chairman: Leon S. Malmud, Temple University Hospital, Philadelphia, PA.

II. PEDIATRIC APPLICATIONS IN NUCLEAR MEDICINE

Chairmen: Gary F. Gates, Good Samaritan Hospital, Portland, OR; Judity Ash, Hospital for Sick Children, Toronto, Ontario, Canada; Philip O. Alderson, Johns Hopkins Hospital, Baltimore, MD.

III. QUALITY CONTROL IN RADIOIMMUNOASSAY: THE STATE OF THE ART

Chairmen: Eileen Nickoloff, Johns Hopkins Hospital, Baltimore, MD; Martin L. Nusynowitz, University of Texas Health Center at San Antonio, San Antonio, TX; Clara M. Heise, Bowman Gray School of Medicine, Winston-Salem, NC.

10:30 a.m.-12:00 p.m.

I. MEASUREMENT OF REGIONAL VENTILATION AND BLOOD FLOW; RADIONUCLIDE DETECTION OF DEEP VENOUS THROMBOSIS

Chairmen: Roger H. Secker-Walker, St. Louis University School of Medicine, St. Louis, MO; Philip O. Alderson, Johns Hopkins Hospital, Baltimore, MD; Fuad S. Ashkar, University of Miami School of Medicine, Miami, FL.

II. TUMOR IMAGING

Chairmen: Paul B. Hoffer, Yale University School of Medicine; William D. Kaplan, Sidney Farber Cancer Institute, Boston, MA.

III. RECENT ADVANCES IN RADIOPHARMACEUTICALS

Chairmen: Michael J. Welch, Washington University, St. Louis, MO; Joanna S. Fowler, Brookhaven National Laboratory, Upton, NY; Michael D. Loberg, University of Maryland School of Medicine, Baltimore, MD.

1:30 p.m.-3:00 p.m.

I. MANAGEMENT OF THYROID CARCINOMA

Chairmen: David V. Becker, The New York Hospital-Cornell Medical Center, New York, NY; William H. Beierwaltes, University of Michigan Medical Center, Ann Arbor, MI; Ernest L. Mazzaferri, University of Nevada, Reno, NV; James R. Hurley, The New York Hospital-Cornell Medical Center, New York, NY.

II. CRITICAL COMPARISON OF BRAIN IMAGING TECHNIQUES

Chairmen: Frederick S. Mishkin, Martin Luther King, Jr. General Hospital, Los Angeles, CA; Frank H. DeLand, University of Kentucky Medical Center, Lexington, KY; Dennis D. Patton, University of Arizona Health Sciences Center, Tucson, AZ.

III. PROGRESS IN NUCLEAR MEDICINE INSTRUMENTATION

Chairmen: James C. Carlson, Hackley Hospital, Muskegon, MI; William R. Hendee, University of Colorado Medical Center, Denver, CO; Trevor D. Cradduck, Victoria Hospital, London, Ontario, Canada.

3:15 p.m.-4:15 p.m.

I. RADIONUCLIDE EVALUATION OF RENAL STRUCTURE AND FUNCTION

Chairmen: Edward G. Bell, Crouse-Irving Memorial Hospital, Syracuse, NY; John C. McAfee, State University of New York, Syracuse, NY.

II. CLINICAL USE OF INDIUM-111 LABELED LEUKOCYTES AND PLATELETS

Chairman: David A. Goodwin, V.A. Hospital, Palo Alto, CA.

III. NUCLEAR MEDICINE COMPUTERS: WHAT THEY DO; HOW THEY DO IT

Chairman: Stephen L. Bacharach, Ph.D., National Institutes of Health, Bethesda, MD.

9:00 a.m.-11:00 a.m.

DIAGNOSTIC APPLICATIONS OF NUCLEAR MAGNETIC RESONANCE: A PROGRAM OF THE COUNCIL ON CORRELATED IMAGING OF THE SOCIETY OF NUCLEAR MEDICINE

Chairman: James J. Smith, Director, Nuclear Medicine, Veterans Administration Central Office, Clinical Professor of Radiology (Nuclear Medicine), George Washington University Medical School;

Moderator: Suzanne B. Knoebel, Krannert Professor of Medicine, Indiana University College of Medicine.

AGENDA

Nuclear Magnetic Resonance Imaging. Paul Lauterbur, Professor, Department of Chemistry, State University of New York at Stony Brook.

In Vivo Measurements of Energy Metabolism Using Nuclear Magnetic Resonance. Eric Fossel, Professor of Biophysics, Harvard Medical School.

Phosphorous Nuclear Magnetic Resonance in the Heart. Donald Hollis, Associate Professor of Physiologic Chemistry, Johns Hopkins Hospital.

In Vivo Blood Flow by Nuclear Magnetic Resonance. Jerome Singer, Professor, Department of Electrical Engineering and Computers, University of California at Berkeley.

The Future of Nuclear Magnetic Resonance Imaging. Waldo S. Hinshaw, Associate Physicist, Massachusetts General Hospital.

DISCUSSION

THURSDAY, JUNE 28, 1979

8:30 a.m.-10:00 a.m. Exhibit Hall

MIXED POSTER SESSION I

RENAL/PULMONARY/BRAIN/ ENDOCRINE/G-I/HA

Chairman: John G. Weir, Jr.
Co-Chairman: William E. Betts

TRANSVERSE SECTION PERFUSION IMAGING IN PERIPHERAL DISEASE. G.L. Brownell, S.Cochavi, D.R. Elmaleh, C.A. Athanasoulis, Massachusetts General Hospital, Boston, MA 02114

Equilibrium imaging following continuous inhalation of $C^{15}O_2$ has been used to determine blood flow in the brain. We have explored the possible application of similar techniques to the measurement of blood flow in disease states of the lower limbs. Both conventional and transverse section images are obtained. Preliminary results in animals and man indicate that the technique may be useful to determine the extent of disease and the effect of therapy. Continuous inhalation of O_2 may yield information on oxygen extraction fraction. Further studies are required to validate the models employed.

Limited studies have been carried out in patients undergoing therapy for cancer in the leg. Marked changes of vascularity before, during and after radiation therapy may be observed. One patient with occlusive vascular disease in the legs was imaged before and after transluminal vessel dialation. Finally animal studies show increased perfusion in tumor and changes in vascularity as a result of hyperthemia.

Tc-99m DMSA RENAL IMAGING: A COOPERATIVE CLINICAL STUDY. A. Khentigan, T.G. Rudd, E. Liff, P.M. Weber, and L.V. dos Remedios. Medi-Physics, Inc., Emeryville, CA, University of Washington Hospitals, Seattle, WA, Kaiser-Permanente Medical Centers, San Francisco and Oakland, CA.

This study was performed to demonstrate the clinical utility of Tc-99m DMSA renal imaging. Renal scintigraphy was usually performed 1 to 2 hours after the administration of 5 mCi of Tc-99m DMSA using Anger type cameras. A total of 206 studies were performed on 192 patients having known or suspected renal disease. Technetium-99m DMSA study findings were compared to the final diagnosis, i.e., presence or absence of renal disease and analyzed for the correlation coefficient (0.94 ± 0.025; $P<0.001$), sensitivity (0.954), specificity (0.988), accuracy (0.969), false positive ratio (0.012) and false negative ratio (0.046). Technetium-99m DMSA studies were similarly compared and analyzed with the results of radiologic procedures (IVP and arteriography), radionuclide renography and tissue examination. The correlation with IVP results were highly statistically significant ($P<0.001$) and in four patients demonstrated the presence of renal parenchymal disease not noted on the IVP. Renal images were safely obtained in patients allergic to radio-opaque contrast media. In the presence of advanced renal failure an unsatisfactory initial study could occasionally be improved somewhat by delaying imaging from 6 to 24 hours. The study demonstrates the diagnositic sensitivity of Tc-99m DMSA in the evaluation of renal parenchymal abnormalities.

IODOHIPPURATE I-123 RENOGRAPHY (I-123 OIH): A COOPERATIVE CLINICAL STUDY. A. Khentigan, T.G. Rudd, L.R. Bennett, P.M. Weber, R.E. Coleman, D.G. Pavel, and T.J. Conway. Medi-Physics, Inc., Emeryville, CA, University of Washington Hospitals, Seattle, WA, University of California, Los Angeles, CA, Kaiser-Permanente Medical Center, Oakland, CA, University of Utah Medical Center, Salt Lake City, UT, University of Illinois, Chicago, IL, and Children's Memorial Hospital, Chicago, IL.

At total of 177 I-123 OIH renography studies were performed on adults (80) and children (75) having known or suspected renal disease including obstructive uropathy, renal failure, inflammatory disease, renovascular disease, and renal transplant complications. Iodine-123 OIH study findings were compared to the final diagnosis, i.e., presence or absence of renal disease, and analyzed for the correlation coefficient (0.90 ± 0.04; $P<0.001$), sensitivity (0.99), specificity (0.88), false positive ratio (0.012), false negative ratio (0.008) and accuracy (0.97) in children and adults. Renography study findings were similarly compared and analyzed with the results of available radiologic procedures (IVP, retrograde pyelography/ cystourography) arteriography/ surgery/ pathology, and ultrasonography/computerized tomography. Iodine-123 OIH study results correlated well with conventional pyelography ($P<0.001$) and provided useful diagnostic data in patients with obstructive uropathy regardless of the level of obstruction. The unique attributes and high photopeak efficiency of I-123 OIH were especially useful in assessing renal function in patients with advanced renal failure, serial transplant evaluations, and in those patients in which other standard techniques might be contraindicated. Iodine-123 OIH was found to be an extremely sensitive indicator of the presence of renal disease.

I-123 FIBRINOGEN SCINTIGRAPHY IN THE DIAGNOSIS OF ALLOGRAFT REJECTION. M.A. Swanson, S. Chatterjee, S.J. DeNardo; University of California Davis Medical Center, Sacramento, Ca

Previous studies with I-125 and I-131 fibrinogen have shown that quantitative uptake determinations with a surface probe detector are unable to differentiate allograft rejection from perirenal hematoma, hydronephrosis or vascular thrombosis. In the present study, 37 transplant recipients were evaluated with I-123 fibrinogen, using both renal scintigraphy and a renal fibrinogen uptake index (RFUI) to identify patients with accelerated renal fibrin deposition associated with rejection.

Following I.V. injection of I-123 fibrinogen, 1-2 mCi, 24° images of transplant (T) and cardiac blood pool (CBP) were obtained with a scintigraphic camera interfaced with a dedicated medical computer. A region of interest computer program was used to determine count/unit time/unit area in each organ from which a RFUI was generated ($counts_T/count_{CBP} \times 100$). Scintigraphic findings and the RFUI were correlated with the presence or absence of rejection based on clinical, biochemical and histologic criteria. Results are shown in Table 1:

	no. of patients	mean RFUI%	range RFUI%
Normal	16	60	51-70
ATN	9	41	27-47
Rejection	10	130	75-262
Perirenal hematoma	2	150	80, 220

RFUI differentiated normal, ATN and rejecting kidneys. Renal scintigraphy was necessary to differentiate perirenal hematomas from rejection. These findings indicate that I-123 fibrinogen is a sensitive and specific agent in the diagnosis of active allograft rejection. Support: ACS PDT 94A

THE USE OF Rb-82 FOR THE DETERMINATION OF RENAL BLOOD FLOW (RBF). J.B. Bingham, S. Cochavi, R.H. Moore, H.W. Strauss, K.A. McKusick, H. O'Brien. Massachusetts General Hospital, Boston, MA and Los Alamos National Laboratories, Los Alamos, NM.

Studies were performed in 11 anesthetized dogs to assess whether Rb-82, a generator produced positron emitting radionuclide with a $T_{\frac{1}{2}}$ of 75 seconds could be used to repeatedly measure RBF. Partial occlusion of the left renal artery was obtained by snare, the right kidney acting as control. A bolus of 10-15mCi of Rb-82 was injected into the left atrium at the same time as 25μ diameter radioactive microspheres (M/S) (I^{125}, Ce^{141}, or Sc^{46}). An arterial blood sample was obtained for 2

minutes following injection of isotopes. Imaging was performed with a positron camera from 2 to 3 minutes after injection. Blood sample was included within the field of view of the camera for calculating absolute RBF. At least 3 measurements were made in each animal. Region of interest analysis was performed on renal uptake of Rb-82 after background correction and of arterial sample. Kidney and blood samples were then counted in well counter to determine M/S content as an independent measure of absolute RBF.

Divided renal uptake of Rb-82 correlated well to M/S distribution (r=0.94) over a range of 0 to 491mls/100g RBF. Repeated measurements of blood flow in the control kidney showed variation of 184 to 530mls/100g. Determination of absolute RBF by Rb-82 showed good correlation with that determined by M/S (r=0.86). These results indicate that Rb-82 is a very suitable isotope for rapid, repeated measure of RBF.

EVALUATION OF RENAL FUNCTIONAL RESERVE WITH CORTICAL REGIONS OF INTEREST. M.D. Blaufox, F.Iloreta, S.Heller, R.Bard and L.Freeman. Divisions of Nuclear Medicine, Albert Einstein College of Medicine, Bronx, N.Y.

Renal cortical regions of interest have been used for prediction of recoverable renal function in obstructive uropathy. Prospective objective evaluation of the technic is sparse in the literature. This study critically evaluates the use of cortical regions of interest in predicting recoverability of renal function prospectively in patients with unilateral or bilateral obstructive uropathy (24 patients,age 14 to 75 yrs). Thirty-four kidneys with acute or chronic obstruction were studied. Renogram curves were generated from areas of interest including the entire kidney and from cortical regions of interest. Pre-op curves were evaluated to determine if the cortical curve improved toward normal compared to the total renal curve. Post-op curves were subsequently evaluated to determine the degree of return of renal function and relief of obstruction. The pre-op cortical curve improved in 64% of patients who improved post-op while 75% of patients who failed to improve post-op were predicted by the cortical curve. Patients with severe impairment of renal function yielded poor correlation of the pre-op cortical curve with post-op results. These data suggest that potential recoverability of renal function correlates well with the ability of the cortical curve to show a reversal pre-op. Of potentially greater use to the surgeon in kidneys with normal or moderate functional impairment is the ability of the cortical curve to predict a poor response to surgery in the immediate post-op period. This test should prove useful to the urologist in choosing those patients in whom surgical repair is indicated or the likelihood of successful surgical repair is poor.

QUANTITATIVE AND REGIONAL EVALUATION OF THE UNEVENNESS OF THE VENTILATION IN CHRONIC OBSTRUCTIVE PULMONARY DISEASE. T. Suzuki, Y. Ishii, D. Hamanaka, K. Yamamoto, K. Torizuka. Kyoto University School of Medicine , Kyoto, Japan.

Radioaerosol scintigraphy provides evidence of regional abnormalities in the airway dynamics in patients with chronic obstructive pulmonary disease(COPD). Though abnormal aerosol deposition is apparant, we may fail to evaluate the regional abnormalities in terms of the overall unevenness of the ventilation. We assessed this unevenness in aerosol scintigraphic findings by correlating them with the single-breath nitrogen washout test. The slope of the phase III in this washout test reflects the ventilation in the small airways and alveoli near functional residual capacity level.

We examined 36 patients with COPD in various stages. Tc-99m aerosol of 2μ or less in size was inhaled during quiet tidal breathing. These scintigraphic images were compared with the single-breath nitrogen washout test and conventional pulmonary function tests performed on the same day.

We classified these findings into 4 grades according to the extent of peripheral irregularity and hot spot formation. We observed a greater correlation of the aerosol grading with the slope of the phase III than FEV1.0(%), but less correlated with closing volume. Closing Volume was well separated only in early stage I and II of the aerosol grading and was zero in the most severe stage IV.

The slope of the phase III is a good index for evaluation of the overall unevenness of aerosol scintigraphy of COPD and it reflects the regional difference in proportion to the severity of airflow obstruction. The combination of the single-breath nitrogen washout test and aerosol scintigraphy gives a quantitative and regional evaluation of airflow obstrution in pheripheral airways in COPD.

GATED REGIONAL SPIROMETRY. J.J. Touya, R.R. Price, J.A. Patton, J. Erickson, J.P. Jones and F.D. Rollo. Vanderbilt University Medical Center, Nashville, TN.

A method for producing quantitative images of regional lung volumes has been developed and the patterns for normal males and females determined. The technique utilizes representative images from resting and forced ventilatory cycles which were obtained by gated analysis of continuously recorded data while the subject rebreaths 3 mCi Xe-133/liter of air. Collected raw data consist of PA and AP views of resting and forced ventilation. Four basic images per view were formed by adding frames corresponding to peaks and valleys on time activity curves from each set of raw data. A fifth image was formed by adding frames corresponding to one second after peaks on the sets of forced ventilation. Using a linear transformation, the images of each view were mapped to correspond with the image of the end of forced expiratory effort. Mapped images (background corrected) were converted from counts per pixel to units of detected volume per pixel. The conversion factors were the ratio between expired air and the difference in counts between inspiratory and expiratory images. Using these images the following parametric images were determined: total lung capacity, residual volume, vital capacity, tidal volume, functional residual capacity, expiratory reserve volume, inspiratory capacity and forced expiratory volume. In thirty-eight normal volunteers normal patterns from apex to base for each parametric image were computed for both males and females and were shown to compare favorably with conventional spirometric volumes determined on the same day. Gated regional spirometry in COPD patients differed significantly from normal.

VALUE OF 24-HOUR TC-99m BRAIN SCANS. H.L. Chandler, and D.R. DeMaster. Mount Auburn Hospital, Cambridge, MA.

We evaluated Tc-99m brain scintigrams performed following long delay (LD) at about 24 hr after radionuclide (RN) administration. From Apr. 1977 to Jan. 1979, 224 LD brain scans were done using Tc-99m DTPA or pertechnetate. All of these also had early (E) scintigraphy at 2 hr or delayed (D) scans at 2-8 hr or both. Of 180 E scans, 19% were abnormal; of 59 D scans 34% were abnormal; and 46% of LD scans were abnormal. The final clinical diagnosis for the 224 LD studies included 106 cortical infarcts, 15 primary or metastatic tumors, and 8 subdural hematomas (SDH). Diagnosis was based on clinical data, CT, arteriography, surgery, and autopsy as available.

Of 106 infarcts, 19% were positive E, 59% D and 74% at LD. No infarct escaped detection at 24 hr when visible earlier, and density of the abnormality was almost always greater at LD.

LD scans uniquely demonstrate abnormalities in stroke patients early after the onset of the CNS event. At 24 hr after onset, 76% of LD scans in 17 patients were positive; within the first 7 days after onset, 69% of 88 patients had positive LD scans.

All 8 SDH patients had positive LD scans, and 6 of 7 E scans were also positive. In all studies, the density of the abnormality was greater at LD.

In tumor patients, 60% of E scans were positive compared with 73% at LD. Several LD scans showed some fading of the abnormality.

Though the ideal time after injection for scans is not known, our data indicate: (1) a higher positive yield and

(2) frequent early diagnosis after infarct by LD scans. The underlying biologic basis for our observations in LD scans deserves study.

RADIONUCLIDE EVALUATION OF SUSPECTED CEREBROSPINAL FLUID SHUNT MALFUNCTION: CLINICAL CORRELATION. P.W. Hayden, T.G. Rudd, D.B. Shurtleff, University of Washington and Children's Orthopedic Hospital & Medical Center, Seattle, Wa.

Experience with radionuclide cerebrospinal fluid (CSF) shunt patency assessment over the past 7 years was reviewed and correlated with clinical outcome in patients studied for suspected shunt malfunction.

640 studies in 273 patients were reviewed: 401 studies were done because of suspected shunt malfunction (221 pts.). The CSF shunt reservoir was entered percutaneously, the pressure determined, then 0.025-0.1 mCi Na pertechnetate was injected and observed for clearance. In all cases the results of the RN test were correlated with final clinical outcome.

233 studies (57%) showed abnormal shunt function; in 142 of these cases the shunt was revised. 168 studies (43%) showed normal shunt function; only 14 of these were revised. Correlation with subsequent clinical outcome was excellent with test results reflecting the true state of shunt function in 95%. The test was extremely sensitive (1% error) for detecting malfunction distal to the reservoir and in most instances specifically localized the level of obstruction including intra-abdominal loculation of CSF. Of the 7 errors in test results, 5 involved intermittent or partial obstruction proximal to the reservoir. In many instances test results significantly altered management; particularly in the symptomatic group with normal shunt studies (38%) for whom emergency or unnecessary shunt revision was avoided. No complications of the test procedure were observed.

Radionuclide assessment of shunt patency and function is a useful clinical tool in management of patients with suspected CSF shunt malfunction.

CALVARIAL MARKINGS ON BONE SCAN--SUTURES OR VASCULAR GROOVES? C.L. Blei, R.A. Cano, G.S. Johnston, A.E. Jones. National Institutes of Health, Bethesda, MD; Walter Reed Army Hospital, Washington, D.C.

Intense circles and lines in the calvaria posterior to the orbits may be confused with metastasis. To study these markings, the authors examined 128 randomly collected known normal Technetium-99m diphosphonate bone scans. These bone scans showed characteristic patterns categorized as 1) coronal and/or lambdoidal lines (sutures), 2) spots posterior to orbits (circles), and 3) horizontal lines curving either backward or forward from the retro-orbital area (vascular grooves).

Of these 128 studies, 100 were adult cases: 50 men and 50 women. Three fourths of the adult cases had symmetric patterns with slightly asymmetric intensities. The 100 cases contained 58 circles, 30 coronal sutures, 26 without markings, 12 vascular grooves, and 3 lambdoidal sutures. The 28 pediatric cases (20 boys and 8 girls, ages 1 to 16 years) contained 11 circles, 10 coronal sutures and 1 posterior vascular groove.

Studies of cadaveric skull and roentgenograms revealed that 1) sutural markings on bone scan correlate with sutural sclerosis on roentgenograms, 2) the circles represent the tunnel of the middle meningeal artery on the inner table of the calvaria below the pterion, and 3) the horizontal lines are the orbital branch and the occipital portion of the anterior branch of the middle meningeal artery.

In conclusion, all of these calvarial patterns investigated are variations of normal anatomy.

REGIONAL LUNG FUNCTION IN ASBESTOS WORKERS. R.Secker-Walker and J.E. Ho. St. Louis University School of Medicine, St. Louis, MO.

We have studied regional lung function in 9 workers whose exposure to asbestos varied from 10-36 years. Detailed clinical evaluation, pulmonary function testing and ventilation-perfusion studies were performed on each man. Regional ventilation was studied in the upright position using Xe-133, with a 3 min washin and subsequent washout breathing air. Four view perfusion scans were obtained with Tc-99m macroaggregates, injected in the upright position. The workers' ages ranged from 48-65 yr, mean 58; asbestos exposure 2-36 yr, mean 25; smoking-pack yr 0-74, mean 34; 8 workers had dyspnea and cough, and 4 chest pains; clubbing was present in 3, basal rales in 6. Pulmonary function tests showed a restrictive pattern in 2,a mixed restrictive and obstructive pattern in 1 and an obstructive pattern in 6. Chest x-rays showed interstitial fibrosis in 7 (lower zones 6, upper zones 1), pleural thickening in 6 and emphysematous bullae in 4. Two perfusion scans were normal, 1 of these men had minimal interstitial fibrosis, the other none. In 6 workers with interstitial fibrosis, defects in blood flow corresponded closely to the regions with interstitial changes, but were also present in the bullous areas when these were visible radiographically. Delayed clearance of Xe-133 was most marked in the fibrotic areas in the 3 workers with the worst fibrosis and the most severe airflow obstruction (maximum mid-flow rate <35% predicted); in the other 4 with interstitial fibrosis, clearance was rapid from the fibrotic areas, but delayed from the rest of the lungs in 3, and normal in 1. Delay in Xe-133 clearance was more closely related to the severity of airflow obstruction and pack-years of cigarette smoking than to asbestos exposure.

QUANTITATIVE GASTRO-CHOLECYSTOSCINTIGRAPHY: COMPARISON OF RESPONSE TO AN ORAL MEAL OR I.V. CHOLECYSTOKININ (Cck). F.Stelzer, L.S.Malmud, R.S.Fisher, R.Tolin, R.Menin, P.T.Makler,Jr., and J. Reilley. Temple University Hospital, Philadelphia, PA

Normal digestion and absorption of nutrients is dependent in part upon coordination between gastric emptying and delivery of bile into the duodenum. A dual-isotope scintigraphic technique, employing 5 mCi Tc-99m HIDA (I.V.) and 250 uCi In-11-DTPA (orally) in a standard liquid meal, has been employed to visualize and quantitate gall bladder and gastric emptying simultaneously. The In-111-DTPA labelled meal was administered one hour following intravenous administration of the Tc-99m-HIDA to a fasting patient and the meal served as a stimulus to gall bladder emptying, as well as, a gastric marker. Gall bladder emptying was significantly delayed in patients with gallstones (GS) and following Bilroth II hemigastrectomy and gastrojejunostomy (BVG), in comparision to normals. When Cck was used as the stimulus for gall bladder emptying, rather than a meal, gall bladder emptying was accelerated in normals, but not significantly so ($p<.05$). In patients with gallstones, either Cck (I.V.) or a standard liquid meal consisting of 80 gm fat, 72 gm protein, 138 gm carbohydrate, in 300 ml, revealed delayed gall bladder emptying. Thirty five patients were studied: 10 normals, 10 patients with gallstones, but no evidence of acute cholecystitis, and 15 patients following BVG. We conclude that delayed gall bladder emptying in patients with gall stones or following BVG, can be demonstrated following either a meal stimulus or Cck, and that the abnormality in emptying cannot be attributed to an abnormality in Cck release.

DEXAMETHASONE SUPPRESSION (DS) ADRENAL SCINTIGRAPHY IN HYPERANDROGENISM. M. Gross, J. Freitas, D. Swanson, and W. Beierwaltes. University of Michigan Medical Center, Ann Arbor, MI.

Hyperandrogenism (HA) is a common endocrinopathy in women. To access the contribution of adrenal androgens in patients with HA, 6β-[I-131]-iodomethylnorcholesterol (NP-59) DS adrenal scintiscans were performed on 31 women with HA. Criteria for HA were increased facial or body hair and irregular or absent menses. DS was performed using either 8 mg for 2 days or 4 mg for 7 days prior to the injection of 1-2 mCi of NP-59 and continued throughout the imaging sequence. Scans were interpreted as abnormal if adrenal visualization occurred prior to 3 days (8 mg DS) or 5 days

(4 mg DS), or if lateralization of uptake was seen on 2 successive days. Plasma testosterone (T) and urinary 17-ketosteroids (17-KS) were obtained on all patients both pre and post DS.

Fourteen (N) of 31 patients had normal adrenal scans. Pre DS, 11/14 of N, had elevated T and 14/14 had normal 17-KS; whereas post DS, 14/14 had suppressed T and 17-KS. Twelve (H) of 31 had scans consistent with adrenal hyperplasia. Mean T and 17-KS in H were higher than in N, but showed a response to DS. The scan diagnosis has been confirmed in 7/12 of H by adrenal venous sampling (AVS). Five (AA) of 31 had localizing scans consistent with adrenal adenoma. T and 17-KS were higher in AA than in N or H and had minimal responses to DS. Adrenal adenomas have been resected in 2 of AA and confirmed in another 1 by AVS.

These data indicate that a significant number of women with HA have adrenal derived androgens as a contributing factor to their disease. DS adrenal scintigraphy can be used in HA as a non-invasive technique to identify those women with adrenal hyperplasia or adenoma.

ADRENAL GLAND AND ECTOPIC ADRENAL TISSUE IMAGING IN CHILDREN WITH CONGENITAL ADRENAL HYPERPLASIA. G.N. Fotiadis, J. Sotos, and S. Vasquez. Children's Hospital, Columbus, OH.

The adrenal imaging radiopharmaceutical 131-I-6β-iodomethyl-19-norcholesterol(NP-59)was used to study 7 children with congenital adrenal hyperplasia(CAH)who were suspected to have nonsuppressible adrenal tissue in the adrenal glands or ectopically in the gonads.

Of 6 patients who had elevated urinary excretion of steroids despite adequate replacement therapy, 5 showed a significant gonadal and/or adrenal uptake of the radiopharmaceutical. Only the testes were visualized(accumulating 0.04 to 0.13% of the injected dose)in 2 males with confirmed histologic diagnosis of adrenal rest cell tumors of the testes; only the adrenal glands were visualized in 2 patients(0.79 to 1.18% uptake)indicating that adrenal was the origin of the nonsuppressed steroids; in a male with known ectopic tumors, the adrenals and the ectopic tumors in the testes accumulated activity indicating a dual source of his nonsuppressible steroids. All ectopic adrenal tissues were biopsy proven and shown to produce corticosteroids.

A female with nonsuppressible steroids showed only faint visualization of her adrenals but no activity was found in the region of her ovaries as postulated.

Finally a male with adrenal rest cell tumors of the testes but successfully suppressed showed no activity in neither the adrenals nor the testes.

The observations indicate that NP-59 is useful in detecting nonsuppressed adrenal adenomatous tissue in either the testes or the adrenal itself in CAH. This technique is also viewed as an aid for the early diagnosis of the complications occurring in children with CAH.

ARTERIAL LIVER PERFUSION SCINTIGRAPHY IN PATIENTS RECEIVING 5-FLUORODEOXYURIDINE INFUSION THERAPY. J. Muz, A. Dincogru, S.S. Figiel and V.K. Vaitkevicius, Harper Division, Harper-Grace Hospitals, Detroit MI

The purpose of this study is to evaluate the usefulness of arterial liver perfusion scintigraphy in patients with neoplastic liver disease receiving 5-Fluorodeoxyuridine (5-FUDR) infusion therapy. Approximately 4mCi of Tc-99m sulfur colloid were slowly injected via a hepatic artery infusion catheter. During and immediately after injection, sequential scintigrams were obtained utilizing a large field of view scintillation camera, and simultaneously forty one-second images were acquired on a medical computer. Subsequently, static images of the liver were obtained in four projections. Thirty-three patients were studied by this technique; 13 had single studies and 20 had multiple studies. Scintigraphic studies were correlated with hepatic angiographic studies performed on these patients. In 17 patients there was normal flow of the radionuclide to both lobes of the liver. Occlusion of the hepatic artery or its branches was demonstrated in eight patients. In four of these eight patients, there was flow to the spleen and from the spleen via splenic vein and portal vein to the liver. Extravasation of the radionuclide was demonstrated in four patients. Three patients experienced abdominal pain during injection. In our experience, arterial liver perfusion scintigraphy is a simple and very useful modality in evaluation of hepatic perfusion during 5-FUDR infusion therapy. It allows us to determine the position and patency of a catheter, the distribution of flow, occlusion of hepatic artery and extravasation.

GALLBLADDER AND BOWEL LOCALIZATION OF BONE IMAGING RADIOPHARMACEUTICALS. J.J. Conway, S.C. Weiss, A. Khentigan, A.J. Tofe, and T.T. Thane, The Children's Memorial Hospital, Chicago, IL

Since October, 1977, approximately 5-10% of bone scans performed at The Children's Memorial Hospital have demonstrated gallbladder and/or bowel localization of the radiopharmaceutical. The most frequent appearance of the radionuclide is within the cecum and ascending portions of the colon. The etiology for this localization is uncertain. Such factors as the patient's sex, age, disease, nutritional status, time of day or week, and pharmaceutical preparation do not seem of significance.

Phosphate radiopharmaceuticals are minimally metabolized by the liver and excreted into the gallbladder and/or small bowel. Its appearance in the cecum presumably is secondary to concentration via water absorbtion. Factors which probably enhance this localization are rapid bowel motility, delayed imaging times, improved resolution of imaging systems, an awareness of its appearance, and unknown factors which may be related to the radiopharmaceutical.

The significance of this finding is to alert practitioners to this variation of distribution of bone imaging radiopharmaceuticals and prevent a misinterpretation of bowel localization as an abnormal finding. The impact upon the evaluation of disorders such as abdominal masses, metastatic disease of the pelvis, and bowel necrosis is evident.

DECISION MAKING AND BAYESIAN ANALYSIS AS DEMONSTRATED BY A CLINICAL QUESTIONNAIRE. H. Agress, Jr. Hackensack Hospital, Hackensack, NJ.

In view of the recent emphasis on decision making and the accuracy of diagnostic testing, a study was performed involving a "test" questionnaire given to 118 physicians and medical students of varying backgrounds. The questionnaire was created to determine the physician's ability to handle the analysis of statistical data (sensitivity, specificity, a priori probability and associated predictive value) in a simplified clinical situation. This study analyzes the physicians' answers, as well as presenting a discussion of the proper approach to such problems. This discussion includes both a non-statistical diagrammatic explanation and a Bayesian analysis, in addition to a graphic demonstration of how predictive values change with increasing a priori values.

Of the 118 examinees, 72%.answered the test incorrectly, and 28% arrived at the correct answer. The main reasons for obtaining the incorrect answers were 1) misunderstanding of the concepts of "false" positives and "false" negatives (i.e., sensitivity and specificity), and 2) underestimation of the marked effect of the disease incidence in the population upon the predictive value of a diagnostic test.

73% felt the test question was a reasonable analogy to daily problems. A practical illustration of the clinical significance of this study would be represented by Thallium-201 myocardial imaging in populations with very low incidence of cardiac disease.

The results of this study demonstrate the necessity for further education of physicians in handling decision making problems.

8:30 a.m.-10:00 a.m. Room 211

CLINICAL APPLICATIONS

RENAL/ENDOCRINE

Chairman: Frank H. Allen
Co-Chairman: Edwin R. Holmes, III

DIURETIC RENAL SCANS IN PEDIATRIC HYDRONEPHROSIS. J.M. Ash, E. Kass, and D.L. Gilday, Hospital for Sick Children, Toronto, Ont.

In children presenting with hydronephrosis or intravenous pyelograms (IVP), it is difficult to be certain whether there is significant renal obstruction. Many kidneys may retain the appearance of persisting obstruction several years post-operatively or have dilated collecting systems for other reasons such as reflux or infection.

In such patients, a renal scan using Tc-99m DTPA without a diuretic agent is initially performed. Sequential timed images of the kidneys are taken up to 30 minutes with the child prone and well hydrated. After voiding, Lasix (0.5 mg/kg) is given intravenously and a second set of sequential timed images taken for another 30 minutes. The first 15 minutes of the diuretic study is recorded into a computer and time-activity curves of the renal pelves generated. These are automatically plotted on a semi-logarithmic scale and clearance half-times calculated.

We have studied 63 renal units in this way. Twenty-eight of the 63 kidneys were clinically normal with normal IVP's and served as controls. All had normal Lasix renal scans. Thirty-five of the 63 kidneys showed hydronephrosis on IVP. Of the 35, 25 which were clinically stable had normal Lasix studies, including 6 with both normal Lasix and Whitaker tests. The remaining 10 hydronephrotic kidneys were subsequently proven to have ureteropelvic junction obstruction at operation. Eight had positive Lasix renal scans and positive Whitaker tests, 2 had positive Lasix scans with negative Whitaker tests.

The diuretic renal scan using clearance half-times has proven to be a clinically valuable method which may replace more invasive ones for diagnosing renal obstruction and for following improvement in drainage post-operatively.

IMAGING RENAL BLOOD FLOW, ANATOMY, AND EXCRETION WITH Tc-99m METHYLENE DIPHOSPHONATE. E.C. Glass, H.H. Hines, J.C.Cronin, A.L. Smith, G.L. DeNardo. University of California, Davis, Medical Center, Sacramento, CA

Tc-99m methylene diphosphonate (MDP) is rapidly excreted by the kidneys. We evaluated its potential use as a renal imaging agent in 20 patients (pts) injected with 10-20 mCi MDP for routine bone imaging. Sequential images of renal blood flow and clearance were recorded on film and on computer disk for 20 minutes immediately after injection.

The first-pass blood flow studies were of high quality. Subsequent images showed a clear, rapid progression of activity from cortex to bladder in 18 nonazotemic pts. Renograms with MDP showed times to peak activity (mean ± SEM) (3.9 ± 0.3 min) that did not differ significantly from those of renograms from 12 normal control pts studied with radiohippuran. Early sequential renal images did not appear perturbed by rib activity, and in 19/20 pts the early images were vastly superior in quality to delayed images obtained at the time of bone scanning. Ratios of renal/vertebral activity were higher in early images than in delayed images obtained at the time of bone scanning (mean ± SEM)(2.56 ± 0.16 vs. 0.54 ± 0.04, $p<.001$). Ratios of renal/infrarenal background activity were also higher in early images (4.26 ± 0.33 vs. 2.60 ± 0.31, $p < .001$). These studies revealed anomalies or abnormalities of renal blood flow, anatomy, or excretion in 11/20 pts, and in 8 of these 11, the abnormalities were undetectable or inapparent on later bone images.

In conclusion, these findings indicate that MDP is a practical agent that is useful in the evaluation of renal blood flow, anatomy and excretory function. Sequential imaging begun immediately after injection provides optimal images for these purposes.

DETECTION OF OBSTRUCTIVE UROPATHY USING TC-99m DTPA. R.B. Grove, T.A. Powers, J.A. Harolds, W.B. Jones, S.C. Orr, R.E. Melton, and R.D. Bowen. Veterans Administration Medical Center, Nashville, TN.

A simple, accurate test with no morbidity which was effective for the detection of obstruction in patients with both normal and impaired renal function would be of significant clinical utility. The purpose of this study was to evaluate the ability of the Tc-99m DTPA renal scan to detect the presence or absence of obstruction of the collecting system. Of 107 patients having recent DTPA studies, 31 had definite confirmation of the presence or absence of obstruction by intravenous urography, retrograde pyelography, or other definitive procedure. Of these 31 patients, 22 had diminished renal function (serum creatinine>1.4 mg%, range 1.4-15.3, median 4.3). Patients were studied in the posterior projection with perfusion images following intravenous injection of 20 mCi of Tc-99m DTPA. Multiple static images of the urinary tract were obtained from 1-30 minutes postinjection. Obstruction was defined as abnormal retention of activity in the collecting system persisting in the delayed images. DTPA correctly identified 13 of 13 patients subsequently proven to have obstruction and 17 of 18 patients found to have no obstruction. One false positive result was due to ectasia of the ureter. There were no false negatives. These data indicate a sensitivity of 100%, specificity of 94%, and accuracy of 97%. The high sensitivity, specificity, and accuracy of the DTPA renal scan in the detection of obstruction indicate that it may provide an alternative to intravenous urography and retrograde pyelography for the detection of obstruction of the urinary tract, particularly in patients with impaired renal function.

NUCLEAR RENAL IMAGING IN ACUTE PYELONEPHRITIS. H. Handmaker B. Young and R. Fay. Children's Hospital of San Francisco, San Francisco, California.

The purpose of this report is to document the success in the use of renal cortical imaging agents (Technetium-99m DMSA and Technetium-99m glucoheptonate) in the initial diagnosis and management of patients with acute pyelonephritis. Patients with acute pyelonephritis typically present with a spectrum of clinical signs and symptoms. There are few diagnostic studies, however, that are currently available to confirm or exclude this entity. A small number of patients, generally those with severe disease, will demonstrate radiographic changes on excretory urography, but the futility of the IVP in early, acute pyelonephritis is well documented. Several radionuclide techniques have been proposed to assist in this clinical problem including the use of Mercury-197 chlormerodrin and Gallium-67 citrate. Over 50 patients have been evaluated over a 4 year period between the ages of 1 week and 50 years of age, with 9 patients showing marked abnormality on the renal cortical images and alteration of the "semi-quantitative" differential renal function study accompanying it. In four of these patients follow-up studies showed reversion towards normal in cortical integrity and function following antibiotic or surgical therapy. Only 1 of these patients showed definite changes on excretory urography. Improved sensitivity, reduced radiation exposure, and a reproducible method for following the response to therapy in patients with acute pyelonephritis appear to represent the advantages of the radionuclide cortical imaging technique. In patients who do not have acute pyelonephritis other renal cortical abnormalities can be delineated accurately by this technique.

A CRITICAL COMPARISON OF Tc-99m GLUCOHEPTONATE AND I-131 HIPPURAN IN THE EVALUATION OF RENAL FUNCTION. M.B. Brachman, D.E. Tanasescu, R.S. Wolfstein, and A.D. Waxman. Cedars-Sinai Medical Center, Los Angeles, CA.

Tc-99m glucoheptonate (TcGH) has been used primarily as a renal scanning agent. This study compares the kinetic characteristics of TcGH with I-131 Hippuran in a normal and abnormal population.

A TcGH flow was followed by two minute images for 14 minutes. I-131 Hippuran four minute images were obtained for 24 minutes. 62 patients, none with renal transplants, were included in this study. The early functional images of both agents were evaluated in a blind fashion by a minimum of two observers. Creatinine estimates were given as less than 1.4 mg% (normal), 1.5-3 mg%, or greater than 3 mg% Any disparity in renal function was recorded. The results are summarized below:

	TcGH	Hippuran
Normal	10/10 (100%)	9/10 (90%)
Abnormal	50/51 (98%)	51/51 (100%)
Differential Function Present	25/28 (89%)	27/28 (96%)
Creatinine Level Estimate	48/62 (77%)	44/62 (71%)

The above data show that both TcGH and I-131 Hippuran are sensitive agents in the detection of abnormal renal function. The ability to detect differential renal function was quite high, with slightly better results for Hippuran. In 4 cases, the degree of overall renal function was more accurately determined with TcGH.

The high correlation of function results with Hippuran and the ability to perform a flow study, blood pool, and delayed high resolution scan with TcGH, would suggest the addition of this agent to the well established Hippuran study in the evaluation of renal disorders.

MARINE-LENHART SYNDROME (GRAVES' DISEASE WITH FUNCTIONING NODULE). F.M.Park, S.F.Zieverink, R.C.Ransburg, Indiana University, Indianapolis, In.

Marine-Lenhart Syndrome (Charkes, J.Nucl.Med.13:885,1972) is a seldom recognized variant of Graves' disease. The diagnosis is based on: (1) Clinical findings of Graves' disease, (2) Initial radioiodine scan revealing a diffuse goiter with a cold nodule(s), (3) T3-suppression test revealing TSH independent paranodular tissue, (4) TSH stimulation scan demonstrating radioiodine uptake by the cold nodule(s).

The incidence of this syndrome was reported to be 2.7% of Graves' disease patients (Charkes). We have observed an incidence of 4.3% in our institution during the last 4 years. A total of 5 cases are reported here.

Pt.	Age Sex	T4 ug% (5.5-11.5)	T3upt.% (25-35)	FT4 Ind (5.5-11.5)	24hr RAIU% (10-35)	T3 Supp Test	Nodular response to TSH
RO*	64F	29.2	30	29.0	26%	33%	+
JR*	42F	26.8	41	36.6	72%	-	+
AL	86F	21.4	37	26.3	39%	-	+
DF	53F	13.2	27	11.9	40%	37%	+
AE	62M	16.8	-	-	81%	-	+

*Surgical resection of the nodule revealed benign adenomas.

The basic abnormality of the gland is diffuse involvement by Graves' disease with incidental presence of benign adenoma. The adenoma appears non-functional under the stimulation of TSI(thyroid stimulating immunoglobulins) of Graves' disease but becomes functional under TSH stimulation.

SIMULTANEOUS TREATMENT OF TOXIC DIFFUSE GOITER WITH I-131 AND ANTITHYROID DRUGS: A PROSPECTIVE STUDY. J.J. STEINBACH and G.D. DONOGHUE. Veterans Administration Medical Center, Buffalo, NY.

Hypothyroidism remains the major drawback of radioactive iodine (RAI) therapy of toxic diffuse goiter.

A prospective study to evaluate the effect of sulfhydryl radical containing antithyroid drugs on the outcome of I-131 (RAI) therapy is reported.

Twenty four male patients with toxic diffuse goiter were assigned by a random process into two treatment groups: A and B. Both groups received a calculated dose of RAI of approximately 5000 rads/treatment. Patients in Group B (control) received no drug preparation. Patients in Group A received antithyroid drug preparation, and RAI was concommitantly administered after attainment of euthyroidism.

The incidence of hypothyroidism at 12 months was 8% for Group A and 36% for Group B ($p<0.001$). During followup of 12-102 months, no additional hypothyroidism was documented for Group A. Two patients with significantly elevated TSH levels were found in Group B during followup of 20-75 months.

The mean time to cure was 15.2 ± 9.1 months for Group B and 19.7 ± 8.2 months for Group A ($p<0.45$). A portion of the time difference between the two groups is accounted for by the 6.5 ± 2.5 months during which patients in Group A were being stabilized and maintained at euthyroidism with antithyroid drugs.

The improved therapeutic outcome of patients in Group A suggests the possibility that pretreatment with antithyroid drugs (containing sulfhydryl radical) minimized the biological variability of the thyroid response to ionizing radiation. Further validation of the method in larger patient population including females is suggested.

I-131 THERAPY (RAI Rx) FOR HYPERTHYROIDISM - LOW VERSUS MODERATE DOSES. R. C. Verma and N. M. Panagiotis. LAC-UCLA Olive View Medical Center, Los Angeles, Ca.

The dose of I-131 for treatment of hyperthyroidism remains very controversial. This study was conducted to compare the short-term outcome of objectively estimated low and moderate doses.

The study included 53 hyperthyroid patients, followed for 2 yrs after RAI Rx. The dose was calculated by the formulae: a) Dose (uCi = Rads to the thyroid/120 x gland wt (gm)/Fractional 24 hr RAIU x 8.1/Biological $T_{\frac{1}{2}}$, and b) Gland wt = area x avg height x 0.31. The dose was estimated to deliver ≈ 4500 rads in the initial 19 (Group A) and ≈ 8500 rads in the remaining 34 (Group B) patients. No thiouracils were used in the first 2 wks after RAI Rx.

The mean dose for Group A was 3.8 mCi and for Group B, 8.5 mCi; these fall within the low and moderate range repectively. At 1 yr follow-up, 74% of Group A and 18% of Group B demonstrated persistent or recurrent hyperthyroidism; 16% of Group A, and 93% of Group B were euthyroid; and ≈ 10% of each group were hypothyroid.

In 20 patients, the initial therapy failed, and retreatment at 1 yr resulted in a mean total dose of 14.5 mCi and a 70% incidence of hypothyroidism at the end of 2 yrs. The latter contrasted sharply with a 13% incidence of hypothyroidism in Group B, 2 yr following a single initial moderate range I-131 dose.

In conclusion, a single initial moderate (8.5 mCi) dose is recommended: a) over the low dose, because the former yields a much higher incidence of euthyroidism with no significant short-term increase in the incidence of hypothyroidism; b) over the multiple doses, since the latter leads to an unusually high (70%) incidence of hypothyroidism at the end of the first year after retreatment.

8:30 a.m.-10:00 a.m. Room 300/301

CLINICAL SCIENCE

CARDIOVASCULAR II

Chairman: B. Leonard Holman
Co-Chairman: Robert Marshall

EXERCISE RIGHT VENTRICULAR RESPONSE IN CORONARY ARTERY DISEASE: CRITICAL ROLE OF CONCOMITANT EXERCISE LEFT VENTRICULAR PERFORMANCE. H.J. Berger, D.E. Johnstone, M.J. Sands, A. Gottschalk, B.L. Zaret. Yale University, New Haven, CT

The right ventricular (RV) response to exercise in coronary artery disease (CAD) was evaluated in 23 patients (pts) and related both to concomitant exercise left ventricular (LV) performance and to the presence of proximal right coronary artery stenosis. RV and LV ejection fractions (EF) were determined at rest and during maximal up-

right bicycle exercise from Tc-99m first-pass radionuclide angiocardiograms using a computerized multicrystal scintillation camera. The normal (nl) cardiac response to exercise was an absolute increase of ≥5% in both RVEF and LVEF (15 nl controls). RVEF was nl (≥45%) at rest in 22/23 CAD pts, while LVEF was nl (≥55%) in 18/23 pts. An abnl RV response to exercise occurred in 12/23 pts, while an abnl LV response occurred in 18/23 pts. All 12 pts with abnl exercise RV performance had abnl exercise LV performance, and all 5 pts with nl exercise LV performance had nl RV performance. RVEF was unchanged by exercise in pts with abnl LV performance (mean RVEF±SEM:rest, 56±1%; exercise, 55±2%, pNS), but increased in pts with nl LV performance (rest, 49±4%; exercise, 63±3%, p<0.001). There was a significant relationship between the direction and magnitude of change from rest to exercise of RVEF and LVEF (r=0.78). With respect to angiographic anatomy, the RV response to exercise was heterogeneous in the 11 pts with right CAD (4 nl and 7 abnl exercise RV performance) and in the 12 pts without right CAD (7 nl and 5 abnl exercise RV performance).

Thus, abnl exercise RV performance occurs frequently in pts with CAD and nl resting RVEF. The major determinant of an abnormal RV response to exercise in CAD is the concomitant exercise LV response and not the presence of right CAD.

RIGHT VENTRICULAR EJECTION FRACTION AT REST AND DURING EXERCISE IN NORMALS AND IN CORONARY ARTERY DISEASE PATIENTS: ASSESSMENT BY MULTIPLE GATED EQUILIBRIUM SCINTIGRAPHY. J. Maddahi, D. Berman, D. Matsuoka, Y. Charuzi, R. Gray, N. Pantaleo, H.J.C. Swan, J. Forrester, and A. Waxman. Cedars-Sinai Medical Center, Los Angeles, California.

The response of right ventricular (RV) ejection fraction (EF) to exercise and its relationship to the location and extent of coronary artery disease (CAD) is not known. We have recently developed a new method for scintigraphic evaluation of RVEF using rapid multiple gated equilibrium scintigraphy (MGES) and multiple RV regions of interest. This study was undertaken to apply 2 min MGES during sitting bicycle exercise (EX) in 10 normals (N)and 18 CAD pts. All CAD pts had significant left anterior descending and/or circumflex disease (>50% stenosis) and 11 had additional right coronary disease (RCAD). Resting RVEF in CAD pts was not significantly different from N (.47±.09 vs. .49±.06, p=ns) (mean±SD). In all of the 10 N at peak exercise, RVEF rose (.49±.06 to .65±.03, p<.001). At peak exercise in CAD pts, mean RVEF did not rise (.47±.09 to .51±.11, p=ns). Importantly, in the subgroup without RCAD, RVEF rose during EX in 7/7 (.42±.06 to .58±.08, p=.001). In contrast, in the subgroup with RCAD RVEF fell or did not change in 10/11 (.50±.1 to .47±.0, p=ns). Discordant RVEF and left ventricular (LV) EF responses to EX were observed in 8/18 pts, including 3/10 with RCAD in whom RVEF fell and LVEF rose during EX. Thus,1)in normals RVEF increases during sitting EX. 2) Although RVEF at rest is not sensitive for CAD, the response of RVEF to EX appears to be related to the location and/or extent of coronary artery disease, either directly to RCA stenosis or to 3 vessel CAD. 3) In some pts with RCAD abnormal RVEF response to EX is not related to abnormal LVEF response.

SIMULTANEOUS ASSESSMENT OF RIGHT AND LEFT VENTRICULAR RESPONSES TO EXERCISE USING MULTIPLE GATED EQUILIBRIUM SCINTIGRAPHY: INCREASED ACCURACY FOR EVALUATION OF THE EXTENT OF CORONARY ARTERY DISEASE. J. Maddahi, D. Berman, M. Freeman, U. Elkayam, H. Staniloff, N. Pantaleo, J. Forrester, H.J.C. Swan, and A. Waxman, Cedars-Sinai Medical Ctr., L.A., CA.

Although abnormalities in the septal (S) and posterolateral (PL) left ventricular (LV) walls are highly specific for left anterior descending and circumflex coronary artery disease (CAD), the inferoapical (IA) area may not be as specific for right coronary artery disease (RCAD) due to overlap in vascular distributions in this region. This study compares rest or exercise (Ex) IA wall motion (WM) abnormality to abnormal right ventricular ejection fraction (RVEF) response to Ex for ability to detect RCAD and their combination with S and PL Ex WM to evaluate the extent of CAD. Of 19 pts studied, 5 had single vessel disease (SVD) and 14 had multiple vessel disease (MVD), including 12 with RCAD. Multiple gated equilibrium scintigraphy was performed using Tc-99m-red blood cells, gamma camera, and computer, both at rest and during graded stages of sitting bicycle Ex. WM was evaluated with a 6 point semi-quantitative scoring system (4=hyperkinesis,-1=dyskinesis). IA WM was abnormal in 10/12 pts with RCAD, but was also abnormal in 5/7 without RCAD. In contrast, Ex RVEF was abnormal in 11/12 RCAD pts, and in only 1/7 pts without RCAD. Analysis of LV WM alone correctly predicted MVD in 11/14, but was not correct in any of 5 pts with SVD, 4 of whom were called MVD. Combined assessment of RVEF and LV WM correctly predicted MVD in 12/14. Importantly, 4/5 SVD pts were correctly assessed. Therefore, 1) assessment of RVEF response to Ex is more specific for RCAD than inferoapical WM abnormality. 2) Combined RVEF + LV WM is more accurate for evaluation of the extent of CAD than LV WM alone.

INTERVENTION RADIONUCLIDE ANGIOGRAPHY: FICK VALIDATION OF SERIAL VENTRICULAR VOLUME RESPONSE TO EXERCISE IN NORMAL MEN. S.G. Sorensen, J.H. Caldwell, J.L. Ritchie, G.W. Hamilton, and J.W. Kennedy. Veterans Administration Hospital, Seattle, WA.

We performed serial, simultaneous Fick (F) and radionuclide (RN) determinations at rest and during exercise in 9 normal men performing 3 symptom-limited, maximum exercise tests: baseline (B), post-nitroglycerin 0.6 mg SL (N) and post-propranolol 0.14 mg/kg IV (P). Serial ventricular time-activity curves were generated at 2 min intervals throughout rest and exercise using an R-wave synchronized camera-computer system. RN cardiac output (CO) was determined as the total counts ejected per minute. Mean percent change (±SEM) in FCO compared with RNCO for each was:

Stage	KPM	B-FCO	B-RNCO	N-FCO	N-RNCO	P-FCO	P-RNCO
I	200	61±11	53±7	56±13	43±10	75±6	64±15
II	400	100±15	83±9	93±11	64±12	95±9	86±17
III	600	137±13	121±13	149±14	105±20	135±14	112±21
IV	800	169±19	156±15	180±27	152±24	195±17	140±24
V	1000	223±39	199±21	215±27	206±32	235±19	167±17*

Mean (±SEM) percent change in count derived end-diastolic volume (EDV) and end-systolic volume (ESV) for each was:

KPM		200	400	600	800	1000	Recovery
	B	3±4	5±3	5±4	5±4	7±5	-11±5
EDV	N	-8±6*	-9±6*	-5±7	1±6	5±7	-21±5
	P	13±5*	14±7	15±8	15±7	12±6	-11±6*
	B	-6±8	-14±5	-23±5	-28±6	-37±5	-62±5
ESV	N	-33±7*	-41±6*	-45±7*	-51±8*	-54±8*	-61±7
	P	9±10	12±7*	11±8*	8±5*	-3±13*	-23±8*

These EDV and ESV changes agree with previous exercise studies. We conclude that 1) RNCO accurately reflects true hemodynamic change, and 2) gated RN permits accurate quantitation of ventricular volume changes and may define mechanisms of response to hemodynamic interventions. (*p<.05)

ONSET AND PROGRESSION OF MECHANICAL SYSTOLE DERIVED FROM GATED RADIONUCLIDE TECHNIQUES AND DISPLAYED IN CINE FORMAT. J.W. Verba, I. Bornstein, N.P. Alazraki, A. Taylor, V. Bhargava, R. Shabetai, M. LeWinter. Veterans Administration Medical Center and University of California, San Diego, CA.

Using radionuclide gated blood pool data, and a mathematical derivative approach applied to the count rate variation at any given point in the image, we have succeeded in visualizing the onset of mechanical systole, or the equivalent of the earliest detectable change in counts. Using high temporal sampled data which we Fourier filter in both the space and time domains, we establish the regional behavior on a Pixel by Pixel basis for the entire cardiac structure. The filtering enhances the statistical reliability so that we can derive volume curves for each individual Pixel over the R to R interval. From these volume curves, the onset of mechanical systole for the individual Pixel can be identified. When the representation of the onset of contraction, ie, the onset of decrease in counts, is superimposed on the cine display of the gated blood pool cardiac image, we are able to visualize the progression of the mechanical wave as it crosses the heart from chamber-to-chamber. Movies of this pattern of the normal wave of the onset of contraction, as well as several abnormal patterns, will be presented. The behavior of

bundle branch blocks and the effects of infarcts will also be shown and discussed. The patterns seen in bundle branch blocks appear to support the possibility that the behavior we are visualizing may actually reflect electrical depolarization of the heart muscle. The potential sensitivity and clinical significance of this technique will be discussed, as well as details, which are required for performing this analysis of the radionuclide gated blood pool study.

A NEW APPROACH FOR ASSESSMENT OF LEFT VENTRICULAR FUNCTION BY FIRST-PASS RADIONUCLIDE ANGIOGRAPHY. R. Slutsky, D. Gordon, J. Karliner, R. Kaiser, A. Battler, K. Peterson. University of California, San Diego.

To identify abnormal left ventricular (LV) function in coronary artery disease (CAD) patients (pts) without exercise stress we analysed radionuclide (RN) angiograms in 32 normals (nls, Group 1, 10 with nl coronary angiograms); 31 pts with CAD and normal contrast ventriculograms (Group 2); and 17 pts with CAD and depressed LV function (Group 3). Total ejection fraction (EF) was computed by standard angiographic methods and from each time-activity curve. During the first third (1/3) of systole EF was determined manually by averaging 3 to 5 beats and compared with 1/3 EF by contrast ventriculography:

	Contrast		Radionuclide	
	Total EF	1/3 EF	Total EF	1/3 EF
Group 1	----------	----------	0.62 ± .04	0.29 ± .04
Group 2	0.65 ± .08	0.23 ± .04	0.59 ± .05	0.18 ± .04**
Group 3	0.42 ± .09#	0.18 ± .04	0.34 ± .09*	0.13 ± .04**

*p< 0.01 vs. 1 & 2; **p <.01 vs. 1; #p <.01 vs. 2

Both total RN EF (r = .95) and 1/3 RN EF (r = .91) correlated well with angiography. Intraobserver and interobserver variation were small, averaging 0.02 ± .02 (range 0- .05). All nls had a 1/3 RN EF ≥ .25. In Group 2, 29 of 31 (94%) had a 1/3 RN EF< .25 and all pts in Group 3 had a 1/3 RN EF< .25. We conclude that 1/3 EF by first-pass RN angiography identifies subtle abnormalities of LV function at rest in over 90% of pts with CAD which may not be recognized by total EF alone.

NONINVASIVE QUANTITATION OF VALVULAR REGURGITATION BY GATED EQUILIBRIUM RADIONUCLIDE ANGIOGRAPHY. S.G. Sorensen, B. Groves, R. O'Rourke, and T. Chaudhuri. Audie Murphy Veterans Administration Hospital and The University of Texas Health Science Center, San Antonio, TX.

Gated blood-pool radionuclide angiography (RNA) noninvasively provides time-activity curve count information proportional to ventricular volumes which may be used for relative volume comparisons within a single chamber for ejection fraction (EF) calculation. Likewise, relative volume comparisons, as differences in ventricular count output (CO), between right (RV) and left (LV) ventricles may permit quantitation of valvular regurgitation and intracardiac shunts.

Using an R-wave synchronized camera-computer system, we performed resting equilibrium RNA in 15 consecutive patients undergoing catheterization (CATH) and quantitative contrast angiography (aortic regurgitation - 7 pts, mitral regurgitation - 7 pts, ASD - 1 pt). RNA regurgitant fraction (RF) was calculated as RF = (LVCO-RVCO)/LVCO. RNA and CATH were within 10 days and without intervening event or medication change. Mean (±SEM) systolic blood pressure (BP), heart rate (HR), LVEF, RVEF, and RF were:

	SBP	HR	LVEF	RVEF	RF
CATH	130±9	79±5	0.47±0.05	---	0.49±0.05
RNA	118±7	72±5	0.48±0.05	0.30±0.04	0.50±0.05
P	0.05	0.05	NS	---	NS

Reproducibilities for RNA measurements were: LVEF (r= 0.99), RVEF (r=0.93) and, RNA RF (r=0.90). In 20 pts (EF range 0.19-0.80) without shunt or regurgitation RVCO correlated well with LVCO (r=0.78). We conclude that the severity of isolated valvular regurgitation may be accurately and reproducibly quantitated by equilibrium RNA.

EXERCISE INDUCED CHANGES IN REGIONAL PULMONARY BLOOD POOL ACTIVITY: ENHANCED DIAGNOSTIC ACCURACY FOR DETECTING CORONARY ARTERY DISEASE. R.D. Okada, G.M. Pohost, H.D. Kirshenbaum, F.G. Kushner, C.A. Boucher, H.W. Strauss. Massachusetts General Hospital, Boston, Massachusetts

To determine if exercise induced changes in regional pulmonary blood pool (PBP) could improve the diagnostic utility of exercise multigated blood pool imaging (MBPI) for the detection of significant coronary artery disease (CAD), 52 patients (pts) who were being evaluated for chest pain had MBPI at rest and during supine exercise. At catheterization, 42 pts had CAD and 10 did not (control). All exercise tests were limited by either angina, dyspnea, or leg fatigue. Two independent blinded observers determined relative PBV activity from the 50° LAO end-diastolic frame for both rest and exercise MBPI by placing a computer derived region of interest over a portion of the left lung. The averaged ratio of exercise/rest counts (PBP ratio) was calculated. Ejection fraction (EF) and regional wall motion (RWM) were determined from rest and exercise MBPI. The mean PBP ratio ± 1 standard deviation (SD) was .94±.06 for controls (n=10), .99±.12 for pts c isolated right CAD (p=NS, n=5), and 1.14±.15 for all other pts c CAD (p<.01, n=37).

Using the standard criteria for a positive exercise MBPI (failure to ↑EF c exercise and/or ↓RWM c exercise) sensitivity was 64% and specificity was 83%. When a PBV ratio ≥1.06 (i.e. ≥control mean + 2 SD) was also considered a sufficient criteria for positivity, the sensitivity increased to 90% (p<.004) and specificity remained at 83%.

Thus, the PBP ratio increases the sensitivity of the exercise MBPI for detecting CAD without changing specificity.

8:30 a.m.-10:00 a.m. Room 201

IN VITRO RADIOASSAY

MEASUREMENT OF FREE THYROXINE

Chairman: Martin L. Nusynowitz
Co-Chairman: Grafton D. Chase

TESTING FOR FREE T4: DO THE ADVANTAGES OUTWEIGH THE PROBLEMS? E.L. Nickoloff, Johns Hopkins Medical Institution, Baltimore, MD.

A COMPARISON OF METHODS FOR THE ESTIMATION OF FREE THYROXINE. L.R. Witherspoon, S.E. Shuler, and M.M. Garcia, Ochsner Medical Institutions, New Orleans, La.

The free thyroxine index (FTI) yields a useful estimate of free thyroxine (FT4) in most clinical situations. The FTI is least useful, however, when binding protein concentrations are markedly abnormal because of limitations in the resin T3 uptake (RT3U). An estimate of FT4 classically required equilibrium dialysis, a time consuming and exacting technique. A direct method utilizing microencapsulated antithyroid antibody (Damon) and a method relating the rate of thyroxine-antibody binding in the presence and absence of endogenous TBG to FT4 (Corning) are now available. We estimated FT4 by these methods and by FTI (T4, RT3U-NML) and compared these results to equilibrium dialysis (Sterling) in 25 euthyroid, euthyroid with elevated TBG, hypothyroid and hyperthyroid patients. Correlation between Corning (r =.91), Damon (r =.86) and FTI (r =.91) and equilibrium dialysis was good. Although discriminating hyper from euthyroid patients the mean FTI was higher in elevated TBG than in normal sera and was frequently normal in hypothyroid patients. The Damon method yielded similar results. Equilibrium dialysis and Corning appeared to be uneffected by TBG concentration and discriminated equally well hyper and hypothyroid patients from normal. Precision was similar in all three assays (between assay CV's, 5 con-

trol sera: dialysis 9-20%, Corning 8-15%, Damon 9-16%). Estimation of FT4 by FTI, Corning or Damon methods provides satisfactory screening information. Confirmation of borderline or clinically suspicious patients should be sought by measuring TSH, total T3 or by TRH response.

SERUM FREE THYROXINE MEASURED BY RIA IN VARIOUS CLINICAL STATES. R. Kleinmann, C. Abreau, P. Brock and L. Braverman University of Massachusetts Medical School, Worcester, Ma.

A radioimmunoassay (RIA) for quantitatively measuring the serum free thyroxine concentration (FT4) without equilibrium dialysis has been developed and evaluated in 49 normal subjects and in 56 patients with thyroid disease, 18 pregnant subjects, and 38 euthyroid, sick patients. FT_4 (RIA) was compared to FT_4 measured by equilibrium dialysis in all subjects and also to the free thyroxine index (FTI) in the sick patients. The method employs T_4 antibody covalently bound to porous glass particles suspended in phosphate buffered saline, pH 7.4, thimerosol to inhibit serum protein binding, ^{125}I-T_4 and plasma based standards containing known concentrations of T_4 and FT_4. Eighty serum samples can be assayed for T_4 and FT_4 (RIA) in 1 hr. There was excellent correlation between FT_4 (RIA) and FT_4 (Equilibrium Dialysis) in the 161 subjects evaluated, irrespective of clinical state ($r = 0.92$, $p < 0.001$). Serum FT_4 (RIA) was increased in all hyperthyroid and decreased in all hypothyroid patients and was significantly decreased ($p < 0.001$) but within the normal range in the pregnant subjects. Serum T_4 was signficantly decreased in the 38 sick patients ($p < 0.001$) and below the normal range in eight. The FTI was low in six of the 8 patients. In contrast, FT_4 (RIA) was elevated in 1 sick patient but was normal in the other 37. As expected, serum T_3 was often low and serum TSH always normal in the sick patients. CONCLUSION: A rapid and reproducible RIA method for quantitatively measuring serum FT_4 correlates well with the FT_4 by equilibrium dialysis in all clinical states, consistently confirms the diagnosis of hypo- and hyperthyroidism, is within the normal range in pregnant subjects, and more accurately reflects thyroid status in sick patients than does the FTI.

A COMPARISON OF FIVE METHODS FOR FREE T4 IN PATIENTS WITH LOW TBG. Linda Merchant and Eileen L. Nickoloff, Johns Hopkins Medical Institutions, Baltimore, MD.

Because of difficulties inherent in the equilibrium dialysis (ED) method for analysis of free T4 (FT4), most clinical laboratories instead provide either a "Free Thyroxine Index (FTI)" determined as the product of the total thyroxine (T4) and the T3 Uptake (T3U), or a "normalized" T4 which simultaneously considers both the TBG binding capacity and the total serum T4 concentration (Mallinckrodt ETR). Two kits for FT4 have recently become available, a kinetic method (Corning) and a so-called "direct" method (Damon). While it would be expected that identical results would be obtained by these methods on euthyroid sera, we decided to examine the effect of low TBG in clinically euthyroid patients by five methods: FTI, ETR, Corning and Damon kits and ED (modified Sterling technique, Nichols Institute).

FTI is usually abnormally low in these cases because correlation between T3U and true TBG levels is not good at extreme TBG concentrations. ED appeared to give results compatible with the patient's clinical condition, as did ETR and the Damon kit. In certain of these patients (6/9), the Corning kit gave elevated FT4 results. There appeared to be no direct relationship between the TBG level (although all were lower than normal) and the elevation seen with the Corning kit. Pure BSA and HSA solutions, with and without added T4 were also run. In all cases, TBG was 0 and the Corning kit gave extremely elevated results. ED gave undetectable FT4, ETR results were variable and FTI were low. The Damon kit gave results which seemed compatible with the amount of T4 added.

It would appear that FT4 results in patients with low TBG must be carefully correlated with clinical findings.

EFFECT OF SAMPLE DILUTION AND TBG CONCENTRATION ON THE MEASURED FT4 USING THE KINETIC REACTION RATE TECHNIQUE. C.M.Heise.Bowman Gray School of Medicine,WinstonSalem,N.C.

Measurement of serum FT4 concentration by the kinetic reaction rate technique has in common with equilibrium dialysis the requirement that the sample be diluted during analysis. Moderate dilution usually does not greatly influence the concentration of unbound ligand as the major plasma binder is TBG, a protein with a very high affinity constant. In earlier studies it was noted that patient samples with very low TBG content gave discordant clinical interpretations when FT4 and FT4I were compared. A study was therefore begun to determine the effect of sample dilution and TBG content on measured FT4 values.

Samples from 25ul to 5ul (corresponding to dilution factors from 1:37 to 1:181) were used in the measurement of FT4 by the usual protocol. In contrast to normal serum, the concentration of FT4 in many patient samples was extremely dependent on sample size. The magnitude and the direction of the effect could be correlated with the quantity of TBG in the assay tube during analysis. When serums of high and low TBG content were mixed in different proportions to cover all observed TBG concentrations, a smooth, continuous distribution of FT4 values was observed in relation to the log of the TBG concentration in the assay medium. All tubes in which the medium contained less than 0.35 ug/ml TBG demonstrated a large dependence of measured FT4 on sample volume.

It is suggested that some artefactually elevated FT4 values are being reported when serum samples of 25 ul do not supply sufficient binding protein to prevent large shifts in equilibrium concentrations of FT4 when the sample is added to the assay tube. Such specimens are common in severely debilitated patients with reduced liver function.

DRUG INTERFERENCE AND PROTEIN MATRIX EFFECTS UPON MEASUREMENT OF FREE THYROXINE IN SERUM. M.Perlstein, A.Herner, R.Rock, E.Nickoloff, B.Almaraz, L.Merchant, D.W.Chan, (The Johns Hopkins Hospital, Balto., MD 21205, and Herner Analytics, Rockville, MD 20852).

Measurement of Free Thyroxine (FT4) in serum is often the final test in the evaluation of thyroid function, and abnormal FT4 results cannot be validated by other common laboratory or clinical procedures. Therefore, technical procedures for this "ultimate" diagnostic test must be critically examined with respect to its analytical integrity. Classically, FT4 is measured by equilibrium dialysis followed by RIA (I) and GLC-EC. Recent technology has provided two new approaches to FT4 measurement: A microencapsulated antithyroid antibody (Damon) (Method III); and a kinetic method using the rate of thyroxine antibody binding to T4 (Corning) (IV). Our results with unusual patient samples suggested that these new procedures may have limitations. Low TBG in the sample matrix produces erroneously high FT4 values (3x normal) with method (IV).

We selected a group of unusual sera (multiple myeloma, hyperlipidemia, and renal disease) and sera from non-human species haveing unique thyroid binding (rabbit, horse, mouse and bovine) to test the effects of variation in protein matrix upon FT4 measurement by all methods. The kinetic method (IV) gave erroneously high FT4 values in samples with low TBG and low, alpha-1-globulins. Method III gave results that correlated better with equilibrium dialysis and GLC. Possible interferences from dilantin and salicylate were studied. They caused variable elevated FT4 values in all procedures. This effect was most profound in (IV). Our data suggest that equilibrium dialysis (I) remains the method of choice.

8:30 a.m.-10:00 a.m. Room 204

INSTRUMENTATION, COMPUTERS, AND DATA ANALYSIS

INSTRUMENTATION

Chairman: Gordon L. Brownell
Co-Chairman: Stephen E. Derenzo

THE PERFORMANCE OF PETT V: A POSITRON EMISSION TOMOGRAPH FOR FAST DYNAMIC STUDIES. M.M. Ter-Pogossian, N.A. Mullani, C.S. Higgins, John T. Hood, and Nancy J. Caston.

We built, tested, and are presently using in physiological studies a positron emission tomograph (PETT V) designed for fast dynamic studies in the human head and in experimental animals. PETT V provides for a maximum field diameter of 25 cm and seven transverse slices simultaneously. The measured resolution of the system is 16.5 mm FWHM and 8.0 mm FWHM (automatically selectible). The sensitivities for seven 16 mm thick slices are 460,000 and 152,000 counts/sec (low and high resolution, respectively) for a 20 cm diameter cylindrical water phantom containing 1 μCi/cc of positron activity. The inherent slice thickness for PETT V is 16 mm FWHM, which can be reduced to 8.5 mm FWHM by the insertion of a collimator. The minimum data acquisition time is 1 second.

PETT V was tested in a series of experiments carried out in the human and in the pigtail monkey by imaging the distribution of carbon-11 labeled carboxyhemoglobin in the brain, and by measuring the rate of egress of oxygen-15 activity from the brain following inhalation of oxygen-15, with the ultimate purpose of assessing regional oxygen metabolism. These preliminary studies indicate that PETT V is capable of providing tomograms of dynamic physiological processes with a data acquisition time of 5 to 10 seconds, and a count density of ~1,200 counts per square cm in the image with the administration of 0.38 μCi per gram (resolution 16.5 x 16 mm) or 2.3 μCi per gram (resolution 8.0 x 8.5 mm) of a positron-emitting activity nearly uniformly distributed in the subject.

A CONJUGATE WHOLE-BODY SCANNING SYSTEM FOR QUANTITATIVE MEASUREMENT OF ORGAN DISTRIBUTION IN VIVO. B.M.W. Tsui, C.-T. Chen, N.J. Yasillo, C.J. Ortega, D.B. Charleston, and K.A. Lathrop. The University of Chicago, Chicago, IL.

We have designed and constructed a whole-body scanning system for quantitative measurement of organ distribution of radioactivity in vivo using the conjugate counting technique. The collection of such quantitative data is important in biokinetic studies and absorbed dose calculation of radiopharmaceuticals in the human.

The scanning system consists of eight opposing pairs of 5x5 cm NaI(Tl) detectors arranged linearly with a separation of 6.35 cm between centers of adjacent detectors. In the conjugate counting mode, each detector is equipped with a 37-hole focused collimator which is designed to have a constant radius of view of about 2.6 cm out to 28 cm from the collimator face. A position-encoded scanning bed moves the patient longitudinally past between the detector arrays and also transversely to provide improved sampling. The scanning system is interfaced with a PDP/11 computer for system control and for data transfer and analysis.

We have modified the conventional conjugate counting technique to include the effects of both attenuation and scatter. A new expression for the geometric mean of the upper and lower detector counts has been derived and is verified by experimental measurements. We have also studied the effects of the size and shape of finite sources on the conjugate counts.

The new scanning system design and the modification of the conjugate counting technique provide improved accuracy in the collection of quantitative organ distribution data over that previously obtainable.

FEASIBILITY OF TOMOGRAPHIC GATED BLOOD POOL IMAGING. W.L. Rogers, T.J. Brady, K.F. Koral, J.W. Keyes, Jr., and J.H. Thrall. University Hospital, Ann Arbor, MI.

Noninvasive detection of patients with coronary artery disease depends upon the identification of global or regional ventricular dysfunction at rest or induced with exercise. Because of geometric constraints regional ejection fractions (REF) and regional wall motion (RWM) abnormalities cannot be detected in standard gated blood pool images. Tomographic images should permit more complete assessment of REF and RWM. To assess the feasibility of this concept a time-coded aperture imaging system was used to obtain end diastolic (ED) and end systolic (ES) images in a dog and several patients. A balloon phantom was also imaged at 200cc and 100cc volumes to simulate ED and ES. All images were acquired on a portable camera interfaced to a minicomputer. High resolution tomograms at 1 cm intervals were calculated using an algebraic reconstruction technique (ART). Qualitative RWM was assessed by viewing cinematic closed loop displays of ED and ES images. Excellent delineation of all wall segments, including posterior wall, was obtained. To assess quantitative REF a commercial edge detection program (MUGE) was used to define the ED and ES boundaries. REFs were calculated by (1) change in pixel area and (2) change in counts (ED-ES/ED). In the phantom study the changes in area agreed well with measured data for each plane. The global EF from the summed phantom tomograms agreed well with the measured value (49.6% vs 50%). There was also close agreement with standard EF's in the dog and patient studies. In conclusion, using coded aperture imaging high resolution tomograms can be obtained from gated blood pool images and this data can be used for quantitative assessment of regional ventricular function.

PERFORMANCE MEASUREMENTS OF AN EMISSION TOMOGRAPHIC BRAIN SCANNER. R.E. Zimmerman, P.F. Judy, T.C. Hill and R. Lovett. Department of Radiology, Peter Bent Brigham Hospital, New England Deaconess Hospital and Harvard Medical School, Boston, MA.

Quantitative measures of the imaging performance of a Cleon 710 Brain scanner have been obtained. The parameters measured were large source sensitivity, small source sensitivity as a function of position, spatial resolution as a function of position and image noise. All measurements were made using a standard 20 cm dia X 35 cm long cylinder with appropriate inserts. Large source sensitivity and image noise were measured by filling the phantom with activity and scanning. Small source sensitivity was measured by loading small cylinders with activity and fixing in various locations within the 20 cm dia water filled phantom. The point spread function was obtained by scanning a capillary tube placed in the phantom perpendicular to the plane being scanned. All quantitative data was obtained by manipulation of reconstructed data using the host computer. The large source sensitivity was found to be 41 kcps/μCi/ml. The small source sensitivity was found to be 0.627 cps/μCi/cc/pixel except in a region about the center which was 74% of this sensitivity. Resolution was found to be independent of position within the phantom with FWHM=10.1±.3 mm and FWTM is 17.1±.9 mm. Noise analysis indicated the variance was correlated with signal, but at higher signal the variance of signal tended to level off, suggesting that while the dominant source of noise was counting statistics, other sources may exist in this system. Attenuation and sensitivity problems do exist. Optimal reconstruction and correction algorithms have not yet been written. These results show further development is warranted on this system to exploit the high resolution and sensitivity of the instrument.

DESIGN AND PERFORMANCE OF A DIGITAL CAMERA. Sebastian Genna and Sing Chin Pang. VA Medical Center and Boston University School of Medicine, Boston, MA.

This paper presents the principles and performance of a one-dimensional camera in which the position of a scintillation is computed digitally from photomultiplier (PM) responses to the event. The method requires initial calibration of each PM (positioned on the crystal assembly) in terms of its response (pulse charge) as a function of positions of a preset light scintillations. From these calibrations, look-up-tables are constructed which give a most probable position and uncertainty for each PM response. Subsequently, analysis of the unknown position of a scintillation event is made by reference to these tables and combination of the results from responding PM's.

The one-dimensional detector reported herein, consists of a linear array of seven 2 inch PM's coupled to a rectangular crystal/light-pipe assembly which has a total thickness of 7/8 inch and is 12 inches long by 1.8 inches wide. Experiments consist of simulation studies and instrument

measurements. In the simulation studies scintillation light was traced to the seven photocathods directly and through one or more reflections from the optical surfaces (up to three generations). From PM responses determined thusly look-up-tables were constructed and resolutions were calculated. The resolution was seen to about 3mm (FWHM) oscillating with minima between photomultipliers and maxima at their centers. Uniformity was seen to be independent of position analysis. Instrument measurements yielded similar calibration curves and tables. Resolution performance was comparable to simulation results. Uniformity measurements confirm that variations in sensitivity are primarily due to shifts in photopeak position.

A MULTI-DETECTOR HIGH PURITY GERMANIUM GAMMA RAY CAMERA FOR NUCLEAR MEDICINE. A.H. Deutchman, W.W. Hunter, Jr., P.A. Schlosser, D.W. Miller, J.W. Steidley, R.T. Profant, M.S. Gerber, K.M. Yocum, and J.R. Hyland.
The Ohio State University, Columbus, OH.

A multi-detector germanium gamma ray camera for nuclear medical imaging has been designed, fabricated, and evaluated. The camera consists of four high purity germanium detectors arranged in a square array. Position sensitive readout from each detector is achieved using a resistive charge splitting scheme. Signals from each detector are processed in parallel by four individual electronic channels. Each channel includes preamplifiers, spatial and energy amplifiers, and a single channel analyzer. The signals from each of the four detectors are multiplexed and displayed as a composite image on a standard display oscilloscope. The dimensions of each detector are 3.2 cm by 3.2 cm by 1.2 cm thick, yielding a total field of view of 41 sq. cm. The intrinsic spatial resolution and energy resolution at 140 keV were measured to be 2 mm and 4%, respectively. A standard high resolution lead foil collimator and a high resolution square hole tungsten collimator were both used.

A series of rats and rabbits were imaged with the germanium camera and then with a state-of-the-art scintillation camera for comparison. Tc-99m pyrophosphate skeletal images of rats taken with the germanium camera through 5.7 cm of scatter showed individual vertebrae. Using Tc-99m pyrophosphate labelled red blood cells, details of cerebral vasculature in the rabbits not seen with the scintillation camera were exhibited with the germanium camera. In all cases the germanium camera images exhibited contrast and in-depth spatial resolution superior to that of state-of-the-art scintillation cameras.

10:30 a.m.-12:00 p.m. Room 210

CLINICAL SCIENCE

RENAL/ELECTROLYTE/HYPERTENSION

Chairman: Harold L. Atkins
Co-Chairman: Alan D. Waxman

COMPARISON OF RENAL EXTRACTION EFFICIENCY OF RADIOACTIVE AGENTS IN THE NORMAL DOG. Z.D. Grossman, J.G. McAfee, G. Gagne, A.L. Zens, F.D. Thomas, P. Fernandes and M.L. Roskopf, Upstate Medical Center, Syracuse, N.Y.

Except for I-131 Hippuran, the renal extraction efficiency (EE) of various radioactive agents has not been reported. Accordingly, during the first hour after intravenous injection their EE was determined in anesthetized normal dogs at 16 time intervals by assay of blood samples drawn from the aorta above the renal arteries and from one renal vein. I-131 Hippuran was injected simultaneously in all experiments, as a control. Blood clearance and urinary excretion were also determined.

EE was calculated as (A-V)÷A, where A=aortic concentration and V=renal venous concentration. The EE of I-131 Hippuran fell steadily from 80% initially to 50% at one hour. EE of all other agents was stable after the first minute.

There was no positive correlation between EE and cumulative concentration in the renal parenchyma. For all Tc-99m renal agents except DMS, the extraction ratio was much higher during the first 30 seconds after injection, as previously observed in first transit extraction measurements (even for inulin) due to rapid initial diffusion through peritubular capillaries.

Tc-99m complexes of DTPA, glucoheptonate, and acetylcysteine were similar, with an average EE of 27-29%. Tc-99m MDP averaged 30%, while EHDP and pyrophosphate were 24-25%. Tc-99m DMS and Hg-197 chlormerodrin had much lower average values of 8% and 14% respectively. Thus, none of the newer agents approached the extraction efficiency of I-131 Hippuran.

PREDICTIVE VALUE OF I-131 HIPPURAN (OIH) KINETICS FOR DETERMINATION OF RENAL TRANSPLANT REJECTION. P.CAHILL, R.MCGOVERN, R.STERRETT, L. TAPIA, L. HO, J. HURLEY, New York Hospital-Cornell Medical Center, NY, NY and Polytechnic Institute of Brooklyn, Brooklyn, NY

The observed intrarenal shifts and changes in the transport kinetics of OIH in renal allografts was studied to predict onset of rejection. In this study, 100 renal allograft rejection episodes were first analyzed retrospectively by 3 nephrologists for the sensitivity of 5 clinical parameters (temperature, weight, urine volume, serum creatinine, creatinine clearance) to predict onset of rejection. These parameters were monitored starting 3-4 days before the patients were treated clinically for rejection and in 30% of the episodes, marked changes were observed. However, in the remaining 70% of the episodes, the clinical parameters were not valid predictors. For 68% of these episodes studies, OIH renograms were analyzed for changes in the % dose in the kidney, rate of uptake, time of appearance of OIH in the bladder, and relative % dose in the outside and middle regions of the kidney, as determined by our nearest neighbor and deconvolution algorithm.* These OIH parameters predicted rejection in 95% of the 30 episodes that had significant changes in the clinical parameters. In most cases, the most marked changes occured in the relative % OIH activity in the middle versus the outside regions of the kidney. In addition, OIH parameters predicted rejection in over 60% of the remaining rejection episodes. In conclusion, intrarenal shifts are normally observed in OIH kinetics at time of rejection and changes in OIH kinetics are more sensitive predictors than the 5 clinical parameters evaluated in this study.*Cahill P,Ornstein E, Ho S, IEEE Trans. Nuclear Science NS-23:555 (1976).

SPECIFICITY OF DISSOCIATION BETWEEN PERFUSION AND CLEARANCE IN Tc-99m-DTPA RENAL STUDIES FOR ACUTE TUBULAR NECROSIS. W.M.S. Shanahan, W.C. Klingensmith III, and R. Weil III. U. of Colorado Medical Center, Denver, CO.

The usefulness of Tc-99m-DTPA studies in differentiating acute tubular necrosis (ATN) and rejection in renal transplants is controversial (Am J Roentgenol 128: 625, 1977). The lack of a reliable clinical method for differentiating ATN and rejection both increases the importance of the Tc-99m-DTPA study and leaves no standard of comparison for determining the usefulness of the Tc-99m-DTPA study. We assumed that during the first four days following transplantation ATN would be common, but rejection uncommon, and that three weeks or more after transplantation rejection would be common, but ATN very uncommon. In an 18 month period 43 Tc-99m-DTPA studies were performed in 38 patients within 4 days of transplantation and 68 studies were performed in 26 patients 3 weeks or more after transplantation (cadaveric transplants only). Each examination consisted of both a Tc-99m-DTPA and I-131 hippuran study. Without knowledge of the time of study or clinical diagnosis, perfusion, clearance, and transit time in the Tc-99m-DTPA study and clearance and transit time in the I-131 hippuran study were visually graded on a 5 point scale with 1 representing normal and 5 representing severe ab-

normality. There were 11 Tc-99m-DTPA studies with perfusion 2 or more gradations better than clearance; all 11 were in the 4 day or less group ($p < 0.01$). Other dissociations did not distinguish between the two groups of studies. Our tentative conclusion is that decreased clearance with relatively preserved perfusion in Tc-99m-DTPA studies is sufficiently specific to be useful in differentiating ATN from rejection.

Tl^{201} AND Tc^{99m} DTPA RENAL IMAGING IN EXPERIMENTAL ACUTE TUBULAR NECROSIS. J.B. Bingham, N.S. Freed, A. Leaf, K.A. McKusick, and H.W. Strauss. Massachusetts General Hospital, Boston, MA.

Relative renal blood flow and glomerular function were evaluated in 11 rats with experimental acute tubular necrosis (ATN).

ATN was induced by clamping of both renal arteries for 45 minutes after the infusion of Ringers solution on one side to prevent thrombosis and Polyethylene Glycol (PEG) in the contralateral side to prevent thrombosis and minimize cell swelling. 24 hours later, Tl^{201} was injected and pin-hole scintillation camera images obtained for 15 minutes as a measure of renal perfusion. This was followed by bolus injection of Tc^{99m} DTPA to measure both flow and glomerular function. Relative blood flow was measured from renal Tl concentration after background subtraction and compared to DTPA uptake up to the first renal peak. Analysis of blood flow using DTPA first pass curves correlated well with Tl^{201} divided uptake ($r=0.83$). Divided flow and function were greater in the PEG treated kidney. The maximum renal peak of DTPA occurred during first transit with little subsequent concentration.

These data suggest that relative renal blood flow can be assessed from either initial DTPA curves or static Tl201 images. Pre-treatment of the kidney with PEG causes some preservation of renal function, confirming that cell swelling plays a role in this disorder.

SEQUENTIAL Ga-67 IMAGING IN DIAGNOSIS OF RENAL ALLOGRAFT REJECTION. P.M. Johnson, R. A. Fawwaz, M. A. Hardy and R. Nowygrod. College of Physicians and Surgeons, Columbia University, New York, NY.

To determine whether Ga-67 renal allograft imaging can differentiate predominantly cellular rejection (CR) from predominantly humoral rejection (HR), serial Ga-67 imaging was performed in 33 renal transplant recipients. Activity in the graft was determined at 24 hrs by 2 observers and graded relative to that in ilium ($=, >$ or $<$). Allograft uptake was graded Positive when $=$ or $>$ than that in ilium, or when demonstrable after previous negative study. During the first post operative week all patients showed intense uptake in the allograft without clinical evidence of rejection. Thereafter, Ga-67 localization decreased and eventually was not demonstrable in all patients whose renal function remained normal (n=5).

Graft biopsies were available in 28 patients after the first post operative week. In 13 patients with CR by biopsy, Ga-67 uptake increased or failed to decrease with time; these patients were free of infection. In 13 patients with HR by biopsy, there was no uptake of Ga-67. In 2 additional patients with CR, examined 2-3 days after treatment with large doses of steroids, renal Ga-67 uptake was also absent.

These results indicate that Ga-67 imaging in renal transplant patients, excluding those with allograft infection or prior treatment with steroids, is useful in differentiating CR from HR. Since immunosuppression is usually effective in reversing CR, but not HR, the method assists selection of appropriate therapy.

PLINT: The PLasma INTegral method for measurement of renal clearance during routine gamma camera renography. TW Ryerson, SM Sviss, Northwestern Memorial Hospital, Chicago, Illinois.

A method is presented for renal clearance determination during routine gamma camera renography which only requires a single timed blood sample and a lateral view of the kidneys, ureters and bladder (KUB). Since KUB acts as a collecting reservoir or intetrator for activity cleared from the plasma, the activity in KUB is directly proportional to both renal clearance (C) and the time integral of the plasma curve P(t); i.e., $C=KUB(t)/\int_0^t P(t)dt$. KUB is depth corrected by a lateral view of the abdomen and pelvis and P(t) is calibrated from a timed blood sample. Using the gamma camera background curve for P(t) results in a spuriously high value for clearance, since the early portion of the background curve is lower than the true plasma curve as measured by a heart probe. An iterative computer program is used to reconstruct the "true" plasma time-activity curve from the gamma camera background curve and KUB, thus eliminating the need for a heart probe. Clearance values from 14 patients using PLINT are compared with a single injection clearance technique with timed plasma and urine collection with good correlation ($r=.95$).

Advantages of PLINT include: (1) only measures activity actually cleared by the kidney without assuming instant mixing of injected bolus or requiring extrapolation of the plasma curve to infinity, (2) does not suffer from poor statistics due to short renal transit time as does the plasma integral method which only includes the kidney.

DMSA SCANNING: AN INDEX OF RELATIVE RENAL PLASMA FLOW. A. Taylor, J. Hollenbeck, and P.L. Hagan. VA Medical Center and University of California, San Diego, CA.

The relative renal accumulation of Tc-99m dimercaptosuccinic acid (DMSA) was evaluated in patients as an index of relative effective renal plasma flow (ERPF) at 25 minutes and 24 hours post injection. Results were correlated with the ERPF determined by computerized I-131 hippuran renography previously validated by conventional split function studies (J. Nucl. Med. 15:102, 1974; J. Urol. 113:595, 1975). Using a previously described method (J. Nucl. Med. 19:178, 1978), renal uptake of DMSA between the 10th and 25th minute post injection was determined using computer assignment of regions of interest over the kidneys. In 24 patients with creatinines ≤ 2.0, the correlation between the relative renal uptake of DMSA (10-25 minutes) and the relative ERPF was 0.91; in 10 patients with serum creatinines > 2.0, the correlation coefficient was 0.51 due to increased DMSA background activity in patients with diminished renal function. Since rat studies showed the 24 hour renal accumulation of DMSA to be 66% of the administered dose, we decided to correlate the relative ERPF with the relative renal accumulation of DMSA in patients at 24 hours. DMSA uptake was determined by taking counts in regions of interest over the kidneys at 24 hours. Results showed excellent correlation with the ERPF (0.93) in 20 patients with creatinines ≤ 2.0 and fair correlation (0.70) in 8 patients with creatinines > 2.0. Relative renal uptake of DMSA determined using a divided field correlated quite well with the relative ERPF (0.94) in 24 patients with creatinines ≤ 2.0, and was 0.76 in 11 patients with creatinines > 2.0. In conclusion, 24 hour DMSA renal scanning may provide a simple and accurate method of assessing relative ERPF particularly in patients with good renal function.

RADIONUCLIDE MEASUREMENT OF ABSOLUTE DIFFERENTIAL GFR. T.A. Powers, R.B. Grove, R.D. Bowen, J.M. Plunkett, S. Kadir, J.A. Harolds, J.A. Patton, and W.J. Stone. Veterans Administration Medical Center, Nashville, TN.

Knowledge of individual kidney GFR could provide an improved basis for diagnosis and therapy of various renal diseases. The purpose of this study was to determine if Tc-99m DMSA and/or Tc-99m DTPA could be used to measure differential GFR as accurately as iothalamate clearances obtained at ureteral catheterization. Five normal adult female mongrel dogs and four with unilateral segmental renal infarction were studied. Differential DMSA uptake was measured on day 1 based on the geometric mean of anterior and posterior views at 4 hr postinjection. On day 2, differential DTPA uptake was measured from 1-3 minutes postinjec-

tion using the posterior view and the GFR calculated from blood samples obtained over 4 hr. On day 3, iothalamate, creatinine, and DTPA clearances were performed by constant infusion after ureteral catheterization. Relative iothalamate clearances and DMSA uptake correlated well ($r = .99$, $y = -.0134 + 1.04x$, $p < .001$). Relative DTPA uptake showed a lesser correlation with iothalamate clearance ($r = .86$, $y = .034 + .77x$, $p < .05$). The bolus injection DTPA two compartment GFR correlated well with the iothalamate clearance ($r = .94$, $y = 7.8 + .98x$, $p < .01$), unlike the single compartment DTPA GFR ($r = .63$, $y = 43 + .78x$, $p > .10$). Absolute differential GFR determined from DMSA uptake and two compartment DTPA GFR data correlated well with differential iothalamate clearance (left: $r = .97$, $y = -.14 + .90x$, $p < .01$; right: $r = .96$, $y = -.46 + .94x$, $p < .01$). The excellent correlation between this technique and ureteral catheter iothalamate clearances strongly suggests that this procedure can replace invasive methods for determination of differential renal function in many clinical applications.

COMPARISON OF DIFFERENTIAL RENAL FUNCTION DETERMINATION BY Tc-99m DMSA, Tc-99m DTPA, I-131 HIPPURAN AND URETERAL CATHETERIZATION. R.R. Price, M.L. Horn, J.P Jones, J.J. Touya, R.B. Grove, J.H. Nadeau, P.A. Branch, R.H. Rhamy, J.W. Hollifield, A.B. Brill, and F.D. Rollo. Vanderbilt University Hospital, Nashville, TN.

The purpose of this study was to compare three different radionuclide methods against ureteral catheterization for the measurement of differential renal function. Forty-eight (48) hypertensive patients were studied with Tc-99m DMSA, Tc-99m DTPA and ureteral catheterization. Twenty patients also had I-131 Hippuran studies. Relative differential renal function was measured from the posterior gamma camera images using computer assisted regions of interest for all radionuclide methods. For DMSA, static images at one hour post injection were used. For DTPA and Hippuran, the relative renal accumulation during the interval from 1 to 3 min. post injection was used. Regression analysis showed excellent correlation of the per cent left renal accumulation of each radionuclide with the relative creatinine clearance (C_{cr}):

DTPA(L) = 7.2 + .82 (C_{cr}) $r = .95$, $p < .001$
DMSA(L) = 0.97 + .92 (C_{cr}) $r = .97$, $p < .001$
Hippuran(L) = 4.7 + .89 (C_{cr}) $r = .97$, $p < .001$

Both DTPA and Hippuran tend to overestimate asymmetric poorly functioning kidneys; however, they did require less than 5 min. of patient time. DMSA is accurate in patients with symmetric and asymmetric renal function, is easier to perform, but requires more time. When the regression equations are used, each of the radionuclide methods is equivalent to the invasive ureteral catheter method for the measurement of differential renal function.

10:30 a.m.-12:00 p.m. Room 211

CLINICAL SCIENCE

GASTROENTEROLOGY I

Chairman: Malcolm Cooper
Co-Chairman: Henry N. Wellman

RADIOISOTOPIC DEMONSTRATION OF ACUTE INTESTINAL BLEEDING. A. Alavi, E. Ring, and S. Baum. University of Pennsylvania School of Medicine, Philadelphia, PA.

Intravenous administration of 99m-Tc sulfur colloid and imaging of the abdomen have successfully demonstrated the site of bleeding in animals. In this report we will describe our preliminary data using this technique in patients. Seventy-five patients are included in this report. Nineteen had positive scans with demonstration of the bleeding site. Of these, 12 had colonic and 7 had small bowel sites of bleeding. The most common disorder among these patients was colonic diverticulosis. Arteriography was done in 11 of these patients. In 6 patients the bleeding site on the scan was detected and corresponded to the site shown on the arteriogram. In 4 patients with definite clinical evidence of bleeding and positive scans, the arteriogram showed no evidence of extravasation. These patients included: one with diverticulosis, one with arteriovenous malformation, one with varices and one with regional enteritis. In one patient who had a positive scan, selective catheterization was impossible because of stenosis of the inferior mesenteric artery. In 7 patients, scans were used to follow the patients' course after proper treatment was instituted. In 8 patients this test played a crucial role in the management of the patient. Compared to arteriography no false negative study has been noticed. Because of its simplicity, noninvasiveness and sensitivity, this test appears to be the examination of choice in the evaluation of a patient with rectal bleeding. The performance of this test before arteriography and endoscopy may prove very helpful in the proper use of these diagnostic modalities.

TECHNETIUM-99m IN VIVO LABELED RED BLOOD CELLS IN THE EVALUATION OF GASTROINTESTINAL (GI) BLEEDING. G.G. Winzelberg, K.A. McKusick, H.W. Strauss, A.C. Waltman, and A.J. Greenfield. Massachusetts General Hospital, Boston, MA.

The timing of arteriography in patients with intermittent GI hemorrhage is critical for localizing the bleeding source. To determine if blood pool tracers could detect intermittent GI bleeding abdominal scans after injection of 20mCi of Tc-99m in vivo labeled red blood cells were performed in 28 control subjects and in 10 patients with suspected lower GI bleeding using a gamma camera. In the control subjects, initial imaging at 3 hours demonstrated tracer activity in vascular structures; gastric activity was noted in 50% and only one patient had colonic activity, while images at 24 hours demonstrated colonic activity in 50%, all of whom had prior gastric activity. Eight of the 10 patients had active hemorrhage documented by guaiac positive stools and falling hcts; seven of these had focal tracer collections in segments of bowel indicating active GI bleeding. Three of the 7 scans were positive by 1 hour; 3 by 5 hours and the 7th positive by 10 hours following tracer injection. The slowest detected bleeding rate was 500ml/24 hours. The one bleeding patient with a negative scan was bleeding at a rate of 50ml/24 hours. Seven of the 8 bleeding patients had angiograms; 3 of these demonstrated extravasation of contrast in the area abnormal on the radionuclide scan. The slowest bleeding rate angiographically detected was 2000ml/24 hours. We conclude that imaging with Tc-99m invivo labeled RBC's is an effective technique to locate sites of active hemorrhage in patients with intermittent GI bleeding but that caution must be used in interpretation of delayed images because of the normal delayed accumulation of tracer in the colon.

DIFFERENTIATION OF PANCREATIC AND OTHER RETROPERITONEAL TUMORS BY POSITRON EMISSION COMPUTERIZED TOMOGRAPHY (ECT). K.F. Hübner, E. Buonocore, W.D. Gibbs, S. Holloway, and B. L. Byrd. Oak Ridge Associated Universities (ORAU), Oak Ridge, TN, and The University of Tennessee Memorial Research Center and Hospital (UTMRCH), Knoxville, TN.

Positron ECT with C-11-labeled DL-tryptophan, DL-valine, and amino-cyclobutanecarboxylic acid (ACBC) has been used in eight patients to differentiate abdominal masses. The tracers were labeled by substituting C-12 with C-11 in rapid synthesis facilitated by modified Bücherer-Strecker technique. The dose of these radiopharmaceuticals did not exceed 15 mCi in any of the patients. Tomographic computer reconstructed images were obtained with a positron tomograph (ECAT). Clinical examples of this presentation include pancreatic carcinoma, pancreatitis, and mesenteric lymphoma. Significant findings of this investigation were: cases with high concentration of C-11-tryptophan and/or C-11-ACBC in pancreatic neoplasms and one case where C-11-tryptophan showed a normal pancreas, while C-11-ACBC concentrated in a lymphoma encasing the pancreas. Despite the limited experience with this technique the results indi-

cate that positron ECT with appropriate biologic tracers visualizing physiologic and metabolic processes in normal and neoplastic tissues hold promise to become a new diagnostic modality in the future.

(ORAU operates under Contract No. EY-76-C-05-0033 with the U. S. Department of Energy. This abstract is based on work supported by USPHS Research Grant CA-14669 from NCI and the OHER-DOE.)

FEASIBILITY OF SINGLE PHOTON TOMOGRAPHIC IMAGING OF THE PANCREAS WITH C-11-TRYPTOPHAN. J. Ryan, M. Zalutsky, P. Kirchner, A. Moossa, P. Harper and M. Cooper.
The University of Chicago, Chicago, IL

Limited availability of positron emission tomographic (PET) instrumentation has impeded the clinical application of native-labeled positron emitting metabolites; therefore, alternative imaging approaches must be developed to exploit the superior in vivo pharmacokinetics of these radiopharmaceuticals. In a previous study with N-13 ammonia we demonstrated that a single photon tomographic (SPT) scanner (Pho/Con) with high energy collimators could effectively image positron emitters. This study examines the applicability of SPT scanning to pancreatic imaging with C-11-tryptophan (C-11-Try).

In 4 patients with abdominal disorders, pancreatic imaging was performed with both C-11-Try (2-8 mCi) and 250 μCi of Se-75-Selenomethionine (SM). Serial 5-20 min images were obtained with C-11-Try up to 1.5 hr post injection. Intense early renal activity diminished rapidly to negligible levels by 15 min. Pancreatic activity increased progressively relative to liver/background, yielding best clinical images after 20 min. The C-11-Try pancreatic images were clearly superior to the Se-75-SM images. In one patient with severe pancreatitis, the pancreas was not visualized with either tracer.

These data suggest that superior images of the pancreas may be obtained with C-11-Try without PET instrumentation. Further, these images, which can be collected serially at 5-20 min intervals, are available immediately. The serial images may provide a dynamic assessment of regional pancreatic function. We recommend C-11-Try as a pancreatic imaging agent for institutions with SPT instrumentation near a cyclotron.

QUANTITATIVE GASTRO-CHOLECYSTOSCINTIGRAPHY (GCG): ENTERO-GASTRIC REFLUX (EGR) IN NORMAL ASYMPTOMATIC SUBJECTS AND POST-GASTRECTOMY PATIENTS. L.S. Malmud, R.S. Fisher, F. Stelzer, R. Menin, P.T. Makler, Jr., and G. Applegate.
Temple University Hospital, Philadelphia, PA

Reflux of bile into the stomach and abnormalities in the pattern of gastric emptying have been implicated as etiologic factors in a variety of gastroenterologic disorders. The technique of GCG was recently developed as a non-invasive test for EGR. The purpose of this study was to detect and quantitate EGR in normal asymptomatic subjects and in a variety of patients following Bilroth II surgery. Thirty patients were studied: 10 normals and 20 gastric ulcer patients subjected to vagotomy, hemigastrectomy and Bilroth II gastrojejunostomy. Post-surgical patients were grouped according to clinical criteria. EGR was detected in normal subjects; however, EGR was significantly increased ($p<.05$) and gastric emptying accelerated ($p<.01$) amongst the entire post-surgical group. In patients with the alkaline gastritis syndrome of postprandial nausea, bilious vomiting, and abdominal pain, EGR was increased significantly compared to other post-surgical patients ($p<.01$) and to normals ($p<.001$). As expected, gastric emptying was delayed and accelerated respectively in the gastroparesis and dumping syndrome patients. In both of these groups, there was increased EGR ($p<.05$) compared to normals. We conclude that quantitative gastro-cholecysto-scintigraphy is a useful non-invasive technique for the evaluation of the pathophysiology of EGR in post-surgical patients, as well as, in normal patients following nutritional loads of varying pH, osolarity, volume, and protein, fat and carbohydrate composition.

EJECTION FRACTION: A NEW OBJECTIVE METHOD OF STUDYING MOTOR FUNCTION OF THE GALL BLADDER. Krishnamurthy, G.T., Bobba, V. R., Kingston, E., Brown, P., Eklem, M., Nuclear Medicine Service, VA Medical Center & UOHSC, Portland, OR.

The motor function of the gall bladder (GB) is poorly understood because of lack of availability of an objective test. A study was undertaken to test if Tc-99m-HIDA could provide an objective means of studying the motor function of the GB following intravenous (IV) cholecystokinin(OP-CCK). Fifteen healthy, adults (5M & 10F) with a mean age of 35 yrs. were chosen. After an overnight fast they were injected with 5-10 mCi of Tc-99m-HIDA (Medi-Physics). Sixty min. after injection a gamma camera fitted with 5mm diameter pin hole collimator was positioned anteriorly to visualize the GB, hepatic, common bile duct and intestines. The detector position was adjusted to prevent any intestinal radioactivity overlying the GB. The analog images were taken at 2 min. intervals & the data was recorded on 64x64 metric size computer at 1 frame/min. for 60 min. Five min. after beginning of the test 2cc's of saline was injected IV & at 10 min. 0.04 microgram/kg of OP-CCK (Squibb) was injected IV. The time activity curves over GB, hepatic & common bile duct were generated. The counts were corrected for physical decay & the background was subtracted from the GB curve.

No contraction of GB was noted following saline injection. After a refractory period of 2.4 ± 0.6 min (mean ± S.E.) following OP-CCK injection, the GB begins to contract. The mean time interval between the beginning to maximum of contraction is 5.3 ± 1.1 min. The mean ejection fraction is 26.1 ± 6.9%. No bile reflux in to hepatic duct is seen during GB contraction. The technique described here offers a new objective means of studying the motor function of the GB.

THE EFFECT OF HISTOLOGIC PATTERN AND VASCULARITY OF GALLIUM UPTAKE IN PRIMARY LIVER CELL CARCINOMA: NON-CORRELATION WITH ALPHA-FETO PROTEIN AND HEPATITIS ANTIGEN A. A.D. Waxman, R.H. Richmond, H.U. Juttner, J.K. Siemsen, M.J. Heffelinger, and E.J. Fink. Cedars-Sinai Medical Center, and LAC/USC Medical Center, Los Angeles, California.

Previous studies have demonstrated gallium sensitivity in primary liver cell carcinoma (PLC) to vary from 71% to 100%. Contradictions are present in the literature with respect to factors responsible for the variation. The present study analyzes the significance of tumor vascularity, histologic pattern, alpha-feto protein (AFP) and hepatitis antigen A (HAA) as factors in determining the degree of gallium uptake in proven PLC.

Seventeen patients with histologically proven PLC underwent conventional Tc-99m sulfur colloid liver scans as well as Ga-67 scintigraphy. Contrast angiography of the liver as well as tissue histology was obtained in each case.

Twelve of 17 patients (71%) showed gallium uptake in the tumor. Eleven of 12 patients (92%) with a moderate or well differentiated PLC showed increased gallium activity in the tumor. The exception was a tumor with a large central area of necrosis. Four of 5 patients with a poorly differentiated or atypical PLC showed absence of gallium activity. Only 6 of 11 patients with a hypervascular tumor showed a marked increase in gallium uptake. Correlation with AFP as well as HAA was poor.

We conclude that a gallium scan in PLC will be positive when the tumor shows a moderate to well differentiated histologic pattern unless significant necrosis is present. If the blood supply is markedly impaired, gallium uptake is reduced. A hypervascular blood supply does not ensure increased gallium avidity. We were unable to demonstrate any correlation with AFP or HAA.

10:30 a.m.-12:00 p.m. Room 300/301

CLINICAL SCIENCE

PERIPHERAL VASCULAR

Chairman: H. William Strauss
Co-Chairman: Kenneth Narahara

REGIONAL COMPARISON OF I-123 FIBRINOGEN SCINTIGRAPHY (SV) AND RADIOPAQUE VENOGRAPHY (RV) IN THROMBOPHLEBITIS (TP). S.J. DeNardo, H.G. Bogren, G.L. DeNardo. University of California Davis Medical Center, Sacramento, CA. Supported by American Cancer Society Grant PDT-94A

SV has been reported to be clinically useful in TP. RV and SV, obtained within 2 weeks of each other, were interpreted blind and rigorously compared in each of five major sites (iliac, upper femoral, Hunter's canal, popliteal, and calf) in 69 legs of 43 patients with 268 areas of adequate technical quality. SV and RV were interpreted using reported criteria. 49 iliac, 11 femoral, 4 Hunter's canal, 4 popliteal and 6 calf sites were inadequately visualized by RV. 2 of 3 iliac sites, which were inadequately visualized by SV, were obscured because of failure to empty the bladder. SV and RV agreed in 26 normal and 37 abnormal legs.

SV vs RV in 69 Legs

		RV +	RV -
SV	+	37	3
	-	3	26

SV and RV disagreed in 4 (9%) patients, 6 (9%) legs and 18 (7%) sites; SV was positive, RV negative in 50% of each group. The results indicate excellent correlation between SV and RV when technically adequate and interpreted by skilled observers. Discrepancies related to factors such as age of disease, size of clot, interval between studies and anticoagulant therapy. SV is non-invasive, readily visualizes the veins of all 4 extremities and the pelvis and has a sound physiologic basis. Ileofemoral TP is routinely detected without injection of the femoral vein.

A COMPARISON BETWEEN TECHNETIUM-99m PLASMIN AND IODINE-125 FIBRINOGEN IN THE DETECTION OF DEEP VEIN THROMBOSIS. P.J. Ell, J.M. Deacon, P.H. Jarritt, P.C. Pearce, and A. Allan. The Middlesex Hospital Medical School, London, UK.

Tc-99m plasmin has recently been reported as being a useful and reliable tracer for the rapid detection of deep vein thrombosis (DVT) in medical patients where thrombosis is suspected clinically.

We have compared the Tc-99m plasmin uptake test with the I-125 fibrinogen uptake test in a series of 40 patients. 20 of these (group A) presented with clinical evidence of DVT. The second group (B) of 20 were cases post abdominal surgery, who were considered to be at high risk of developing DVT, but without clinical evidence of it.

The protocol for I-125 fibrinogen involved intravenous injection of 100 uCi and external probe counting at 24 hours or later. The protocol for Tc-99m plasmin involves intravenous injection of 500 μCi and external probe counting at 15 and 30 minutes.

Group A - 17 out of 20 patients showed concordant results. In three cases, the Tc-99m plasmin test was negative at the time the I-125 fibrinogen test was positive. In at least one of these three cases, insufficient labelling of the plasmin was proven.

Group B - In all patients, concordant results were obtained.

In conclusion, this data ($P < 0.05$) supports the evidence that Tc-99m plasmin has the effective potential for early and rapid screening for DVT 15 minutes after its intravenous administration. The test is safe, quick (less than 15 minutes) and easy to perform by non-qualified staff.

EVALUATION OF TC-99m SULFUR COLLOID UPTAKE IN EXPERIMENTAL DEEP VIEN THROMBOSIS. F. Vieras, E. L. Barron, and G. A. Parker, Armed Forces Radiobiology Research Institute, Bethesda, MD

This study was undertaken to evaluate the potential of Tc-99m sulfur colloid (Tc-SC) as a radiopharmaceutical for thrombus imaging. Deep vein thrombosis was experimentally induced in anesthetized dogs by passing an electrode through a femoral vein into the inferior vena cava, and applying a direct 5-ma current for 1 hour with a 12-volt power supply. A 2- to 3-mCi dose of Tc-SC was injected intravenously on the contralateral rear extremity at various time intervals, and the animals were sacrificed 1 or 2 hours later. The area of thrombosis was dissected and tissue samples were collected for in vitro counting. The mean thrombus-to-blood (T/B) uptake ratios, for thrombi that were 24 hours old at the time of Tc-SC injection, were 11.38 ± 2.33 S.E. and 12.0 ± 5.21 S.E. for the groups of animals sacrificed at 1 and 2 hours postinjection, respectively. The T/B ratios were comparably high for younger and older thrombi (up to 72 hours). The T/B ratios were significantly lower for a group of five control dogs that received Tc-99m pertechnetate instead of Tc-SC ($\bar{X}$ = 1.35 ± 0.24 S.E.). Intravenous heparin administration (5,000 I.U.) 2 hours prior to injection of Tc-SC caused a significant depression in T/B ratios ($\bar{X}$ = 4.90 ± 1.27 S.E.) but did not totally block Tc-SC uptake. The T/B ratios with Tc-SC are sufficiently high for imaging studies. Tc-SC appears to have potential as a clinically useful thrombus-imaging radiopharmaceutical.

NONINVASIVE EVALUATION OF VASCULAR TRAUMA USING Tc-99m SULFUR COLLOID ANGIOGRAPHY. F.L. Datz, M. Gordon, S.E. Lewis, D.C. Hickey, W. Krupski, and R.W. Parkey. Univ. Texas Health Science Center at Dallas, TX.

This study evaluated the utility of Tc-99m sulfur colloid (Tc-SC) angiograms for the diagnosis of traumatic vascular injuries.

Thirty-five patients with possible peripheral vascular injuries from blunt or penetrating trauma were studied. Following the bolus intravenous injection of 8 mCi of Tc-SC in an uninjured extremity, dynamic images were recorded at 3-second intervals for one minute using a gamma camera and computer. Immediate and 15 minute delayed static images were obtained for 200,000 counts. Positive scan criteria were either: 1) an abnormal flow pattern or 2) a focal region of increased activity on static views, suggesting extravasation. Following the radionuclide study all patients underwent contrast angiography. Surgical exploration was performed in those patients with evidence of major vascular injury on conventional studies.

All 10 patients with evidence of vascular disruption on contrast angiography had positive radionuclide studies including: 1 pseudoaneurysm, 1 A-V fistula, 4 occluded vessels, 2 intimal flaps, 1 puncture wound of a vessel and 1 external compression of an artery secondary to hematoma. Two patients with bone fractures showing extravasation on static images had normal contrast angiograms. Twenty-five patients had negative Tc-SC studies and all had normal contrast angiograms. Overall sensitivity was 100%, with 8% false positive and no false negative studies.

We conclude that Tc-SC angiography may be of significant value as a screening procedure for patients with suspected traumatic peripheral vascular injury.

VENOUS VOLUME CHANGES ASSESSED BY BLOOD-POOL IMAGING. I. P. Clements, D. A. Strelow, G. P. Becker, R. E. Vlietstra, and M. L. Brown. Mayo Clinic and Mayo Foundation, Rochester, MN.

This study, in six normal subjects, compares a standard plethysmographic method of assessing forearm venous volume changes with a technique using forearm blood-pool imaging by in vivo Tc-99m labeled red cells. Venous compliance curves were determined from forearm volume changes measured by a Whitney, mercury in silastic, strain gauge. Upper arm collecting cuff pressure was increased from 0 to 80 mm Hg and returned to zero in 20 mm Hg steps. Allowing

one minute between each step for stabilization, forearm volume and counts per minute over the forearm were determined simultaneously. Changes in volume and counts were also compared during rapid inflation of the collecting cuff to 40 mm Hg. Compliance curves constructed using both forearm volume and count changes were similar. There was a close linear relationship between the percent change in forearm volume and percent change in forearm counts/minute in each individual (r = 0.94 to 0.99). Changes in forearm volume and counts during rapid cuff inflation were also highly correlated (r = 0.97 to 0.99). However, after the 18-minute experimental period, when counts/minute at 0 mm Hg had returned to baseline, forearm volume was 1.2 ml/100 ml of forearm (range 0.4 to 2.0) above initial volume. This may represent tissue fluid accumulation. Forearm blood-pool imaging using Tc-99m labeled red cells provides precise measurements of forearm venous blood volume changes which may aid in evaluating the venous circulation in clinical conditions and after therapeutic interventions, and, when combined with a plethysmographic method, tissue fluid accumulation may be quantified by this technique.

ACCURATE DETECTION OF PERIPHERAL ARTERIAL DISEASE WITH EXERCISE TL-201 LEG IMAGING. J. Seder, S. Rahimtoola, E. Botvinick, J. Goldstone, D. J. Effeney, D. Price. University of California, San Francisco, California.

Obstructive peripheral arterial disease (PAD) was evaluated by injection of 2 mCi of Tl-201 at peak leg exercise with a scintillation camera. Images of thighs (T) knees (K), and calves (C) were obtained at exercise and on redistribution, and stored on a 64x64 computer matrix. Counts/pixel/minute were obtained in symmetric regions of interest (T,K,C) in the right (R) and left (L) limbs and ratios derived. Additionally, T/K and C/K ratios were calculated and examined in both R and L extremities.

In 11 control subjects without PAD, normal values (mean ± SD) of ratios were: LT/RT .96 ± .04, LC/RC 1.0 ± .1; R limb: T/C 1.1 ± .15, T/K 4.9 ± 1.3, C/K 4.5 ± 1.2; L limb: T/C 1.1 ± .2, T/K 4.8 ± 1.05, C/K 4.4 ± 1.1.

In all patients (pt) with arteriographically proven bilateral PAD, 3 or more of the above ratios were abnormal (>2 SD). Abnormal interextremity ratios (T/T, C/C) were always related to the side and local site of angiographically documented vascular narrowing (4/5 pt). Intraextremity ratios (T/C,T/K and C/K) served to further localize disease within an extremity and aided identification of bilateral disease.

Knee counts decreased with redistribution demonstrating their relationship to skin, muscle and bone perfusion. An increased T/K ratio at stress was a valuable indicator of distal disease in the ipsilateral extremity. In patient with PAD, redistribution generally occured in all areas and was a diagnostic aid.

In pts. with bilateral PAD, an integrated evaluation of relative regional radioactivity allows accurate estimation of regional arterial disease.

NON-INVASIVE DETERMINATION OF ISCHEMIC ULCER PERFUSION: PRELIMINARY REPORT. M.E. Siegel, C.A. Stewart, I. Sakimura, W. Wagner, and A. Bessman. LAC/USC Medical Center and Rancho Los Amigos Hospital, Los Angeles, CA

The purpose of this paper is to present a technique and data for non-invasively determining, objectively and subjectively, the relative perfusion of, so-called, ischemic ulcers, as a prognostic indicator of ulcer healing.

After obtaining informed consent peripheral vascular perfusion scans, using 1.5 mCi of Tl-201, have been performed in 15 patients with ischemic ulcers of the lower extremities. Two of the patients have ulcers of an amputation stump. After intravenous administration of the tracer the distribution of perfusion is subjectively evaluated by peripheral perfusion scanning of the extremities and objectively via point counting over the ulcer and surrounding normal tissue. From the point counting data the degree of hyperemia of the ulcer, or lack of it, is determined.

Preliminary data reveal all 7 non-stump ulcers with a relative hyperemia greater than 1.5 have healed or are healing while 5 of 6 non-stump ulcers with a relative hyperemia less than 1.5 have required amputation or are not healing. The two stump ulcers had ratios of 1.5 and are healing. The mean degree of hyperemia for the healing ulcers is 2.6± .5 while for the non-healing ulcers it is 0.9± .6.

Preliminary data suggest that non-invasively determined "ischemic ulcer" perfusion may be a clinically useful indicator of healing ability.

10:30 a.m.-12:00 p.m. Room 201

CONJOINT SESSION IN VITRO RADIOASSAY RADIOPHARAMCEUTICAL CHEMISTRY

MECHANISM OF REACTION AND EPIDEMIOLOGY OF PEPTIDE AND STEROID HORMONE RECEPTORS

Chairman: Danielle J. Battaglia
Co-Chairman: H. Donald Burns

ASPECTS OF EPIDEMIOLOGY OF BREAST CANCER. Elizabeth P. Anderson, National Cancer Institute, Bethesda, MD.

STEROID RECEPTORS IN BREAST CANCER. Marc Lippman, National Cancer Institute, Bethesda, MD.

MEASUREMENTS AND DISORDERS OF PEPTIDE HORMONE RECEPTORS. Len Harrison, National Institute of Health, Bethesda, MD.

10:30 a.m.-12:00 p.m. Room 204

INSTRUMENTATION, COMPUTERS, AND DATA ANALYSIS

PHYSICS

Chairman: A. Bertrand Brill
Co-Chairman: Lesley Rogers

EFFECT OF ACCIDENTAL COINCIDENCES IN POSITRON EMISSION COMPUTED TOMOGRAPHY. E.J. Hoffman, M.E. Phelps, S.C. Huang, D.E. Kuhl. University of California, Los Angeles, CA.

Errors caused by detection of accidental coincidences (ACs) and techniques for removing these events from image data were investigated in terms of their effect on quantitation in Positron Emission Computed Tomography (PCT). Removal of ACs is accomplished by simultaneous measurement of total coincidence events and ACs followed by an on line subtraction of the ACs from the total coincidences. Sequential phantom studies with short-lived positron emitters, which were performed with increasing scan times to compensate for isotope decay, gave images of constant true coincidence counts and variable AC fractions (0-50%). Images of pure ACs were obtained with phantoms containing TC-99m.

Errors in measured isotope concentrations in images were linearly related to AC fractions and are a function of size and shape of cross section and isotope distribution. For a 20 cm diameter uniform distribution of activity, a 50% (25%) AC rate contributed 46% (23%) of counts at center of cylinder, giving overestimates of 85% (33%) for concentration of positron emitter. Images of pure ACs show

count distributions varying 2 to 1 from center to edge of field of view with a definite geometric pattern of 10-20% oscillations superimposed. This pattern, due to differences in true and accidental detection efficiencies, is removed by the on line AC subtraction technique.

ACs were found to create significant and correlated errors in PCT, indicating a need for accurate correction techniques which take into account the nature of this source of error.

ANALYSIS OF COINCIDENT SCATTER FOR POSITRON CAMERAS USING LARGE AREA DETECTORS. F.B. Atkins, P.V. Harper, R. Scott, and R.N. Beck. Walter Reed Army Medical Center, Washington, D.C., and The Franklin McLean Memorial Research Institute, The University of Chicago, Chicago, Il.

The design of positron cameras which employ large area detectors, either position sensitive or discrete arrays, have been criticized on the basis that the coincident scatter component will be excessive. These conclusions are drawn largely from data obtained with well collimated, single slice systems which have been extrapolated to the virtually uncollimated geometry of the area-type systems. To obtain more direct evidence, we have investigated the coincident scatter response for this type of geometry under a variety of conditions; namely, as a function of the thickness of the scattering medium and baseline setting. The analysis involved both Monte Carlo computer simulations, and experimental measurements. The experimental studies were performed with a positron camera designed with two Searle LFOV cameras as the detectors.

It has been found that the extrapolations overestimate the coincident scatter fraction, which is defined as the ratio of the number of coincident events in which at least one of the annihilation photons has scattered to the number of unscattered coincident events. The experimental measurements are consistant with the simulated data; in particular, for a 24 cm. thick medium and a narrow window (approx. 20%), the coincident scatter fraction for a point source at the center is about 0.30. In an actual clinical situation the scatter fraction will depend on the source distribution, and scattering geometry. However, analysis of the coincident spectra from several patient studies involving N-13 ammonia imaging of the myocardium, indicates an average scatter fraction of about 25-30%.

OPTIMIZATION OF SHIELDING DEPTH FOR CIRCULAR POSITRON TOMOGRAPHS. S.E. Derenzo. Donner Laboratory, University of California, Berkeley, CA.

In positron emission transverse section tomography, the image is derived from unscattered coincident annihilation pairs. Even though shielding is used to restrict the activity seen by the detectors, image contrast is degraded by scattered coincident annihilation pairs and accidental coincidences of unrelated annihilation photons. The rates for these events are given by:

$$\text{image events: } C_i = K_i\, \rho S^2/C$$
$$\text{coincident scattered events: } C_s = K_s\, \rho S^3/(CT)$$
$$\text{accidental events: } C_a = K_a\, \rho^2 S^4/T^2$$

where ρ is the activity density (μCi/axial cm), S is the shielding gap (cm), C is the detector circle radius (cm), T is the shielding depth (cm) and K_i, K_S, and K_a are appropriate constants. Increasing the depth of the shielding (T) reduces the backgrounds but also increases the diameter of the detector circle and reduces sensitivity. The tradeoff between sensitivity and contrast may be described by a figure of merit Q which is proportional to the square of the ratio of the image signal to the statistical noise: $Q = C_i^2/(C_i+C_s+C_a)$.

For the Donner 280-crystal NaI(Tl) system and activity distributed in a 20 cm cylinder of water, K_i=310, K_S=740, and K_a=1.45 (20 nsec timing window). These constants may be used with the above equations to estimate the optimum shielding depth T for NaI(Tl) systems, given a patient port 2(C-T), an activity density ρ, and a shielding gap S. For a 50 cm patient port, ρ=200 μCi/cm and S=2 cm, the optimum shielding depth (T) is 23 cm which results in a detector circle diameter of 96 cm. For a 25 cm patient port and the same ρ and S, the optimum T is 15 cm which results in a detector circle diameter of 55 cm.

GEOMETRIC RESPONSE OF A GAMMA CAMERA COLLIMATOR WITH PARALLEL HOLES. C. E. Metz, F. B. Atkins*, and R. N. Beck. Dept. Radiology and the Franklin McLean Memorial Research Institute, The University of Chicago, Chicago, IL, and *Walter Reed Army Medical Center, Washington, D.C.

Previous studies of gamma camera collimators have been restricted largely to empirical measurements of the combined collimator-camera system. We have developed a theoretical approach that allows the geometric component of camera collimator response to be predicted independent of other system characteristics, and which thus provides a powerful tool for collimator design and camera system analysis. To deal with the positional dependence of a point source image due to the collimator hole array, we define an effective or average point spread function as the normalized image of a point source that would result if the collimator were randomly translated (but not rotated) during image formation, with the source and camera fixed. We have shown that the corresponding geometric component of the collimator transfer function is given by a general expression of the form

$$OTF_G(\vec{\nu}) = |A\{[1+(Z+B)/L]\vec{\nu}\}|^2$$

where $A(\vec{\nu})$ is the normalized two-dimensional Fourier transform of the aperture of a single hole, L is the collimator thickness, Z is the collimator-source distance, and B is the distance from the collimator to the effective image plane of the camera crystal. Closed-form expressions have been obtained for the common hole shapes: round, hexagonal, square and triangular. Monte Carlo simulations and experimental measurements of collimator geometrical response have shown this approach to be highly accurate, with disagreement typically less than 0.005 at all spatial frequencies.

THE EVALUATION OF IMAGING SYSTEMS WITH Tl-201 USING THE PERFORMANCE INDEX AS A TOTAL SYSTEM PERFORMANCE CRITERION. J.A. Patton and F.D. Rollo, Vanderbilt University Medical Center, Nashville, TN 37232

Line spread functions (LSF) and plane source (S) measurements have been used for many years to measure resolution and sensitivity respectively. Modulation transfer functions (MTF) calculated from LSF data predict the resolution of systems over an entire range of spatial frequencies and include the effects of scatter. To more closely approximate the clinical situation, the contrast efficiency function (Ec), calculated from the MTF, has been defined to measure an imaging system's ability to detect a spherical void of activity. To obtain a measure of total system performance, the performance index (PI) has been introduced to combine spatial resolution performance (Ec) with plane sensitivity measurements (S). Also a phantom is available (Rollo phantom) based on this concept and therefore, imaging systems can be evaluated and compared simply by comparing images obtained for equal accumulation times. These concepts are used to evaluate the performance of systems in imaging Tl-201 distributions in the myocardium. Computer programs provide plots of MTF, Ec, and PI function calculated from LSF and S data. The calculated PI values, when compared to imaging evaluations using the Rollo phantom show good agreement. PI functions measured for an Ohio Nuclear mobile camera show that for equal counting times, there is virtually no difference in imaging with the high sensitivity collimator and a 20% window and the medium energy collimator with a 30% window for lesion diameters less than 2 cm. For larger lesions, the former configuration is superior. Clinical studies verify these results.

QUANTITATIVE COMPARISON OF SOLID STATE AND SCINTILLATION CAMERAS. J. W. Steidley, Radiation Monitoring Devices, Watertown, MA. D. W. Miller, P. A. Schlosser, A. H. Deutchman, and J. R. Hyland The Ohio State University, Columbus, OH.

The imaging capabilities of solid state and scintillation cameras with energy resolution from 1% to 14% FWHM at 140 KeV was studied in a qualitative fashion experimentally and in a quantitative fashion with a computer simu-

lation. A germanium camera with 1.8 mm FWHM spatial and 4% energy resolution was experimentally compared to an Anger camera with 3.6 mm spatial and 13% energy resolution. Lead and tungsten collimators of 8.3 mm and 3.2 mm resolution at 10 cm depth were used. As a result of better spatial and energy resolution capabilities, the solid state camera showed qualitatively improved phantom and animal images.

To quantitate, and thus highlight, the effects of improved energy resolution a computer program was written to control the variables of detector spatial resolution, efficiency, uniformity, dead time, linearity, energy window, film and observer interpretation. Imaging at 140 KeV of 3 mm to 9 mm diameter spherical regions at 10 cm depth and of 10% to 50% contrast was simulated. As an example, consider a detector of 3 mm spatial resolution and regions of 24% inherent contrast which are imaged at 12% contrast (i.e., at 50% modulation transfer). When the energy resolution is improved from 13% to 4%, volumes which are 2.2 and 5.1 times smaller are imaged with the lead and tungsten collimators respectively. This quantitatively illustrates the improved performance of high energy resolution cameras which was qualitatively demonstrated experimentally.

COMPARATIVE QUANTITATIVE MEASUREMENT OF SPATIAL RESOLUTION IN-DEPTH USING TOMOGRAPHY AND NON-TOMOGRAPHIC INSTRUMENTS. B. Brunsden, P. Kirchner, E. Lands, T. Brown and M. Cooper. The University of Chicago, Chicago, IL.

Instrument selection for specific clinical imaging problems should consider the variation of spatial resolution with distance. To measure this parameter for the Pho/Con, the LFOV camera, and the Ohio-84 rectilinear scanner, a special phantom was constructed. An acrylic plate was sloped 45° in a container. In the plate, six parallel pairs of grooves defined line separations of 30, 20, 15, 10, 7.5, and 5mm. The grooves were made finer for lesser line separations, so that uniform tracer concentration in the grooves produced a constant count density across the phantom.

The distances from the collimator at which any given line separation was still resolved was measured for each instrument in air, water and background activity (isotope in water), using Tc-99m and each major Ga-67 peak.

Compared to results in air, the LFOV had significantly smaller range-of-resolution in scattering medium and even less in background activity; e.g., for Tc-99m, 15mm line separation seen to a distance of 18cm in air, 16.5cm in water, 14.2cm in low background, and 9.4cm in high background activity. In constrast, the resolution range of the Pho/Con was not affected by scatter or background activity: 15mm line separation was resolved in Tc-99m permeated water from 3 to 14cm depth. The Ohio 84 resolution was poor but similarly unaffected. Identical measurements with Ga-67 provided similar results.

These results support the use of longitudinal tomography in clinical circumstances where deeply placed lesions, such as pancreatic cancer and para-aortic or retroperitoneal disease are sought.

2:00 p.m.-3:30 p.m. Room 210

CLINICAL SCIENCE

PEDIATRICS

Chairman: Hirsch Handmaker
Co-Chairman: Gary F. Gates

SCINTIGRAPHIC EVALUATION OF GASTROESOPHAGEAL REFLUX (GER) IN CHILDREN. P.G. Devos, P. Forget, M. De Roo and E. Eggermont. KUL School of Medicine, Leuven, Belgium.

Because of the difficulty in assessing the clinical significance of GER in children, as demonstrated by RX, we tried to evaluate it by means of quantitative dynamic scintigraphy, using a modification of the method introduced by Fisher ea (1976). 0.2 - 0.5 mCi Tc-99m sulfur colloid in 100 - 300 ml glucose 5 % were administered through a nasogastric tube and the supine patient was studied during 30 minutes. GER-index was computed as the mean value of the time-activity curve over the esophagus, expressed as % of the measured maximal initial gastric activity; one could expect this value to reflect both quantity and duration of GER.

In 8 controls (age 2 m - 8 y) GER-index was 0.66 ± 0.12 % (mean ± SEM), ranging from 0.30 to 1.30 %; in 5 patients (age 1 - 3 m) with benign vomiting the index was 0.67 ± 0.12 %, range 0.45 to 1.03 %. In 8 patients with peptic esophagitis (age 2 m - 16 y) however the index was 3.66 ± 0.81 %, ranging from 1.72 to 7.82 % and differing significantly ($p < 0.01$ in Mann-Whitney U test) from the controls. 3 patients (1 - 2 y) who underwent fundoplication showed a value from 0.26 to 0.98 %.

Using endoscopic and anatomopathologic diagnosis of peptic esophagitis as ultimate proof for the presence of a significant GER, there were neither false positive nor false negative results with the scintigraphy, whereas RX missed 2/7 patients and had 4/16 false positive results.

These preliminary results look promising and point to the possibility of an easy and accurate detection, follow-up and perhaps quantification of cardia-malfunction.

SCINTIGRAPHIC DETECTION OF GASTROESOPHAGEAL REFLUX IN CHILDREN. J.D. Blumhagen, T.G. Rudd, D.L. Christie. Children's Orthopedic Hospital and Medical Center, and the University of Washington Medical School, Seattle, WA.

We investigated the clinical efficacy of radionuclide gastroesophagography in detecting pathologic gastroesophageal reflux in children clinically suspected of reflux. Forty-six patients between one month and 16 years of age were studied with the acid reflux test, barium esophagography and the scintigraphic technique.

Each fasted patient drank 200 μCi Tc-99m sulfur colloid in a small volume followed by fruit juice until sated. The patient was then imaged anteriorly in the supine position continuously for 30 to 60 minutes with a gamma camera while data were collected for 30-second intervals. Esophageal activity/time curves were plotted. Following the continuous monitoring, abdominal compression was applied in an attempt to induce reflux. Acid reflux testing was performed with a pH probe in the distal esophagus after instillation of an acidic solution into the stomach. Barium studies included the water siphon test.

The acid reflux test was considered the standard of comparison and was positive in 33 patients, among whom there were 28 positive and 5 negative scintigraphic studies. There were 10 positive and 3 negative scintigraphic studies among the 13 patients with negative acid reflux tests. Barium studies agreed with scintigraphic results in 35 cases. Among the 10 patients with false positive scintigraphy, 7 showed only a minor degree of reflux of doubtful significance.

The radionuclide gastroesophagogram is a promising technique for the diagnosis of gastroesophageal reflux. It has the advantages of being physiologic and allowing continuous monitoring of esophageal activity for prolonged periods.

DETECTION OF PULMONARY ASPIRATION IN INFANTS AND CHILDREN Sombat Boonyaprapa, Philip O. Alderson, Darryl J. Garfinkel and Henry N. Wagner, Jr. Johns Hopkins Medical Institutions, Baltimore, Md.

Recurrent pneumonia in children may be caused by trans-tracheal aspiration of gastric contents following gastro-esophageal (GE) reflux or through a tracheoesophageal (TE) fistula. To determine if pulmonary aspiration could be diagnosed in children using radionuclides, 19 patients aged 1 mo-14 yrs (mean age = 29 mos) drank 500 uCi of Tc-99m sulfur colloid mixed with infant formula or orange juice. Gamma camera images (100 K) of the chest (ant, post, lat views) were obtained immediately after

feeding, and 4 and 24 hrs later using a high sensitivity, high contrast computer oscilloscope to record the images. No artificial means were used to increase intra-abdominal pressure during the radionuclide study. Fourteen of the children also had G-E contrast studies using abdominal compression and standard radiographic techniques. These studies were never performed the same day as the radionuclide study. Four children (24%) showed abnormal pulmonary activity. One child with lung activity seen immediately after ingestion of Tc-99m colloid had a radiographically confirmed TE fistula. Two children had lung activity present at 4 hrs; one had reflux and aspiration seen during his contrast study. One child showed lung activity only after sleeping overnight. His contrast study was normal. The other 15 children had negative radionuclide aspiration studies. Eleven had G-E contrast studies; 8 were normal and 3 showed GE reflux, but no evidence of aspiration. Radionuclide studies represent a noninvasive means for diagnosing pulmonary aspiration under physiologic conditions in infants and children.

USEFULNESS OF RADIONUCLIDE STUDIES IN DETECTION OF GASTRO-ESOPHAGEAL (GE) REFLUX AND PULMONARY ASPIRATION IN CHILDREN. S.Thirunavukkarasu, A.R.Siddiqui, R.Wyllie, H.Eigen, E.A.Franken, H.N.Wellman, J.L.Grosfeld, J.F.Fitzgerald, Indiana University School of Medicine, Indianapolis, IN.

We studied usefulness of radionuclide (RN) techniques in evaluation of children with GE reflux and recurrent pneumonias. Two mCi of technetium-99m sulfur colloid were administered in upright position through a NG tube and stomach was distended with saline. Images were obtained in upright and supine position with and without manual abdominal pressure. Four and 24 hrs delayed images were obtained over the chest to detect pulmonary aspiration (PA).

A total of 43 patients (pts) were studied, 30 of which had clinical and/or laboratory evidence of GE reflux and the remaining were controls (cts). All pts also underwent barium UGI studies, gastroesophageal manometry, measurement of esophageal pH (Tuttle test) and endoscopy. Seventeen of 30 pts with GE reflux had RN evidence of reflux. All 13 cts had normal RN studies. Barium studies were positive in 15 of 30 pts with reflux and negative in all cts. Six pts had positive RN studies but negative radiographs and 4 pts had positive radiographs with normal scans. At least one study was positive in 21 of 30 pts. All pts had positive Tuttle test. PA was not demonstrated in any pt by any technique, although 17 pts had clinical findings suggestive of it. CONCLUSION: 1) Tuttle test is very accurate. 2) RN and barium studies are complimentary and very specific, but not as sensitive as Tuttle test. 3) The RN technique was not suitable for detection of PA; however, it was not done ideally, i.e., dosing pts at bedtime and imaging in the morning (J Nucl Med 18:1079, 1977)

VENTRICULAR FUNCTION AT REST AND DURING EXERCISE IN CYSTIC FIBROSIS (CF). Bradley E. Chipps, Philip O. Alderson, Jean-Michel A. Roland, Shirley Yang, Andries van Aswegen, Beryl L. Rosenstein, Henry N. Wagner, Jr. The Johns Hopkins Medical Institutions, Baltimore, Md.

The cardiac function of 19 children (aged 4-17 years) and two young adults (26,27 yrs) with CF was studied using radionuclides and M-mode echocardiography (ECHO). The patients exhibited a wide range of clinical and pulmonary function abnormalities. Right ventricular ejection fraction (RVEF) was determined during the first pass of Tc-99m human serum albumin (HSA) using a multicrystal camera. Left ventricular (LV) function was studied at rest in all patients and during exercise in 8 patients (pts) ($\bar{x}$ age 15, range 10-27) after Tc-99m HSA equilibration using an ECG-synchronized camera-computer system and by ECHO. The first transit RVEF was abnormally low in 13/18 pts (72%) at rest; an additional 4 pts had abnormal septal motion on ECHO. LVEF was abnormal at rest in 4 pts (19%); each showed generalized LV hypokinesis. The ratio of the LV pre-ejection period over LV ejection time (PEP/LVET) as determined by ECHO significantly increased (i.e., worsening LV performance) with deterioration of the chest radiograph score ($p < .001$) and forced expiratory volume in 1 second ($p < .05$). Three of eight pts with normal LVEF at rest showed an abnormal response to supine bicycle exercise; LVEF fell in 2 pts and was unchanged in 1. Thus, LV dysfunction was observed in 7 of the 21 pts (33%) and was demonstrated only during exercise in 3 of them. The results confirm the high incidence of RV dysfunction in CF and show that LV dysfunction also occurs. The findings suggest that exercise testing should be performed when evaluating LV function in pts with CF.

SIMULTANEOUS Tc-99m PARABUTYL-IDA AND I-131 ROSE BENGAL EXAMINATION IN JAUNDICED NEONATES. B.D. Collier, S. Treves J. McAffee, G. Subramanian, M.A. Davis, and S. Heyman. Harvard Medical School and Children's Hospital Medical Center, Boston, MA and Upstate Medical Center, Syracuse, NY

The principal goal of hepatobiliary scintigraphy in jaundiced neonates is the identification of complete or near complete obstruction of the extrahepatic biliary tract. Nine jaundiced patients, 6 with neonatal hepatitis and 3 with biliary atresia, were examined. Tc-99m-parabutyl-IDA (50 μCi/kg) and I-131 rose bengal (200 μCi) were injected simultaneously with imaging at 15 minutes, 30 minutes, 45 minutes, 1 hour, 4 hours, 24 hours, and as late as 7 days if small bowel activity was not seen. By showing passage of activity into the small bowel, I-131 rose bengal correctly separated 5 neonates with neonatal hepatitis from 3 neonates with biliary atresia. Tc-99m-parabutyl-IDA failed to show small bowel activity in 3 patients with neonatal hepatitis. The advantages of lower patient dose and higher photon flux from the Tc-99m agent are offset by its limited ability to demonstrate late passage of bile into the small bowel. I-131-rose bengal remains the hepatobiliary agent of choice in the jaundiced neonate.

DOSIMETRY CONSIDERATIONS FOR THE LIVER, SPLEEN AND METAPHYSEAL GROWTH COMPLEXES IN CHILDREN UNDERGOING Ga-67 CITRATE SCANNING PROCEDURES. S. R. Thomas, M. J. Gelfand, J. G. Kereiakes, G. S. Burns, R. C. Purdom and H. R. Maxon. Eugene L. Saenger Radioisotope Laboratory, Cincinnati General Hospital, Cincinnati, OH.

Ga-67 citrate scanning procedures have been used extensively in the diagnosis of inflammatory disease in adults. More recently, the efficacy of Ga-67 scintigraphy in pediatric patients has been evaluated. To date, dosimetric estimates for children have simply been extrapolated from adult data. We have obtained initial results concerning Ga-67 citrate dosimetry for the liver, spleen and metaphyseal growth complexes of the distal femur and proximal tibia in a small group of children ranging from 2 to 17.5 years old. In-vivo dosimetric measurements for Ga-67 are complicated by the high degree of non-specificity of this radiopharmaceutical. Quantitative conjugate view counting techniques have been applied for the determination of the radioactivity in the given organ, with corrections as required for surrounding diffuse non-target organ activity and/or "overlapping" discrete regions of uptake (e.g., spine). The uncertainties involved in these calculations are described. In the case of the metaphyseal growth complexes, additional ambiguities arise for some patients in the spatial differentiation of the metaphyseal growth complex from adjacent metaphyseal and epiphyseal bone and marrow. The effective halflife for these organs was determined from serial measurements over a period of days to be essentially 78 hours (i.e., equal to the physical halflife of Ga-67). The dose per administered activity for the liver and spleen was found to be in the range 1 - 4 rad/mCi and 1 - 5 rad/mCi respectively. For the metaphyseal growth plates, the results indicated a range 3 - 10 rad/mCi.

2:00 p.m.-3:30 p.m. Room 211

CLINICAL APPLICATIONS

PULMONARY

Chairman: Robert J. Lull
Co-Chairman: Robert J. Kaminski

VENTILATORY ABNORMALITIES INDUCED BY PULMONARY EMBOLUS: DEMONSTRATION BY V/Q STUDIES. H. Hricak, D.S. Marks, and W.R. Eyler. Henry Ford Hospital, Detroit, MI.

We wish to report on several patients in whom pulmonary embolism appears to have induced airway changes. None of these patients had a previous history of airway disease.

Eight patients with a clinically confirmed diagnosis of pulmonary embolism demonstrated concomitant perfusion and ventilation abnormalities during V/Q studies. In three cases embolism was confirmed by angiography, one case by venography and in the remaining four by clinical presentation and/or serial scans. All patients had matching perfusion defects and delayed wash-out on ventilation. Four also had matching abnormalities on the single-breath (wash-in) phase of ventilation. Follow-up studies were performed on six patients, and showed resolution of both perfusion and ventilatory abnormalities. Since no patient had pre-existing airway disease, the ventilation changes appear to have been induced by the emboli.

While we do not feel that the findings interfered with the diagnosis of emboli in any of the cases, this is the largest series (to date) reporting on the simultaneous occurance of V/Q changes secondary to emboli. One is thus reminded that matching ventilation and perfusion abnormalities may not exclude the diagnosis of pulmonary emboli.

REGIONAL VENTILATION AND PERFUSION IN PATIENTS WITH UNRESECTABLE CARCINOMA OF THE BRONCHUS STUDIED BEFORE AND AFTER PALLIATIVE RADIOTHERAPY. F. Fazio, T.A. Pratt, C.G. McKenzie, and R.E. Steiner. Hammersmith Hospital, London, U.K.

Ventilation/perfusion ($\dot{V}/\dot{Q}$) scans were obtained in 45 patients with inoperable carcinoma of the bronchus. Thirty-five patients were re-investigated following radiotherapy and 17 of them had further follow-up studies.

Both $\dot{V}$ and $\dot{Q}$ were always abnormal in the lung affected by the tumor, $\dot{Q}$ being usually more impaired than $\dot{V}$. These abnormalities were difficult to detect or to evaluate from an assessment of regional perfusion and ventilation derived from the standard chest radiograph. Following radiotherapy, a significant improvement of both $\dot{V}$ and $\dot{Q}$ was observed, which was associated with amelioration of breathlessness. Slow but progressive deterioration of regional $\dot{V}$ and $\dot{Q}$ and dyspnea were subsequently observed. This was often associated with the development of radiation fibrosis. Tests of overall lung function (VC, $FEV_{1.0}$) were moderately impaired at the initial assessment (probably due to co-existing chronic airways obstruction), and did not show significant changes after radiotherapy or during follow-up. Isotope studies of regional perfusion and ventilation proved more sensitive and more specific than tests of overall lung function for the assessment and follow-up of patients with unresectable carcinoma of the bronchus.

VENTILATION/PERFUSION LUNG SCANS IN COLLAPSE AND CONSOLIDATION. J.D. Lavender and J.D. Armstrong, R.P.H.S. and Hammersmith Hospital, London, United Kingdom.

The major application of radioisotope lung scans is in the detection of pulmonary embolic disease. However, with detailed images of regional ventilation and perfusion available from the use of Kr-81m/Tc-99m, lung scanning can be of value in acute respiratory disease.

The present analysis is based on a review of four hundred scans performed over the last twelve months. Fourteen patients with pneumonic consolidation (five with follow-up scans), fifteen with lobar, segmental or subsegmental collapse and eight with pulmonary infarction associated with pulmonary embolic disease, have been reviewed in detail. Three patients have had two acute respiratory disease processes simultaneously. Acute pneumonic consolidation examined during the first seven days shows relatively well preserved perfusion and absent ventilation. An acutely collapsed lung shows some reduction (approximately 50%) in perfusion and absent ventilation. Lung infarcts show defects of both perfusion and ventilation with frequently more extensive defects of perfusion. Calculated V/Q ratios therefore for pneumonia and collapse are low (less than 0.5), for infarcts, 1.0. Multiple pathologies occurring in the same patient can be identified by consideration of relative perfusion and ventilation.

DETECTION OF BRONCHIECTASIS IN CHILDREN BY MEANS OF LUNG SCINTIGRAPHY. J. Vandevivere, M. Spehl, I. Dab, D. Baran and A. Piepsz. St-Peter Hospital, Free University of Brussels, Belgium.

This study was undertaken to evaluate the validity of lung scintigraphy in detecting bronchiectasis.
Between 1970 and 1978, 76 children clinically suspected of bronchiectasis have been examined by means of chest X-ray, bronchography and Tc-99m HAM perfusion scintigraphy. 102 unilateral bronchographies were available for the purpose of comparison. Additional Kr-81m ventilation lung scans were obtained in 16 patients. All these investigations were performed 3 to 6 months after the last pulmonary infection. Evidence of bronchiectasis was demonstrated by bronchography in 26 lungs and discarded in the 76 others. On this basis, for the chest X-ray alone a sensitivity of 73 % and a specificity of 76 % were obtained. For the lung scan alone sensitivity was 92 % and specificity 60 %. When both chest X-ray and lung scan were considered, sensitivity reached 96 % and specificity fell to 53 %. Preliminary data with Kr-81m gave the same information as perfusion scintigraphy.
It is concluded that bronchiectasis may be almost excluded when both chest X-ray and lung scan are negative. When either chest X-ray or lung scan were positive, the presence of bronchiectasis was confirmed in about 40 % of the cases. Lung scan, combined with chest X-ray, therefore represents an excellent guide when a decision of bronchography should be taken in children.

VENTILATION-PERFUSION LUNG SCANS WITH Xe-133 IN INFANTS AND CHILDREN. L.D. Samuels, S. Godfrey and B. Warshaw, Hadassah University Hospital, Jerusalem, Israel.

This study was undertaken to evaluate a simple yet effective means of documenting regional pulmonary function in infants and young children.

Fifteen infants and young children with suspected congenital anomalies of the lung or with acquired abnormality in pulmonary function were studied with a combination of Xe-133 perfusion-washout studies following injection of Xe-133 in saline and by Xe-133 inhalation studies, usually administered via nasal catheter, utilizing both sequential multi-imaging and computer analysis of regional ventilation after serial acquisition of data.

Examples to be shown include hypoplastic lung, congenital lobar emphysema, bronchial obstruction, bronchomalacia, pulmonary vascular disease and hyperlucent lung syndrome.

We conclude that Xe-133 scans by this technique are a safe, rapid and effective screening test for both congenital and acquired respiratory problems of infancy and children.

VENTILATION/PERFUSION LUNG SCANNING IN PEDIATRICS. I. Gordon, P. Helms, and F. Fazio. The Hospital for Sick Children, Great Ormond Street, London, U.K.*

We obtained Kr-81m ventilation and Tc-99m perfusion lung scans in anterior, posterior and oblique views in 105 children (age range 14 days to 15 years) with various pediatric problems.

On reviewing these studies we found four main areas of clinical usefulness:
a) Establishing the diagnosis: in a relatively small number of patients the lung scan was essential for either establishing the exact diagnosis or directing the attention to the abnormal area. b) Refuting a diagnosis: the two main groups in this category include possible bronchiectasis and inhaled foreign body. c) Establishing the extent of the disease: isotope studies enable one to assess and follow up the extent of the disease in children with lower respiratory problems: a lung scan may obviate the need for bronchography in bronchiectatics failing to respond to medical treatment and for whom surgery is considered; repeat studies are useful in following the natural history or the response to treatment of various lung conditions. d) Assessing the success of surgical procedures on the heart and on abnormal pulmonary arteries.

We indicate that Kr-81m ventilation/Tc-99m perfusion scanning is particularly useful in small children in whom tests of overall pulmonary function cannot reliably be carried out because of lack of cooperation.

*Work done in cooperation with the M.R.C. Cyclotron Unit, Hammersmith Hospital, London, U.K.

ENHANCED DIAGNOSIS OF VENOUS THROMBO-EMBOLIC DISEASE EMPLOYING ROUTINE RADIONUCLIDE VENOGRAM (RNV'S) IN CONJUNCTION WITH PULMONARY VENTILATION-PERFUSION (V/Q) SCINTIMAGING. A.R.Siddiqui, D.J.Bruns, H.N.Wellman, E.C.Klatte, Indiana University School of Medicine, Indianapolis, IN.

RNVs using Tc-99m macroaggregates of albumin (Tc-MAA) were performed on 90 patients (pts) who were referred for V/Q scintimaging for suspected pulmonary emboli (PE). The RNVs were performed on completion of Xenon-133 ventilation scans, during the injection of Tc-MAA for perfusion studies according to the technique described by Ryo et al (J Nucl Med 18:11, 1977).

Forty pts had RNVs consistent with venous thrombotic disease. Contrast venograms (CVs) were available for comparison in 39 limbs of 24 pts. All 13 limbs with abnormal CVs had abnormal RNVs. There were no false negatives; however, there were 4 false-positive RNVs, two of which were due to post-exercise punctate hang-up in the calves. The overall accuracy of RNV, when compared to CV, was 90%.

V/Q studies were interpreted to be consistent with either PE (30), normal (12), indeterminate (12) or consistent with chronic lung disease (36). RNVs were abnormal in all 9 pts with clinical thrombophlebitis; 6 of which had V/Q studies consistent with PE. In the 81 pts without clinical thrombophlebitis, 20/27 pts with PE had abnormal RNVs, whereas 11/54 RNVs were abnormal in the rest. Three pts with indeterminate V/Q studies had abnormal RNVs and all of them subsequently developed PE. When all pts with final diagnosis of PE (33) are grouped together, the use of RNVs enhanced the diagnosis of venous thrombotic disease from 18% (6/33) to 80% (26/33).

RNVs are accurate and add only about 20 minutes to V/Q studies. Routine RNVs may increase the certitude of presence or absence of thrombo-embolic disease.

TOURNIQUET PRESSURE (TP) AND LOWER EXTREMITY VENOUS FLOW DYNAMICS. R. C. Verma, M. M. Webber, and J. I. Eisenman. LAC-UCLA Olive View Medical Center, Los Angeles, CA.

The highly variable results of radionuclide venography from various centers are partly due to differences in technique, one such being the amount of TP applied to occlude the superficial veins (SV). Investigations into the effect of TP on flow through the SV and deep veins (DV) of the lower extremity are in progress and early observations are reported below.

A 21 gauge scalp vein needle is placed into a dorsal pedal vein in a supine subject. The needle tip is pointed towards the toes to direct flow through the plantar plexus. The popliteal systolic and diastolic pressure are recorded. A blood pressure (BP) cuff is applied above the ankle. Fifty uCi of TcMAA are injected and flow through the calf noted. The TP is sequentially increased by 20 mmHg and the above procedure repeated. The minimum pressure necessary to occlude SV and DV is recorded. With the pressure in the above-ankle cuff set to occlude the SV, the above procedure is repeated with a cuff above the knee.

Preliminary results in 9 patients studied so far reveal that higher pressures may actually diminish flow through DV possibly because of occlusion of arteries. Release of TP or flexion/extension of foot may be more helpful than flushing with additional saline to evaluate interrupted sluggish flow (sometimes misinterpreted as occlusion) through DV. The minimum pressure required to occlude SV varies tremendously and bears no correlation to the subjects' systolic or diastolic BP. In 2 patients with extensive occlusion of DV, even systolic pressure did not prevent flow through SV.

2:00 p.m.-3:30 p.m. Room 300/301

CLINICAL SCIENCE

CARDIOVASCULAR III

Chairman: Ismael G. Mena
Co-Chairman: Harvey Berger

THE EFFECT OF ORAL PROPRANOLOL ON LEFT VENTRICULAR FUNCTION AT REST AND DURING EXERCISE IN NORMALS AND IN PATIENTS WITH CORONARY ARTERY DISEASE AS DETERMINED BY RADIONUCLIDE ANGIOGRAPHY. G. Wisenberg, R. Marshall, H. Schelbert, C. Rue. UCLA School of Medicine, Los Angles, CA.

Reports on the effects of oral propranolol (P) on left ventricular performance at rest and during exercise in patients with coronary artery disease (CADP) have been conflicting and preclude prediction of the response to P in the individual patient. Therefore, this study was undertaken to define the effects of P on left ventricular ejection fraction (EF) at rest and during graded supine bicycle exercise in 4 normal controls and 9 angiographically documented CADP, using gated equilibrium radionuclide angiography. All subjects were studied prior to and during P therapy, the controls studied at 160mgm/day and at maximum beta blockade, as determined by treadmill exercise. Peak daily P doses averaged 533±92 (SD) mgm in normals and 154±44 mgm in CADP. In normals, peak exercise HR declined from 164±21* to 128± 17 and to 113±8.0*(P<.025) at intermediate and peak P doses respectively, the corresponding values in CADP being 119±14 to 97±8 (P<.005). P did not significantly change resting EF either in normals (69.7%±4 vs 74.6±2.5) or CADP (60±11.6 vs 62±9.7). In normals on P, there was a significant decline in mean exercise EF from 82.3±3.1* to 77±2* to 75±3.5* (P<.05) on intermediate and maximal therapy, while in CADP the increase was not significant (55±16.0 vs 62±11.6). However, the mean change in EF from rest to exercise (+or-) was significantly less in both groups while on P, 12.7±1.5 to 4.3±2.1 to 0.7±1.1 (P <.005) in normals, and 10.9±7.3 to 4.2±4.5 (P<.025) in CADP. We conclude that (P) does not alter resting EF, and minimizes the change in EF during exercise regardless of the pretreatment response.

EFFECT OF NITROGLYCERINE ON LEFT VENTRICULAR FUNCTION AND VOLUME DURING EXERCISE IN CORONARY ARTERY DISEASE. D.E. Manyari, T.D. Cradduck, L.J. Melendez, A.A. Driedger, and A.C. MacDonald. Victoria Hospital, University of Western Ontario, London, Canada.

The purpose of this study was to evaluate the changes produced by nitroglycerine (GTN) upon the left ventricular ejection fraction (EF) and end-diastolic volume (EDV) as

assessed by radionuclide angiography. 24 patients with proven coronary artery disease (CAD) and 10 normal subjects (N) underwent equilibrium cardiac scintigraphy at rest (R) and during supine bicycle exercise (EX), before and after GTN administration. In N subjects, the EF increased from 49 ± 3 (% mean ± SE) at R, to 59 ± 4 during EX ($p < 0.01$); after GTN administration the EF increased at R (57 ± 4, $p < 0.01$), but not during EX (62 ± 5, $p > 0.10$). In patients with CAD the EF decreased from 44 ± 3 at R to 38 ± 3 during EX ($p < 0.001$); after GTN administration the EF increased at R (47 ± 3, $p < 0.0001$) when compared to pre-GTN values.

During EX, EDV did not change significantly in either group. After GTN administration the EDV decreased ($p < 0.01$) at R in N and CAD subjects, but during EX only CAD patients showed a significant reduction ($p < 0.01$).

The aforementioned changes occurred despite similar blood pressure-heart rate products during EX before and after GTN administration in both N and CAD groups. The observation that GTN improves the EF only when accompanied by significant reduction on EDV, at R and during EX in N and CAD subjects, supports the concept that the beneficial effect of GTN in ischemic heart disease may be related solely to its peripheral action upon the venous capacitance vessels.

IMPROVED GLOBAL AND REGIONAL VENTRICULAR PERFORMANCE WITH NITROPRUSSIDE IN ACUTE MYOCARDIAL INFARCTION. P.K. Shah, D. Berman, M. Pichler, F. Shellock, J. Maddahi, A. Waxman, and H.J.C. Swan. Cedars-Sinai Medical Center, L.A., CA.

Multiple gated equilibrium scintigraphy (MGES) is well suited to serial assessment of left ventricular (LV) function during pharmacologic intervention. This study was to apply MGES in evaluating the effects of nitroprusside (NP) in the setting of acute myocardial infarction (AMI).

Nitroprusside (NP) was infused to lower elevated arterial pressure (AP) and/or pulmonary capillary wedge pressure (PCW) in 16 pts with AMI. MGES was performed using Tc-99m-RBC's in 45° left anterior oblique (LAO) and anterior views along with hemodynamic assessment before and during NP infusion to determine LV and right ventricular (RV) ejection fractions (EF). Normalized wall motion score (NWMS), a semiquantitative index of regional wall motion (RWM), was derived from assessment of RWM of 9 LV segments according to a 6 point scoring system (4 hyperkinesis, -1 dyskinesis). The results are shown below:

	HR	AP mmHg	PCW mmHg	CI L/m	SVR Units	LV EF	LV NWMS	RV EF
C	92±12	110±22	19±6	2.4±.7	24±10	.33±.10	.37±.2	.40±.10
NP	91±14	91±13*	11±4*	2.4±.7	21±9*	.38±.10*	.46±.2*	.50±.10*

C=control, SVR=systemic vascular resistence, CI=cardiac index, HR=heart rate. *p<.01 Mean±SD

Of the 67 abnormally contracting LV segments, RWM improved in 18, remained unchanged in 48 and deteriorated in 1. Conclusion: Careful reduction of elevation of AP and/or PCW in AMI with NP improves global and regional ventricular performance suggesting decrease in ischemia in reversibly hypofunctioning LV segments. MGES represents a useful noninvasive method for monitoring the potent effects of this drug.

THE DETECTION OF CORONARY HEART DISEASE (CHD) AND CARDIOMYOPATHY (CM) USING MULTIPLE GATED TECHNETIUM-99M (MUGA-Tc^{99m}) CARDIAC BLOOD POOL SCINTIGRAPHY DURING THE COLD PRESSOR (CP) TEST. R.J. Wainwright, D.A. Raper, A.J.W. Hilson, E. Sowton, M.N. Maisey. Guy's Hospital, London S.E.1., England.

MUGA-Tc^{99m} studies were performed in 50 normotensive patients (22 normals, 24 CHD, 4 CM) before and during CP stimulation to assess this intervention in the detection of abnormal ventricular wall movement (VWM) and ejection fraction (EF) response. In all subjects a significant increase in mean heart rate (18%) and blood pressure (22%) was produced by CP stimulation.

i) Normal subjects had no change or a significant increase ($p<0.005$) in left ventricular (LV) EF and preserved normal myocardial wall motion.

ii) 22/24 (92%) CHD patients had a significant decrease ($p<0.001$) in LVEF and 10 developed localised VWM abnormalities in regions supplied by severely stenosed coronary arteries.

iii) All patients with CM had a significant fall in LVEF ($p<0.001$).

iv) 12 patients with CHD had normal LV function at rest and a normal rest 12 lead electrocardiogram (ECG). 11 patients developed abnormal CP:MUGA-Tc^{99m} studies whereas only 6 patients had an abnormal exercise ECG (single V5 lead) ($p=0.03$).

It is concluded that:

a) the CP test in resting patients provides a stimulus sufficient to cause abnormal LV function detectable by MUGA-Tc^{99m} scintigraphy.

b) CP:MUGA-Tc^{99m} is more sensitive than the single lead exercise ECG to detect patients with CHD.

EXERCISE INDUCED CHANGES IN LEFT VENTRICULAR FUNCTION IN PATIENTS WITH MITRAL VALVE PROLAPSE. M. Ahmad, T. Sullivan*, H. Haibach*, K. Sandock*, K. Logan*, and R. Holmes. Veterans Administration and University Hospitals, Columbia, MO.

To characterize the response of left ventricular (LV) function to exercise in patients (pts) with mitral valve prolapse (MVP), we studied 30 pts with MVP and normal resting LV function confirmed by LV cineangiography. Equilibrium cardiac blood pool imaging was performed in 45° left anterior oblique projection following in vivo red blood cell labeling with Tc-99m pertechnetate. Images were obtained at rest and during symptom-limited maximum exercise stress test in the upright position on a bicycle ergometer. LV ejection fraction (EF) and wall motion were examined. All pts had normal resting EF. A >5% increase/decrease in EF from rest to exercise was interpreted as a change. In 12 pts without associated coronary artery disease (CAD) (Group I), EF increased with exercise in 6, remained unchanged in 4, and decreased in 2. The 2 pts with EF reduction during exercise developed exertional chest pain without ischemic changes. In 18 pts with associated CAD (Group II), EF remained unchanged during exercise in 15, increased in 1, and decreased in 2. The 2 pts with EF reduction had angina and ischemic ST depression at peak of exercise. All 4 pts with decreased EF during exercise (Groups I,II) developed localized LV wall motion abnormality. Heart rate and blood pressure responses were not significantly different between Groups I and II. These data suggest: 1) In pts with isolated MVP, LV function changes variably during exercise with increase of EF being most common. 2) Exercise-induced reduction in EF is not specific for CAD and may occur in pts with isolated MVP. 3) EF reduction in pts with isolated MVP and in those with associated CAD correlates with development of chest pain during exercise.

EXERCISE VENTRICULOGRAPHY: COMPARISON OF RIGHT ANTERIOR OBLIQUE WALL MOTION ANALYSIS BETWEEN RADIONUCLIDE AND CONTRAST VENTRICULOGRAPHY. T.J. Brady, J.H. Thrall, K. Lo, J.A. Walton, J.F. Brymer, and B. Pitt. University of Michigan Medical Center, Ann Arbor, MI.

Wall motion (WM) analysis of equilibrium gated radionuclide ventriculography (RNV) has been shown to correlate well with resting contrast ventriculography (CV). Patient motion and varying heart rates during acquisition are inherent problems of exercise radionuclide ventriculography (ERV), that may adversely affect interpretation of ventricular WM. We studied 38 patients (PTS) at rest and then during supine bicycle exercise (EX) using both RNV and CV, at similar exercise levels within 72 hours of each other. Twenty-one PTS had a ≥ 70% stenosis in one or more coronary arteries. Seventeen PTS had no evidence of coronary artery disease (CAD).

Cinematic closed loop display of 10° right anterior oblique (RAO) radionuclide and cineangiographic display of 30° RAO contrast ventriculograms were analyzed independently by two observers. Five standard segments (SEG) were compared using the grading system: normal = 3+, mild hypokinesis (H) = 2+, marked H = 1+, akinesis = 0, and dyskinesis = -1. RNV failed to define the diaphragmatic SEG in 11% and the posterior basal SEG in 60% of cases.

A total of 163 resting and 165 EX SEGS were evaluated. There was complete agreement between RNV and CV WM analysis

in 89% of resting and 85% of EX SEGS. Agreement within 1 WM grade was present in 98% of resting and 98% of EX SEGS. Using only abnormal WM both RNV and CV had similar sensitivity (RNV of 81% and CV of 76%) and the same specificity of 94% in detecting patients with CAD. In conclusion, analysis of RAO ERV wall motion compares favorably with WM analysis obtained by EX CV.

RADIONUCLIDE VENTRICULOGRAPHY: EVALUATION OF AUTOMATED AND VISUAL METHODS FOR REGIONAL WALL MOTION ANALYSIS. R.A. Steckley, M.W. Kronenberg, M.L. Born, T.C. Rhea, J.M. Bateman, F.D. Rollo, G.C. Friesinger, Vanderbilt University Medical Center, Nashville, TN.

We examined the accuracy of regional wall motion (RWM) detected by gated radionuclide ventriculograms (RVG's). We evaluated RWM in 18 patients undergoing gated equilibrium RVG's immediately prior to contrast ventriculography (CVG). In the left anterior oblique projection, end-systolic and end-diastolic borders were traced on a video monitor from unprocessed moving RVG images. The RVG and CVG borders were aligned, digitized, and analyzed using both 8-segment and 4-segment rectangular and radial coordinate systems. The same segments were analyzed visually by two experienced observers (graded 0-6). There were strong correlations for the sector area shrinkage of 90° sectors corresponding to the apex and posterior wall ($r=.85$, $P<.001$) and for the five 45° sectors from mid-septum through posterior wall ($r=.82$, $P<.001$). Corresponding visual methods were similar ($r=.80$, .77, $P<.001$). Rectangular area shrinkage and radial shortening had slightly weaker correlation in these 5 segments ($r=.77$, .75, $P<.001$). The mitral, aortic, and proximal septal segments had much weaker relationships to CVG data ($r=.22-.67$). Conclusion: Quantitative RWM in radionuclide ventriculograms compared favorably with near-simultaneous contrast ventriculograms in non-overlapping structures. Visual and automated methods accurately measured RWM in the left anterior oblique projection, supporting the premise that radionuclide ventriculography is useful for analyzing and quantitating regional as well as global left ventricular function.

2:00 p.m.-3:30 p.m. Room 201

RADIOPHARMACEUTICAL CHEMISTRY: TECHNETIUM CHEMISTRY

Chairman: Dennis R. Hoogland
Co-Chairman: Samuel E. Halpern

A TETRADENTATE LIGAND DESIGNED SPECIFICALLY TO COORDINATE TECHNETIUM. A. Davison, M. Sohn, C. Orvig, A.G. Jones, and M.R. LaTegola. Department of Chemistry, Massachusetts Institute of Technology, Cambridge, MA. and Department of Radiology, Harvard Medical School, Boston, MA.

Based on the results of studies investigating aspects of the ligand preferences of technetium(V), a new chelate has been formulated and synthesized which will both firmly bind the element and also allow the introduction of a variety of noncoordinating functional groups. The molecule is N,N'-bis(benzoylmercaptoacetamido)ethylenediamine ($PhCOSCH_2CONHCH_2CH_2NHCOCH_2SCOPh$). Addition of sodium dithionite to a solution containing Tc-99 pertechnetate and the chelate at pH 13 leads to the formation of an anionic complex, which can be quantitatively isolated as the salt $[Ph_4As][TcO(SCH_2CONCH_2CH_2NCOCH_2S)]$ with tetraphenylarsonium chloride. The nature of this anion has been established by several methods.

Preliminary animal studies indicate that the distributions at the carrier and tracer levels are identical, with up to 80% of the injected dose appearing in the bladder within 20 minutes. Comparative computer studies in the same animal with I-131-iodohippurate sodium show that similar time-activity curves over the left kidney and bladder are obtained; 4% of the dose shows clearance through the liver and intestines, thus interfering with activity profiles over the right kidney. These experiments on the unsubstituted ligand will form a baseline for future structure-activity studies of variants of the basic chelate itself and of versions which incorporate different functional groups.

OXOTECHNETIUM(V) COMPLEXES. A.G. Jones, A. Davison, H.S. Trop, B.V. DePamphilis, C. Orvig, and M.A. Davis. Department of Radiology, Harvard Medical School, Boston, MA. and Department of Chemistry, Massachusetts Institute of Technology, Cambridge, MA.

Using Tc-99 we have found that oxotechnetium(V) complexes can be readily synthesized and isolated. Three basic types of such complexes have been obtained in this work and in that of others, and they can most conveniently be categorized on the basis of their oxotechnetium cores: (a) TcO^{3+}, (b) TcO_2^+, (c) $Tc_2O_3^{4+}$. All contain a terminal Tc=O bond. Those of type (a) are either five-coordinate [e.g. $TcO(SCH_2COS)_2^-$, $TcOCl_4^-$] or six-coordinate [e.g. $TcO(NCS)_5^{2-}$], depending on the nature of the ligating groups. A number of this class have been characterized by X-ray analysis. Complexes of type (b) [e.g. $TcO_2(CN)_4^{3-}$] have a trans-dioxo arrangement, while those of type (c) [e.g. $Tc_2O_3(Et_2NCS_2)_4$] have a linear O=Tc-O-Tc=O structure in which each technetium is six-coordinate, binding in this example two bidentate diethyldithiocarbamato ligands. The infrared spectra of the complexes show one terminal Tc=O stretching mode in the region 1050-800 cm^{-1}. The occurrence of this absorption cannot be used diagnostically to distinguish between the various types. Type (c), however, can be identified by an intense infrared absorption due to the Tc-O-Tc moiety near 600 cm^{-1}.

The isolation of complexes of this type shows that the chemistry of technetium(V) resembles that of oxorhenium(V) and oxomolybdenum(IV).

PREPARATION AND PARTIAL CHARACTERIZATION OF AMINOETHANETHIOL COMPLEXES OF CARRIER FREE TECHNETIUM-99m. H.D. Burns, R.F. Dannals, L.G. Marzilli and H.N. Wagner. The Johns Hopkins Medical Institutions, Baltimore, MD.

The design of bifunctional 99m-technetium (Tc-99m) radiopharmaceuticals which bind to intracellular receptors (such as estradiol receptors) has been hindered by the lack of information on the structure of Tc-99m-complexes. The majority of Tc-99m complexes studied have been highly charged molecules and, thus, limited to an extracellular volume of distribution, precluding interaction with intracellular receptors.

As part of a program aimed towards identifying ligands which will form neutral, stable complexes with Tc-99m, we have investigated the Tc-99m complexes of bidentate aminoethanethiols (AET) by an electrophoretic technique used to determine the ligand:Tc-99m stoichiometry and the net charge of these complexes at carrier free levels. Several substituted AET ligands were synthesized

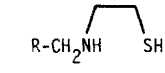

R = neutral, negatively charged and positively charged functional groups

and their Tc-99m complexes prepared. Results of mixed ligand experiments indicate that AET ligands form bis complexes with Tc-99m under the conditions studied. Neutral, lipid soluble complexes were obtained from simple AET ligands provided the R group did not possess functional groups which are charged at physiological pH. These findings indicate that the AET ligands may be useful for incorporation into bifunctional Tc-99m radiopharmaceuticals for which an intracellular volume of distribution is desired.

COMPLEXES OF Tc-99m WITH CYCLAM. D. E. Troutner, W. A. Volkert, J. Simon, A. Ketring, and R. A. Holmes, Department of Chemistry and Radiology, University of Missouri, and Veterans Administration Hospital, Columbia, MO.

Macrocyclic amines are used commercially as metal chelators and have a distinct advantage due to their small molecular size. Their ability to complex Tc-99m was assessed and its potential as a radiopharmaceutical evaluated. Of the group of macrocyclic amines investigated, cyclam (1,4,8,11, tetracyclotetradecane) has proven to be the most efficient compound to chelate Tc-99m. Reduction of Tc-99m pertechnetate by $SnCl_2$, hydrazine or electrolysis with Sn or Zr metal electrodes in the presence of cyclam produces complexes (Tc-CyC) with 95 percent labeling efficiency determined by chromotography and electrophoresis. The highest yields of Tc-CyC occurred in the pH range 7-12. Their molecular structure was stable after standing in air for 24 hours or when exposed to 0.05 M NaOH or 1.5% H_2O_2 for one hour, but unstable in 0.05 NHcl. Electrophoresis of the Tc-CyC demonstrated a single sharp peak at the cathode indicating a positively charged complex. Biodistribution of the Tc-CyC was determined in unanesthesized mice. Tc-CyC cleared rapidly from blood and localized in the liver and kidneys. Tc-CyC cleared by the kidney was excreted into the bladder and previous studies using a Tc-complex of a CyC derivative indicated renal clearance by glomerular filtration. Complexes produced in excellent yields from 10^{-4} solutions of Tc-99m are used to characterize its long term stability and chemical properties. Side chain derivatization has been accomplished and early studies have shown it to alter the biodistribution of the basic Tc-CyC complex.

COMPARISON OF HEPATOBILIARY RADIOPHARMACEUTICALS IN AN IN-VITRO MODEL. D.W. Porter, M.D. Loberg, P.I. Eacho, M. Weiner. University of Maryland, Baltimore, Md.

Numerous Tc-99m labeled radiopharmaceuticals have been developed as hepatobiliary agents. In vivo analysis of the agents in animals is laborious and does not truly reflect the clinical situation. This is especially true in those patients in which elevated serum bilirubin alters the in-vivo kinetics. We have developed a simple in-vitro model to study the hepatic uptake mechanism and the effect of protein binding and bilirubin on the hepatic uptake. Isolated rat hepatocytes were obtained by a collagenase perfusion technique. The isolated hepatocytes at a concentration of 2 - 3 x 10^6 cells/ml were incubated with various radiolabeled compounds. Cell uptake curves were generated as a function of time and inhibitor concentration by centrifugation of 200 µl samples of the cell suspension through a layer of silicone oil into 3M KOH. The diffusable tracer ^3H_2O and the cell impermeable tracer ^{14}C dextran were added to the cell suspension so that the cell volume could be computed. Compounds studied were ^{131}I-rose bengal (RB), ^{14}C-taurocholic acid (TCA), ^{99m}Tc-HIDA, ^{99m}Tc-diethyl IDA (DIDA), and ^{99m}Tc-p-isopropyl-IDA (PIPIDA). The % of the dose concentrated in the cells after 30 min. of incubation was 87, 43, 37, 21, and 20 for TCA, ^{99m}Tc-DIDA, ^{99m}Tc-PIPIDA, RB, and ^{99m}Tc-HIDA respectively. The % cell uptake was depressed by increasing bilirubin concentration. At bilirubin levels of 11.5 mg% the % uptake for ^{99m}Tc-PIPIDA, RB, and ^{99m}Tc-HIDA was 32., 4.5, and 4.0 respectively. Protein binding did not appreciably alter the uptake of the ^{99m}Tc compounds but did substantially reduce the equilibrium value for the highly protein bound compounds RB and TCA. This is a facile method of comparing hepatobiliary radiopharmaceuticals.

INHIBITORY EFFECT OF SULFOBROMOPHTHALEIN ON THE HEPATIC UPTAKE AND BILIARY EXCRETION OF ^{99m}Tc-N-(2.6-DIMETHYL-PHENYLCARBAMOYL-METHYL) IMINODIACETIC ACID AND -PYRIDOXYLIDENE-ISOLEUCINE IN RATS. K. Kitani, S. Kawaguchi, M. Iio, Y. Sasaki, S. Kanai and K. Someya. Tokyo Metropolitan Institute of Gerontology. Tokyo Metropolitan Geriatric Hospital. St. Marianna University School of Medicine.

The biliary excretion mechanism of ^{99m}Tc-labeled compounds has not been studied in the past. The present study was undertaken to know the property of hepatic transport of ^{99m}Tc-N-(2.6-dimethylphenylcarbamoyl-methyl) iminodiacetic acid (HIDA) and ^{99m}Tc-pyridoxylidene-isoleucine (Pi) in relation to sulfobromophthalein (BSP). Hepatic uptake and biliary excretion of ^{99m}Tc-HIDA and -Pi were compared for 60 min between control rats and rats excreting sulfobromophthalein (BSP) at a maximal rate with a continuous infusion of BSP (0.25mg/100g/min). The biliary recovery of ^{99m}Tc-HIDA 60 min after the injection was 33.6±10.0 % of the dose (n=8), while it was 77.0±5.6 % (n=6) in control rats; a marked depression in the biliary excretion of HIDA in BSP Tm state rats. The Pi recovery in BSP Tm rats was also depressed (51.2±5.8 %,n=10) compared with control study (78.3±7.2 %,n=11), but the extent of depression was less than with HIDA. On the other hand, there was less delay in plasma clearance of HIDA by BSP than there was with Pi activity. It was concluded that BSP inhibits both the hepatic uptake and biliary excretion of ^{99m}Tc-HIDA and -Pi but that its effect is stronger on Pi for uptake and,converesely, stronger on HIDA for excretion.

HEPATOBILIARY TRANSPORT MECHANISM OF Tc-99m-N,α-(2,6-DIETHYLACETANILIDE)-IMINODIACARBOXYLIC ACID (DIETHYL-IDA). A.R. Fritzberg, W.P. Whitney, and W.C. Klingensmith III. University of Colorado Medical Center and Denver Veterans Administration Hospital, Denver, CO.

Recent clinical evaluations have demonstrated the superiority of Tc-99m-diethyl-IDA and related iminodiacetate complexes for hepatobiliary imaging. Interpretations of studies under various disease and genetic conditions require knowledge of the hepatobiliary transport mechanism of these complexes. In order to determine if Tc-99m-diethyl-IDA is excreted via anion dye, bile acid, quarternary amine pathways or a pathway unique to metal complexes the kinetics of biliary excretion of the complex were evaluated while the various pathways were saturated with compounds representative of the pathways. The effects were monitored in rats by collection of bile from the common bile duct after either constant infusion or bolus administration of the radiopharmaceuticals.

Administration of sulfobromophthalein (BSP) at levels of 2.5 µmol/min/kg reduced bile output of Tc-99m-diethyl-IDA and I-131-Rose Bengal under both constant infusion and bolus injection conditions. Taurocholate at 13 µmol/min/kg increased bile output of both agents with a return to steady state conditions. Administration of a dose of 20 mg/kg of procaine amide ethobromide also increased the bile output of both agents. These results indicate that Tc-99m-diethyl-IDA is transported by the dye anion pathway which includes BSP, Rose Bengal and bilirubin. Net anionic charge on Tc-99m iminodiacetate complexes is apparently more important than structural similarities to quarternary amines resulting from participation of the imino nitrogens in the complexes.

2:00 p.m.-3:30 p.m. Room 204

INSTRUMENTATION, COMPUTERS, AND DATA ANALYSIS: MINI-SYMPOSIUM

EDGE DETECTION AND PINHOLE TOMOGRAPHY

Chairman: Barbara J. McNeil
Co-Chairman: Steven Bacharach

METHODS AND LIMITATIONS OF EDGE DETECTION FOR NOISY IMAGES. S.M. Pizer, University of North Carolina, Chapel Hill, NC.

A NEW METHOD FOR COUNT-BASED BORDER DEFINITION WHICH EMULATES VISUAL FUNCTION-APPLICATION TO RADIONUCLIDE VENTRICULOGRAPHY. J.L. O'Connor, M.W. Kronenberg, S.B. Higgins, R.W. Pederson, T.C. Rhea. Departments of Medicine and Pediatrics, Vanderbilt University Medical Center, Nashville, TN.

Fast, consistent, objective border definition is desirable for analyzing radionuclide regions of interest (ROI).

Present edge-detection methods are based on thresholding or count-rate change alone one-dimensional, linear sections. We constructed an algorithm for border definition, based on two-dimensional image components, specifically adapted to cardiac blood pool imaging. The user supplies cardinal points A,B,C, at approximately the center, apex, and left ventricular (LV) septum. The program constructs a "guiding ellipse", and radii are constructed every five degrees. For each radius point Q, a normal to the ellipse is constructed with specific inner and outer limits. At each point P on the normal, is constructed a "bordon", a structure of two adjacent 5 x 2 rectangles, one rectangle outside and one inside the point. Count ratios between rectangles are calculated. The greatest ratio defines the border point P. Optionally, the contiguous left atrium or aorta may be excluded from the ROI. The border algorithm runs in 6 sec. on unsmoothed, unthresholded images, and the borders appear highly accurate. The algorithm has been incorporated into a software system which defines the LV ROI, selects the retrocardiac background, and calculates the LV ejection fraction (EF). In a series of 18 patients, the radionuclide EF compared favorably to the contrast ventriculographic EF ($r=.93$ $p<.001$). We concluded that this new method of border definition, based on two-dimensional principles, provided rapid, visually accurate LV borders, and gave quantitatively accurate definition of global LV function.

A SIMPLE EDGE-FINDING ALGORITHM FOR GATED CARDIAC IMAGES
J.P. Jones, R.R. Price, and F.D. Rollo, Divisions of Nuclear Medicine and Radiological Sciences, Vanderbilt University Medical Center, Nashville, TN 37232

This algorithm is part of a set of FORTRAN programs we have developed and routinely use to analyze gated blood pool studies. Image processing is always performed first (weighted smoothing in both time and space). The edge-finder examines each horizontal line of the processed images independently, using a combination of the count profile slope and an isocount level to define the edges. Program output is used to determine the ventricle volume curve, ejection fraction, and overlaid end systole and end diastole edge outlines.

Besides simplicity, the program is fast (<10 seconds/frame), requires moderate memory (<12 K words), needs little operator interaction, and has minimal user dependence. One must draw a single searching region and enter the isocount level. Within reason, the exact region used does not matter, and an isocount level of 50%-60% usually works best. (Image isocounters can be examined beforehand to see which best fits the ventricle free wall.) However, a prominent atrium will sometimes not be distinguished from the ventricle, so the searching region should include as much end diastole ventricle and as little systole atrium as possible--rarely a prohibitive constraint. In correlation studies, the ejection fraction has correlated well with phantoms ($r = 0.85$) and patients under-going x-ray contrast ventriculography ($r = 0.86$, 12 patients).

INTERPOLATIVE BACKGROUND USE IN ASSESSMENT OF LEFT VENTRICULAR EJECTION FRACTION, END-DIASTOLIC VOLUME AND SEGMENTAL WALL MOTION. J.R. Perry and R.C. James. University of North Carolina, Chapel Hill, N.C.

Methods for background correction of cardiac blood pool images were sought which would compensate for uneven background activity and gamma camera nonuniformity in the region of interest. Planar and weighted bilinear interpolative background methods were used for first-pass RAO and equilibrium LAO images respectively. The patient studies were carefully matched for heart rate, drug effect, and close proximity in time of the two studies. Left ventricular (LV) ejection fraction (EF) was derived from the equilibrium LAO study and compared to the EF from single plane contrast angiography with a correlation of $r=.95$, $n=25$; and reproducibility CV=2%, $n=5$. LV end-diastolic volume was derived from the first-pass RAO study and compared to that of single plane contrast angiography with a correlation of $r=.99$, $n=12$; and reproducibility CV= 9%, $n=5$. Segmental wall motion functional images generated from the background corrected chamber images of both views agreed well with contrast angiography. Interpolative background correction methods for cardiac blood pool imaging demonstrate optimal compensation for background nonuniformity and relative immunity from gamma camera nonuniformity by excellent agreement with contrast angiography for global and regional function.

CURRENT STATUS OF THE SEVEN PINHOLE TOMOGRAPHIC TECHNIQUE.
D.L. Kirch, R.A. Vogel, M.T. LeFree, and P.P. Steele. The Veterans Administration Medical Center, Denver, CO.

The method developed for performing myocardial perfusion tomography using a large-field Anger camera (J Nucl Med 19: 683) has been modified for use with small-field cameras, applied to other organ systems and extended to the study of gated studies and temporal processes. Scaling down and adjusting the dimensions of the seven pinhole collimator provides a volume of reconstruction having a 12.7 cm diameter for small-field cameras. We have operated two small-field collimators on a Picker 4/11 (19 PMT's and a 0.5 inch thick crystal) and a Picker Dynamo (37 PMT's and a 0.25 inch thick crystal). Both demonstrated clinical results which were equivalent to the large-field system. Using a multiple-layer, cardiac phantom, the Dynamo was found to provide superior tomographic resolution to that of the large-field system because of its excellent intrinsic resolution (FWHM = 3.8 mm) and the thin crystal. For application of this method to the brain, heart, and thyroid the pinhole geometry of the large-field collimator was modified to achieve 20.3 cm, 12.7 cm and 8.3 cm volumes of reconstruction, respectively. The new geometry accommodates the different organ sizes with a steeper viewing angle (32^{o}) for the outside pinholes than was used previously (26.5^{o}). The computer programs which accomplish the tomographic reconstructions have been made faster (3 minutes on the ADAC C.D.S.) which makes it practical to process sequences of gated blood pool tomograms, and have been improved to produce linear reconstructions necessary for study-to-study comparability in determining the rate of Tl-201 uptake and washout from the myocardium. These developments have significantly enhanced the clinical usefulness of the seven pinhole tomographic method.

TOMOGRAPHIC GATED BLOOD POOL SCINTIGRAPHY USING A WIDE-FIELD SCINTILLATION CAMERA. R.A. Vogel, D.L. Kirch, M.T. LeFree, J.O. Rainwater, D.P. Jensen, and P.P. Steele. Denver Veterans Administration Medical Center, Denver, CO.

A new method for performing multi-planar (longitudinal) gated blood pool tomography is presented. LAO or RAO projection imaging is performed utilizing a seven pinhole collimator and a wide-field (38 cm diameter) scintillation camera. Using 25 mCi Tc-99m in vivo red cell labelling, 8 frame per cardiac cycle imaging is accomplished in approximately 3 minutes. Each of the 8 128x128 pixel matrix frames is then individually processed into 10 tomograms spaced on the average 1 cm apart utilizing a reconstruction algorithm and an on-line digital computer. Eight frame cyclical motion pictures are then assembled for each of the 10 tomographic depths. This 30 minute technique results in images possessing excellent chamber definition with approximately 10 to 1 ventricular cavity to septum or background count density ratios. In addition to visual interpretation, ventricular wall motion is quantitatively analyzed through use of a second computer program. End systolic and diastolic frames for all planes cutting through the ventricular cavities first undergo chamber edge detection using maximum radial gradient criteria. Sixty measurements of the distance from the ventricular center (diastolic) to the chamber edge are calculated in a circumferential fashion (at 6^{o} spacing) for both ventricular cavities of each tomogram, thus allowing for quantitative comparison of diastolic and systolic myocardial wall dimensions. This tomographic gated blood pool imaging technique enables segmental myocardial wall motion analysis to be done in a three-dimensional fashion.

MULTIPLE-GATED TOMOGRAPHIC BLOOD POOL IMAGING (BASIC): MUGTM I. W. Chang, R.E. Henkin, Loyola Univ.Med.Ctr., Maywood, IL.

Multi-pinhole tomography for cardiac imaging has been previously reported on. The applications of this technique have been predominantly to thallium imaging. We adapted this technology to gated blood pool images (MUGA). We expected more accurate identification of edges due to the defocusing of off-plane activity.

MUGA acquisitions were accomplished with a super-fine (4.5mm) 7 pinhole collimator in a 64x64 matrix. Existing reconstructive programs were modified by us for the acquisition format of MUGA data and to provide display of reconstructed data. Modified normalization routines for blood pool imaging were also created.

The FWHM with a 99mTc line source was 1.2 cm through a plane parallel to and 14.6 cm from the collimator. Depth resolution was 4.1 cm at that distance. FWHM decreased with distance from the collimator. Planar resolution (FWHM) was 1.1 cm at 12.3 cm distance and 1.6 cm at 18.3 cm. Depth resolution behaved in a like fashion. Clock' phantom studies demonstrate the tomographic images to be at their predicted depths. An oscillating phantom (MUGA phantom) was reconstructed to simulate cardiac motion. This demonstrated, in a cine format, the tomographic effect in a multi-gated situation. Reconstruction time for a 14 frame study is approximately 20 minutes per plane. The above data demonstrates that multi-gated tomography of the heart is clinically feasible.

MUGTM has acceptable depth resolution as outlined above. Clinical data on wall motion and regional ejection fraction imaging is discussed separately.

SINGLE PHOTON LONGITUDINAL TOMOGRAPHY WITH A 7 PINHOLE HIGH ENERGY COLLIMATOR. P.V. Harper, W. Fox, D.B. Charleston, G. Rutkowsky, V. Stark, J. Ryan, B. Brunsden, J. Goodman, K.G. Chua, and L. Resnekov. The University of Chicago, Chicago, IL.

The demonstration by Vogel et al. of a bedside technique for myocardial tomographic imaging using a 7 pinhole collimator with Tl-201 suggested the possibility of extending this approach to high energy emitters, such as nitrogen-13 ammonia, which would permit rapid sequential studies due to the 10 min half-life, and provide an available initial count rate many times greater than that for thallium-201. A collimator was designed and built with thick shielding (2-1/2" of lead) which largely preserved the geometry of the low energy system. Interchangeable pinhole inserts of tungsten (Kennametal) and depleted uranium were constructed with diameters of 4mm and 6mm. The entire assembly weighed 515 pounds when adapted to a Searle LFOV gamma camera. Point source response function measurements with the 4mm uranium and tungsten inserts showed with uranium a 1.4mm improvement in resolution (FWHM) in the primary pinhole images and a 20% reduction in count rate due to reduction of penetration of the pinhole edges. The background from the uranium was only 1% of the initial count rate following injection of 20 mCi of nitrogen-13 ammonia. The existing commercially available software functioned well with the MDS and DEC Gamma-11 systems with very little adaptation. Tomographic images produced from phantoms and clinical studies appear quite satisfactory. Exercise studies show a very rapid (10-15 min) redistribution of the nitrogen-13 ammonia activity with filling in of exercise-induced uptake defects. Sequential studies of patients with myocardial infarction have shown substantial uptake defects preceding by a period of days the extension of an infarction.

SIMPLE OPTICAL BACK-PROJECTION OF KIRCH COLLIMATOR (7-PINHOLE) IMAGES FOR TOMOGRAPHIC RECONSTRUCTION. B.S. Brundsden, P.T. Kirschner, D. Charleston, and P.V. Harper, The University of Chicago, Chicago, IL.

(See page 608 for abstract)

EFFECT OF CAMERA LINEARITY CORRECTION UPON N-PINHOLE TOMOGRAPHY. K.F. Koral, W.L. Rogers, J.W. Keyes, Jr., J H. Thrall, G.F. Knoll, M.C. Bennett and D.R. Strange. University of Michigan Medical Center and Medical Data Systems, Ann Arbor, MI.

Multiple pinhole pictures are currently being used as the data base for longitudinal tomographic reconstructions of the heart by several devices. It is tacitly assumed in these devices that each projection ray accurately measures the radioactivity along that ray. However, camera nonlinearities of the type that produce non-uniform floods also produce variations from the correct ray sums. While present camera corrections do produce uniform floods, they do not properly correct these ray sums. In the seven pinhole tomograph, a calibration involving a point-source image and a flood source image only partially compensates for camera nonlinearity and in the 72-pinhole time-coded tomograph perfect linearity is assumed.

A microprocessor-based device which corrects camera non-linearities has been applied to N-pinhole-tomography data acquisition. This device, which is electronically placed between the camera and the camera interface of a digital computer, applies a position correction to each event from the camera in real time. The magnitude of the correction is derived by interpolation from initial calibration images of a flood taken through a parallel line mask oriented sequentially in the vertical and horizontal direction. Resultant computer images are free of non-linearities. Phantom studies show that using this corrector produces a computer data base which leads to reconstructions having better resolution than the standard reconstructions. Results of using the corrector for patient cardiac studies are also shown.

4:00 p.m.-5:30 p.m. Room 210

CLINICAL SCIENCE

ONCOLOGY

Chairman: Carlos Bekerman
Co-Chairman: Stuart M. Spies

GALLIUM-67 SCANNING IN CLINICAL STAGING OF LUNG CANCER: A MULTI-IMAGING APPROACH. K. Rezai-Zadeh, P.T. Kirchner, T.R. DeMeester, H. Golomb, and M. Cooper. University of Chicago, Chicago, IL.

The efficacy of Ga-67 scanning in the clinical staging of lung cancer was evaluated against other imaging modalities in 100 patients with proven lung cancer. The protocol included colloid liver scan, bone scan, CT of the brain and multiplane longitudinal emission tomography (Pho/Con) 48-72 hours after a 10 mCi dose of Ga-67. Independent interpretations of each scan were retrospectively compared with final diagnosis, surgical findings, and x-ray or tissue verification of suspected metastases.

Ga-67 localized in 96% of primary lung cancers. In 66 patients with surgical evaluation of the mediastinum, Ga-67 uptake yielded 90% probability of tumor involvement, whereas, a negative Ga-67 study gave only a 67% probability of normal mediastinal nodes.

Forty patients had proven metastases. The Ga-67 scan identified 11 of the 12 patients with occult metastases and detected 7/7 liver, 9/14 brain, 9/11 bone, 4/4 soft tissue and 1/4 contralateral lung metastases. Ga-67 yielded no false positives, whereas, bone scans produced 6. We have since then improved brain lesion detection with selective tomography of the head. Abnormal extra-thoracic Ga-67 uptake produced a 90% probability of metastasis and served as a guide for biopsy confirmation. Twelve post-mortems done within 3 months of Ga-67 scans, confirmed the presence or absence of metastatic disease in 11/12.

Whole body gallium scanning may thus suffice for initial metastatic screening in lung cancer; specific organ scans may be best applied in symptomatic patients with negative Ga-67 scans or for clarification of indeterminate Ga-67scans.

GALLIUM UPTAKE IN HILAR AND MEDIASTINAL STRUCTURES IN PATIENTS WITH PULMONARY TUMORS: THE SIGNIFICANCE OF LOCATION AND CELL TYPE ON SENSITIVITY AND SPECIFICITY. A.D. Waxman, P. Julian, M. Komaiko, M.B. Brachman, D.E. Tanasescu, R. Wolfstein, and D.S. Berman. Cedars-Sinai Medical Center, Los Angeles, California.

Previous studies have shown gallium to be a sensitive but nonspecific indicator of hilar and/or mediastinal spread of pulmonary tumors from a peripheral site. This study evaluates the influence of tumor histology and mediastinal distribution of gallium on the sensitivity and specificity of hilar and/or mediastinal metastasis detected by gallium scintigraphy.

Fifty patients with histologically proven pulmonary tumors were included in this study. The sensitivity and specificity for hilar and/or mediastinal metastasis detection according to gallium location are summarized as follows:

Ga-67 Location	Sensitivity	Specificity
Mediastinum and/or hilum (any site)	32/33 (96%)	9/17 (56%)
Unilateral hilum or mediastinum	22/33 (66%)	16/17 (94%)
Bilateral hilar only	10/33 (30%)	10/17 (59%)

No correlation was found between cell tyne and degree of gallium uptake in primary or metastatic foci. Four patients with negative Ga-67 uptake in the peripheral primary tumor showed positive ipsilateral hilar uptake proven to contain tumor.

The results clearly show unilateral hilar or mediastinal uptake of Ga-67 to have a high specificity for tumor (94%). Bilateral hilar uptake was nonspecific. Mediastinal uptake was independent of gallium-67 uptake by the primary tumor or tumor cell type. This suggests that mechanisms other than direct tumor cell uptake of Ga-67 may be operative in the determination of gallium avidity within the hilar or mediastinal soft tissue structures.

FLUORINE-18-5-FLUOROURACIL IMAGING IN HUMANS. L.M. Lieberman, B. Wessels, S.J. Gatley, A.L. Wiley, R.J. Nickles, and D. Young. University of Wisconsin Hospitals, Madison, WI.

We have investigated Fluorine-18-5-fluorouracil (F-18-FU) in sixteen patients with cancer to evaluate the usefulness of this radiopharmaceutical as a tumor scanning agent. F-18-FU was synthesized by the method of Fowler et al. (1) as modified by Wessels, and millicurie amounts prepared.

Patients with known malignant tumors were given 500-4000 μCi of F-18-FU IV in 20-60 mg of FU. Imaging was performed 2-10 hours after injection using a Picker 12.5 cm Magnascanner.

Accumulation of radioactivity was noted in primary tumor sites of two patients with adenocarcinoma of the colon, two patients with carcinoma of the base of the tongue, one bronchogenic carcinoma of the lung and one chondrosarcoma of the pelvis. Positive scans were noted only in patients who had not received prior FU therapy.

Plasma clearance studies in nine patients and three normal volunteers showed no significant difference in the halftime clearance of F-18.

Six of 16 patients have shown positive accumulation of F-18 in the tumor site from F-18-FU given IV. These results support previously reported animal studies suggesting that FU sensitive tumors may concentrate F-18 more avidly than non-sensitive tumors (2). Continued investigation of this agent as a tumor scanning agent seems warranted.

(1) Fowler, J.S., Finn, A.D., Lambrecht, P.M. and Wolf, A.P.: J. Nucl. Med. 14:63-64, 1973
(2) Shani, J. and Wolf, A.: Cancer Res. 37:2306-2308, 1977

EFFICACY OF HIGHLY IODINATED FIBRINOGEN IN PATIENTS WITH CANCER. S.J. DeNardo, G.L. DeNardo, M.A. Swanson, J.D. Trelford, K.A. Krohn. University of California Davis Medical Center, Sacramento, CA. Supported by American Cancer Society Grant #PDT-94A)

We have reported enhanced tumor concentration of highly iodinated fibrinogen in the mouse KHJJ tumor model (2x that of Ga-citrate or authentic fibrinogen) as well as its accelerated clearance from the blood and the animal. The purpose of the present study was to determine the efficacy of this radiopharmaceutical in patients with cancer (PC). Total body and tomographic scintigraphy were performed <1, 4-6 and 16-24 hrs after administration of I-123-fibrinogen iodinated at 40 atoms I/molecule of fibrinogen (40 I/F) to 48 PC. Blood was obtained for clearance, clottability and precipitability studies. 40 I/F was 88% clottable, 94% precipitable and cleared from the blood 4x as rapidly as authentic fibrinogen ($T_{\frac{1}{2}}$=14 and 52 hrs, respectively). Normal tissues did not concentrate 40 I/F except for iodide-concentrating tissues, e.g., stomach, which were most evident at 16-24 hrs. Images of the abdomen, head and extremities were more readily interpreted with 40 I/F than with Ga-67-citrate. Abnormal uptake was found in 43/45 PC at time of study. Primary site, local recurrence or extention were detected in 42/43 and metastases in 11/16 PC. Osseous metastases were detected infrequently. Thrombophlebitis was incidentally detected in 10 PC. There was little or no uptake in cancer at <1 hr. Intensity of localization in cancer was equal or greater at 4-6 hrs compared to 16-24 hrs whereas the reverse was the case for benign disease.

The results suggest 40 I/F to be an efficacious oncophilic radiopharmaceutical.

CANCER LYMPHOSCINTIGRAPHY BY RADIOIMMUNO-DETECTION. F.H. DeLand, E.E.Kim, J.Primus, R.Corgan, E.Spremulli, N.Estes, D.M.Goldenburg. University of Kentucky and V.A. Medical Centers, Lexington, Kentucky.

Radiocolloids have been used for lymphoscintigraphy to demonstrate the presence of metastatic disease, as inferred from negative evidence. Based on our experience with the in vivo detection of carcinoma by means of I-131 labeled antibodies to carcinoembryonic antigen, these antibodies were administered subcutaneously in the feet or hands to evaluate the role of CEA antibodies in the detection of metastases in regional lymph nodes. Twelve patients were studied, six with breast carcinoma, one vulvar carcinoma, one melanoma, and 4 controls. In all patients with breast carcinoma increased concentration of radioactivity in the ipsilateral axillary lymphnodes was observed and bilateral activity in two patients with centrally located breast lesions. Positive findings were also observed in the patients with vulvar carcinoma and melanoma. In one control patient initial bilateral axillary concentration of radioactivity was detected that disappeared by 72 hours and in another unilateral inguinal activity persisted. No radioactivity was found in 2 other control patients. In three patients, surgical specimens were imaged and the distribution of radioactivity correlated with the pre-surgical images. I-131 labeled antibodies to CEA does concentrate in lymphnodes with metastatic carcinoma, however, transient concentration has been observed in nodes without carcinoma possibly due to Fc receptors on mononuclear cells. This study has demonstrated the feasibility of using radiolabeled antibodies to detect malignant tissue in regional lymphnodes.

VISUALIZATION OF PROSTATIC LYMPHATIC DRAINAGE WITH Tc-99m-ANTIMONY SULFIDE COLLOID. W.D.Kaplan, W.F.Whitmore III, and R.F.Gittes. Depts. of Radiology & Urology, Harvard Medical School & Sidney Farber Cancer Institute, Boston, MA.

Lymph node involvement in patients with cancer of the prostate is frequent, even in early disease. Contrast lymphangiographic studies are generally unable to fill and permit visualization of commonly involved nodal groups. Intraprostatic injections of Au-198 colloid in animals and man suggested the feasibility of Tc-99m-radiocolloid injections to delineate lymphatic drainage by external imaging.

We used Tc-99m-antimony sulfide(Sb_2S_3)to define prostatic lymphatic drainage in dogs and man. Nine mongrel dogs received bilobar 0.1-0.2ml intraprostatic injections of 1.0 mCi of Tc-99m-Sb_2S_3. Eight animals were injected after suprapubic incisions to expose the prostate; in one animal, a transrectal injection was performed. A 64-yr old male with Stage A2 prostatic cancer was also injected transrectally. Six animals were imaged from 0-3 hrs, 5 from 3-5 hrs, and 4 between 20-24 hrs. Four of the animals were

imaged at only one point in time. The patient was imaged immediately and 14 hrs after injection.

Using a scintillation camera, 19 nodes were seen in the 9 animals; 7 nodes were seen in the patient. In the dogs, an increasing number of nodes were seen for the first 3 hrs after injection; no additional nodes were seen after 5 hrs. Excised nodes from both dogs and man were histologically normal and scintiphotographic examinations confirmed radiocolloid uptake.

Tc-99m-Sb2S3 imaging of prostatic lymph drainage may be useful for preoperative estimates of metastases, intraoperative definition of draining nodes, and selecting appropriate modes of therapy.

ABDOMINAL-MEDIASTINAL LYMPHOSCINTIGRAPHY IN PATIENTS WITH OVARIAN CARCINOMA. Robert D. Katz, Neil B. Rosenshein, Philip O. Alderson and Henry N. Wagner, Jr. Johns Hopkins Medical Institutions, Baltimore, Md.

The abdominal-mediastinal lymphoscintigrams of 35 patients (pts) with ovarian-tubal (O-T) carcinoma and 11 pts with other gynecologic tumors were reviewed to investigate the relationship between thoracic node visualization and diaphragmatic involvement by tumor. Each pt received a 5 mCi intraperitoneal injection of Tc-99m SC in 250-500 ml of normal saline, and one or more 100K anterior images of the upper abdomen-thorax region were obtained 2-6 hrs later. Twenty-four pts had adequate peritoneal dispersion of the SC plus inspection of the diaphragm during laparotomy. Fourteen of these pts had O-T cancer and 10 had other gynceologic tumors. The lymphoscintigrams in 19 of 21 pts (90%) with normal diaphragms showed normal visualization of thoracic nodes. However, 2 of 3 studies in pts with diaphragmatic metastases (2 ovarian, 1 endometrial carcinoma) also showed good node visualization. There was a poor relationship between node visualization and prognosis. Twenty-five pts with O-T carcinoma were followed as long as 38 mos after surgery. Ten pts died and one developed recurrent disase. Only 11 of 21 pts with visualized nodes remained disease-free. Three of 4 pts without visualized nodes were also disease-free. Similarly, there was a poor relationship between node visualization and the laparotomy-proven tumor stage in these pts. Abdominal-mediastinal lymphoscintigraphy performed with Tc-99m SC has limited utility in pts with ovarian-tubal carcinoma.

4:00 p.m.-5:30 p.m. Room 211

CLINICAL SCIENCE

BONE/JOINT

Chairman: Manuel L. Brown
Co-Chairman: Wilfrido M. Sy

RESOLUTION OF SCINTIGRAPHIC SKELETAL ABNORMALITIES FOLLOWING RENAL TRANSPLANTATION
R.S. Hattner, F. Vincente, A. Hull
University of California, San Francisco, California

Several classes of skeletal scintigraphic abnormalities have been reported in patients with renal osteodystrophy and have been attributed variously to secondary hyperparathyroidism and abnormal calciferol metabolism. To evaluate the validity and natural history of these findings a prospective study was done.

Tc^{99m} MDP bone scans were obtained in 106 patients immediately after transplantation and at approximately three monthly intervals up to one year. One to six scans were obtained per patient (mean 2.5). The following features were qualitatively graded 0-3: 1) skull (S); 2) costochondral junctions (CCJ); 3) metaphyseal regions (M); 4) long bones (LB) and; 5) extra-skeletal calcification (ESC).

The following results were obtained: (means ± S.D.)

	S	CCJ	M	LB	ESC
0-3 MO	1.4±1.3	1.4±1.2	1.6±1.1	0.9±1.0	0.4±0.8
3-6 MO	1.4±1.1	0.9±1.0	1.3±1.1	1.0±1.0	0.3±0.6
6-9 MO	1.6±1.2	1.0±0.8	1.1±0.9	0.5±0.7	0.3±0.6
9-12 MO	1.7±1.1	0.9±0.9	1.1±1.0	0.6±0.7	0.3±0.6

Analysis of variance showed the changes in CCJ, M, and LB were significant ($p<.05$).

Relative activity of CCJ, M, and LB appear to be valid signs of renal osteodystrophy and improve following reestablishment of renal function. An interesting observation was made in the ten diabetic patients. Their CCJ, M and LB scores were significantly lower ($p<0.01$-0.05) than the non-diabetic patients at all sampling times. Diabetes appears to protect the skeleton from the scintigraphic manifestations of renal osteodystrophy.

PROSPECTIVE SCINTIGRAPHIC EVALUATION OF AVASCULAR NECROSIS (AVN) OF THE FEMORAL HEAD IN RENAL TRANSPLANT RECIPIENTS
A. Hull, R.S. Hattner, F. Vincente;
University of California, San Francisco, California

AVN in renal transplant recipients has an incidence of 10-25%. Early diagnosis of AVN might lead to interdiction of progression by manipulation of the immunosuppresive chemotherapy. Since bone scans exhibit a characteristic evolution in idiopathic AVN in children, similar findings were sought in a prospective series of renal transplant recipients.

Tc^{99m} MDP bone scans were obtained in 106 patients immediately after transplantation and at three monthly intervals thereafter. Between one and six scans were obtained per patient (mean 2.5) spanning up to one year. Femoral head localization was graded 0-3 (0-normal-3 markedly decreased) and abnormally increased activity was simply noted. Grades 2 and 3, and increased uptake were considered abnormal.

15 patients developed AVN (14% incidence). Four of the 15 were non-evaluable because the lack of scans spanning the evolution of the AVN. Of the reamining 11, 10 had abnormal scans (90%). Radiographs were obtained at times comparable to scans in 9 of the 15 patients. Scans became abnormal prior to radiographs in 4 of the 9 patients (44%). In one patient radiographic changes occured prior to scan abnormalities. In eight patients serial scans were obtained prior to and after the onset of symptoms. Five of the 8 (63%) developed abnormalities before symptoms (mean 4 mo.). Evolution of scan abnormalities entailed decreased activity, increased activity in the capital epiphysis, then diffusely increased activity. Radiographs were usually abnormal in the presence of increased activity. Scan abnormalities are sensitive early indicators of AVN, and may permit intervention to halt progression.

IDENTIFICATION OF MUSCLE DAMAGE IN ACUTE ELECTRICAL BURNS WITH TECHNETIUM-99m PYROPHOSPHATE (Tc-99m-PYP) SCINTIGRAPHY
S.E. Lewis, J.L. Hunt, C. Baxter, D.C. Hickey, and R.W. Parkey. Univ. Texas Health Science Center at Dallas, TX.

High voltage electrical burns are often associated with extensive deep local and regional muscle damage in addition to a limited cutaneous burn. This study evaluated the utility of Tc-PYP scintigraphy for detection and localization of both regional and focal muscle necrosis in burn patients with electrical injuries. Fourteen patients with total body surface area burns averaging 15% (range: 25 to 45%) were studied between the first and fifth days post-injury with multiple studies obtained in 6 patients. Large field-of-view gamma camera images, normalized for time, were obtained at delays of 1 to 2.5 hrs following intravenous injection of 15 mCi Tc-PYP over areas of clinically apparent muscle damage and over areas of suspected, but clinically inapparent injury. Muscle damage was identified by an increased cellular uptake of the tracer. All 14 patients had gross and histologic evidence of muscle necrosis at sites identified on the Tc-PYP scintigrams. Muscle necrosis was identified as early as 24 hrs and as late as 6 days post-injury. The extent of muscle damage, relative amount of tissue debridement necessary or level of amputation was correctly ascertained preoperatively

in all patients. We conclude that Tc-PYP scintigraphy can accurately identify and localize muscle necrosis caused by electrical injury.

BONE SCANNING IN THE EVALUATION OF NON-UNITED FRACTURES. A. Alavi, A. Desai, J. Esterhai, C. Brighton, and M. Dalinka. University of Pennsylvania School of Medicine, Philadelphia, PA.

Recent advances in the treatment of non-osseous fracture union have made it imperative to differentiate fibrous union from true pseudoarthrosis and other complicated fracture sites. While patients with fibrous union usually respond favorably to percutaneous electrical stimulation, those with complications do not. However the prediction of unfavorable response is difficult before surgery. We used 99m-Tc diphosphonate or methylene diphosphonate bone scans to study 75 patients with non-united fractures considered for electrical stimulation. The scans were obtained 2½-3 hours after intravenous administration of 20 mCi of the radiopharmaceutical. A scintilation camera was used to image the fracture site. Multiple views of the area of interest were obtained in each subject. On these scans two patterns of radioconcentration were noticed: 1) Intense activity at the fracture site, which appeared quite homogeneous; 2) A line of decreased activity at the fracture site (negative defect) surrounded by increased uptake in both sides. Of 66 patients with intense increased activity at the fracture site on the scan, 62 have shown evidence of complete healing with electrical stimulation. In 9 patients scans revealed a negative defect at the fracture site. Eight patients in this group did not respond to closed percutaneous electrical stimulation. Based on this preliminary data it is concluded that bone scanning is of value in proper selection of patients for electrical stimulation and diagnosis of complicated non-united fractures.

BONE SCANNING IN MULTIPLE MYELOMA. J. M. Woolfenden, M. J. Pitt, B. G. M. Durie, and T. E. Moon. University of Arizona Health Sciences Center, Tucson, AZ.

Bone scans (SC) in multiple myeloma (MM) are often said to be of limited use, but only a few small series support this contention. This study was done to evaluate the clinical utility of SC in a large number of patients with MM, and to correlate SC with skeletal radiographs (SR) and clinical extent of MM as assessed by quantitative immunoglobulin levels, myeloma cell mass, and in 4 patients by osteoclast activating factor (OAF) levels.

Sixty-seven SC using Tc-99m phosphate complexes were done on 51 patients; SR done within 2 weeks of SC were correlated at a total of 561 anatomic sites. At 186 sites with SR changes typical of MM, SC agreed with SR at 25%, showed less extensive disease at 22% and were normal at 53%. Pathologic fractures were present at 34% of the sites that were abnormal on both SC and SR; the rest had varying degrees of bone destruction. SC showed increased uptake at 96% of the abnormal sites, and decreased uptake at 4%. Abnormalities were seen only on SC at 76 sites; followup data are limited, but serial SC showed 7 cases in which SC were abnormal before SR, and also 4 cases in which abnormal SC reverted to normal while SR remained abnormal.

No differences in agreement between SC and SR were seen when patients were grouped according to treatment status, myeloma type, cell mass, or level of serum M-component ($p > 0.20$). The 2 patients with the highest OAF levels had poor agreement between SC and SR.

SC underestimate the extent of skeletal involvement in MM, but may provide useful information by showing early abnormalities not evident on SR. However, the primary method for evaluating skeletal disease in MM remains radiography.

IMAGING IN MULTIPLE MYELOMA: THE ROLE OF GALLIUM SCINTIGRAPHY. A. Waxman, J. Siemsen, S. Levine, D. Holdorf, R. Suzuki, F. Singer, and J. Bateman. Cedars-Sinai Medical Center, and LAC/USC Medical Center, Los Angeles, California.

Because of the characteristics of bony abnormalities in multiple myeloma, nuclear scintigraphy has often failed to detect abnormalities demonstrated on radiographs. This study evaluates the x-ray, bone scan, and gallium study in an attempt to define the significance of each modality.

Twenty-two patients with proven multiple myeloma were studied with x-ray, technetium phosphate complex bone scan (TcP), and Ga-67 citrate scintigraphy. The studies were evaluated on a site as well as patient basis. Osseous abnormalities were considered as separate from soft tissue abnormalities. The results are summarized below:

Total Sites	X-Ray +	TcP+	Ga(Osseous)+
91	77(85%)	43(47%)	38(42%)

Any Site	X-Ray +	TcP+	Ga(Osseous)+	Ga(Soft Tissue)+
22 Patients	17(77%)	14(64%)	10(45%)	9(41%)

Areas with multiple small lytic abnormalities were most easily detected by x-ray and often missed by bone scan and gallium. Small areas of healing were most readily detected on bone scan. The gallium scans were intensely positive when a plasmacytoma was associated with the bony abnormality, or when lytic lesions of the bone were accompanied by a large cellular component of active myeloma.

We conclude that x-ray, bone scan, and gallium scintigraphy are important in the evaluation of the myeloma patient. Gallium scintigraphy is valuable in determining the activity of the myelomatous process, especially when lytic abnormalities or severe demineralization is present on x-ray. In addition, soft tissue uptake is useful in determining an appropriate biopsy site to aid in the staging of the disease.

TIME SEQUENCE OF BONE AND GALLIUM SCAN CHANGES IN ACUTE OSTEOMYELITIS: AN ANIMAL MODEL. S.F. Dye, R.J. Lull, R.J. McAuley, B.E. Van Dam, W. Young. Letterman Army Medical Center, San Francisco, CA.

This study was undertaken to evaluate the time at which Tc-99m-MDP bone scan and Ga-67-citrate scan abnormalities develop in acute osteomyelitis in order to determine which study provided earliest diagnosis. Nine New Zeland white rabbits were inoculated with Pseudomonas Aeruginosa (right tibia) and Staph Aureus (left tibia) using the Norden technique (Norden CW: Experimental osteomyelitis: a description of the model. J INF DIS 122: 410-418,1970). Tc-99m-MDP bone scans and Ga-67-citrate scans were performed at 1,3,6,11,16,21 and 26 days following inoculation using a large field scintillation camera. All animals were sacrificed on day 32 when tibiae were removed and cultured. Staph Aureus could not be recovered from any tibia, but Pseudomonas was recovered from 7/9 right tibiae and 2/9 left tibiae. Scan results were evaluated in all culture positive tibiae.

During the first week after inoculation, 4/9 lesions (44%) were detected by Gallium scan but only one of these lesions was abnormal on bone scan. In no instance was the bone scan abnormal before the Gallium scan became abnormal. During subsequent weeks after inoculation, 8/9 lesions (89%) were detected by both Gallium and bone scans. One lesion was not visualized by either scan technique.

This study suggests that Gallium scanning is more sensitive than bone scanning in detecting acute osteomyelitis in its earliest stages. Bone scanning should not be used as the sole screening test in cases of suspected acute osteomyelitis. In such cases, a Gallium scan should be performed whenever the bone scan is normal.

4:00 p.m.-5:30 p.m. Room 300/301

CLINICAL SCIENCE

CARDIOVASCULAR IV: POSTER SESSION I

Chairman: Daniel Berman
Co-Chairman: Sherman Sorenson

SINGLE PASS EXTRACTION OF N-13 AMMONIA BY MYOCARDIUM AND ITS RELATIONSHIP TO MYOCARDIAL BLOOD FLOW. S.C. Huang, H.R. Schelbert, M.E. Phelps, E.J. Hoffman, C.J. Selin and D.E. Kuhl. UCLA School of Medicine, Los Angeles, CA.

Myocardial single pass extraction fraction (E) and its relationship to myocardial perfusion (F) was determined in 5 open chest dogs. Flow probes were placed around the left circumflex coronary artery (CIRC) and calibrated using intra-atrial injections of radioactive microspheres (8μ) and the arterial reference sampling technique. Studies were performed at control flows and during CIRC hyperemia induced by intracoronary papaverine (1mg). For each study a bolus of N-13 ammonia was injected into the CIRC and myocardial activity monitored continuously by an external detector. Immediately after injection, the time activity curve reached a maximum, followed by a fast and a slow clearance component. E was determined by the fraction of the slow component to the peak of the curve. Two to five measurements at different CIRC flows were performed in each dog resulting in a total of 23 studies. E was found to decrease as flow increases, similar to that observed by us previously using the in-vitro counting technique. At F equal to 100, 200, and 300ml/min/100gm, E is 0.82.0.65 and 0.57, respectively. The relationship between E and F can be represented by E=1-0.635 exp (-121/F) with an average standard deviation of 0.059. This relationship does not match exactly that of CRONE'S extraction model, in which ln(1-E) is inversely proportional to F. The discrepancy can be interpreted as either 1) that the permeability surface area product (PS) is 0.455F+121 ml/min/100gm, a linear function of flow, or 2) that there are two distinct extraction mechanisms in myocardium, one with PS=121 ml/min/100gm and the other with PS >>300 ml/min/100gm.

MANGANESE-52 M POSITRON EMISSION TRANSAXIAL TOMOGRAPHY FOR DETECTING MYOCARDIAL INFARCTION. J.C.K. Hui, H.L. Atkins, P. Som, T.H. Ku, R.G. Fairchild, L.O. Giwa and P. Richards. Department of Surgery and Radiology, S.U.N.Y. at Stony Brook, N.Y. and Medical Department, Brookhaven National Laboratory, Upton, N.Y.

This investigation was undertaken to determine the resolution and sensitivity of positron emitting manganese-52m as a quantitative measurement of the size, extent and location of myocardial ischemia. Left thoracotomy was performed on seven mongrel dogs and a loose silk ligature for later occlusion was placed around the second diagonal branch of the left descending coronary artery. Serial cross-sectional images of control, occlusion and 60 minutes after occlusion with 4 mCi of Mn-52m administered i.v. at the beginning of each period were performed with the positron emission transaxial tomograph (PETT III). Mapping of the distribution of myocardial perfusion was obtained for each period with left ventricular injection of microspheres labeled with Sr-85, Cr-51 and Ce-141. Comparison between the microsphere mappings and Mn-52m images taken at 1.5cm levels has revealed that an ischemic area down to the size of 2.5 sq.cm. with 50% of the normal myocardial perfusion can be seen in the Mn-52m images. In addition, a relative change of 10% or more of the normal perfusion in the ischemic area can also be observed. Mn-52m would be a useful agent for evaluating the efficacy of any therapeutic or pharmacological interventions that can improve ischemic perfusion by more than 10% of normal myocardial flow.

NON-INVASIVE MEASUREMENT OF RIGHT AND LEFT VENTRICULAR PRESSURE. M.H. Bourguignon, and H.N. Wagner, Jr. The Johns Hopkins Medical Institutions, Baltimore, MD.

We have developed a simple method for measuring right or left ventricular systolic pressure based on automated analysis of the ventricular time-activity curve, obtained with the scintillation camera after intravenous injection of Tc-99m albumin or red blood cells.

The method is based on 3 principles: (1) intraventricular pressure equals force per area of the aortic opening; (2) force equals mass (of blood) times its acceleration; (3) acceleration can be derived from the ventricular volume curve. The following differential equation was derived: $dP/dt = \rho/A^2 \cdot \alpha^2 \cdot da/dt \cdot d^2a/dt^2$, where dP/dt=first derivative of ventricular pressure; ρ=density of blood; A=area of aortic opening; α=ratio of blood volume to radioactivity (a) measured within ventricle; da/dt=first derivative (velocity) of activity (a) within ventricle; and d^2a/dt^2=second derivative (acceleration). The integration of this equation is readily accomplished. We assumed that the area of the aortic opening is readily constant, that blood flow is laminar, and that the pressure pulse travels with the velocity of blood through the aortic opening. In validation studies in dogs, theoretical and observed ventricular curves were nearly identical in shape. Preliminary studies in normal persons and patients yielded several different types of curves. In patients with various types of ventricular dysfunction, including aneurysms, asymmetrical and striking double-peaked left ventricular pressure curves were observed.

The procedure can be performed easily, and the calculation can be made within minutes. The method can provide non-invasively pressure and volume which are valuable in characterizing the function of the heart as a pump, at rest and during graded exercise.

QUANTITATION OF REGIONAL MYOCARDIAL BLOOD FLOW BY POSITRON EMISSION COMPUTERIZED TRANSAXIAL TOMOGRAPHY. G.Wisenberg, H. Schelbert, G. Robinson, C. Selin, E. Hoffman, M. Phelps. UCLA School of Medicine, Los Angeles, CA.

Positron emission computerized transaxial tomography (PCT) offers the potential of measuring non-invasively tissue concentrations of radioactive indicators, but this has yet to be established for the heart. Also, count recovery is affected by object size and may be limited in small structures e.g. myocardium. Therefore, the potential of PCT for non-invasive quantitation of regional myocardial blood flow (RMBF), was studied in 7 open chest dogs, with 30 imaging procedures and 2 planes/study. Ungated PCT imaging was begun 30 sec after microspheres (8-15u) labeled with Cu-62 ($t_{\frac{1}{2}}$=9.7 min, positron emitting) were injected together with gamma microspheres (9u) into the left atrium. Following control study, subsequent images were obtained after repeat injections of both microspheres while circumflex flow was altered from 9 to 464 ml/min/100gm. After sacrifice, myocardial tissue samples were counted for gamma activity, RMBF determined by the arterial reference technique and compared to RMBF calculated from regions-of-interest in the PCT images with cpm/cm^2 converted to ct/gm by a calibration factor, and to ml/min/100gm using the reference sample. Based on phantom studies, corrections were made for dependence of count recovery on wall thickness, as measured by in-vivo echocardiography. Uncorrected RCT RMBF correlated poorly with in-vitro RMBF, while data corrected for wall thickness correlated linearly and in a one to one relationship by y=5.25+1.06x(r=0.85) and by y=16.0+97x n=60(r=0.95) for the anterior and posterior LV wall regions respectively. The results indicate that PCT accurately measures myocardial indicator concentrations when corrections are made for object size. With further developments, non-invasive measurement of myocardial flow and metabolism by PCT is feasible.

MYOCARDIAL METABOLIC RATE FOR GLUCOSE DURING SUPPLY-DEMAND IMBALANCE IN THE ISOLATED ARTERIALLY PERFUSED RABBIT SEPTUM. R.C. Marshall, W.W. Nash, K.E. Shine, M.E. Phelps, N. Ricchiuti and I. Whitehorn. UCLA School of Medicine, Los Angeles, CA.

Quantitative evaluation of regional myocardial metabolic rate for glucose (MMRGlc) during ischemia is possible using 18-fluorodeoxyglucose (FDG) and emission computerized axial tomography (ECAT). Previous investigations have shown that MMRGlc declines in ischemia due to low flow (cellular hypoxia reduced flow) and accelerates during anoxia (cellular hypoxia, maintained flow). Myocardial ischemia can also result from excessive oxygen demand without a concomitant increase in supply (supply-demand imbalance) (SDI) - situation simulating anoxia (cellular hypoxia, maintained flow). If MMRGlc could be evaluated during SDI in an experimental model and shown to accelerate, then FDG and ECAT could potentially be used to distinguish SDI from low flow

ischemia in man. The isolated arterially perfused rabbit septum (IAPRS) was adapted to serve as an experimental model to study MMRGlc during SDI. SDI is produced by introducing a paired stimulus without increasing flow. Oxygen consumption (OC) and MMRGlc were determined during control, normoxic high work (NHW), and SDI in 4 preparations. MMRGlc increased (+SD) 109%+ 3.2 and 91%+ 3.0 in NHW and SDI respectively ($p < .05$). OC increased 113% ±6.2 in NHW, but only 31% ±3.6 in SDI ($p < .001$). In 3 other preparations, SDI was exaggerated by progressively increasing demand without changing flow: OC declined 17% from moderate to severe SDI while MMRGlc increased 15%.

The IAPRS has been adapted as an experimental model to study MMRGlc during SDI. Preliminary data suggest that anaerobic glycolysis occurs in SDI.

ASSESSMENT OF CORONARY DISEASE BY REST AND EXERCISE RADIONUCLIDE ANGIOCARDIOGRAPHY AND TREADMILL PROCEDURES. G.E. Newman, S.K. Rerych, M.T. Upton, D.C. Sabiston, Jr., R.H. Jones, Duke Medical Center, Durham, NC

Multistage treadmill test (ETT), rest (R) and exercise (E) radionuclide angiocardiography (RNAC) and cardiac catheterization (CC) were performed in 72 patients (pts) with symptoms of coronary artery disease (CAD). Fourteen normal subjects had RNAC alone (Gp I). Pts were grouped by the number of major vessels (V) with >75% luminal stenosis, and 15 pts had insignificant CAD (Gp II), 16 had 1-V (Gp III), 17 had 2-V (Gp IV) and 24 had 3-V CAD (Gp V). Left ventricular ejection fraction (EF), end-diastolic volume (EDV), end-systolic volume (ESV) and wall motion abnormality (WMA) were determined by RNAC at R and E. The normal response (R to E) was defined by increases in EF (>5%) and EDV (<25%), a decrease in ESV and no WMA. RNAC and ETT results are tabulated (*R to E $P<0.03$).

	Gp I	Gp II	Gp III	Gp IV	Gp V
EF-R %	66± 9	69± 9	62±16	57±15	57±12
EF-E %	79± 8*	75± 9*	57±17*	50±16*	47±14*
EDV-R ml/m^2	53±16	55±18	70±30	76±25	76±28
EDV-E ml/m^2	63±19*	71±22*	97±28*	104±37*	109±31*
ESV-R ml/m^2	19± 9	18± 9	31±28	36±22	36±24
ESV-E ml/m^2	13± 7*	18± 9	44±33*	57±33*	61±29*
Positive RNAC	0	5	15	17	22
Negative RNAC	14	10	1	0	2
Positive ETT	--	2	6	13	17
Negative ETT	--	6	4	1	4

The sensitivity of ETT was 80% in 53 pts (74%) with adequate ETT and 95% in 72 pts by RNAC. Moreover, the magnitude of EF, EDV and ESV changes from R to E appeared to correlate with the anatomic severity of CAD. Thus, RNAC appears useful for the characterization of pts with CAD.

STRESS INDUCED PULMONARY THALLIUM-201 UPTAKE IN PATIENTS WITH CORONARY ARTERY DISEASE. F.C. Kushner, R.D. Okada, H.D. Kirshenbaum, C.A. Boucher, F.W. Strauss, and G.M. Pohost. Massachusetts General Hospital, Boston, Mass.

Increased pulmonary thallium-201 (Tl) activity may occur on initial post stress myocardial images (SMI) in some patients (pts) with coronary artery disease (CAD). Accordingly, initial (init) and 2 hour post stress Tl images were collected and reviewed in 49 pts. Computer determined pulmonary Tl activity (PUL-Tl) was expressed as a percent of maximal myocardial activity for init and delayed images. PUL-Tl) was compared to the angiographically determined extent of CAD, ejection fraction (EF) and the number of abnormal Tl myocardial segments. In 10 control pts without CAD, the mean init PUL-Tl was 37±6±5%. Ten pts with single vessel CAD has a mean init PUL-Tl of 45.5±3.6% (p=NS from controls), while 29 pts with double and triple vessel CAD and an elevated mean init PUL-Tl of 53.5±2.1% ($p<.001$). Those pts with CAD and a normal mean init PUL-Tl had a higher resting EF (66±2%) than those CAD pts with an abnormal mean init PUL-Tl more than 2 standard deviations above control, >47%, (EF=58±2.5%)$p< .05$. Those pts with 4 or 5 abnormal segments on their SMI's had a higher mean init PUL-Tl (59±4.9%) than those pts with one or no abnormal segments on SMI (44.5±2.0%)($p<.01$). When an init PUL-Tl over 2 standard deviations above the control mean was defined as abnormal, pts having both a positive SMI (perfusion defect) and an abnormal mean init PUL-Tl all had CAD (n=17). The 3 pts with a positive SMI but no CAD had normal mean init PUL-Tl.

Thus, the finding of an elevated pulmonary Tl-201 activity after stress is associated with multivessel CAD, a reduced rest EF, and more abnormal Tl myocardial segments. This suggests that PUL-Tl may be a marker of abnormal ventricular function.

Tl-201 REDISTRIBUTION IN PATIENTS WITH ACUTE MYOCARDIAL INFARCTION. L.M. Zir, H.W. Strauss, H. Gewirtz, W.H. Shea, S.A. Forwand, P.C. Voukydis, and G.M. Pohost. Massachusetts General and Mount Auburn Hospitals, Boston, Massachusetts.

Patients with acute myocardial infarction (MI) and no previous MI underwent serial Tl imaging and gated blood pool studies within 12 hours of the onset of chest pain in order to determine the ability of serial imaging of Tl with redistribution (RD) analysis to differentiate between ischemic and infarcted myocardium. All patients (pts) showed initial Tl defects. Serial imaging was performed over a two hour period after Tl administration. Nine pts demonstrated some RD into the region of MI, while 7 did not. On gated blood pool scan, those with RD had ejection fractions (EF's) of 58.2±5.3 (SEM) while those without RD had EF's of 46.5±5.0 ($p<.01$). Although regional wall motion abnormalities (WMA) corresponded to Tl defects in regions of acute infarction, the severity of WMA did not relate to the presence or absence of RD. Eleven of these pts demonstrated RD in segments remote from those which were acutely infarcted. Four pts who had both defects in the MI site and remote from it underwent coronary angiography within 2 weeks of radionuclide study. In each case, the remote defects were associated with severe coronary artery narrowing. These preliminary data indicate the following: 1) RD occurs into zones of acute MI in the early hours and is presumed evidence of a reversible ischemic component; 2) RD pts have better EF's than non-RD pts;) RD occurs in areas remote from the acute MI is most likely related to other severe coronary artery disease involvement; 4) These preliminary data from this ongoing protocol suggest the potential utility of serial Tl imaging during the early hours of acute MI to determine the degree of reversibility and to detect additional coronary artery disease.

TIME-ACTIVITY ANALYSIS OF NORMAL ZONES IN THALLIUM SCANS OF PATIENTS WITH CORONARY ARTERY DISEASE. H. Gewirtz, M.J. Sullivan, D.R. Shearer, D. Delude, A.K. Fitzgibbons, and A.S. Most, Rhode Island Hospital, Brown U., Providence,R.I.

Stress Thallium (Tl) images (Im) in patients (Pt) with coronary artery disease may show areas of apparently normal Tl uptake in regions supplied by diseased vessels. To determine if occult ischemia as evidenced by delayed Tl clearance occurs in such areas the following study was done. Fifteen Pts with ≥75% stenosis of ≥1 coronary artery and 10 with angiographically normal coronary arteries were exercised maximally and then imaged over 2-3 hr starting 2-3 min after injection. All Im were taken for 300K counts in a 128X128 matrix and acquisition time noted. The normal zone (NZ) in each initial Im was defined by the computer as the set of 5X5 myocardial pixel arrays with Tl activity (determined at the $P<.05$ level) ≥80% of the activity in the highest single 5X5 array. Background corrected changes in Tl activity in the NZ were computed after early (20-30 min after Tl) and late Im were spatially realigned relative to the initial one. Two NZ were analyzed (1 each in anterior and LAO views) for each Pt. A ≥75% stenosed coronary artery supplied 19/30 NZ in 13/15 Pts. In these, activity (% initial, mean±SD) early (92±9%) and late (72±9%) after Tl was given did not differ significantly from early (94±9%) or late (72±7%) activity in the NZs of normal Pts. In addition failure of Tl activity to decrease by >2SD between initial and early views was seen in 5/10 normals (4NZ-no change, 2NZ-increased) as well as in 4/15 Pts with coronary disease (4NZ-no change, 1NZ-increased). Thus, normal zones in Tl scans of Pts with coronary artery disease have Tl kinetics similar to those in normal Pts and thus may be used appropriately as an internal standard for estimating relative differences in Tl activity in other regions of the heart.

INFLUX OF RADIOACTIVE CALCIUM INTO ISOPROTERENOL DAMAGED RAT HEART. A. Owunwanne, A. Durakovic, E. Schenk and R.E. O'Mara. University of Rochester Medical Center, Rochester, NY

It has been postulated that the abnormal localization of Tc-99m-PPi in the myocardium damaged by infarction is related to calcium influx. Isotopic, autoradiographic and histologic studies of the influx of calcium ion into damaged myocardial cells were performed. Necrotic changes were induced in the myocardial cells of experimental rats by the use of isoproterenol and confirmed by histologic studies. Isoproterenol was injected subcutaneously 1, 2, 4, 6 and 24 hours prior to sacrifice. Rats which did not receive isoproterenol served as the control group. Ca-45, Ca-47 and Tc-99m-PPi were injected intraperitoneally 30 min prior to sacrifice with each time group having 4 rats studied.

The hearts of both experimental and control rats were individually counted for Ca-47 or Tc-99m activity. Autoradiographic studies were performed on myocardial sections and optical densities of the autoradiographs were made with a Macbeth densitometer. There was an increase in uptake of Ca-47 and Tc-99m-PPi in the damaged heart as compared to the control by a factor of nearly 2:1. The optical density of the autoradiograph of a section of the damaged heart also increased by a factor of nearly 2:1 over a comparable autoradiograph of a section of the control heart. This calcium influx reached a peak at 6 hours isoproterenol injection.

These results have confirmed that there is an influx of calcium ions into the damaged myocardium of the rat. This calcium influx paralleled the uptake of Tc-99m-PPi in such hearts. The results are consistent with the hypothesis that abnormal Tc-99m-PPi uptake is due to increased calcium influx into myocardial cells that have suffered infarction.

MYOCARDIAL IMAGING AND MEASUREMENT OF MYOCARDIAL FATTY ACID METABOLISM USING ω-I-123-HEPTADECANOIC ACID. K. Vyska, A. Höck, C. Freundlieb, M. Profant, L.E. Feinendegen, H.J. Machulla, G. Stöcklin. Institute for Medicine and Institute for Nuclear Chemistry, Nuclear Research Center Jülich, Western Germany

Previous animal experiments had demonstrated the suitability of ω-I-123-heptadecanoic acid (IHA) for imaging and for the determining metabolic turnover of fatty acids (FA) in the myocardium (1). The present paper describes an improved method and results of imaging and metabolic studies in 20 normal (nl) persons, in 35 patients (pts) suffering from coronary heart disease and 3 pts with old myocardial infarctions. 0.5 - 1.0 mCi IHA dissolved in 2 ml of pts serum was i.v. injected. Activity distribution in the chest was registered with an Anger-γ-camera with computer. 20 minutes after injection of IHA, 300 μCi of NaI-123 were i.v. given for the purpose of correcting for the iodide beeing released during the catabolic degradation of IHA and so to achieve an optimal contrast between myocardium and other tissue; infarcted zones are clearly visualized as defects of activity accumulation; moreover, ischemic regions in the myocardium are detectable at rest. The release of the activity from myocardium was determined from the background corrected time activity curves and served as parameter for the regional metabolic turnover of FA. The average clearance half-time in nls was 25 ± 5 min, the values for ischemic zones ranged from 35 to 50 min. IHA seems to be an excellent radiopharmaceutical for myocardial imaging and for noninvasive assessment of energy metabolism of normal and pathological myocardium.

(1) Machulla, H.J. et al.: J.Nucl.Med. 19, 298-302 (1978)

BLOOD FLOW AND MYOCARDIAL UPTAKE OF Tl-201 AND Tc-99m-PPi. H. Nishiyama, R. Adolph, S. Lukes, M. Gabel, J. Blue and V. Sodd. FDA, Nuclear Medicine Laboratory, Cincinnati, OH.

Because myocardial infarcts imaged with Tl-201 (Tl) and Tc-99m-PPi (PPi) frequently show size discrepancy, we studied this in relation to myocardial blood flow. Seven dogs with 48-hr infarcts received PPi, Tl, and I-125 labeled microspheres (10-μ size) at 2 hr, 15 min, and immediately before sacrifice, respectively. Multiple samples from seven transmural layers were made totalling 1307 samples. Each sample weighed about 100 mg. Higher blood flow and Tl uptake were seen in the mid to inner layers of the normal myocardium, and the best correlation between the two was also seen in the same regions. Blood flow and Tl uptake in the infarcted regions were as low as about 10% in the middle of the infarct and as high as 100% of normal in the bordering zone, where no clear-cut demarcation was seen by means of either blood flow or Tl uptake. Most of the time PPi showed the highest uptake in the mid-portion of the infarct, not in the bordering zone, where blood flow ranged from 40% to 80% of mean values. Increased PPi uptake was observed beyond the infarct as defined by either blood flow, Tl uptake, or histological confirmation.

The following conclusions were made: (1) A wide range of normal blood flow and normal Tl uptake were noted; (2) Surprisingly high blood flow and Tl uptake were seen in the infarcted area, especially in the periphery at 48-hr infarct, suggesting that evolution of the infarct has taken place; (3) PPi uptake tended to show higher than normal uptake beyond the infarcted area where blood flow and Tl uptake were within normal range. Thus, Tl underestimates infarct size, while PPi overestimates infarct size. These changes will, however, differ depending upon the stage of infarct.

EFFECTS OF CORONARY BLOOD FLOW ON Tl-201 UPTAKE. H. Nishiyama, R. Adolph, M. Gabel, S. Lukes and C. Williams. FDA, Nuclear Medicine Laboratory and Cincinnati General Hospital, Cincinnati, OH.

This study assessed the effects of ischemia and reactive hyperemia on Tl-201 (Tl) myocardial uptake in dogs. In the ischemia study, Tl was given at the onset of a 2-min occlusion of the circumflex coronary artery and in the hyperemia study 30 sec after 2-min occlusion. Data were collected using a gamma camera with a computer in the LAO position. Ultrasonic segment-length gauges and flow meters assessed functional changes. As an average, circumflex blood flow reached 3 times higher than the control value at 1-min post occlusion and returned to the control value in less than 5 min. Segmental systolic shortening occurred during occlusion return to the control value in less than 15 min. Tl uptake in the anterior wall served as a control; uptake was about 60% at 5-min and 100% at around 50-min post injection (PI), when Tl activity in the blood pool (BP) was about 8% and 1.8%, respectively. With ischemia, the posterior wall showed an initial relatively rapid uptake in the first 20 min, followed by slow uptake to equilibrium with the anterior wall at about 120-min PI when about 1.5% Tl activity was in BP. With hyperemia, the posterior wall showed 150-300% uptake at 15-20 min PI, followed by relatively rapid decrease to reach equilibrium at 240-340 min. In ischemia study, the posterior wall uptake increased continuously despite low Tl activity in BP; in reactive hyperemia study, net loss of Tl activity from the posterior wall exceeded that from the anterior wall. The major determinant of the Tl uptake is coronary blood flow. Redistribution can best be understood as the relative balance of net gain compared to net loss of Tl as coronary blood flow and myocardial function return to the normal state.

REVERSE REDISTRIBUTION: WORSENING OF THALLIUM-201 IMAGES FROM EXERCISE TO REDISTRIBUTION. H.S. Hecht, J.M. Hopkins, D.E. Blumfield, M. Wong and J.G. Rose. Wadsworth VA Hospital Center and the University of California, Los Angeles, CA.

One hundred eighty-five consecutive thallium-201 exercise and redistribution scans for the evaluation of coronary artery disease were reviewed for the presence of reverse redistribution (RR), i.e. worsening of images from exercise to redistribution. Fourteen patients (7.6%) were noted to have this pattern; 8 had reversible defects consistent with ischemia in addition to redistribution defects. Ten of the RR defects were noted on a single view; 3 in the anteroposterior projection, 4 in the left lateral, 1 in the left anterior oblique and 2 in the right anterior oblique. Three patients had RR defects in 2 views and 1 in 3 views. There were 13 inferior RR defects, 1 anterior and 1 anteroseptal.

Ten patients underwent cardiac catheterization; 7 had triple vessel, 2 double vessel and 1 single vessel disease. Seven patients had RR defects in the distribution of totally occluded vessels and 1 in a vessel with 99% occlusion; 7 had wall motion abnormalities in the distribution of these vessels. All 8 areas were supplied by collateral vessels. Of the remaining 2 patients, 1 had a RR defect in an area supplied by a vasospastic vessel and the other in the distribution of a diffusely narrowed vessel distal to a 50% stenosis.

In summary, 7.6% of all patients undergoing thallium-201 scanning had RR defects and 80% of those with angiographic data had RR in areas supplied by collateral vessels. One of the underlying mechanisms may be exercise induced increased collateral flow resulting in normalization during exercise in an area that is underperfused in the redistribution state.

SEQUENTIAL BAYESIAN ANALYSIS OF MULTIPLE NONINVASIVE TESTS FOR THE ACCURATE DETECTION OF CORONARY ARTERY DISEASE. H. Staniloff, G. Diamond, M. Hirsch, D. Berman, Y. Charuzi, M. Freeman, U. Elkayam, R. Vas, A. Waxman, J. Forrester. Cedars-Sinai Medical Center, Los Angeles, California.

Multiple noninvasive testing has become increasingly important in the assessment of coronary artery disease (CAD); however, discordant test results frequently lead to clinical uncertainty. Accordingly, 43 pts with suspected CAD were evaluated by thallium scintigraphy (TS), fluoroscopy (Fl) for coronary calcification, treadmill stress ECG, and cardiokymography (CKG). The data were analyzed quantitatively using Bayes' theorem; for each pt, a single likelihood (L) for CAD was calculated, based on a pretest estimate by age, sex and symptoms, and the sensitivity and specificity of each test. L was then correlated with subsequent coronary angiography. There were 46 (27%) incorrect test responses occurring in 30 of the 43 (70%) pts (10 TS, 13 Fl, 12 ECG, 11 CKG; p=ns). Mean L after testing was 7.0±3% in the 12 non-CAD pts, 84.2±7% in the 11 1-vessel CAD pts ($p<0.0001$) and 99.5±0.2% in the 20 multivessel CAD pts ($p<0.001$). To further validate the L calculation, the 15 possible combinations in each of the 43 patients was evaluated. There was a highly linear correlation between CAD prevalence and L in these 645 actual combinations of test results ($r=0.964$, $p<0.01$). The prevalence of CAD was 22% in pts with 0-20%L, only 35% of whom had multivessel disease; 67% in pts with L between 40-60%, 47% of whom had multivessel disease; and 98% in pts with L of 80-100%, 76% of whom had multivessel disease. Therefore sequential Baysian analysis produces an accurate prediction of subsequent angiographic CAD in individual patients and allows a meaningful resolution of discordant test results.

MONITORING RUBIDOMYCIN TOXICITY WITH PYROPHOSPHATE AND MUGA HEART SCANS. L.D. Samuels, B. Lewis, A.Weiss and E. Naperstak, Hadassah University Hospital, Jerusalem, Israel

This study reports early results of a protocol established for the regular cardiac evaluation of patients who are receiving rubidimycin therapy. It was established after the onset of severe myocardial decompensation in a patient receiving intensive therapy for acute myelogenous leukemia was clearly documented by Tc-99m pyrophosphate (PYP) myocardial scans and Tc-99m RBC MUGA scans of wall motion.

Patients who have received significant doses of rubidomycin therapy for leukemia and lymphoma, as well as certain solid tumors, receive 15mCi Tc-99m PYP and undergo myocardial scans from three projections between 1-2 hrs.later. Those who show signs of cardiac decompensation also receive 15mCi Tc-99m RBC and undergo MUGA studies of wall motion and cardiac function.

In ten patients receiving rubidomycin therapy for leukemia and lymphoma, four have been shown by scans to have sufficient myocarditis to warrant termination of therapy. In one patient without evidence of clinical myocardial involvement but with scan evidence of myocarditis one additional dose of rubidomycin produced acute heart failure. A second series of patients with solid tumors is also being followed with this protocol.

We feel that heart scans with Tc-99m pyrophosphate and Tc-99m RBC MUGA studies are important routine procedures to periodically evaluate cardiac status in patients who are receiving rubidomycin therapy.

COMPARISON OF ECHOCARDIOGRAM (ECHO) AND FIRST PASS RADIONUCLIDE VENTRICULOGRAM (RVG) IN THE DETERMINATION OF LEFT VENTRICULAR EJECTION FRACTION (LVEF) AS CORRELATED TO CONTRAST VENTRICULOGRAM. E.D. Folland, D.E. Tow, A.F. Parisi, S. Karaffa, C.A. Dilts and F.C. Basilico. West Roxbury VA Medical Center and Harvard Medical School, Boston, MA.

The study was undertaken to compare the two non-invasive imaging methods in determining LVEF in 50 consecutive CAD patients undergoing cardiac catheterization. Echocardiographic LVEF was determined from LV dimensions just below the mitral leaflets at end diastole (LVD) and end systole (LVS). The fractional shortening was taken as EF: (LVD-LVS)/LVD. RVG EF was obtained from the representative beat constructed for the first pass of the 15 mCi bolus of Tc-99m pertechnetate through LV using a high count rate multicrystal scintillation camera and 30° LAO with 30° caudal tilt position. 39/50 echocardiograms and all RVG examinations were suitable for measuring EF. Results were compared to EF calculated from contrast examination (cine EF) and shown in Table 1. Correlations of RVG EF with cine EF was better ($r=0.86$, $p < 0.001$) than ECHO EF ($r=0.55$, $p < 0.01$). When only data from patients with transmural infarction was compared, r for ECHO EF showed no improvement (0.51). When CINE EF ≤ 0.30 was taken as indication of poor LV function, RVG was 100% sensitive. ECHO was 57% sensitive. The specificity was 100% for ECHO, and 95% for RVG, Table 2. It is concluded that RVG is a better non-invasive method for the state of art in determining LVEF.

CORRELATIVE ROLE OF ECHOCARDIOGRAPHY (EC) AND RADIONUCLIDE ANGIOCARDIOGRAPHY (RN). R.W. Myers, R.P. Bails, and E. Drasin. Herrick Memorial Hospital, Berkeley, CA.

To determine the correlative role of conventional M-mode EC and RN, 21 patients (pts) were studied in conjunction with contrast ventriculography (CVG) (16 biplane, 5 RAO only). Segmental wall motion abnormalities (WMA) were assessed on EC both subjectively and by measuring left ventricular (LV) wall excursions and on RN and CVG by subjective evaluation of 7 LV segments. When anteroseptal WMA were considered present if any anterior or septal segment was abnormal on CVG, sensitivity (SN) and specificity (SP) were 40% and 91% for EC and 90% and 100% for RN. If only septal WMA were considered, the SN and SP were 80% and 91% for EC and 100% and 91% for RN. For inferior WMA the SN and SP were 27% and 100% for EC and 79% and 100% for RN. Apical segment WMA on CVG were detected by RN in 9 of 10 pts but not identified by EC. Five of these pts had no segmental WMA on EC. Ejection fraction (EF) was determined by LV dimensional changes on EC and from the area/length method on RAO first pass RN and CVG. The correlation for EF was slightly better for RN ($r = .96$, $p < .001$, SEE = .06) than EC ($r = .77$, $p < .001$, SEE = .14). Cardiac diagnoses made by EC but not by RN (e.g. LV hypertrophy, mitral stenosis) occurred in 52% of cases.

This study suggests that when compared to EC, RN in multiple projections is more accurate for evaluating global and at least more sensitive in evaluating segmental LV function. The lower SN for WMA by EC may be due to limited visualization of the LV by the single dimension ultrasound beam. SP for WMA of the two techniques is similar; however, EC appears to offer additional specific information about other cardiac disease states not available from RN.

THE BIFOCAL DIVERGING COLLIMATOR: A METHOD FOR SIMULTANEOUS BIPLANE IMAGING OF THE HEART. C.A. Boucher, H.W. Strauss, R.D. Okada, H.D. Kirshenbaum, F.G. Kushner, K.A. McKusick, P.C. Block, J. Leask, G.M. Pohost, Mass. General Hospital, Boston.

Because coronary artery disease affects left ventricular

(LV) wall motion regionally, simultaneous rapid imaging of the heart in two views during acute interventions, such as exercise or pacing, would be desireable. To accomplish this we constructed a bifocal diverging collimator (BDC) capable of recording 2 views of the heart 50° apart on each half of a standard 25 cm imaging field. In this study, simultaneous biplane multigated blood pool scans (BPS) using the BDC were compared to the same 2 separate views obtained using a conventional all purpose parallel hole collimator (PHC) and to left ventricular (LV) angiography (A). BPS was performed at rest using ^{99m}Tc in-vivo labelled red blood cells in 20 patients (pts) undergoing cardiac catheterization. LV ejection fraction (EF) and regional wall motion (RWM) was determined by 3 observers for BDC, for conventional single plane anterior and LAO BPS using PHC, and for A. LVEF by BDC correlated closely with PH (r=0.94) and A (r= 0.88) with an interobserver variability (±1 S.D.) of 6%. LV wall motion was scored for 6 LV segments (3 in anterior and 3 in LAO) on a 5 point scale from 3 (normal) to -1 (dyskinesis). The % agreement in scores for a segment, defined as a difference ≤1, between BDC and PH was 88%, varying from 100% in the anterolateral to 80% in the inferior segment. The % agreement between BDC & A and PH & A was identical, 79%.

In summary, the BDC for a single BPS acquisition provides information about global and regional LV function in two planes comparable to that of PHC. By adding a second view, evaluation of the effect of acute interventions on RWM should be enhanced.

PERIPHERAL RADIONUCLIDE ANGIOGRAPHY: A NEW DIAGNOSTIC MODALITY. P. Matin, E.C. Glass, J. Villarica and R.F. Carretta. Roseville Community Hospital, Roseville, Ca., and University of California, Davis, Ca.

Peripheral radionuclide angiography is a new and useful clinical nuclear medicine modality which arose from the need for noninvasive study of the vessels of the extremities. The technique is simple, completely benign and relatively inexpensive. It requires neither arterial puncture nor the administration of allergenic contrast agents. Positioning a high resolution scintillation camera over the extremity allows imaging of the arteries of the distal extremities with a simple antecubital venous injection of 15 mCi of 99mTc. The technique can be performed in almost every nuclear medicine department and in addition, quantitative data can be obtained in those departments where data processing equipment is available. To date we have studied over 300 patients with preliminary diagnoses of stenosis, obstruction and aneurysm of the distal arteries. We have been able to visualize aneurysms and stenoses of the arteries as distal as the vessels of the wrist and fingers. In many cases treatment or surgery was performed without additional x-ray contrast studies. However, where x-ray contrast studies were performed, the correlation was excellent. Ninety-two percent of the cases showed essentially identical findings. The quantitative data was often more useful to the vascular surgeons than the arteriographic data in deciding whether to graft a stenosed vessel. The technique has proved extremely useful in the diagnosis and follow-up of a variety of clinical problems related to the peripheral system such as paresthesias, "cold limbs" and intermittent claudication. The quantitative data has removed much of the subjectivity in the diagnosis and follow-up of these arterial problems.

4:00 p.m.-5:30 p.m. Room 201

RADIOPHARMACEUTICAL CHEMISTRY POSTER SESSION I

Chairman: David A. Goodwin
Co-Chairman: Kenneth A. Krohn

TECHNETIUM LABELED HEPARIN AND THROMBOEMBOLISM. J. P. Esquerré and R. Guiraud. Hôpital Purpan, Toulouse, France.

We used Technetium 99m heparin as an approach to heparin pharmacokinetics which might lead to clinical applications in thromboembolism diagnosis and treatment. We performed kinetics studies in 7 normal subjects. In I8 patients diagnosed as, or suspected of having a leg veinous thrombosis we performed a legs'scintigraphy, but we were more strongly interested in kinetics studies especially blood clearance as a possible index of thrombotic disease.

In normal subjects both external detection and blood samples radioassay showed a biphasic blood clearance curve with fast (t I/2 = 8 ± 3 mn) and slow (T I/2 = 240 ± 30 mn) components. The half life of the anticoagulant effect as measured by thrombin clotting time (60 mn), was different from the half life of heparin concentration (240 mn). With regard to patients, in I2 cases out of I8 the scintigrams showed a more or less increased uptake by the pathologic limb. The results are inconstant because of a probable saturation of endothelial heparin binding sites by previously injected therapeutic heparin. In thrombotic patients, the kinetics studies showed a very significantly increased clearance : the slow component half life was T I/2=I20±40 mn. In addition we showed that heparin clearance depends on its plasma concentration : the lower the concentration, the higher the clearance.

Our results suggest that Technetium heparin is a reliable tool which might be usefull to understand better how heparin works. More immediatly, it should be a means of early diagnosis of thrombotic disease by imaging damaged blood vessels and, more importantly, by showing changes in heparin kinetics since an increased clearance appears to be a constant and early feature of thromboembolism.

A RAPID METHOD FOR LABELING IgG WITH ^{99m}Tc. L. G. Colombetti, J. Goldman, G. C. Patel, M. Goldman and S. Pinsky. Michael Reese Hospital and Medical Center, Chicago, IL.

Several methods for radioactive labeling of proteins are in common usage. However, these techniques often are associated with undesirable effects such as colloid formation or partial denaturation. The technique originally proposed by Wong et al has been adapted to the labeling of immunoglobulin G (IgG) resulting in a rapid, simple and effective method which enables the production of ^{99m}Tc-IgG with high specific activity and minimal denaturation. The procedure is carried out by adding 1 ml of a solution containing 2 to 4 mCi of $^{99m}TcO_4^-$ to a vial containing 0.1 ml of aqueous solution of 100 µg of $SnCl_2$. The vial is flushed with nitrogen for 2 minutes. 1 ml of veronal buffered saline, pH 7.5 containing 2 mg purified rabbit IgG is added and after mixing for 5 seconds, this solution is incubated for 15-20 minutes at 37°C. Labeled IgG is then separated from unbound ^{99m}Tc by passage through a 1x4 cm column containing Sephadex G50. Instant thin layer chromatography and immunoelectrophoresis combined with autoradiography revealed greater than 90% binding of ^{99m}Tc and no significant alteration of size, charge and antigenic properties of the IgG.

NEW COMPLEXES OF Tc-99 IN LOWER OXIDATION STATES. A. Davison, A.G. Jones, and H.S. Trop. Department of Chemistry, Massachusetts Institute of Technology, Cambridge, MA. and Department of Radiology, Harvard Medical School, Boston, MA.

Two complexes of technetium in the (+3) oxidation state have been isolated and characterized. Both contain pi-acid ligands. They are readily oxidized to either the (+4) or (+5) state.

The treatment of TcI_6^{2-} with cyanide ion in methanol-water gives yellow-orange solutions from which $K_4Tc(CN)_7 \cdot 2H_2O$ has been isolated. It has been characterized by elemental analysis and infrared spectroscopy. The latter shows ν CN, 2089, 2046 cm^{-1}, consistent with its having D_{5h} geometry, identical to the known rhenium complex. Solutions of this complex are air sensitive, and are oxi-

dized in the presence of CN^- to give the yellow oxotechnetium(+5) ion $TcO(CN)_5^{2-}$. The latter shows ν CN, 2095, 2075, 2035 cm^{-1} (consistent with C_{4v} symmetry) and ν Tc=O, 910 cm^{-1}. Pure $K_2TcO(CN)_5$ hydrolyzes in water in the absence of CN^- ion to give $K_3TcO_2(CN)_4$. The presence of only one Tc=O stretching mode in the infrared spectrum shows this to be a trans-dioxotechnetium(+5) ion (IR: ν CN, 2120, 2070 cm^{-1}; ν Tc=O trans, 785 cm^{-1}).

The reduction of $(NH_4)_2$ $Tc(NCS)_6$ in the absence of nonligated NCS^- by hydrazine in methanol gives a yellow solution. The addition of Bu_4NCl gives well-formed crystals of $[Bu_4N]_3[Tc(NCS)_6]$. The latter is also easily oxidized to the purple (+4) complex $[Tc(NCS)_6]^{2-}$. Cyclic voltammetric studies show that both $[Bu_4N]_3[Tc(NCS)_6]$ and $[Bu_4N]_2$ $[Tc(NCS)_6]$ in CH_3CN/Bu_4NClO_4 at a Pt electrode show a reversible one-electron change at $E_{\frac{1}{2}}$ = 0.18 v vs S.C.E. The species are thus $Tc(+4)(NCS)_6^{2-} + e^- \rightleftharpoons Tc(+3)(NCS)_6^{3-}$.

THE PREPARATION OF A KNOWN TECHNETIUM COMPLEX WITH A VARIETY OF REDUCING AGENTS. C. Orvig, A.G. Jones, A. Davison, H.S. Trop, B.V. DePamphilis, and M.A. Davis. Department of Chemistry, Massachusetts Institute of Technology, Cambridge, MA. and Department of Radiology, Harvard Medical School, Boston, MA.

Many radiopharmaceutical preparations involve the reduction of technetium in aqueous solution from the heptavalent state to some lower oxidation state in order to allow ligand substitution. None of the active species incorporating Tc-99m have yet been fully characterized. Recently, however, two new anionic complexes of Tc(V) with thiol-containing ligands similar in nature to some already evaluated as radiopharmaceuticals, have been identified. These are $[TcO(SCH_2CH_2OS)_2]^-$(I) and $[TcO(SCH_2CH_2S)_2]^-$(II). This study examined the effectiveness of selected reducing agents in preparing the known complex (II) in aqueous solution. The reagents used were dithiothreitol, formamidine sulfinic acid, sodium dithionite, hydrazinemonohydrate, hydroxylamine hydrochloride and 50% hypophosphorous acid. Standard aliquots of NH_4TcO_4 (0.15 millimol) and ethanedithiol (0.84 millimol) were placed in 25 ml of water, and the reducing agent added. The effect of reductant concentration, pH, temperature and time were studied. Complex (II) was precipitated by the addition of tetraphenylarsonium chloride (0.34 millimol) as the salt $[Ph_4As][TcO(SCH_2CH_2S)_2]$. This was then purified by recrystallization from acetone-water.

The results showed that although several of the reducing agents have good yields of (II) in the pH range 5-9, quantitative yields were only obtained with dithionite at pH 11, with a reaction time of 10 minutes at room temperature.

RADIOLYTIC PRODUCTION OF PEROXIDES IN TECHNETIUM-99m SOLUTIONS. A.K. Thornton, V.J. Molinski and J.T. Spencer. Union Carbide Corporation, Tuxedo, NY.

The purpose of this study was to determine whether radiolytic products were affecting the stability of Tc-99m labeled radiodiagnostic kits.

Water solutions of radiopharmaceuticals are decomposed by the action of ionizing radiation, producing molecular H_2 and H_2O_2 and, in the presence of dissolved oxygen, hydroperoxy radicals. An average value for the time-integrated deposited energy is 360 rads (3.6×10^4 erg/g) for an initial concentration of 1 mCi Tc-99m/ml.

The analytical method used for the determination of peroxides was a modified iodometric colorimetric determination utilizing a starch indicator system. Using this method, it was shown that substantial quantities of hydrogen peroxide and hydroperoxy radicals are formed during Tc-99m decay. The H_2O_2 production is dependent on the total activity present in solution. Dissolved oxygen in solution also plays an important part in peroxide buildup in Tc-99m solutions. Radioactive kits which use stannous ion as the reducing agent and which are prepared with large amounts of activity could have a serious oxidation problem if they are allowed to stand for many hours before use.

Possible remedies to this problem are: the use of oxygen-free saline to elute generators and to dilute Tc-99m solutions; addition of an antioxidant to Tc-99m eluate; heating Tc-99m eluates; and limiting the decay time of the Tc-99m in the Tc-99m radiodiagnostic.

THE INTERACTIONS OF Tc-99m PHOSPHORUS RADIOPHARMACEUTICALS AND SERUM PROTEINS. A. Owunwanne, R.E. O'Mara and C. O'Brien. University of Rochester Medical Center, Rochester, NY

Equilibrium dialysis and precipitation methods were used to study the interactions of different serum proteins with Tc-99m phosphorus radiopharmaceuticals. Unfractionated human serum proteins and fractionated albumin, alpha-, beta- and gamma-globulins to which Tc-99m-MDP, -HEDP and -PPi had been added in standard amounts, were separately dialyzed in physiologic saline, using pure regenerated cellulose sacs at 25°C for 24 hr. The serum proteins were also precipitated from an aliquot of the serum with 5% trichloracetic acid and centrifuged at 2000g for 10 min. Both serum proteins and the dialysate/filtrate were separately counted in a NaI well-type device.

Radiopharmaceutical binding to human serum proteins was found in the following increasing order: Tc-99m-MDP<-HEDP <-PPi. Tc-99m-MDP and -PPi were bound to different proteins in the following order: albumin<gamma-<beta-<alpha-globulins, whereas, the protein binding of Tc-99m-HEDP resulted in: albumin<gamma-<alpha-<beta-globulins.

The binding order of the unfractionated human serum protein is consistent with the blood clearance rate of the Tc-99m phosphorus radiopharmaceuticals (Tc-99m-PPi<-HEDP<-MDP) with the Tc-99m-PPi preparation having the slowest clearance rate and the greatest protein binding. The binding of different proteins to these bone scanning agents might help to explain the uptake of these agents in non-osseous tissues, many of which contain globulins. The knowledge of Tc-99m radiopharmaceuticals and serum protein interactions may aid in design and development of new technetium labeled radiopharmaceuticals as well as assist in the differential diagnostic possibilities in clinical nuclear medicine.

AN INVESTIGATION OF LOW TAGGING YIELDS OF Tc-99m DTPA KITS. P.J. Robbins and C.C. Williams. FDA, Nuclear Medicine Lab and University of Cincinnati Medical Center, Cincinnati, OH.

This investigation was performed to test the validity of the maximum quantity of Tc-99m prescribed by some package inserts and to determine if it is well chosen in the interest of proper tagging and economical use of DTPA kits. Some package inserts prescribe a maximum as low as 100 mCi Tc-99m. Radiochromatographic assay of Tc-99m DTPA preparations from our clinical facility during 1976-77 showed that the tagging yield frequently drops below 90% when more than 300 mCi Tc-99m is used to reconstitute the kit. Tc-99 carrier effects were studied by adding known amounts of Tc-99 to kits and measuring radiochemical yield by paper and thin layer chromatography. Levels of Tc-99 equivalent to 560 up to 1670 mCi Tc-99m from a Mo-99 generator on Monday morning were used. The effect of oxidant on the tagging yield was determined by adding hydrogen peroxide (HP) to the kits and determining the radiochemical yield. The HP concentrations were equivalent to and exceeded the concentration of oxidant found by iodometric analysis in Tc-99m solutions from a new generator on Monday morning. Carrier Tc-99 up to 2.1×10^{-8} moles Tc had no effect on tagging yield and HP at a concentration range of 4×10^{-4} to 4×10^{-3} M caused a decrease in tagging yields. These levels of HP were greater than the level determined in first elutions on Monday. We concluded that the cause of the low yields was due to (1) unusually high levels of oxidant in the Tc-99m, (2) instability of the Tc-99m DTPA complex 2-3 hr after preparation, (3) a kit-to-kit variability, or (4) other unknown causes. Radiochemical quality control tests should be an integral part of the daily preparation of radiopharmaceuticals.

KINETIC STUDIES OF A NEW AND SUPERIOR Tc-99m DIPHOSPHONATE BONE IMAGING AGENT. J.S. Arnold, W.E. Barnes, N. Khedkar, T. Milo. Hines VA Medical Center and Pathology Dept. Stritch Medical School, Loyola University, Maywood, IL.

In the course of clinically evaluating a new diphosphonate imaging agent, hydroxy methane (HDP), it was found that bone uptake was very rapid in lesions as well as control bone. Pursuant to an explanation of the greater fixation of HDP in bone and bone lesions, kinetic studies of the uptake of HDP were performed in ten patients and compared with similar studies using EHDP and MDP.

Studies were performed with 10 mCi of Tc-99m labeled diphosphonate. Sequential digital LFOV images were made of the posterior pelvis continuously for one hour and intermittently for 24 hours. A venous blood curve was collected. Bone curves were corrected for blood and soft tissue background, decay, camera sensitivity, and mass absorption. Net bone and blood curves were fitted to a compartmental model where blood communicates with three bone compartments corresponding to loosely, tightly, and an irreversibly bound imaging agent. The transfer coefficients between blood and bone compartments were calculated.

This data revealed that (1) the efficiency of bone extraction of blood HDP and MDP are approximately equal and > HEDP (2) that transfer rates from blood to (a) the loosely bound compartment were equivalent for HDP and HEDP and > MDP and that to (b) the irreversibly bound compartment was greatest for HDP > MDP > HEDP.

The tighter binding of HMD in bone is thought to be principally responsible for its observed superior performance as a skeletal imaging agent. The ratio of activity in lesions to that in normal bone is comparable for HDP and MDP.

PARA-AORTIC LYMPH NODE VISUALIZATION IN DOGS USING Tc-99m-Sn-PO_4. G.P.Basmadjian, D.L.Gilliland, J.C.Leonard,* A.S.Kirschner, and R.D.Ice. College of Pharmacy, University of Oklahoma HSC and Nuclear Medicine Department, Children's Memorial Hospital*, Oklahoma City, OK.

Technetium-99m-Sn-PO_4 is a radiopharmaceutical prepared by the addition of Pertechnetate-99m to a solution of stannous phosphate pH 9.0. This radiopharmaceutical has been shown to be a mixed metal soluble complex in which Tc is present in the III^+ oxidation state and Sn is an integral part.

Subcutaneous injection of a 1:100 diluted, pH 9.0 buffered preparation of a Tc-99m-Sn-PO_4 solution in rats, rabbits and dogs visualized the popliteal or axillary lymphatic nodes depending upon site of injection, hind or fore paws.

Intratesticular injection in dogs showed the lymph channels draining from the testes in less than 3 min. post injection and within 30 min. the para-aortic lymph nodes could be clearly visualized.

The mechanism of uptake of this radiopharmaceutical in the lymphatics is probably due to the in-vivo microcolloid formed with interstitial Ca(II) ions and resulting entrapment in the lymph nodes.

Studies under way to evaluate other injection sites, e.g. the spermatic cord, could result in a diagnostic agent for studying the involvement of para-aortic lymph nodes in testicular carcinoma.

PREPARATION AND BIODISTRIBUTION OF NEUTRAL, LIPID SOLUBLE Tc-99m COMPLEXES OF BIS(2-MERCAPTOETHYL)AMINE LIGANDS. H.D. Burns, H. Manspeaker, R. Miller, V. Risch, J. Emrich and N.D. Heindel. Hahnemann Medical College, Philadelphia, PA

Oldendorf has recently suggested that lipid soluble Tc-99m complexes which have octanol/water partition coefficients greater than 0.5 may be useful for the evaluation of regional brain blood flow. As part of a project aimed towards identifying ligands which form stable, neutral, lipid soluble complexes with Tc-99m, we have studied the Tc-99m complexes of a series of bis-(2-mercaptoethyl)-amines. The ligands were synthesized by reacting an alkyl halide with diethanolamine to give the substituted alcohol which was converted to the nitrogen mustard by reaction with thionyl chloride. Treatment of the nitrogen mustards with thiourea gave the isothiouronium salts which were hydrolyzed to the desired bis-(2-mercaptoethyl)amines.

$R\text{-}N(CH_2CH_2SH)_2$ R = H, METHYL, ETHYL, BUTYL, HEXYL

The Tc-99m complexes were prepared using either stannous chloride or sodium borohydride as reducing agents. Chromatography and electrophoresis demonstrated that these ligands formed neutral complexes, provided that R did not possess any functional groups which are charged at physiological pH. Octanol/saline partition coefficients of the Tc-99m complexes were determined and ranged from a low of 0.45 (R = H) to a high of 38 (R = Hexyl). Biodistribution studies in mice showed that at 30 minutes post injection the Tc-99m complex of the methyl substituted compound was able to penetrate the blood:brain barrier giving a blood:brain ratio of 1.3:1. This finding suggests that Tc-99m complexes of these ligands may be useful for the evaluation of regional brain blood flow.

EVALUATION OF FIRST-PASS AND EQUILIBRIUM CHARACTERISTICS OF TECHNETIUM-99m-LABELED VASCULAR MARKERS. M. Grissom, W. Alter, J. Hill, F. Vieras, W. Eckelman, and J. Phillips. Armed Forces Radiobiology Research Institute, Bethesda, MD, and George Washington University, Washington, DC

Tc-99m(TC)-labeled human serum albumin (HSA) and red blood cell (RBCs) were compared to I-125 human serum albumin (RISA) on a first-pass and equilibrium basis to determine which would be a better vascular marker for use in dual isotope extraction analysis studies. Anesthetized dogs were injected with a mixture of HSA or RBCs and RISA. Blood samples were drawn at intervals of 10 seconds for the first minute from the coronary sinus, and at 1 hour from the femoral vein. Both HSA and RBCs showed a higher first-pass in terms of uCi/g blood/kg body weight than RISA ($p<0.1$). This first-pass peak activity occurred in the 30-second samples for all 3 agents. The coefficients of variation at the peak were similar for RISA and RBCs (59.6% vs 60.3%), with HSA being greater (90.3%). There was no significant difference ($p>0.5$) between HSA and RBCs for the first-pass samples. Tissue analysis after sacrifice (1 hour postinjection) indicated that significantly greater elution of TC occurred from HSA than from RBCs ($p<0.1$) RBCs had higher splenic levels than HSA or RISA. HSA differed from RISA in kidney cortex and medulla, thyroid, liver, and urine levels ($p<0.1$) at equilibrium. It is suggested that the lower amount of TC elution for RBCs compared to HSA contributed to the smaller coefficients of variation seen in the first-pass blood data. In conclusion, although some RBCs were sequestered in the spleen, it is evident that less free TC, as seen in the RBCs to HSA comparison, makes RBCs better vascular markers due to a reduction in non-vascular compartment components.

GENTISIC ACID: A NEW STABILIZER FOR LOW TIN SKELETAL IMAGING AGENTS. A.J. Tofe, J.A. Bevan, M.B. Fawzi, H.S. Whitehouse and M.D. Francis. Miami Valley Labs, The Procter & Gamble Company, Cincinnati, OH.

Instability associated with Tc-99m stannous radiopharmaceuticals is a direct result of oxidants, either radiolytically induced or through chemical contamination.

In vitro stabilization for low tin bone imaging agents has been demonstrated with ascorbic acid and in this paper gentisic acid is shown to be an equally effective antioxidant for the hydroxyethane diphosphonate (HEDP) and hydroxymethane diphosphonate (HDP) skeletal agents. In vitro studies show less than 2% free or hydrolyzed-reduced pertechnetate-99m at 24 hours with the gentisic acid stabilizer.

Studies in guinea pigs at 3 and 24 hours using both C-14 and H-3 labeled gentisic acid show no effect upon the biodistribution of either bone agent by the addition of the gentisic acid stabilizer.

	Percent Dose Per Gram (3 hr)			
	Tc-99m HEDP (alone)	Tc-99m with HEDP	C-14 GA	C-14 GA (alone)
Bone	1.66 (1.60-1.71)	1.62 (1.49-1.71)	0.005 (0.004-0.007)	0.007 (0.005-0.011)

	Tc-99m HDP (alone)	Tc-99m HDP with H-3 GA		H-3 GA (alone)
Bone	1.91 (1.79-2.03)	2.0 (1.93-2.07)	0.005 (0.005-0.006)	0.006 (0.005-0.007)

Gentisic acid is an effective stabilizer and clinical studies have shown equivalency with ascorbic acid.

COMPARATIVE EVALUATION OF THREE DIPHOSPHONATES: IN VITRO ADSORPTION (C-14 LABELED) AND IN VIVO OSTEOGENIC UPTAKE (Tc-99m COMPLEXED). M.D. Francis, D.L. Ferguson and A.J. Tofe. The Procter & Gamble Company, Miami Valley Labs, Cincinnati, OH.

Recent studies comparing Tc-99m labeled diphosphonate skeletal imaging agents suggest fundamental uptake differences among agents depending upon the state of calcification and presence or absence of a hydroxyl group on the geminal diphosphonate carbon of the ligand. In order to elucidate the mechanism responsible for these observations, both in vitro and in vivo experiments were designed. In vitro studies involved quantitating adsorption of C-14 labeled hydroxy diphosphonates or non-hydroxy diphosphonates onto crystalline hydroxyapatite (HA) or amorphous calcium phosphate (ACP). In vivo studies involved the uptake of the Tc-99m complexes of hydroxy diphosphonates or non-hydroxy diphosphonates on sites of induced osteogenesis in Sprague-Dawley rats by subcutaneous implantation of acid insoluble bone matrix.

The results of the in vitro study indicated similar affinity of HEDP and MDP for HA but a significantly higher uptake with the smallest member of the hydroxy diphosphonate family, hydroxymethane diphosphonate (HDP). All three diphosphonates exhibited a greater adsorption on ACP than on HA per mole calcium. HDP had a significantly higher uptake on ACP than the other two. In vivo findings show the retention of Tc-99m HDP in the osteogenic site was also significantly ($p<.05$) greater than either HEDP or MDP. Since active sites of osteogenesis are believed to contain ACP, these studies form a working hypothesis for the clinically observed contrast of HDP between normal bone and soft tissue and between tumor and normal bone.

QUALITATIVE AND QUANTITATIVE DIGITAL COMPARISON OF TC-99m-HMDP AND MDP. N. Khedkar, J.S. Arnold, T. Milo, W.E. Barnes, G. Gergans. VA Medical Center, Hines, IL. and Stritch School of Medicine, Loyola University, Maywood, IL.

In an evaluation of two Diphosphonate agents which differ only by a hydroxyl group, MDP and HMDP (Hydroxyl methane Diphosphonate), we have compared scan quality and measured bone uptake in quantitative digital images. Images were obtained with both agents in 12 patients within a 4 to 7 day interval. Quantitative bone uptake was measured over pelvic bones at 1/2, 3, and 24 hours. All data was corrected for camera sensitivity, isotope decay and was normalized for the same injected dose.

The most consistent finding in analog images was low background activity at 4 and 24 hours with HMDP. Imaging techniques used tended to make the density of the bone equivalent in the two studies making it impossible to determine whether the bone was increased or the background decreased. Scan quality is superior in 50% of patients with HMDP and comparable in remaining patients. Subjectively, appearance of lesions was better with HMDP.

Digital data showed net bone uptake to be 30 to 60% higher with HMDP in normal bone at 3 and 24 hours. Background activity is 0 to 25% higher at 3 hours and 10 to 30% lower at 24 hours with HMDP. Few bone lesions studied showed comparable increase in net bone uptake of HMDP over MDP in normal bone and lesions at 24 hours and even in earlier images of 1/2 hour. Lesion to non-lesion ratios were the same at both times.

HMDP with a hydroxyl group appears to be a better bone scanning agent due to greater skeletal retention even at 1/2 hour and may facilitate earlier imaging of hot bone lesions.

MECHANISM OF TUMOR LOCALIZATION OF GALLIUM: EFFECT OF TUMOR pH. S.R. Vallabhajosula, J.F. Harwig and W. Wolf. Radiopharmacy Program, University of Southern California, Los Angeles, CA.

We have shown previously that radiogallium at high specific activity is, in blood, exclusively bound to and transported to the tumor site by transferrin, but the process by which transferrin-bound Ga is converted to tumor-bound Ga is not fully understood. The extracellular fluid in many animal tumors is known to be slightly acidic (pH 6.5-7.0) due to increased anaerobic glycolysis and lactic acidosis. To evaluate this factor we have studied the effect of pH on the in vitro stability of Ga-transferrin and the in vivo tumor uptake of Ga.

Blood samples were obtained from rabbits 15 min post Ga-67 citrate injection. Plasma was dialysed at 37°C in barbital-acetate buffer at pH 6.5, 7.0 and 7.5. Within 5 hr of dialysis, 55% gallium dissociated from plasma (transferrin) at pH 6.5, while only 30% dissociated at pH 7.5. Dialysis of Ga-transferrin formed in vitro showed similar results. Tumor uptake of Ga was studied in 2 groups of rats bearing Walker-256 carcinosarcoma. The tumor pH in the test group was reduced an additional 0.5 unit minimum by the known technique of glucose administration, while the control group did not receive glucose. Six hr post Ga-67 citrate injection, rats were sacrificed and the % I.D./g tumor was determined. Test rats showed a 30% increase in mean Ga uptake ($0.025 < p < 0.05$).

These results demonstrate that the stability of Ga-transferrin is pH dependent and suggest that dissociation of the complex due to decreased pH at the tumor site may be involved in tumor localization and binding of Ga. Clinical differences in Ga uptake by various tumor types may, in part, reflect differences in tumor pH.

IN VIVO AND IN VITRO STUDIES OF Tc-99m HIDA UPTAKE. L.R. Chervu, E.B. Robbins, S.S. Huq, M.D. Blaufox, Albert Einstein College of Medicine, Bronx, NY.

Tc-99m-HIDA has proven to be useful for evaluating acute cholecystitis and biliary duct pathology. However, there have been few studies directed at its handling by the liver and factors enhancing or impeding its uptake. In vivo liver fractionation was used in this study in an attempt to localize the intracellular binding sites for Tc-99m-HIDA. Liver homogenates were subjected to differential centrifugation or polyacrylamide gel electrophoresis and Sephadex gel filtration. Most of the Tc-99m-HIDA is recovered in the cytosol fraction. Binding with macromolecular constituents could not be demonstrated with these techniques although loose or easily reversible binding could not be ruled out. In vitro cell culture systems were also used to identify factors responsible for Tc-99m-HIDA uptake. Chicken embryo liver cells of various ages as well as other cell types have been cultured and the pattern of intracellular Tc-99m-HIDA concentration has been investigated under diverse conditions. Inhibition of protein synthesis, DNA synthesis and the 'Na pump' causes no significant change in Tc-99m-HIDA uptake. Decrease in temperature causes a marked reduction in uptake while a decrease in extracellular Ca (II) concentration causes a substantial increase in uptake. Protein binding of the agent appears to play no significant role. HeLa cells do not take up the activity but chick embryo fibroblasts and kidney cells also accumulate significant activity raising the question of less than total dedifferentiation or common transport systems. The availability of an in vitro system for studying the uptake and disposal of radiopharmaceuticals at the cellular level significantly aids in the elucidation of the mechanisms involved.

ENVENOMATION OF MICE WITH I-125 COBRA VENOM: LABELING AND TISSUE DISTRIBUTION. F.P. Castronovo, S.Y. Kopiwoda, and H.W. Strauss. Massachusetts General Hospital, Boston, MA.

The tissue distribution of radiolabeled cobra venom (Naja naja Kaouthia), which possesses both neuro and cardio toxins, was investigated in anethesized mice. The crude venom was labeled with I-125 via the ICL method and

fractionated on a Sephadex G50-80 column with distilled water. Three major peaks resulted whose partition coefficients (K) were 0.57, 1.17 and 1.7, while dextran and I-125- NaI had values of 0.96 and 3.78 respectively. Studies of the toxicity of each venom fraction in mice resulted in an LD-100 at 1 hr. of 20 mg/kg. for the first fraction (the most toxic). Radiolabeled venom from this toxic peak were administered iv to groups of 6 mice and the content of radioactivity in various organs was determined at 5, 15 and 30 minutes. Similar values were determined for NaI-I-125. The tissue results are expressed as % Dose/organ, (mean values):

	I-125	Cobra	Venom A		I-125	NaI
organ	5m	15m	30m	5m	5m	30m
blood	24.49	17.33	14.01	16.87	14.79	8.03
liver	6.56	5.72	4.52	3.98	2.57	2.44
spleen	0.435	0.313	0.386	0.289	1.03	0.205
lung	0.938	0.385	0.591	0.773	0.609	0.484
thyroid	0.383	0.743	1.01	1.60	1.80	3.19
kidney	6.46	4.86	4.50	1.74	1.86	1.25
muscle	24.13	13.27	15.13	15.01	13.21	9.83
carcass	41.47	37.19	27.19	-----	-----	----

These results indicate that the most toxic peak of radioiodinated cobra venom distributes primarily in the blood, liver and muscle after iv administration.

ANTI-β-hCG ANTIBODY AS A POSSIBLE TUMOR-LOCALIZING AGENT. R. Verma, B. Chang, M. Webber, and D. Buffkin. UCLA, School of Medicine, Los Angeles, California.

Many neoplasms produce ectopic human chorionic gonadotropin (hCG), which often is fixed on tumor cell surfaces with little or no circulating hCG. Antibodies raised to whole hCG or α subunit show cross-reactivity to LH, TSH, and FSH, since α subunit is very similar in these hormones. Antibodies to β subunit however show little, if any, cross-reactivity. For specific antibody production, a healthy male goat was chosen. One mg. of highly purified β-hCG was dissolved in 2 ml of sterile saline and emulsified with 2 ml of Freund's complete adjuvant. The antigen was injected i.d. at 40 sites on the goat's back. Three boosters followed. Serial blood samples were collected. The antibody titer in sera was between 1:1000 and 1:10,000.

The IgG fraction was purified by passing through DEAE-cellulose column. IgG was then conjugated with fluorescein isothiocyanate. Fluorescein conjugated IgG was used as a detector for the presence of hCG antigen. IgG from control serum (serum before immunization) and normal lymphocyte cells were used as negative controls.

Two human tumor culture lines (HEP-2, BeWo) were studied for the presence of hCG. Hep-2 failed to show any fluorescence under the microscope, while BeWo cells successfully demonstrated the presence of fluorescence. This confirmed the same results as radioimmunoassay. The culture media and homogenized BeWo cells demonstrated 630-960 MIU/ml(mg) of hCG, while Hep-2 contained less than 2 MIU/ml(mg) of hCG in media or cell.

Purified goat anti-βhCG is therefore a potential agent for the detection of the presence of hCG and hence an indicator of the site of malignancy. It can be fluorescein-labeled, peroxidase-labeled, or radiolabeled.

EFFECT OF CARRIER ON GA-67 AND MN-54 IN A TUMOR MODEL. PART I. S.E. Halpern and P.L. Hagan. VA Hospital and University of California, San Diego, CA.

Gallium (Ga) and manganese (Mn) concentrate in tumor tissue, form useful tumor (T)/background (Bkg) ratios for imaging and have isotopes which could be used with positron detectors. In this study variations were made in the time sequence of carrier-tracer administration in an effort to improve the T/Bkg ratios by altering the pharmacodynamics of the cations.

The experiments were performed in hepatoma bearing rats. Carrier (C) Ga was injected I.V. 2 hrs. prior, simultaneously with and 2 hrs. following C free Ga-67. Six animals received C free Ga-67 only. The same experiment was repeated using Mn-54 and C Mn. The percent injected dose of tracer/gram of blood (B), liver (L), kidney (K), heart (H), muscle (M), femur (F) (Ga only), viable (VT) and nonviable tumor (NVT) was then calculated.

Carrier Ga decreased the concentration of Ga-67 in all tissues except F and K regardless of sequence, however, if C were administered 2 hrs. after the tracer, less Ga-67 was lost from the VT and NVT than from the normal tissues (except F and K). Carrier Mn markedly decreased Mn-54 concentrations in L, K, H, and M (but not B) if given simultaneously with Mn-54. Little effect was noted at other time periods. Concentrations of Mn-54 by VT did not decrease regardless of when C Mn was injected. These manipulations improved some 4 hour post injection VT and NVT/Bkg ratios as much as 2-3 fold for both Ga-67 and Mn-54.

It is concluded that carrier material injected at the appropriate time may be a useful mechanism for improving T/Bkg ratios at early time periods.

EFFECT OF CARRIER ON GA-67 AND MN-54 IN A TUMOR MODEL. PART II. S.E. Halpern and P.L. Hagan. VA Hospital and University of California, San Diego, CA.

Gallium (Ga) and manganese (Mn) form useful tumor (T)/background (Bkg) ratios in an animal model. These can be enhanced by carrier (C). The following experiment was designed to further study movement of the ions following a C load.

Hepatoma bearing rats were injected I.V. with carrier free (CF) and carrier added (CA) Mn-54. Forty and 10 minutes prior to killing, SO4-35 and I-125 HSA (interstitial fluid space (ISFS) and blood markers) were injected I.V.. Groups were killed at 4 and 24 hrs. after Mn-54 injection. The same protocol was used for Ga-67 except the C was administered 2 hrs. prior to death instead of concomitantly. Tumor and multiple organs were taken, urine (U) and feces collected and the percent of dose/gram of all tracers determined. Manganese-54 and Ga-67/ISFS ratios (Tracer Distribution Index or TDI), was computed for viable tumor (VT) and muscle (M).

The C Mn increased 4 and 24 hr. Mn-54 excretion (ex) X 4, decreased all tissue uptake except blood (B) and VT and decreased the TDI for M by a factor of 4 without changing the TDI for VT. Carrier increased Ga-67 U but not gut ex, decreased all 4 hr. values except femur and kidney and decreased the TDI for both M and VT X 3. Only B decreased at 24 hrs. with no difference between control and experimental TDI's.

We conclude that the rat hepatoma is less able than healthy tissues to decrease its clearance (CL) of Mn-54 in the presence of C. Ga-67 CL is limited by C, yet once fixed in cells, Ga-67 cannot be displaced by C. Carrier also enhances both Mn-54 and Ga-67 T/Bkg ratios.

BLOOD CLEARANCE AND IN VITRO STABILITY OF PROTEINS CONTAINING A CONJUGATED INDIUM-111 CHELATE. C.H. Paik, D.C. Herman, W.C. Eckelman, and R.C. Reba. George Washington University Medical Center, Washington, D.C.

A new bifunctional chelating agent, N'-(p-diazoniumbenzyl)-N,N,N'',N''-diethylenetrinitrilotetraacetic acid (DTTA) was synthesized. The compound was coupled to methyl p-hydroxybenzimidate and the resulting azoimidate was attached to human serum albumin(HSA) via the amidination reaction. The chelating agent conjugated to HSA(AAHSA) was shown to be chemically and radiochemically pure with respect to the HSA monomer, the conjugation site by amidination, and the binding of In-111. Blood clearance of [In-111]-AAHSA in rabbits was biphasic. The first phase had a clearance indistinguishable from that of [I-125]-HSA. During the second phase, the [In-111]-AAHSA was cleared more rapidly so that between 24 hours and 48 hours the percent of the injected dose of [In-111]-AAHSA in the blood was significantly lower than that of [I-125]-HSA. Highly conjugated [In-111]-AAHSA(0.9 DTTA/HSA) showed accelerated clearance at 24 and 48 hours compared to lightly conjugated protein(<0.9 DTTA/HSA). In-vitro indium exchange between [In-111]-AAHSA and transferrin showed that 17% of the radioactivity in the serum was bound to transferrin at 48 hours. This is similar to that of [In-111]-DTPA.

The level of conjugation appears to be the critical parameter controlling the blood clearance. Since rapid blood clearance is important for high target-to-blood ratios, the proper approach to labeling such proteins as antibodies is to balance altered substrate specificity caused by modification against accelerated plasma clearance.

THE QUEST FOR AN IN VIVO VASOPRESSIN (ADH) RECEPTOR ASSAY--IODINE-123 LABELED ADH A POSSIBLE RECEPTOR SCAN AGENT. A. Kagan, W. Fried, J. Ernst, S. Thomson, and E. S. Himelstein. Coney Island Hospital, Brooklyn, N.Y.

The principles of in vitro receptor assays (developed by Roth and Associates) make for intriguing possibilities if used in vivo. Purified injection labeled ADH should preferentially bind to ADH receptor sites (in kidneys) allowing for a "receptor scan" and thereby proving and localizing the presence of these sites. Utilizing iodination and purification procedures developed in this laboratory (Kagan & Glick), iodinated ADH was injected into 14 rabbits, kidney localization was prompt (within 5 minutes) and scans could be obtained. Computer analysis of scans also demonstrated greater medullary concentration. The more specific the localization, the more one would expect the labeled AVP to reside in the medulla as compared to the cortex. Tissue medulla counts/gm to cortex counts/gm ratios (mean: 1.45; n-14; S.D.± .127) were greater than control rabbits given free iodine (mean: 1.06; n-14; S.D.± .154). The difficulty in obtaining even sharper differences is probably explained by the expected receptor sites in the cortex normally seen in rodents as opposed to primates.

Iodine-123 ADH is potentially an ideal scanning agent for this system. Adapting our iodination methods to Iodine-123 has yielded successful labeling AVP 62%, Damage 0%, Free Iodine 38% (which after purification approaches 99%). Even better initial iodination should eventually be achieved by proper refinement of buffer and oxidizing agent concentrations.

These studies show that the eventual development of an in vivo ADH receptor site scan is possible.

4:00 p.m.-5:30 p.m. Room 204

INSTRUMENTATION, COMPUTERS, AND DATA ANALYSIS

MATHEMATICS

Chairman: Bernard E. Oppenheim
Co-Chairman: Sebastian Genna

RENAL FUNCTIONAL MAPPING TO DETECT SEGMENTAL ARTERIAL LESIONS. T.B. Stibolt and P.R. Bradley-Moore. National Institutes of Health, Bethesda, MD.

This study was conducted to test the sensitivity of functional maps to occlusion of segmental renal arteries.

Five dogs were studied before and 10 days to 3 months after partial ligation of a segmental renal artery. Data was collected using a gamma camera and high resolution collimator on digital tape for twenty minutes following injection of 5-10 millicuries of I-123 Ortho-iodo-hippurate. Routine images were also obtained directly from the camera during the study at two minute intervals. The digital data was processed using a minicomputer system to produce whole kidney time-activity curves and functional maps. Parameters mapped were: time to maximum counts, clearance half time, and an approximation of the exponential washout constant. Renal arteriography was also performed on each dog.

Pre-operatively, each dog had a minimum of two studies. No abnormalities in either the whole kidney time functions or the functional maps was observed.

Post-operatively each dog was studied twice. The first study was 10 to 21 days post surgery, the second at 2 to 3 months. Renal arteriograms were performed at 6 weeks. The arteriograms showed no cortical defects or convincing arterial lesions in any dog. The whole kidney time functions showed little change post-operatively. Routine images were not remarkable. In three dogs, well defined regions of delayed clearance of I-123 Ortho-iodo-hippurate were clearly seen on the functional maps in the distribution of the partially occluded artery.

Functional mapping appears to be more sensitive than other techniques currently used in the detection of mild segmental renal arterial disease.

A NEW METHOD FOR FUNCTIONAL RENAL IMAGING. B.E. Oppenheim and C.R. Appledorn. Indiana University School of Medicine, Indianapolis, IN.

The functional renal image is a single image which demonstrates the time-related changes in renal uptake and excretion of a radiolabeled tracer which are conventionally displayed in a sequence of images. The image has superior ability to demonstrate subtle asymmetries and regional abnormalities in function. It is formed by constructing the time-activity curve for each pixel in the image, measuring some parameter of curve shape for each curve, and displaying the parameter values as a digital image. The parameter most often utilized for this purpose is t_{max}, the time to peak for the time-activity curve.

Unfortunately, functional renal images are usually noisy, since the time-activity curve for each pixel in the image is very count-limited and hence quite noisy. We have developed a method which produces greatly improved functional images. By using factor analysis, a smooth curve is fit very rapidly to each noisy time-activity curve, and the parameter of curve shape is identified from this smooth curve. Given the noisy curve $\underline{r}$ (normalized to unit area), we find the smooth fitted curve $\underline{r}^*$ by first computing the factor weightings $f_i=(\underline{r}-\underline{r}_{av})^T\underline{e}_i$ (i=1,2) and then computing $\underline{r}^*=\underline{r}_{av}+f_1\underline{e}_1+f_2\underline{e}_2$ (the average curve $\underline{r}_{av}$ and the eigenvectors $\underline{e}_1$ and $\underline{e}_2$ have previously been determined from a large representative set of renogram curves).

The method has been applied to renal studies performed with Tc-99m DTPA, I-123 Hippuran and I-131 Hippuran. The functional images provide information about anatomy, uptake rates and transport times that is not observable in the conventional sequence of images. The method is fast, and the images are consistently superior to those obtained through more direct approaches to functional imaging.

EXTRINSIC CARDIAC MOTION AND ITS EFFECT ON NUCLEAR MEDICINE IMAGING. M. W. Groch, P. L. Von Behren, and G. K. Lewis. Research Department, Searle Diagnostics Inc., Des Plaines, IL

Heart motion is two facetted: Intrinsic motion due to the contraction of the myocardium and extrinsic motion (EHM) from respiration (RESP) and patient motion. EHM has a degrading effect on ECG gated imaging, but is 3-dimensional motion of a deformable body and thus the simple assumption of planar rigid body motion used for analog motion correction circuitry is not adequate. Centroids of photon activity were monitored as a function of time from regions of interest (ROI) in the transverse (TRANS) and longitudinal (LONG) planes of blood pool scintigrams and CO-57 point sources sutured on the epicardium of canines. Centroids from LONG ROI's were displayed simultaneously with the signal from a pressure transducer monitoring RESP and a correlation was found. The centroid motion was Fourier analyzed by a minicomputer to determine significant frequency components. The Fourier transforms from centroids generated along LONG projections showed a spike in the Fourier spectrum corresponding to RESP in both the RAO and anterior projections; the peak was more significant in the RAO, although not as significant as typically obtained from LONG liver sections. No peak was observed at RESP frequency for centroids obtained from TRANS ROI's. Thus, motion correction circuitry may correct motion in the LONG dimension but not in the TRANS dimension. ECG gated and motion corrected cardiac images using currently available circuitry were dissimilar when compared to images which were both ECG and RESP

gated. Conventional 2-dimensional motion correction circuitry is inadequate when applied to ECG gated cardiac imaging and a hybrid 1-dimensional circuit may be required.

FAVORABLE EXCHANGE OF PHOTON COUNT FOR BLUR REDUCTION IN NUCLEAR IMAGING OF MOVING ORGANS. R.E. Wernikoff, K.A. McKusick, and H.W. Strauss. Brattle Instr. Corp., Cambridge, MA and Massachusetts General Hospital, Boston, MA.

Reducing motional blurring of Tl-201 cardiac images by gating without increasing study time--hence by choosing to accept a reduction in photon count--results in improved edge definition and in increased apparent wall thinning and certainty of defect detection. This finding is a special case of a general result that applies to any photon-limited system, and follows from the theory of threshold detection. The theory predicts that, for certain ranges of the relevant variables, image improvement from reduced motion may more than offset image deterioration from reduced photon counts. Specifically, given a circular threshold lesion of radius R moving one-dimensionally with amplitude ± M about its mean position, if its motion can be reduced to ± αM (α<1) by reducing counts, the image will be improved (in the sense that the lesion will still be detectable, with no increase in error probability and improved definition of any edges in the image) if γ, the fraction of counts that is accepted, satisfies,

$$\gamma \geq [k(\alpha M)/k(M)]^2 \left[1 + \frac{4}{\pi}\left(\frac{M}{R}\right)\alpha\right]\left[1 + \frac{4}{\pi}\left(\frac{M}{R}\right)\right]^{-1} \quad (1)$$

where k(M) and k(αM) are threshold constants. A similar relation holds for lesions of arbitrary shape. The organ's motion regime and the gating strategy define possible pairs of α and γ; pairs that satisfy (1) result in image improvement in the sense defined above. Although the method is tolerant for moderate (<20%) departures from (1), whenever the method is applied without adjustments for individual patients it is best to record the ungated as well as the gated image, with exposures equalized.

THE APPLICATION OF THREE DIMENSIONAL FOURIER FILTERING TECHNIQUES TO NUCLEAR CARDIAC STUDIES. J. Verba, I. Bornstein, V.A. Medical Center, San Diego, CA., J. Almasi, T. Goliash, R. Eisner, and D. Nowak, General Electric Medical Systems Division, Milwaukee, WI.

The interpretation of nuclear cardiac images is hampered by the inherently poor statistical quality of the acquired data. Our three dimensional Fourier filtering technique is shown to greatly improve image quality in both the spatial and temporal domain. This improvement is due to the matching of the three dimensional Fourier filter function to the temporal and spatial content of the cardiac data, and the properties of the imaging system. Our scheme has definite advantages over less sophisticated digital filtering approaches. For example, we are able to extract the phase and amplitude structure of the harmonics of the cardiac cycle. This allows better definition of region of interest and associated background assignment. Care must be taken in devising the appropriate form of the filter kernel. The use of rectangular cut-off windows is shown to produce ring artifacts which emanate from sharp edges in the image. We have determined the effects of different roll-off filters on simulated and actual cardiac image data. An adaptive Hanning window is shown to produce substantial reduction in ringing with no apparent loss in resolution. Proper filtering of nuclear data is necessary both for correct image visualization and as a prerequisite for further image processing such as boundary detection.

LIMITATIONS OF THE SIMPLE GEOMETRIC MEAN FOR ATTENUATION COMPENSATION IN ECT. T.F. Budinger and G.T. Gullberg. Donner Laboratory, Univ. of California, Berkeley, CA.

Computed tomographic images of single photon emitting sources contain important dortortions due to attenuation. The simplest of many methods posed to remove these distortions is to apply the geometric mean to the projection data before application of computed tomography algorithms. The geometric mean is the square root of the product of projection values from opposing views. For a point source of unit concentration and constant attenuation μ, the geometric mean gives $(\exp(-\mu x_1) \times \exp(-\mu y_1))^{\frac{1}{2}} = \exp(-\mu/2 \times \text{thickness})$ where x_1 is the distance from the source to the edge for one projection ray and y_1 is the distance in the opposing 180° view from the source to the edge. Unlike the situation in positron tomography where the detection of an annihilation event is a multiplicative probability, the detection of single photon events from one view is independent of the detection from another view; thus, for more than one source along a projection ray, the projected events are $\Sigma A_i e^{-\mu x_i}$ where A_i and x_i's are the source strengths and distances. The projection data for the conjugate view is $\Sigma A_i e^{-\mu y_i}$. When performing the geometric mean we find exponential terms present which contain the cross values between sources and opposite distances. This results in large distortions in the reconstructed distribution for distributed sources in a constant or variable attenuating medium.

For a single point source the geometric mean is adequate and for multiple point sources placed in the central ½ of an attenuating disc, the relative change in concentration will be less than 25%. However, the true concentration of the center source is 60% less than a source of equal concentration at the object edge for a 20 cm disc (μ=0.15 cm^{-1}).

CONVOLVERS WHICH COMPENSATE FOR CONSTANT ATTENUATION IN SINGLE GAMMA EMISSION COMPUTED TOMOGRAPHY. G.T. Gullberg. Donner Laboratory, Univ. of California, Berkeley, CA.

Convolvers were evaluated for a convolution algorithm proposed by Tretiak and Delaney for attenuation compensation in single photon transverse section tomography. The reconstruction of projection data which has been attenuated by a constant attenuation coefficient μ is performed by first modifying the projection data at the angle θ and lateral sampling ξ so that they conform to projections represented by the integral equation

$$p(\xi,\theta) = \int \rho(\hat{x})\, e^{\mu \underset{\sim}{\theta}^{\perp}\cdot\hat{x}}\, \delta(\xi - \underset{\sim}{\theta}\cdot\hat{x})\, d\hat{x}$$

where ρ is the transverse section tomogram and the symbol · denotes the dot product between the position vector $\hat{x}=(x,y)$ and the vectors $\underset{\sim}{\theta} = (-\sin\theta, \cos\theta)$ and $\underset{\sim}{\theta}^{\perp} = (\cos\theta, \sin\theta)$. After this modification, the convolution is performed with a convolver which has been previously determined for a particular attenuation coefficient μ by a least-squares fit of the attenuated back-projection of the convolver to a desired point response function. The filtered projections are then back-projected using the attenuated back-projection operator. This algorithm gives a reconstructed image $\hat{\rho}$ which can be represented by the formula

$$\hat{\rho}(\hat{x}) = \int_0^{2\pi}\int_{-\infty}^{\infty} c(\hat{x}\cdot\underset{\sim}{\theta} - \xi)\; p(\xi,\theta)\, d\xi\; e^{-\mu \underset{\sim}{\theta}^{\perp}\cdot\hat{x}}\, d\theta$$

where c is the convolution function.

The results indicate that in the case of constant attenuation, attenuation can be compensated for in emission computed tomography using an attenuation dependent convolver which reconstructs the transverse section reliably and requires little computer memory and very little computer time.

FRIDAY, JUNE 29, 1979

8:30 a.m.-10:00 a.m. Room 210

CLINICAL SCIENCE

HEMATOLOGY AND INFECTIOUS DISEASE

Chairman: Robert E. Henry
Co-Chairman: R. Edward Coleman

THE EFFECT OF INTERNAL IRRADIATION WITH Pd-109-HEMATOPORPHYRIN ON RAT CARDIAC ALLOGRAFT SURVIVAL. R.A. Fawwaz, M.A. Hardy, S. Oluwole, R. Nowygrod, D.I. Sung, K. Reemtsma, and P.M. Johnson. College of Physicians and Surgeons, Columbia University, New York, NY.

Lymphatic tissue plays an important role in allograft rejection. Since lymphocytes are vulnerable to irradiation, the effect of beta irradiation delivered by systemic injection of Pd-109-hematoporphyrin (PdH) with and without rabbit antirat lymphocyte serum (ALS) in preventing cardiac allograft rejection was studied.

Lewis rat recipients were subjected to the following treatments prior to allografting: (A) none; (B) PdH, 16 mCi/kg iv on day -4; (C) ALS, 10 mg sc on days -2 and 0; (D) PdH, 16 mCi/kg iv on day -4 and ALS, 10 mg sc on days -2 and 0. Treated Lewis, L, (AgB 1/1) rats received cardiac allografts from either Fisher, F, (AgB 1/1) or ACI (AgB 4/4) rats. In the Fisher to Lewis combination the median survival time (MST) in days was as follows: (A) 10.9 $\pm$ 2.51; (B) 12.3 $\pm$ 1.32; (C) 30 $\pm$ 4.3; and (D) indefinite (>300 days). In the ACI to Lewis combination the MST was as follows: (A) 6.83 $\pm$ 0.4; (C) 14.14 $\pm$ 3.4; (D) 28.14 $\pm$ 7.51. When Lewis rats were subjected to higher doses of PdH (24 mCi/kg) followed in quick succession by administration of ALS, 1.5 x 10^8 bone marrow cells and ACI cardiac allograft, they remained in good health and continued to demonstrate allograft survival at more than 100 days post transplantation.

In conclusion, selective lymphatic ablation combined with ALS treatment greatly reduces the immunologic rejection potential of the host. The resultant state of acquired tolerance of cardiac allografts may have clinical application.

LABELING MECHANISM AND LOCALIZATION OF INDIUM-111 IN HUMAN PLATELETS. C.J. Mathias and M.J. Welch. Department of Radiology, Washington University School of Medicine, St. Louis, MO.

Indium-111 labeled platelets have been shown to effectively accumulate at sites of atherosclerotic lesions and venous thrombi. To evaluate the labeling mechanism and location of indium-111-oxine in platelets, several approaches were utilized.

Labeled platelets were suspended in various media and the release of indium-111 measured. Only when excess 8-hydroxyquinoline is present in the media is the metal released. Platelets were then labeled substituting tritiated oxine to chelate the indium. The characterization of the oxine as only a metal carrier was demonstrated; after the labeling and washes, 0.01% of the tritiated oxine remains associated with the platelets. Other studies executed with carrier indium metal present demonstrated that the degree of elution of oxine from the cells was not altered.

Gel filtration, gel electrophoresis, thin layer chromatography and sucrose gradient separations were carried out to study the subcellular binding of the label. Results from gel electrophoresis and gel filtration indicate that 65% of the radioactivity is weakly bound to a protein whose molecular weight is approximately 400,000, possibly myosin. By labeling human platelet-myosin with indium-114m and using the complex as a tracer in the platelet labeling procedure and subsequently separating myosin, 102% yield of the protein and 70% recovery of the radioactivity were achieved. The other 35% of the indium is membrane bound, however the bond is too weak to be analyzed with the techniques used.

CLINICAL EVALUATION OF INDIUM-111 LEUKOCYTE SCANS IN DIAGNOSIS OF INFLAMMATORY DISEASE. P.W. Doherty, D. Fawcett, D.A. Goodwin, J.R. Heckman, J.E. Baumert, R.L. Lantieri and I.R. McDougall. Division of Nuclear Medicine, Stanford University Medical Center and Palo Alto Veteran Administration Hospital, Stanford, CA.

The results of 146 In-111 white cell scans have been compared with clinical, laboratory, radiological, surgical or follow up information in 143 patients. The cells were isolated using 5% hetastarch and differential centrifugation and labeled with 200 µCi to 2.0 mCi In-111 as In-111 oxine. Whole body images of cell distribution were obtained at 18-24 hours in all patients with additional spot views or delayed scans in selected cases.

25 females and 118 males were studied, average age 51 years (range 3-81). In 3 studies donor white cells were used, in 143, autologous cells.

66 scans (45%) were abnormal and a definite cause was found in 65. Pathological causes of the abnormality included 14 abdominal abscesses, osteomyelitis or septic arthritis in 18, renal disease such as pyelonephritis or transplant rejection in 8, colitis or pancreatitis in 8.

7 out of 7 acute myocardial infarcts were not visualized and, in general, white cell scan as a blind test in patients with F.U.O. did not demonstrate an abscess. In 2 out of the 81 patients with negative scans, liver abscesses were present, one was sterile, the other grew out candida. A third patient had a pelvic abscess found at surgery 3 days after a negative scan.

The preparation and labeling of white cells are not difficult to perform. The test has a high degree of both specificity and sensitivity.

INDIUM-111 OXINE LABELED LEUKOCYTES IN THE DIAGNOSIS OF OCCULT INFLAMMATION OR ABSCESS. L. Forstrom, D. Hoogland, L. Gomez, G. Saecker, B. Weiblen, J. McCullough, and M. Loken. University of Minnesota Hospitals, Minneapolis, MN.

Indium-111 oxine was used to label granulocyte-rich leukocyte suspensions by previously reported methods. 83 studies with this agent (In-111-WBC) have been performed in 78 subjects, including six normal volunteers and 72 patients with clinically suspected occult inflammatory disease. 43 female and 29 male patients, ranging in age from 1½ to 83 years, were studied. In most cases (66), autologous cells were used for labeling. However, in granulocytopenic patients (12), leukocytes for labeling were obtained from an ABO-compatible donor. Images were obtained by means of a rectilinear scanner or scintillation camera at 24 hours after administration of 0.3-0.5 mCi In-111-WBC (adult dose). In-111-WBC images showed positive uptake in 30 of 33 confirmed sites of inflammation or abscess, for a diagnostic sensitivity of 90%. Calculated specificity of the test was 85%, yielding an overall diagnostic accuracy of 87%. Diagnostic efficacy of In-111-WBC scanning did not differ significantly between groups of patients receiving homologous versus autologous labeled leukocytes. Neither did results differ significantly in 24 patients studied in outside hospitals with leukocyte preparation and labeling in our laboratory. These data substantiate the usefulness of In-111-WBC imaging in the detection of occult inflammatory disease, and demonstrate the feasibility of this procedure with cells (autologous or homologous) radiolabeled in a centralized nuclear pharmacy.

INDIUM-111 LABELED LEUKOCYTES IN THE EVALUATION OF SUSPECTED INFLAMMATORY PROCESSES. D.M. Welch, W.J. Baker, R.W. Beightol, and R.E. Coleman. University of Utah Medical Center, Salt Lake City, UT.

Prompted by experimental studies demonstrating the potential advantages of indium-111 labeled autologous leukocytes,

this report summarizes our clinical experience in imaging inflammatory processes with this agent. Ninety-three studies were performed in 75 patients. Leukocytes from approximately 40ml of heparinized blood were separated and labeled with indium-111 oxine in a dilute plasma solution. Labeling efficiency has ranged from 16-90% (mean 52%). Images were obtained 3 and 24 hours after administration of the labeled leukocytes. Indications for the leukocyte imaging studies included 66 for suspected abdominal abscess, 20 for bone or joint infection and 7 for other inflammatory diseases.

Adequate follow-up has been obtained for 88 studies. Of 35 proven inflammatory processes, 30 studies correctly identified the location. Fifty-two of 53 studies correctly indicated absence of inflammation. Overall accuracy was 93%.

Adequate follow-up was obtained for 65 studies performed for suspected abdominal abscess. Ten proven abscesses were associated with abnormal accumulation of leukocytes. Thirty-nine studies were normal and no inflammatory processes were identified. Fifteen studies disclosed abnormal leukocyte accumulation indicating processes other than abscesses.

Adequate follow-up was obtained in 16 studies for suspected bone or joint infection. In 8 studies of patients with proven inflammatory processes, only 4 had abnormal leukocyte accumulations at the inflammatory site.

These results indicate indium-111 leukocyte imaging is highly sensitive in detecting abdominal abscesses. Our limited experience in patients with suspected bone or joint infections suggests less sensitivity.

GALLIUM-67 CITRATE (GA) KINETICS IN INFECTED AND NON-INFECTED SUBCUTANEOUS POLYETHYLENE CHAMBERS (SPCs) IN RABBITS. A.R.Siddiqui and R.R.Tight. Indiana University School of Medicine, Indianapolis, IN.

The kinetics of Ga were studied in rabbits with surgically implanted SPCs (practice golf balls, 2/rabbit). Holes in the SPC walls permitted serial interstitial fluid (ISF) sampling and inoculation of bacteria. After IV injection of Ga (200 uCi/kg) into non-infected rabbits, radioactivity in the SPCs was present within 15 mins and peaked at about 24 hrs, after which there was a gradual fall. This was true for one-week old as well as 3-month old implants. Gamma camera images showed symmetrical activity in both SPCs. Minor traumas of needle aspiration of ISF were of no consequence. Infected rabbits received injections of 10^8 Streptococcus fecalis directly into one SPC (ISPC) with the other one in the same rabbit acting as control (CSPC). Ga was given IV 6 hrs after inoculation. The Ga kinetics in CSPC were the same as in non-infected rabbits; however, by 2 hrs radioactivity in ISPC was 2.5 times that of CSPC and at 24 hrs the ratio increased to 10. After 24 hrs the activity in the CSPC declined gradually whereas the activity in ISPC increased slightly, gradually increasing the ratio between ISPC and CSPC (35 on day 6). The infected rabbits were treated with ampicillin starting a week after bacterial inoculation. After 3 days of therapy the ISF from ISPC was sterile; however, the Ga images after reinfection were still positive and ISF from ISPC had 10 times the radioactivity of CSPC. Conclusion: 1) In bacterial infections scans can be positive within 2 hrs of Ga injection. 2) Abscess to background ratio continues to increase with time. 3) Ga can localize in the infection site even after adequate therapy.

ROLE OF ENHANCED CAPILLARY PERMEABILITY AND IRON BINDING PROTEINS ON GALLIUM-67 ACCUMULATION. K.Y. Tzen, Z.H. Oster, H.N. Wagner, Jr., and M.F. Tsan. Johns Hopkins Medical Institutions, Baltimore, MD.

The role of increased capillary permeability and iron binding proteins on Ga-67 accumulation in rabbits was studied. Ga-67 accumulation was quantified using Ohio-Nuclear 150 Data System.

Intramuscular (IM) injection of histamine (H), but not normal saline or albumin, caused accumulation of intravenously (IV) injected Ga-67 citrate as well as Tc-99m DTPA. Likewise, IM injection of transferrin (T) or lactoferrin (L) caused accumulation of IV injected Ga-67. No accumulation of Tc-99m DTPA was observed at the site of T injection, while there was a slight accumulation at the site of L injection. Prior saturation of T or L with ferric ions abolished the effect of accumulating Ga-67. In order to assess the relative contribution of free and T-bound Ga-67, Ga-67 was first bound to T by incubating with T followed by dialysis. This T-bound Ga-67 did not accumulate at the site of H or T injection; while there was a slight accumulation at the site of L injection. Analysis of Ga-67 in the plasma after IV injection of Ga-67 citrate using dialysis, revealed that there was a significant amount of Ga-67 remaining in the free form, e.g., 69,23,10,5, and 2% at 1.5, 3, 6, 12 and 24 hours after injection respectively.

Our results suggest that increased capillary permeability and iron binding proteins can cause accumulation of Ga-67, and that free Ga-67 plays a more important role than T-bound Ga-67 in the accumulation of Ga-67. Since these factors are present at the site of inflammation, they may contribute to the accumulation of Ga-67 in inflammatory lesions.

8:30 a.m.-10:00 a.m. Room 300/301

CLINICAL APPLICATIONS

CARDIOVASCULAR

Chairman: Ben C. Berg, Jr.
Co-Chairman: John L. Floyd

SENSITIVITY AND IMPROVED SPECIFICITY OF A LOCALIZED PATTERN OF ^{99m}Tc PYROPHOSPHATE MYOCARDIAL SCINTIGRAPHY FOR THE DIAGNOSIS OF ACUTE MYOCARDIAL INFARCTION. K.P. Lyons, H. Olson, W. Arcnow, J. Kuperus, R. Collins, and R. Evans. VA Medical Center, Long Beach, CA.

One thousand and seventy-seven patients with suspected acute myocardial infarction (AMI) had a Tc-99m pyrophosphate myocardial scintigram 3.8 ± 1.4 days after admission to the Coronary Care Unit with the following results:

Diagnosis	No. Patients	Positive Study	% Positive	% Localized
AMI Group	361	331	92	66
Transmural	206	197	96	82
Anterior	98	95	97	
Inferior	91	86	95	
Posterior	13	13	100	
Lateral	4	3	75	
Subendocardial	144	126	88	44
Left Bundle Branch Block	11	8	73	5
No AMI Group	716	184	26	
Chest Pain Syndrome	390	53	14	
Unstable Angina	201	69	34	
Resuscitated Patients	30	18	60	
Heart Failure	61	33	54	
Acute Pericarditis	34	11	32	

Of the 206 patients with a transmural infarction, 169 (82%) had a localized pattern. In the subendocardial group 64 (44%) showed a localized pattern. With few exceptions, non-AMI patients demonstrated a diffuse pattern.

Therefore, based on the criterion of intensity of Tc-99m pyrophosphate activity in the heart, the procedure is very sensitive but nonspecific for the diagnosis of AMI. Using the criterion of a localized versus a diffuse pattern, the specificity increases as the sensitivity decreases.

Tc99m RBC MUGA VENTRICULAR PACING FOR DETERMINATION OF OPTIMAL PACING RATE IN PATIENTS WITH PERMANENT PACEMAKERS. H. Atlan, A. Weiss, D. Tzivoni, A. Rein, J. Salomon, D. Warshaw, L.D. Samuels, M. Gotsman, Hadassah University Hospital, Jerusalem, Israel.

Patients with permanent implanted ventricular pacemakers require different pacing rates. This is adjusted today in most cases at a rate of about 70 per min. With the use of multiple gated blood pool cardiac scan (MUGA) at different pacing rates, it is possible to evaluate

the rate which yields maximum ejection fraction and/or maximum cardiac output. Patients with permanent implanted pacemakers are studied routinely at pacing rates of 60-100 per minute on 30° RAO and 45° LAO projections. Left ventricular end diastolic, end systolic activity and Ejection Fraction were calculated from the LAO projection. Stroke counts times heart rate gave the isotopic cardiac output. The change in pacing rate was performed with the aid of an external magnet and at each pacing rate imaging was performed for 2.5-4 minutes. All patients tolerated the examination well and no side effects were observed. It is assumed that MUGA at different ventricular pacing rates can determine the optimal pacing rates for each patient with permanent implanted pacemaker.

MONITORING CARDIAC FUNCTION WITH RADIONUCLIDES IMMEDIATELY AFTER HEART SURGERY. W. Covitz, C. Eubig, A.T. Truman, R. Shelnutt, B.B. Sellers, H.V. Moore and M. Brown. Medical College of Georgia, Augusta, Georgia.

The purpose of this study was to develop a practical approach to monitoring cardiac function after heart surgery to aid in patient management. Cardiac output and shunting were assessed in 11 children 2-3 hours after heart surgery with first pass (FP) images of a bolus of Tc-99m albumen in the anterior projection, an equilibrium image, and serial blood samples. Gated blood pool (GBP) images in left anterior oblique projection were obtained at 0.5, 2 and 3 hours after injection to measure ejection fraction (EF) and left ventricular end-diastolic (LVED) activity. LVED volume was derived from FP and 0.5 hour data and equated to LVED activity. Change in LVED activity in subsequent GBP studies corrected for loss of blood activity reflected the change in LVED volume allowing CO to be calculated at 2 and 3 hours. FP CO's of right and left heart were in close agreement in 8 children without shunts r=.95, $p < .01$. In 2 children with shunts, the left ventricle reflected CO plus the shunt, but the right atrium reflected CO only since it was proximal to the shunt. The Tc-99m blood activity curves from which blood volume was determined described a two compartment distribution possibly related to cardiac state, bleeding, and high glomerular filtration. EF was 0.47-.71(m=.59) at 0.5 hour. EF and HR fell slightly by 2 and 3 hours. Cardiac index was 2.2-5.6 (m=3.7) at 0.5 hour with a 30% drop at 2, and 6% additional drop at 3 hours. A high initial CO dropped into a low normal range. This method provided serial measurements of CO, LVED volume, and EF after a single isotopic injection. CO and albumen clearance were high early and fell to lower levels by 3-6 hours following surgery.

COMPARISON OF THALLIUM SCINTIGRAPHY TO Q-ST AND R-WAVE CHANGES FOR DETECTION OF CORONARY DISEASE. N. Venkatesh, M.F. Wilson, E. Schechter, E.W. Allen, University of Oklahoma and Veterans Administration Medical Center, Oklahoma City, Oklahoma.

To assess the clinical value of 201-Thallium myocardial perfusion scintigraphy (Tl-MPS) to exercise electrocardiography (Ex ECG) when R-wave amplitude changes were added to Q and ST criteria 18 patients who had coronary angiography (CA) for evaluation of chest pain were studied. Pathological Q-waves (0.04 seconds or greater in width), ischemic ST depression (ST segment depression of 1mm or greater), abnormal R-wave response (V_5R immediate post exercise greater than or equal to pre-exercise) and transient or fixed perfusion defects in Tl-MPS were considered positive for the presence of coronary artery disease (CAD). Significant CAD (SCAD) by CA (70% or greater narrowing of any given vessel) was found in 11 patients (61%).

CRITERIA	SENSITIVITY TP/TP + FN	SPECIFICITY TN/TN + FP	ACCURACY TP + TN/TOTAL
Q-ST	9/11 (82%)	6/7 (86%)	14/18 (78%)
R-WAVE	8/11 (73%)	1/7 (14%)	9/18 (50%)
QSTR	11/11 (100%)	1/7 (14%)	11/18 (61%)
Tl-MPS	9/11 (92%)	6/7 (86%)	15/18 (83%)
QST-Tl	11/11 (100%)	5/7 (71%)	16/18 (89%)

In this series Tl-MPS was the best single test for detection of SCAD. By combining Q-ST criteria with Tl-MPS both sensitivity and accuracy showed improvement. Inclusion of R-wave criterion improved sensitivity of Ex ECG, but reduced the specificity and the accuracy primarily by increasing the incidence of false positives. (Supported by the Veterans Administration Research Service).

THE EVALUATION OF LEFT VENTRICULAR REGIONAL WALL MOTION USING REST AND EXERCISE MULTIGATED BLOOD POOL IMAGES AND REST CONTRAST VENTRICULOGRAM: A STUDY OF INTEROBSERVER VARIANCE. R.D. Okada, H.D. Kirshenbaum, F.G. Kushner, R.E. Dinsmore, H.W. Strauss, C.A. Boucher, and G.M. Pohost. Massachusetts General Hospital, Boston, Massachusetts.

Multigated acquisition blood pool imaging at rest (MUGR) and with exercise MUGEx) has been widely employed for the evaluation of left ventricular regional wall motion (RWM). The accuracy of this test is dependent on interobserver variance (IV). 59 patients had MUGR and MUGEx during peak bicycle exercise, and rest left ventriculography (LVGRAM) during cardiac catheterization. 49 patients had significant coronary artery disease and 10 did not. MUGR, MUGEx, and LVGRAM RWM were graded by 3 independent observers on a 5 point scale. The ventricle was divided into anterolateral (AL), apical (AP), inferior (INF), septal (SEP), AP-INF (AI), and posterior (POST) walls. The variations between observers were analyzed by a 2-way analysis of variance and expressed as ±2 standard deviations:

	AL	AP	INF	SEP	AI	POST
MUGEx				1.46	1.30	.94
MUGR	.60	.78	.76	1.02	1.00	.74
LVGRAM	.76	.98	.76	.66	.98	.92

IV for all MUGEx areas were greater than the corresponding areas on MUGR($p<.01$). IV for MUGR AL, AP, and POST walls were lower ($p<.05$), SEP wall higher ($p<.01$) and INF and AI walls not significantly different than the IV's for the corresponding walls by LVGRAM.

The IV in RWM determinations from MUGR are comparable to those determined from LVGRAM except for the SEP wall. The results offer a framework in which exercise induced changes in multigated blood pool image RWM can be interpreted.

A NON-GEOMETRIC METHOD FOR SCINTIGRAPHIC DETERMINATION OF LEFT VENTRICULAR VOLUME: CONTRAST CORRELATION. S.E. Lewis, G.J. Dehmer, M. Falkoff, L.D. Hillis, and J.T. Willerson. University of Texas Health Science Center, Dallas, Tx.

Equilibrium multiple-gated blood pool imaging using in vivo labeled red blood cells was performed in 25 patients within 24 hrs of cardiac catheterization to assess the utility of a geometry-independent scintigraphic method for determining left ventricular volumes. Indications for catheterization were: evaluation of coronary artery disease (15), valvular heart disease (7) and cardiomyopathy (3). Angiographic volumes (V) were determined from single-plane right anterior oblique cine ventriculograms by the area-length method and the Kennedy regression formula. Scintigraphic volume estimates (S) were obtained from the end-diastolic and end-systolic frames of a modified 35° left anterior oblique study via an algorithm which considered: left ventricular activity corrected for background and normalized for radioactivity per ml of peripheral venous blood, total study acquisition time, number of frames acquired per cycle, and the % of the cycle acquired. Excellent correlation between angiographic and scintigraphic methods was demonstrated. Linear regression analysis yielded: $V = 5.04(S) + 6.79$ ($r = .981$, SEE = ± 10.3 ml). Volumes ranged from 13 to 768 ml. Excellent agreement was also noted for left ventricular ejection fraction calculation ($r = .975$). Interobserver variation was 7.5% for scintigraphic measurements and 8.2% for angiographic measurements.

We conclude that non-geometric radionuclide methods may be utilized for accurate left ventricular volume determinations in man.

THE PARADOX IMAGE: NON-INVASIVE INDEX OF REGIONAL LEFT VENTRICULAR DYSKINESIS. B.L. Holman, J. Wynne, J. Idoine, J. Zielonka, J. Neill. Harvard Medical School and Peter Bent Brigham Hospital, Boston, MA.

The paradox image, a functional image of regional dyskinesis derived from the equilibrium (gated) radionuclide ventriculogram, was constructed by subtracting the background-corrected end-diastolic frame from the background-corrected end-systolic frame. In the eleven patients with dyskinesis by contrast ventriculography, the percent of left ventricular picture elements containing paradox ranged from 3.6 to 55.6% (21.44% ± 4.45 SEM). In the eleven patients with normokinesis and in the eight patients with hypokinesis by contrast ventriculography, the left ventricular picture elements demonstrating paradox was less than 1.1% in all cases. We considered a segment dyskinetic if 10% or more of the total left ventricular picture elements containing paradox were in that anatomic segment. Using these criteria, 16 of 16 dyskinetic segments on contrast ventriculography were correctly identified, while 15 of 17 segments without dyskinesis were also correctly identified. The correlation between the percent of total left ventricular picture elements containing paradox and global left ventricular ejection fraction was excellent (%P = 49.64-1.04EF; r = 0.85; $S_{x.y}$ = 8.13). The advantages of the paradox image are that it provides: 1) a sensitive measure of the presence of dyskinesis; 2) a precise indicator of the location of dyskinesis; 3) a method for the separation of focal from diffuse dyskinesis and 4) a quantitative estimate of dyskinesis, permitting comparisons at various times during or following medical and/or surgical interventions.

REVERSIBLE LEFT VENTRICULAR DYSFUNCTION: UNMASKING BY 2-VIEW NUCLEAR ANGIOGRAPHY. C. Hellman, J. Carpenter, T. Garner, W.D. Johnson, and D.F. Schmidt. University of Wisconsin-Mt. Sinai Medical Center, Milwaukee, Wisconsin.

The degree of left ventricular dysfunction (LVD) is often a limiting factor in the consideration of myocardial revascularization surgery (MRS). However, the LVD may be reversible. This study was designed to assess the ability of simultaneous 2-view first pass nuclear angiography (FPNA) after sublingual nitroglycerin (NTG) to recognize reversible LVD. 10 patients (pts) with severe coronary artery disease and LVD were prospectively studied before and after MRS using a newly designed bilateral collimator with a multicrystal camera system allowing 30° RAO and LAO view FPNA with a single radiopharmaceutical dose. All pts had control and NTG FPNA studies 1 day pre-MRS and a control study 7 days post-MRS. Regional wall motion (RWM) was assessed by dividing each RAO and LAO image into 6 segments; ejection fraction (EF), end diastolic volume (EDV), and heart rate (HR) were assessed by generation of computer derived data. The following significant ($p<0.05$) mean values were noted:

	HR	EF(%)	EDV(CC)
Pre-MRS control	75	39.8	157
Pre-MRS NTG	85	46.7	130
Post-MRS control	101	49.8	122

33 of 62 initially hypokinetic RWM segments improved after NTG; 30/33 improved post-MRS. Of 30 initially akinetic segments, 13 improved after NTG; 12/13 improved post MRS. No dyskinetic segments improved after NTG or MRS. 11 RWM segments that improved post-MRS were not predicted by NTG FPNA. Of note is that in 4 of the 10 pts, reversible LVD was seen in only 1 view.

Thus, the rapid, noninvasive, 2-view NTG FPNA technique is highly specific to unmask potentially reversible LVD and is more sensitive than a single view alone.

8:30 a.m.-10:00 a.m. Room 201

RADIOPHARMACEUTICAL CHEMISTRY CYCLOTRON PRODUCED RADIOTRACERS

Chairman: Alfred P. Wolf
Co-Chairman: Alun G. Jones

EARLY DETECTION OF NEOPLASMS WITH RADIOLABELED SUGAR ANALOG. P. Som, H.L. Atkins, D. Bandyopadhyay, J.S. Fowler, R.R. MacGregor, K. Matsui, Z.H. Oster, D.F. Sacker, C-Y Shiue, and A.P. Wolf. Brookhaven National Laboratory, Upton, NY.

Increased metabolic demand of cancer cells for glucose has been well documented. Many glucose analogs have therefore been investigated as potential glucose antemetabolites to inhibit glycolysis of tumor cells and thereby tumor growth. This study was undertaken to investigate [18-F]-FDG, a structural analog of glucose, as a potential probe for tumor detection both in spontaneous and transplanted tumors in different host systems. Tumors studied were: spontaneous adenocarcinoma, L-1210, spontaneous leukemia, ependyomoma, pituitary tumors, fibroadenoma, squamous cell carcinoma, Greene melanoma, amelanotic melanoma and spontaneous seminoma.

High uptakes were found in certain tumors at 30 minutes and remained relatively constant up to 120 minutes. Tumor to blood (T/B) and tumor to normal tissue (T/NT) ratio at 60 minutes ranged from 2.1-17.8 and 1.3-9.2 depending on the type and age of tumors. There was about a two fold increase in [18-F]-FDG-6-P activity in tumor tissues as compared to corresponding normal tissues, indicating an increase in hexokinase activity in neoplastic cells. Comparative imaging studies with Ga-67 in a dog with seminoma showed a high quality image with [18-F]-FDG. It is concluded that [18-F] -FDG could be used to detect neoplasm early because of its high uptake and low body background.

PREPARATION OF OPTICALLY ACTIVE C-11-AMINO ACIDS, G.A. Digenis*, D.L. Casey*, D.A. Wesner*, L.C. Washburn+ and R.L. Hayes+. *University of Kentucky, Lexington, KY. and +Oak Ridge Associated Universities (ORAU), Oak Ridge, TN.

C-11-DL-Phenylalanine (C-11-DL-Phe, 375 mCi) was synthesized from C-11-cyanide (2.4 Ci) by a modified Bucherer-Strecker reaction. The chemical yield was 65% and the total time for synthesis and purification (ion-exchange chromatography) was 40 min. Resolution of C-11-DL-Phe into its D- and L- isomers was accomplished in 35 min (including purification) by oxidative deamination using immobilized L- and D- amino acid oxidase (L-AAO and D-AAO), respectively; the yields for C-11-D- and L- Phe were 19 mCi and 27 mCi. The optically active amino acid obtained in each case was separated from phenylpyruvic acid (the production of which was monitored colorimetrically in developmental work) by cation exchange chromatography and the optical purity was established by ORD. L-AAO was immobilized on diazotized arylamine glass beads and D-AAO was bound to cyanogen bromide-activated Sepharose 4B. Immobilized L-AAO and D-AAO were incubated at 37° with buffered DL-Phe solutions at pH's of 6.8 and 9.0, respectively. Whole body retention data revealed that loss of C-11-DL- and D-Phe in the rat was very low (less than 2% during the first hour after I.V. injection). For C-11-L-Phe, pancreas was the tissue of highest uptake, whereas for C-11-D-Phe kidney was highest.

This method should be applicable to resolution of other C-11-amino acids, producing potential agents for a wide range of radiodiagnostic and dynamic studies. (ORAU operates under contract number EY-76-C-05-0033 with the U.S. Department of Energy; U.K. work was supported by NCI grant CA17786).

ENZYMATIC SYNTHESIS OF C-11 ACETYL CARNITINE. L. Spolter, M.B. Cohen, C.C. Chang, and N.S. MacDonald. V.A. Medical Center, Sepulveda and UCLA, Los Angeles, CA.

Fatty acids are the main substrate for aerobic energy production in the myocardium, but many previous studies utilizing radio-labeled fatty acids have had limited success because of relatively low uptake. Fatty acids are metabolized by the myocardial mitochondria, but fatty acids can only cross the mitochondrial membrane with the help of the carrier substance, carnitine. Radio-labeled acyl carnitine may be a better agent for the study of myocardial fatty acid metabolism than the labeled fatty acid. A

method has, therefore, been devised to synthesize C-11 acetyl carnitine.

C-11 acetyl carnitine was synthesized by the following sequence: C-11 carbon dioxide, produced by the UCLA Bio-Medical Cyclotron in a (p,α) reaction, was reacted with methyl magnesium bromide to yield C-11 acetic acid. The latter was reacted with adenosine triphosphate (in the presence of acetate kinase) to yield C-11 acetyl phosphate. This product reacted with coenzyme A (CoA) (in the presence of phosphotransacetylase) to give C-11 acetyl CoA which in turn was reacted with carnitine (in the presence of carnitine acetyltransferase) to yield C-11 acetyl carnitine.

The C-11 acetyl carnitine was separated from the other labeled constituents of the incubation mixture (acetate, acetyl phosphate, acetyl CoA and other negatively charged substances) on an AG 1-X8 anion exchange column. The identity of the labeled acetyl carnitine was established by paper and column chromatography using C-14 labeled acetate, in addition to C-11 acetate, in the incubation medium. The availability of C-11 acetyl carnitine will permit further study of myocardial metabolism.

C-11-TRYPTOPHAN: SYNTHESIS AND PURIFICATION USING HIGH PRESSURE LIQUID CHROMATOGRAPHY. M. Zalutsky, J. Wu, T. Wickland, P. Harper and A. Moossa. University of Chicago, Chicago, IL.

C-11-tryptophan(Try) is a promising radiopharmaceutical for in vivo assessment of amino acid metabolism in pancreas and brain. However, the current production method requires high levels of C-11 activity to produce useful quantities of C-11-Try because of low chemical yield and long synthesis and purification time. Therefore, in order to make C-11-Try a more suitable agent for use on a routine basis, we have developed a modified production method which utilizes high pressure liquid chromatography (HPLC) for radiopharmaceutical purification. The synthesis of C-11-Try was similar to the modified Strecker procedure developed at Oak Ridge. Differences were that the first reaction step was reduced to 3 min and the reaction temperature was increased to 245°C for both steps. The pH was adjusted with glacial acetic acid before injection into a Waters HPLC for purification with a 30 cm, μBondapak C-18 column with a mixture of 0.01M NaAc/HAc/EtOH as the solvent. With a flow rate of 2 ml/min, the unreacted C-11-cyanide elutes in 2 min and the C-11-Try elutes in 6 min. Using these methods, we have routinely produced and purified C-11-Try in 30 min with radiochemical yields of 45-50%. The specific activity of the product is 0.5 Ci/mmole; however, the C-11-Try can be produced in high yield with 100 times higher specific activity by eliminating carrier cyanide. In conclusion, we have increased the available activity of C-11-Try per mCi of C-11-cyanide by greater than threefold by halving the synthesis and purification time and by increasing the chemical yield by 50%. These modifications have simplified the production of C-11-Try and made its production more suitable for routine use. These results support the use of HPLC for purifying other radiopharmaceuticals.

ORGAN IMAGING WITH N-13-L-GLUTAMATE. A.S. Gelbard, R.S. Benua, J.M. McDonald, R.E. Reiman, J.J. Vomero, and J.S. Laughlin. Memorial Sloan-Kettering Cancer Center, New York, N.Y.

We have been evaluating N-13-L-glutamate as an organ and tumor imaging agent in normal volunteers and cancer patients. The amino acid is enzymatically labeled in a manner suitable for clinical studies by utilizing glutamate dehydrogenase immobilized on activated Sepharose. Quantitative whole body scans were carried out 5 minutes after intravenous injection of up to 10 mCi of N-13-L-glutamate. Radioactivity localized in salivary glands, heart, liver and pancreas. The amount of activity in various organs was determined from scan data by the method of Clarke (Med. Phys. 3:324, 1976). The fraction of administered N-13 activity which localized in myocardium averaged 5.7% ±1.2% in 10 subjects with excellent visualization of the myocardium in all cases. This compared with 4.2% ±0.7% of the activity in the heart following injection of N-13 ammonia in 3 cases.

The pancreas was clearly visualized in normal subjects with N-13-L-glutamate. In those cases where a clear separation of liver from pancreas permitted quantitation, the fraction of administered radioactivity in the pancreas ranged from 8-12% and the pancreas/liver concentration ratio was estimated to be 9:1. Three patients with pancreatic cancer were studied. In one case the cancer produced a filling defect in the head of a well visualized pancreas. The pancreas was not visualized in the other two cases.

The excellent visualization of the human myocardium and normal pancreas with N-13-L-glutamate could not be predicted from results obtained in animals.

SYNTHESIS OF CARRIER-FREE FLUORINE-18 FLUOROETHANOL. T.J. Tewson and M.J. Welch. Department of Radiology, Washington University School of Medicine, St. Louis, MO.

Although several radiopharmaceuticals have been utilized to measure regional perfusion only labeled microspheres have ideal in vivo behavior. A radiopharmaceutical suitable for measuring regional perfusion should have the properties of a constant extraction fraction, preferably 100%, following arterial delivery to the organ of interest, and be totally retained within the tissue throughout the period of measurement. Previous work by us and others using low specific activity material suggest that fluoroethanol is such an agent. Alcohols generally are 100% extracted and fluoroethanol is known to bind irreversibly to an enzyme in the Krebs cycle. Unfortunately, fluoroethanol is extremely toxic and is only useable at extremely high specific activities. We have previously described a method for preparing anhydrous carrier-free fluorine-18 cesium fluoride impregnated on silver wool. A solution of α-p-toluene sulphonyl ethyl glycolate in ether is added to the silver wool and the ether is evaporated. The silver wool is heated to 140°C for 40 minutes and then extracted with ether to give 40-45% yield of fluorine-18 α-fluoroethyl-acetate. Reduction at 0°C with sodium dihydro-bis[methoxy-ethoxy] aluminate for 30 minutes gives quantitative conversion to carrier-free fluorine-18 fluoroethanol. Gas chromatography of this solution gives no detectable mass signal under conditions when a solution of 10^{-7} molar fluoroethanol gives full scale response and both gas and high pressure liquid chromatography showed radiochemical purities of >98%.

PREPARATION OF RADIOBROMINATED PROTEINS USING MYELOPEROXIDASE. K. D. McElvany and M. J. Welch. Mallinckrodt Institute of Radiology, Washington University School of Medicine, St. Louis, MO.

Myeloperoxidase, an enzyme isolated from human leukocytes, has been found to catalyze carrier-free radiobromination and radioiodination of proteins at pH 7. It is desirable to label proteins with radioisotopes of bromine since bromine forms a stronger bond to carbon than does iodine. The only other described methods to achieve direct carrier-free radiobromination of proteins involve the enzymes chloroperoxidase and bromoperoxidase. The chloroperoxidase method requires a pH of 2.8, which is too acidic for most protein molecules. Bromoperoxidase, on the other hand, can be used to prepare radiobrominated proteins at pH 7. The stabilities of radiobrominated proteins prepared using myeloperoxidase are comparable to those prepared with bromoperoxidase. Myeloperoxidase has the advantage that it can be isolated from a readily available source, whereas bromoperoxidase can only be obtained from certain species of red algae.

Optimum efficiencies for carrier-free radiobromination at pH 7 can be achieved by mixing protein (25 μg), myeloperoxidase (12 μg), carrier-free Br-77 as NaBr in aqueous solution, and 20 nmoles of hydrogen peroxide in a total volume of 0.25 ml. The reaction is complete after 1 hr at 37°C. In vitro hydrolysis studies on proteins labeled with Br-77 using the myeloperoxidase method have shown the label to be completely stable toward hydrolysis at pH 7 for at least 7 days. This gentle technique for radiobromination is applicable even to the labeling of fragile proteins such as fibrinogen, as evidenced by in vitro clottability studies (>85%) and in vivo clearance studies on fibrinogen labeled with Br-77 using this method.

8:30 a.m.-10:00 a.m. Room 206

IN VITRO RADIOASSAY

RECENT ADVANCES IN CARDIOLOGY AND TUMOR MARKERS

Chairman: Stanley J. Goldsmith
Co-Chairman: Avir Kagan

RADIOIMMUNOASSAY OF MYOGLOBIN: TECHNICAL AND CLINICAL ASPECTS. Stanley J. Goldsmith, Mt. Sinai Medical Center, New York, N.Y.

SERUM MYOGLOBIN BY RADIOIMMUNOASSAY IN SCREENING FOR ACUTE MYOCARDIAL INFARCTION. L. Reese and P. Uksik, St. Joseph's Hospital and University of Western Ontario, London, Ont., Canada.

We evaluated serum myoglobin levels by radioimmunoassay in the diagnosis of Acute Myocardial Infarction (A.M.I.).

Over an eight month period 289 consecutive admissions to the Coronary Care Unit were studied. Two samples were taken, one on admission, and a second one at the next routine collection time. The myoglobin results were -

Diagnosis	# of Patients	Negative	Positive
No A.M.I.	164	156	8
A.M.I.	125	32	93

Sensitivity 0.74 Specificity 0.951 Predictive Value 0.92

It was noted that of the 32 false negatives 29 were outside a 5-15 hour time frame. Restricting our analysis to those patients sampled during this period gave -

Diagnosis	# of Patients	Negative	Positive
No A.M.I.	94	92	2
A.M.I.	70	3	67

Sensitivity 0.957 Specificity 0.979 Predictive Value 0.97

Of the 70 A.M.I.'s sampled in the 5-15 hour time frame 67 had positive myoglobin tests but only 44 had a C.P.K. elevation at that time. Because of conflicting clinical history two of the three false negatives could well have been outside the 5-15 hour time frame.

Of the eight false positives four also had an elevation of C.P.K. isoenzyme. Six of these eight had conditions known to increase myoglobin in the absence of A.M.I. The only true false positives were a patient with angina and one with no pathology.

Taken in the proper time frame, serum myoglobin determination is a quick, simple, sensitive, specific test with an excellent predictive value.

MODIFICATION OF A DIGOXIN RADIOASSAY FOR STAT PROCEDURE. I.W. Chen, M. Sperling and H.R. Maxon. Eugene L. Saenger Radioisotope Laboratory, University of Cincinnati, Cincinnati, OH.

The recently available stat procedure of a commercial digoxin radioassay (Beckton Dickinson) involves doubling of the amount of antibody used in the regular procedure and incubating the reaction mixture at 37°C to compensate for the decrease in binding due to a shorter incubation time (10 min). Use of a double amount of antibody has two obvious disadvantages: an increase in the material cost per assay and a decrease in sensitivity due to an increase in the binding capacity of the assay.

We modified the stat procedure and kept the binding capacity constant by reducing the incubation volume while maintaining a normal amount of antibody. We found that a 1.5-fold increase in the antiserum concentrations would result in a 30% increase in binding. We incubated 50ul of sample or standard, 600ul of I-125 digoxin, and 100ul of antibody at 37°C for 10 min, followed by charcoal addition, centrifugation, and counting of the supernate for 0.5 min. Total binding and the rate of binding at 10 min incubation were 50.4 $\pm$ 0.7% (mean $\pm$ 1 SD, n=12) and less than 1.3% per min, respectively. The standard curve was superimposable on that of the manufacturer's recommended regular (non-stat) procedure. The within- and between-assay coefficients of variation were less than 4.0%. The digoxin values obtained by our modified stat procedure correlated well with those obtained by the manufacturer's regular procedure (r=0.9918, y=0.023 + 0.951x, Sxy=0.10, n=60), and the clinical correlation of the results was excellent (48 nontoxic and 28 toxic, n=76).

β-THROMBOGLOBULIN RADIOIMMUNOASSAY: EVALUATION OF REAGENTS AND SAMPLING TECHNIQUE. P.A. Bardfeld, S.J. Goldsmith and H. Lipsyck. Mt. Sinai Med. Ctr., New York, NY

β-Thromboglobulin (BTG), a protein released during platelet aggregation, may be a convenient marker to determine platelet integrity and function in hemostatic and thrombotic disorders. A commercially available reagent kit was evaluated for clinical use.

The kit contains ^{125}I-BTG, standards, rabbit anti-BTG sera, NH_4SO_4 sol. for separation, and blood sampling tubes with EDTA and Theophylline (to retard BTG release). Procedure includes 50μL samples; incubation 60 min. Sensitivity (determined by assaying tracer aliquot) < 20 ng/ml. Normal range (N=8) 20-46 ng/ml. Aggregation of platelets with collagen produced levels > 260ng/ml at 1:1 dil. The recommended sampling technique (EDTA/Theophyllin tubes, no tourniquet compression, and 4°C storage prior to centrifugation) was evaluated. No increase in BTG levels were observed with tourniquet use, even with compression up to 2 min. (Range 24-44ng/ml, N-6). Hemolysis produced marked elevation of BTG activity. EDTA alone, heparin and failure to store samples at 4°C produces elevations of basal levels (68-258ng/ml).

Ice water storage of samples and special anticoagulant tubes are necessary but routine blood drawing techniques may be used in assessing clinical utility of BTG assay.

URINARY EXCRETION OF L-DOPA, DOPAMINE AND 3-O-METHYLDOPAMINE BY PATIENTS WITH MELANOMA. B. A. Faraj, D. Nixon, D. Murray, Y. Tarcan, M. Camp, F. A. Ali and W. Stacciarini. Departments of Radiology (Division of Nuclear Medicine) and Medicine, Emory University School of Medicine, Atlanta, Ga.

The biochemistry of malignant melanoma is essentially that of accelerated activity of enzymes involved in the biosynthetic and/or degrative pathways of tyrosine metabolism and the subsequent formation of excessive amounts of melanogens such as dopamine (D), and L-dopa (DO). We have recently developed a specific and sensitive enzyme-radioimmunoassay (E-RIA) for these catechols (Faraj et al, J. Nucl. Med. 19, 1217, 1978; ibid, 18, 1027, 1977). The technique involved on the conversion of D to its respective O-methylated metabolite by the enzyme catechol-O-methyltransferase (COMT) and S-adenosylmethionine (SAM) followed by the simultaneous determination of the formed 3-O-methyldopamine (MD) by RIA. In the case of DO, it is necessary to incubate the sample in the presence of COMT enriched with a decarboxylase preparation. With the availability of this method, we were able to evaluate the role of these metabolic intermediates in patients with melanoma. The results indicated that patients with malignant melanoma excreted significant quantities of D (av. 750 μg/24 hr), DO (av. 102 μg/24 hr) and MD (av. 104 μg/24 hr) in their urine as compared to normal controls (av. 160, 3 and 40 μg/24 hr) and patients with amelanotic melanoma (av. 177, 2, and 32 μg/24 hr), respectively. Following surgery and chemotherapy, there was a substantial decrease in urinary levels of these compounds in those cases where the presence of melanoma was associated with increased production of catechols. The E-RIA of D, DO and MD may provide a valuable diagnostic tool for melanoma as well as to help stage the disease and follow its progress.

RADIOIMMUNOASSAY FOR SERUM PROSTATIC ACID PHOSPHATASE: COMPARISON WITH ENZYMATIC ACID PHOSPHATASE MEASUREMENTS AND BONE IMAGING. R.B. Shafer, J.H. Eckfeldt, and M.K. Elson. V.A. Medical Center, Minneapolis, MN.

We previously reported the relative insensitivity of the enzymatic determination of prostatic acid phosphatase (PAP) compared to bone imaging in the diagnosis of bony metastasis of carcinoma of the prostate (CAP). Radioimmunoassay (RIA) is an attractive alternative to the enzymatic method because the immunological activity of PAP is more stable during serum collection, storage and assay. We evaluated an RIA kit by a commercial supplier, available for investigational use pending clinical release. The assay employs PAP isoenzyme #2 for standards, I-125 PAP as a tracer and a second antibody separation of bound and free antigen. The assay is reproducible; between assay coefficient of variation were 7%, 3% and 10% for samples at various concentrations. To evaluate sensitivity and specificity of the assay, 41 patients referred for routine bone imaging had measurement of PAP by both RIA and enzymatic methods. The patient group included 19 patients with CAP, 15 with other malignancy and 7 patients with nonmalignant disease. In 19 patients with CAP, PAP (RIA) was elevated in 5/6 patients with stage IV and 3/7 with stage III disease, PAP (enzymatic) showed similar results. Bone scans were positive in 5/6 of stage IV patients and in 1/7 of stage III patients. In other malignancies, 13/15 patients had normal PAP by both methods. False positive elevations were found in 2 patients by RIA and in 2 additional patients by enzymatic method. No false positives by either method were found in nonmalignant disease. Conclusions: (1) PAP by both RIA and enzymatic methods lacked desired sensitivity. (2) Bone imaging remains a sensitive indicator of metastatic disease in CAP.

8:30 a.m.-10:00 a.m. Room 204

INSTRUMENTATION, COMPUTERS, AND DATA ANALYSIS

IMAGE PROCESSING

Chairman: Michael L. Goris
Co-Chairman: Nathaniel M. Alpert

COMPUTER-ASSISTED MEASUREMENT OF LIVER IMAGE INHOMOGENEITY BY TEXTURE INDEX T2. E.A. Eikman, V.K. Jain, G.A. Mack, J.A. Madden, D.L. Flower, S.R. Witenhafer. University of South Florida and James A. Haley VA Medical Center, Tampa, Fl.

Some patients with liver disease show inhomogeneous distribution of radioactivity on radiocolloid liver images; observer variation in the interpretation of this index is large. The purpose of our work was to objectively and automatically measure image inhomogeneity as a diagnostic feature.

The image of the right lateral projection of the liver was recorded with a gamma camera, digitized, filtered, and transformed prior to the formation of spatial dependence probability matrices, which represent 1st order radioactivity level differences. From these matrices a number of indices of inhomogeneity may be extracted. One promising index, T2, is a measure of squared difference over the image.

We have assessed the diagnostic use of T2 on a sample population of 112 independently diagnosed patients. In patients with a texture index of ≥19, the probability of liver disease was 0.95. The specificity of the test using this criterion was 0.98. The sensitivity was 0.20.

Although the sensitivity of the index is modest at this point in development, T2 shows promise as a component in a multivariate approach to liver disease diagnosis.

AN ADAPTIVE FILTER FOR THE COMPUTER PROCESSING OF DIGITAL IMAGES. C.R. Appledorn, B.E. Oppenheim, H.N. Wellman. Indiana University Medical Center, Indianapolis, IN.

We present an adaptive (linear, nonstationary) filter for the computer processing of digital images. This filter has been compared with three conventional filters of current interest in the nuclear medicine literature: 1) a nine point smooth (linear, stationary), 2) a nine point median level smooth (nonlinear, stationary), and 3) a general restoration filter (linear, stationary). All filters programmed in Fortran required approximately thirty seconds for execution (without hardware multiply/divide) when operating on 64x64 integer array images. Initial efforts have been directed towards contrast improvement in stress and rest thallium images of the left ventricular myocardium.

The adaptive filter provides edge enhancement in regions of high counts and provides background smoothing in regions of low counts. A cross section of this filter is realized as

$$Y_n=[-a_nX_{n-2} + X_{n-1} + (2+2a_n)X_n + X_{n+1} - a_nX_{n+2}]/4$$

where a_n is parametrized as a function of local image statistics $a_n=-2/3 + SQRT[8/3(QX_n+R)-5/9]$.
The parameters Q and R are chosen before processing. Q is a function of the noise-to-signal ratio of the image and R is a function of the maximum smoothing desired in regions of low counts.

In a series of stress and rest thallium images, we found the smoothing filters blurred edges separating normal and abnormal myocardium. The restoration filter improved this contrast at the expense of noise amplification in background regions. The adaptive filter provided the necessary compromise between edge sharpening and background smoothing. Best results were obtained when identifying cold abnormalities in hot target regions.

DYNAMIC DENSITOGRAPHY AND TOMOGRAPHY OF THE BREATHING LUNG. F. Deconinck, A. Bossuyt, R. Lepoudre, M. Jonckheer. Academisch Ziekenhuis, V.U.B., Brussels, Belgium and E. Huffer, Research and Application, SA Informatek, Orsay, France.

A new technique based on computerized gammadensitography and tomography is described. The technique allows the local study of the breathing mechanism of the lung (expansion - magnitude and timing) and of vascular pulsations (distribution and magnitude). Dynamic changes in the shape of lung and chestwall are studied by means of tomographic reconstructions.

There is no tracer administration to the patient. The transmission images which yield all the necessary data are obtained with a 5 mCi Tc-99m source at 2 m from the crystal plane of an Elscint Dymax LF Gamma Camera without collimator. Hence, the camera is used at maximum sensitivity and at intrinsic resolution. The radiation exposure to the patient is less than 10^{-6} rad.

Dynamic changes in transmission of x or γ rays through the lungs stem principally from local expansion perpendicular to the direction of the transmission during the respiratory cycle, from organ displacement associated with the respiration and from local variations in blood volume due to vascular pulsations.

All are clearly visualised and readily quantitated regionnally using either static image processing, tomographic reconstruction methods or temporal Fourier analysis on an Informatek Simis 3 processing system.

We have developed a method which allows a new approach to basic problems in lung physiology and pathology. The obtained information is either completely new or obtained by much less agressive methods than before.

A NEW COMPUTER PROGRAM FOR THE EXTRACTION OF GLOBAL AND REGIONAL BEHAVIOR OF ALL FOUR CARDIAC CHAMBERS FROM GATED RADIONUCLIDE DATA. J.W. Verba, I. Bornstein, M.P. Alazraki, A. Taylor, V. Bhargava, R. Shabetai, and M. LeWinter. Veterans Administration Medical Center and University of California, San Diego, CA.

We have developed a completely automated computer program for the batch mode reduction of gated radionuclide data. The program is designed to operate retrospectively on list mode (event by event) data presented on 9-tract magnetic tape and to yield both global and regional analysis of all four cardiac chambers. The program will handle data from very short acquisitions (less than 2 minutes) even if these acquisitions are at relatively low counting rates (between 5 and 10 thousand events per second). To

preserve detail throughout the cardiac cycle, the data is weighted with respect to its proximity to an initiating or termination R-wave. The data is 3-dimensionally filtered in both the space and time domains to increase statistical reliability. We make extensive use of Fourier transforms for both the filtering and for the automatic determination of regions of interest. Background is assessed by a technique which takes into account not only the underlying and overlying activity but also the activity arising from the other cardiac chambers and the great vessels. A complete functional global analysis can be extracted for each of the four chambers. The program analyzes regional behavior for the various chambers in several alternate ways. Extensive care has been made to present the final output in a comprehensible manner.

We plan to present details on both the coding and on our experience with the development of the coding of this program and to show examples describing the methodologies applied at various steps of the analysis.

INEXPENSIVE PORTABLE DATA COLLECTION AND IMAGE ANALYSIS SYSTEM FOR SCINTILLATION CAMERAS J. Carter, S.L.Ho, P.Cahill, D.V. Becker, New York Hospital-Cornell Medical Center, NY,NY, and Polytechnic Institute of New York, Brooklyn, NY

To combat the increasing cost of satellite medical computing systems, a novel, inexpensive ($5000) portable microprocessor computer system has been developed for data collection and image processing. The system to be described utilizes the standard S-100 bus, allowing a wide choice of microprocessors, can build histogram scintillation images at a throughput greater than 1 microsecond, stores data on floppy disc, and displays images in black-white or color. To build the scintillation image, a hardware processor maps each pixel into a 16 bit word using a novel method of multiplexing the bus. In addition, the system is capable of building 16 dynamic histograms gated by processed EKG information. The operating system utilizes Fortran based programs along with our nearest neigbor edge detection algorithm* Flexibility of data transfer to larger computers for storage and information retrieval is equally available.

In summary, this portable microprocessor system has met the needs of our laboratory for a portable scintillation camera for heart and renal studies from an operational and economic point of view.

* Cahill P,Ornstein E, Ho S, IEEE Trans. on Nuclear Science, NS-23:555 (1976).

SIMULTANEOUS MULTIPLANE DECONVOLUTION IN FOCAL PLANE TOMOGRAPHY, D. Pickens, J. Patton, D. Pearse, R. Price, and A.B. Brill, Vanderbilt University Hospital, Nashville, TN 37232

The objective of this study is to characterize blur artifacts contributed by off plane information, inherent in focal plane tomography, by determining the relationships between blur contributions and interplane separation distance during multiplane deconvolution.

The method of Chang, Macdonald, and Perez-Mendez (IEEE Transactions on Nuclear Science, Vol. NS-23, No. 1, Feb. 1976) has been applied to images collected with a high resolution rectilinear scanning system consisting of nine high purity germanium detectors with collimators focused at a common point. Back projection of the data from a point source yields multiple tomographic images with blur components spread into all planes, as does back projection of the data from a planar object source. The system response for each plane was derived from scans of point sources. Deconvolution of back projected images was carried out using the measured system response functions. Varying the back projection plane separations before deconvolving the images produces changes in: signal-to-noise ratios; amount of blur removal during deconvolution; and intraplanar resolution.

The results are demonstrated with Tc-99m scans of planar objects in air for six planes simultaneously. Deconvolution yields a reduction in the projection artifacts in all object planes. Image enhancement is dependent on plane separation, input signal-to-noise ratios, and number of planes specified during deconvolution. Comparison studies with a digitized Searle Pho/Con system are expected to provide further information on the nature of the blur artifacts.

10:30 a.m.-12:30 p.m. Room 300/301

CLINICAL SCIENCE

CARDIOVASCULAR V: POSTER SESSION II

Chairman: Heinrich Schelbert
Co-Chairman: John Verba

RIGHT VENTRICULAR EJECTION FRACTION ASSESSMENT BY RAPID MULTIPLE GATED EQUILIBRIUM SCINTIGRAPHY: DESCRIPTION, VALIDATION, AND APPLICATION OF A NEW TECHNIQUE. J. Maddahi, D. Berman, D. Matsuoka, J. Forrester, H.J.C. Swan, and A. Waxman. Cedars-Sinai Medical Center, Los Angeles, CA.

Previously described right ventricular (RV) ejection fraction (EF) by the first pass method does not allow serial measurement without reinjection. This study assesses the validity and applies rapid multiple gated equilibrium scintigraphy (MGES) in 76 pts for determination of RVEF using Tc-99m RBC's, gamma camera, and computer. In 20 pts multiple gated images of the right heart were acquired during FP. Immediately following FP, MGES was performed in LAO view. For both types of imaging multiple (M) regions of interest (ROI) were used for RVEF. MGES RVEF was also determined by single (S) ROI. Excellent correlation for RVEF was found between MGES and FP (r=.94); however, SROI MGES severely underestimated FP EF and showed poor correlation (r=.60). For RVEF with MROI, inter and intra observer variations were small (r=.91 and r=.98).

Twenty pts had 2 minute MGES as well as standard 6 min MGES, and RVEF correlated well (r=.98). In 15 normals mean RVEF was less than left ventricular EF (.48± .05 vs. .63± .08, mean ± SD) (p= <.001). In 21 pts with coronary disease subgrouped by degree of right coronary artery stenosis, RVEF was not significantly different from normal in any subgroup.

Thus, 1) this new method for RVEF using multiple gated equilibrium scintigraphy is highly accurate and reproducible and requires the use of multiple regions of interest. 2)The technique is well suited to rapid serial assessment of RV function during exercise. 3) Right coronary artery stenosis is not usually associated with abnormal RVEF at rest.

RIGHT VENTRICULAR EJECTION FRACTION: WHICH METHOD? R.N. Pierson, Jr, P.J. Huang, W.A. Tansey, M.I. Friedman. St. Luke's Hospital Center, New York, N.Y.

Right ventricular ejection fraction (RVEF) has been rarely available by traditional catheterization angiography, and has been successfully added to the cardiology armamentarium by the first pass radionuclide time activity (TA) method using the multi-crystal camera. In order to extend this method to Anger camera users, and to compare time-activity with area-volume methods, systematic comparison was made between a TA method, a new simple regional wall motion (RWM) method, and a contrast validated A-V method, using 99m-Tc albumin radiocardiography.

The TA method uses dead-time corrected count rates at end diastole (ED) and end systole (ES) over 3-5 beats during RV transit. The regional wall motion(RWM) method uses the global average of percent shortening along 8 individual axes, measured from computer reconstructed images of the RV in right and left anterior oblique views. Results from TA and RWM are compared with the AV method proposed by Gorlin, which is applied to lanimetered measurements from these reconstructed images: Volume = 0.6 RAO area x LAO area/RAO + 3.9, (Circ: 52: 608-615, 1975).

RVEF measurements in 15 normals, and 47 patients with heart disease, ranged from 22 to 76%. The TA method showed a slope of

0.65, and correlation coefficient of only 0.76; 6 subjects, or 9% showed results > 2 S.D. different from the AV method.

The RWM method showed an r of 0.89, with no results > 2 S.D different from AV.

The simplified RWM method requires RAO and LAO views, but is more reliable than TA in predicting RVEF from radiocardiography.

LEFT VENTRICULAR FUNCTION ASSESSMENT OF PATIENTS WITH CORONARY ARTERY DISEASE. R.E. Sonnemaker, E.G. DePuey, J.L. Floyd, W.L. Thompson, J.A. Burdine. Baylor College of Medicine, Houston, TX., Wilford Hall Medical Center, San Antonio, TX.

In order to assess their potential as screening parameters, resting left ventricular (LV) function indices of global contractility and compliance were compared in normals (N=18) and angiographically defined (>70% intraluminal narrowing) coronary disease patients (N=18). First-pass radiocardiograms were obtained in the fasting state using a dual detector cardiac probe. LV, background, and ECG data were digitized at 5 msec intervals permitting minicomputer analysis of high-resolution, single-cycle, LV volume curves. Calculated indices included ejection fraction, isovolumic contraction time (ICT), ICT/R-R, LV ejection time (LVET), LVET/R-R, ICT/LVET, rapid filling time (RFT), RFT/R-R, slow filling time (SFT), SFT/R-R, SFT/RFT, first third ejection fraction (FTEF), mean circumferential fiber shortening velocity and mean systolic ejection rate. Normal values were similar to those reported in the literature. Using Student's t-test for non-paired data, no parameter showed significant difference comparing normals to patients with coronary disease and normal ventricular function (N=6) or to patients with coronary disease and abnormal ventricular function (N=12). The inability of FTEF, a sensitive index of ventricular contractility and SFT/RFT, an index of ventricular compliance, to identify patients with coronary disease is contrary to data reported by others. In conclusion, resting parameters of global LV function are unable to identify patients with coronary artery disease.

CHARACTERISTICS AND INCIDENCE OF REGIONAL ASYNCHRONY IN CORONARY ARTERY DISEASE. B.L. Holman, J. Wynne, J. Neill, and J. Idoine. Harvard Medical School and Peter Bent Brigham Hospital, Boston, MA.

Spatial asynergy at end-systole has been well characterized in patients with coronary artery disease. Assessment of regional asynchrony has been hampered by technical constraints. We developed a computer-assisted method for analyzing regional asynchrony from the ECG-gated radionuclide ventriculogram. Indices of regional asynchrony were determined for 6 regions of the left ventricle. Twenty patients with normal wall motion (9 with a normal coronary arteriogram (NCA) and 11 with coronary artery disease (CAD)) and 18 patients with asynergy during contrast ventriculography (ASY) were studied. The earliest evidence of regional asynchrony occurred in early systole. Regional ejection fraction at 1/3 systole was 34.9±1.2 (SEM) in NCA, 25.4±1.4 in CAD ($p<0.001$) and 11.9±1.3 in regions in ASY ($p<0.001$). 9/11 (82%) patients with CAD had abnormal regional ejection fractions at 1/3 systole. In ASY patients, severe forms of regional asynchrony appeared in both early systole and early diastole. Early systolic paradox was present in 61% of ASY patients; regional prolongation in peak ejection fraction was present in 67% of ASY patients; % peak ejection fraction at global end-systole was reduced in 78% of ASY patients and early diastolic relaxation was present in 15% of ASY patients. 94% with spatial asynergy at end-systole had one or more forms of severe regional asynchrony. We conclude that regional asynchrony is a frequent companion of coronary artery disease. Regional asynchrony during early systole precedes the appearance of asynchrony at end-systole. As the severity of CAD increases, early systolic paradox appears and peak regional ejection becomes delayed.

GLOBAL AND REGIONAL FUNCTION IN ACUTE MYOCARDIAL INFARCTION: ASSESSMENT BY QUANTITATIVE RADIONUCLIDE VENTRICULOGRAPHY. J. Wynne, M. Sayres, J. Idoine, J.S. Alpert, J. Neill, B.L. Holman. Peter Bent Brigham Hospital and Harvard Medical School, Boston, MA.

Global and regional left ventricular performance (LVP) was assessed in 55 patients (pts) with acute myocardial infarction (AMI) by gated radionuclide ventriculography. Regional LVP in 3 regions was determined by analysis of regional time-activity curves corrected for regional background. Followup studies were obtained at 2 weeks (29 pts) and 4 months (24 pts). Regions with Q waves on corresponding locations on the ECG demonstrated depressed function in 79% (77/99) of regions; function was also depressed in 41% (28/68) of regions without Q waves. Eight pts who succumbed within one month of admission had more severely depressed global LVP than survivors (22±4 vs 41±3%; $p<.05$); function was worse in regions with (20±4 vs 44±3%; $p<.0025$) and without (36±7 vs 69±3%; $p<.0005$) Q waves. Anterior transmural AMI demonstrated more severe impairment of function than inferior AMI in regions with (37±4 vs 63±8%; $p<.0005$) and without (61±6 vs 78±4%; $p<.005$) Q waves. Function improved at 4 month followup in regions without Q waves in both anterior (61±6 vs 98±4%; $p<.0025$) and inferior (78±4 vs 98±4%; $p<.0025$) AMI; regions with Q waves improved only with inferior AMI (63±8 vs 89±14%; $p<.05$). Thus, prognosis and clinical functional class after AMI is related to LVP in regions with and without Q waves, and dysfunction in regions without Q waves plays a significant role in the response to infarction. Improvement in regional LVP occurs after infarction, and involves improvement in function in regions both with and without Q waves.

NONINVASIVE ASSESSMENT OF LATENT MECHANICAL FUNCTION: COMPARISON OF LEFT VENTRICULAR SEGMENTAL WALL MOTION RESPONSES IMMEDIATELY POST-EXERCISE AND FOLLOWING NITROGLYCERIN. U. Elkayam, D. Berman, M. Freeman, H. Staniloff, J. Maddahi, H.J.C. Swan, J. Forrester, A. Waxman. Cedars-Sinai Medical Center, Los Angeles, CA.

Improvement of left ventricular (LV) wall motion abnormalities (WMA) with nitroglycerin (NTG) has been shown to be a predictor of latent myocardial mechanical function. Using multiple gated equilibrium scintigraphy (MGES), we observed similar changes in segmental wall motion immediately following sitting bicycle exercise (Ex). To compare the relationship between these phenomena, we evaluated 15 patients undergoing sitting bicycle Ex with MGES, and Tc-99m-RBC's. Prior to Ex, 2 control (C) left anterior oblique (LAO) images were obtained. The immediate post-exercise (IMPEX) image was collected during the initial 2 min following Ex. After 30 min rest, two LAO C images were performed prior to NTG, and after NTG, serial MGES was performed. The LV was divided into 5 segments and scored with a 5 point system (3=normal, -1=dyskinesis). Evaluation of MGES was performed by 2 blinded experienced observers, and disagreements were mediated by consensus. Of 44 abnormal segments, 37 showed identical response IMPEX and to NTG: 25/37 segments did not change and 12/37 segments improved. Four segments showed no change IMPEX and improvement following NTG, whereas 3 segments demonstrated augmentation of motion IMPEX with no improvement after NTG. LV volume was usually reduced from control both IMPEX and with NTG. Therefore, 1) the immediate post-exercise and NTG responses of LV regions with WMA are similar, probably reflecting reduced pre-load conditions associated with both states; 2) the IMPEX response may provide a simple, useful, noninvasive method for assessment of latent mechanical LV function.

DETERMINATION OF LEFT VENTRICULAR END-DIASTOLIC VOLUME (LVEDV) FROM GATED CARDIAC IMAGES:COMPARISON WITH CONTRAST VENTRICULOGRAPHY. J.B. Bingham, E.J. Taroli, N. Alpert, C.A. Boucher, R.D. Okada, K.A. McKusick, G.M. Pohost, and H.W. Strauss. Massachusetts General Hospital, Boston, MA.

LVEDV's were determined in 31 patients from both multiple gated cardiac blood pool images and contrast ventriculograms performed within two weeks. The LVEDV'S

were determined independently by two observers for each method using a geometric method based on the assumption of an ellipsoid form for the left ventricle (area-length method of Dodge). The tracer LVEDV was calculated from light pen outline of the end-diastolic image in the anterior, LAO 45° or LPO 30° projection using two of the three views with correction of the horizontal dimensions for nonorthogonality. Calibration of the image field was obtained using a bar phantom. Contrast LVEDV's were calculated from single plane 30° RAO end-diastolic outlines of the LV calibrated with a grid pattern filmed at the level of the LV. LVEDV's ranged from 82-403 mls. Inter-observer error (IOE) (1SD) and the correlation (r) between the mean volumes for each pair of observers were:

	Cath	Ant-LAO	LPO-LAO
IOE (ml)	±30.0	±49.4	±35.6
r		.80	.88

These data suggest that tracer determination of LVEDV correlates well with that obtainable from contrast ventriculography and the interobserver variance is similar to that of catheterization values. The LPO-LAO tracer calculated LVEDV's proved to be more reproducible than Ant-LAO LVEDV's because of better definition of the mitral valve plane.

QUANTIFICATION OF LEFT VENTRICULAR REGURGITANT FRACTION BY FIRST-PASS RADIONUCLIDE ANGIOCARDIOGRAPHY. W.R. Janowitz, M. Read, A. Fester, and A.J. Gilson. Mount Sinai Medical Center, University of Miami, Miami, FL.

The ability to non-invasively measure left ventricular regurgitant fraction (RF) would aid in the management of patients with valvular disease. A new technique for quantifying RF from first-pass radionuclide angiocardiographic studies has been developed.

On the first pass of a tracer through the heart the amount of activity ejected from the RV, (C_R), must equal the amount ejected from the LV, (C_L). Theoretically, it can be shown that in the presence of aortic or mitral regurgitation $RF = (C_L - C_R)/C_L$. C_R and C_L can be measured from time-activity curves of the RV and LV by summing the difference between end-diastolic and end-systolic counts for every identifiable heartbeat.

Five normal volunteers and ten patients undergoing cardiac catheterization have been evaluated using a multicrystal camera-computer system. 20 mCi. of Tc-99m HSA were injected using a saline flush technique. Time-activity curves were obtained from the right and left ventricles and C_R and C_L were measured. Values of RF obtained by this technique have correlated excellently with catheterization values (r = 0.98, all subjects; r = 0.96 normals excluded).

This method appears to be a simple and accurate technique to non-invasively measure RF.

COMPARISON OF THE EFFECTS OF ISOMETRIC AND DYNAMIC EXERCISE ON EJECTION FRACTION (EF) AND SEGMENTAL WALL MOTION (SWM) IN NORMAL CONTROLS AND PATIENTS WITH CORONARY ARTERY DISEASE USING RADIONUCLIDE ANGIOCARDIOGRAPHY. J. A. Jengo, R. Conant, R. Freeman, M. Brizendine and I. Mena, Divisions of Nuclear Medicine and Cardiology, Harbor-UCLA Medical Center, Torrance, CA 90509

EF and SWM were evaluated in 9 normals and 20 patients with coronary artery disease (CAD) at rest, during bicycle exercise (BE), and during isometric handgrip exercise (HE) to compare the effects of the two types of exercise on left ventricular function. Patients were imaged in the 30° RAO position while seated upright on a stool or bicycle ergometer. Radionuclide angiograms were done using a 15 mCi bolus of 99m Tc pertechnetate, i.v.. HE injections were made after 3 min. of 33% max handgrip. In the normal group EF increased during BE from .62±.02 to.83±.03 (mean± SEM) p<.0005. During HE, EF increased to a mean of .71± .04 (p<.025); this represents an increase in EF in 7 and a decrease in 2 patients. No abnormalities in SWM occurred. In the CAD group, EF showed no significant change during BE: from .39±.03 to .40±.04 (p>.10); half of the patients showed a decrease in EF. During HE, EF also showed no significant change: to 0.37±.02 (p>.10); 60% of the pts. had no change or a decrease in EF. Similar SWM abnormalities developed with both BE and HE: either no improvement of a pre-existing defect or the development of a new defect. It is concluded that variable changes in EF occur during HE in both normals and CAD, and variable changes in EF also occur during BE in CAD. However, SWM abnormalities uniformly appeared in all patients with CAD during either BE or HE. Therefore isometric handgrip exercise may be an appropriate substitute for bicycle exercise testing when SWM is also evaluated.

COMPARISON OF RV FUNCTION EVALUATION BY GATED FIRST-PASS, EQUILIBRIUM GATED, AND LIST-MODE FIRST PASS RADIONUCLIDE VENTRICULOGRAPHY. R.B. Grove, J.A. Harolds, T.A. Powers, R.W. Pederson, and R.D. Bowen. Veterans Administration Medical Center, Nashville, TN.

The purpose of this study was to evaluate gated first-pass (GFP) and equilibrium gated (EG) techniques for right ventricular (RV) function measurement compared to the list mode first-pass (LMFP) procedure. In 21 patients, after predosing with pyrophosphate, a basilic vein bolus injection of Tc-99m pertechnetate was performed. Using 2 mini-computers interfaced in parallel to an Anger camera, simultaneous GFP and LMFP studies of the RV in the RAO projection were performed. After repositioning, an equilibrium gated LAO blood pool study was obtained. The GFP studies were acquired for 6 seconds using standard software and processed using semiautomated edge detection. LMFP studies were acquired at 25 frames/second for 15 seconds. A background subtracted time-activity curve was then generated from the RV. EG LAO studies were acquired for 2-6 min and processed using manual RV end-systolic, end-diastolic regions of interest. RV EF's ranged from .27 to .66 in this unselected patient group. RV EF's obtained by GFP and LMFP techniques correlated well ($r = .97$, $y = 1.02x - .004$, $p < .001$). The EG procedure had a significantly lesser correlation with LMFP by each of 3 experienced observers ($r = .75$, $y = .65x + .13$, $p < .001$; $r = .53$, $y = .63x + .13$, $p < .05$; $r = .30$, $y = .25x + .32$, $p > .10$). Interobserver variability was high for the EG procedure ($r = .41, .48, .43$). The GFP study required the least processing time and provided superior delineation of tricuspid and pulmonic valve planes. The GFP technique allows the evaluation of RV EF as accurately as the more complex LMFP procedure and provides the additional information of RV wall motion.

MUGA ATRIAL PACING AS A TEST FOR MYOCARDIAL ISCHEMIA. H. Atlan, D. Tzivoni, A. Weiss, J.L. Rod, J. Salomon, D. Warshaw, L.D. Samuels and M. Gotsman, Hadassah University Hospital, Jerusalem, Israel.

The aim of this study is to detect patterns of changes in left ventricular (LV) function at increasing heart rates triggered by right atrial pacing, as indicators of myocardial ischemia. After injection of 15-20mCi of 99mTc in vitro labelled RBC, multi-gated blood cardiac imaging (MUGA) was performed in the 45° LAO and 30° RAO at several pacing rates for 2.5 to 4 minutes each. The test was terminated after reaching a maximum pacing rate of 150/min, if the patient complained of severe chest pain, or if a 3mm ST depression was recorded on ECG. Wall motion abnormalities were looked for and the following parameters were measured at rest and each rate: Ejection Fraction (EF), LV volumes, stroke volume and cardiac output. Twelve patients were studied and the results compared with angiography performed the day before, when 5 had normal coronaries and 7 advanced coronary artery disease (>60% narrowing in at least one major vessel).

Under atrial pacing EF increased or did not change significantly in the normal group (66% to 68%) while it decreased significantly in the CAD group (64% to 48% p= 0.05). No side effects were observed. Similar results have been reported by several authors after inducing myocardial stress by exercise, but MUGA atrial pacing is easier than MUGA exercise, by avoiding body motion and keeping constant heart rate during each recording. It is concluded that MUGA atrial pacing is a method of providing precise information on changes in ventricular function during induced myocardial ischemia.

A SIMPLIFIED METHOD FOR THE CALCULATION OF LEFT VENTRICULAR VOLUME BY EQUILIBRIUM RADIONUCLIDE ANGIOGRAPHY. R. Slutsky, A. Battler, D. Gordon, S. Walaski, J. Verba, L. Lief, K. Peterson, I.P. Murray, W. Ashburn. University of California, San Diego.

We have recently described a method correlating left ventricular (LV) volume by contrast ventriculography (CV) with radionuclide volume units developed from the counts in the LV derived from equilibrium angiographic (EA) time-activity curves. This method (I) used plasma radioactivity concentrations. To study a new method, which involves correcting for counts in whole blood (II), we studied 10 pts just prior to CV. Each pt underwent EA with 15-20 miC^{99m} Tc-HSA. Ten ml of blood was withdrawn during the mid-point of the EA study. Four ml was suspended over the collimator to develop a "blood" radioactivity concentration. The other 6 ml spun to yield 1 ml of plasma and counted in a well counter. End-diastolic (ED) and end-systolic (ES) counts developed from a semiautomatic computer program, corrected for heat beats, time per frame and either plasma (I) of blood (II) radioactivity was then compared with CV EDV and ESV. When CV volume is correlated with method I; for EDV r = .98 and ESV r = .98, and for method II; r = .98 for EDV and .96 for ESV. Method I and II correlated well r = .99 for EDV and ESV. The effects of LV attenuation was small though seen in the slightly smaller slope of the regression equation for EDV than ESV in both methods. In only 1 extreme case was soft tissue attenuation noticeable. We conclude LV volume can be calculated using blood or plasma radioactivity by means of EA. Only in rare extreme cases is attenuation a significant problem in volume calculations.

REPRODUCIBILITY OF EJECTION FRACTION AND LEFT VENTRICULAR VOLUME BY GATED EQUILIBRIUM RADIONUCLIDE ANGIOGRAPHY AFTER ACUTE MYOCARDIAL INFARCTION. R. Slutsky, J. Karliner, A. Battler, M. Pfisterer, W. Ashburn. University of California, San Diego.

To validate the repeated use of radionuclide equilibrium angiography for determining left ventricular (LV) ejection fraction (EF), end-diastolic (ED) and end-systolic (ES) volume (V), we studied 25 patients (pts) an average of 9.1 days (range 4-21) after acute myocardial infarction (MI). Data was collected at rest for 10 minutes each hour for up to 4 hours. Blood pressure and heart rate remained stable. At the start of each study a first pass EF was obtained. Data was processed with a semi-automatic computer program which develops an averaged volume curve from an assigned left ventricular region-of-interest. LV EDV and ESV were calculated in 8 pts and derived from a method which correlates well with contrast ventriculography (r = .98). Initial equilibrium EF averaged .46 ± .15 (range .19 - .71) and correlated well with first pass (r = .92). Comparison between initial and subsequent equilibrium EF 1,2,3 and 4 hours later showed correlations of .97, .95, .98, and .94 respectively. Excluding 3 anginal episodes the variation between studies averaged .03 ± .02 (range .00 - .09). Similarly initial and subsequent EDV and ESV showed correlations of .99, .98, .98 and .97. One minute before angina in 3 pts EF decreased from .45 ± .10 to .40 ± .11; during angina there was a further decrease to .32 ± .10; and 6 minutes after angina relief with nitroglycerin EF averaged .49 ± .13. We conclude that gated equilibrium radionuclide angiography is a reliable and reproducible method for serial evaluation of EF, EDV and ESV in pts after acute myocardial infarction and may prove useful in intervention studies.

ASSESSMENT OF RIGHT AND LEFT VENTRICULAR FUNCTION IN PATIENTS WITH CHRONIC PULMONARY DISEASE BY GATED CARDIAC ANGIOGRAPHY. M.J. Chamberlain, P. Mathur, D. Ahmad, W.J. Kostuk. University Hospital, London, Ontario.

Gated synchronous cardiac acquisition is a noninvasive technique permitting measurement of right and left ventricular (RV, LV) ejection fraction (EF). After in-vivo labelling of red blood cells with Technetium 99m, studies were obtained in a modified left anterior oblique position with a gamma camera linked to a dedicated computer. Following background subtraction, generation of a time-activity curve for each ventricle permitted calculation of EF. In 11 normal adults EF averaged 57±8% (mean±S.D.) for the RV and 67±11% for the LV. Based on the criteria of the American Thoracic Society, three patient groups were studied. Group A consisted of 16 patients (pts) with chronic airflow obstruction (CAO) alone; group B, 13 pts with CAO together with cor pulmonale (CP); and group C, 6 pts with diffuse interstitial fibrosis (DIF) and CP. For group A, both RV and LV EF at 52±7 and 67±13 respectively were similar to normals. In both groups B and C the RV EF was markedly diminished (33±7, 26±11 respectively $p<0.001$), while the LV EF was well preserved (60±18 and 55±13) respectively. Although pts in group B and C were more hypoxic than those in group A, the degree of hypoxia did not correlate with the degree of RV impairment. In summary, both RF and LV EF can be determined non-invasively in pts with chronic lung disease. RV EF is reduced only in pts with cor pulmonale and does not correlate with the degree of hypoxia, hypercapnia or the degree of airway obstruction. LV is well maintained in CP in spite of hypoxia.

NON-INVASIVE MONITORING OF LEFT VENTRICULAR FUNCTION IN ARRHYTHMIAS. E.F. Camargo, K.S. Harrison, H.N. Wagner, Jr., M.H. Bourguignon, P.P. Reid, P.O. Alderson, and R.H. Baxter. Johns Hopkins Medical Institutions, Baltimore, MD.

Beat-to-beat monitoring of left ventricular performance in arrhythmias was undertaken to evaluate hemodynamic differences between normal and abnormal beats. Validation experiments were performed in 3 dogs, in which a close relationship between the ventricular time-activity curve and the changes in aortic blood flow, aortic pressure and left ventricular pressure was shown. Left ventricular hemodynamic monitoring was also carried out in 16 patients with premature ventricular contractions (PVC) and 15 male volunteers. After intravenous injection of 20 mCi of Tc-99m HSA, the left ventricular time-activity curve was obtained with a cardiac probe (nuclear stethoscope, NS) and the following parameters were measured: ejection fraction (EF), ejection rate (ER), filling volume (FV) and stroke volume (SV). In the volunteers, the relative standard deviation was 9% for EF, 16% for ER, 13% for FV and 11% for SV. In the patients, the PVC showed EF 49±15%, FV 51±18% and SV 59±16% lower than the patients' normal beats. Compensatory beats had EF 22±10% and SV 26±16% higher than the patients' normal beats. These changes were significantly different ($p<.01$) from the deviation of the normal beats in the control population. Stroke volume was proportional to end-diastolic volume in the normals ($r=.93$) and in the patients ($r=.70$). The PVC time-activity curves showed 3 types of ejection: incomplete, complete and over-emptying, respectively, in 75%, 62% and 18% of the patients. Combination of the first two types occurred in 50% of the patient population.

Thus, the NS provided a means of quantifying the hemodynamics of normal and abnormal beats, non-invasively, at the patient's bedside.

HANDGRIP VS. BICYCLE EXERCISE FOR STRESS RADIONUCLIDE VENTRICULOGRAPHY. J. Lindsay Jr., M. Kamkar, and N.G. Nolan. Washington Hospital Center, Washington, D.C.

Radionuclide left ventricular angiography during exercise stress is useful for detection of ischemic heart disease and for assessment of its severity. Most investigators have used bicycle exercise (BE) but some have employed hand grip (HG) for this examination. We compared the effectiveness of these two forms of stress in inducing global and segmental changes in left ventricular performance.

Thirty patients underwent multiple-gated radionuclide angiography of their left ventricular blood pool following in vivo labelling of their red blood cells with Tc-99m. Each was examined at rest, during HG and during supine BE. Segmental wall motion (SWM) was normal at rest in 18. Of these, 12 became abnormal during HG, and 10 during BE. Five remained normal. In the 12 patients with abnormal

SWM at rest, deterioration occurred in 10 with HG and in 7 with BE.

Global ejection fraction (GEF), was normal at rest in 29. Decline in GEF ≥ 10% was observed in 4 during BE and 7 during HG. No patient had a decline of ≥ 10% during both. Increase in GEF ≥ 10% was observed in 6 during BE. No increases of this magnitude occurred during HG.

Thus, HG appears to be at least as effective as BE in inducing SWM abnormalities, and produces abnormal decline in GEF in certain patients in whom this is not evident during BE. Response to HG may provide additional information regarding left ventricular function.

RIGHT-TO-LEFT SHUNT QUANTITATION USING ONLY A GAMMA CAMERA WITH A SYNCHRONIZED SCANNING TABLE. C.J. Armstrong, T.F. Brown, P.T. Kirchner, and B.S. Brunsden. University of Chicago Hospitals and Clinics, Chicago, IL.

After Tc-99m MAA/microsphere injection, the ratio of extra-pulmonary-activity to whole-body-activity has been shown to be an accurate measure of right-to-left shunts. For performing this measurement without the usual computer analysis of multiple static camera images, we have developed a simple, reliable technique using only a gamma camera and synchronized scanning table (Searle Scintiscan).

Total body counts obtained in scanning mode can be related to lung counts in static mode by a factor based on scan speed and pass width (aperture) settings:

$$\text{Counts}_{\text{scanning mode}} = [\text{cpm static mode}]\frac{16 \times \text{aperture length (cm)}}{15 \times \text{scan speed (cm/min)}}$$

This relationship was experimentally verified for all combinations of scan speed and pass width settings, using a simple Co-57 phantom and subsequently a Tc-99m filled multiple-area phantom simulating activity in brain, lungs, and kidneys. Each phantom was studied 12 times. The maximum difference between calculated total counts and actual total counts was <4% with Co-57 and <6% with Tc-99m, producing a maximum error of 4% in the calculated right-to-left shunt. In patients our shunt estimations were in close agreement with values obtained at catheterization.

This method of right-to-left shunt quantitation agrees well with computer-assisted techniques, but is simpler, easier, and faster. It may be applicable for regional uptake quantitation in other diseases, e.g., metastatic thyroid cancer and bone marrow disorders.

QUANTIFICATION OF INTRA-PULMONARY SHUNTING IN SUPERIOR VENA CAVA-RIGHT PULMONARY ARTERY (GLENN) ANASTOMOSIS. B. Pastakia, L.M. Lieberman, J. Levy, D.S. Moodie and R.E. Polcyn. University of Wisconsin Hospitals, Madison, WI.

Intrapulmonic arteriovenous shunting, development of venous collaterals and closure of ventricular septal defects are complications of the Glenn procedure (end to end anastomosis of the superior vena cava to the right pulmonary artery). Intrapulmonic shunting can be detected by contrast echocardiography but accurate quantification of the degree of shunting is possible only with computer assisted pulmonary radionuclide angiograms.

We studied three patients who developed complications after the Glenn shunt procedure. We injected 200 μCi/kg Tc-99m-MAA intravenously and used a large field of view gamma camera with a dedicated PDP 11/40 computer. Two patients had intrapulmonary A-V shunting quantified. In addition, abnormal venous collaterals were demonstrated between the superior vena cava and the inferior vena cava in one patient while anomalous connection of the superior vena cava and the right pulmonary artery was shown to be present in another patient.

We conclude that computer assisted radionuclide angiograms can provide important information on the quantification of intrapulmonary shunting in addition to showing other unexpected complications. The technique is safe, non-invasive, requires only an intravenous injection, and is easily performed as an outpatient procedure.

RADIONUCLIDE ANGIOGRAPHY IN THE DIAGNOSIS OF TRICUSPID REGURGITATION. P.A. Germon, A. Patil, F.J. Lumia, and V. Maranhao. Deborah Heart and Lung Center, Browns Mills, NJ.

To assess the accuracy of first pass radionuclide angiography (RA) with Tc-99m pertechnetate in the diagnosis of tricuspid regurgitation (TR), the results of RA were correlated with contrast right ventriculography (RVG).

68 patients were studied with both RA and RVG, 58 were included in our study. Of these, 36 were female and 16 male with an average age of 55 years. 45 patients had RHD, 4 had CAD, 4 had mitral valve prolapse and 1 had both CAD and mitral valve prolapse.

Group I included 12 patients with no TR on RVG. On RA, 10 had no TR and 2 had minimal to mild TR. Right atrial mean transit time (RAMTT) was 2.7 ± 1.2 seconds (S.D.), the right ventricular mean transit time (RVMTT) was 3.8 ± 1.9 seconds.

Group II included 22 patients with mild to moderate TR on RVG(1+-2+). On RA, 19 had mild to moderate TR, 3 had no TR. The RAMTT was 6.3±3 sec. and the RVMTT was 8±4.2 seconds.

Group III had 20 patients with severe TR by RVG (3+-4+). On RA, 18 had moderate to severe TR and 2 had mild TR. The RAMTT was 10±3.8 sec. and the RVMTT was 12±5.7 sec.

The RAMTT and RVMTT increased with the severity of the TR and the increases in each group were significant.

In summary, 39 of 42 patients with TR by RVG had TR by RA. 8 of 10 patients without TR on RVG had no TR by RA. There were 2 false positive and 3 false negative RA studies giving a sensitivity of 93% and a specificity of 83%.

These data suggest that first pass radionuclide angiography is an accurate screening procedure for the presence of TR.

CARDIAC TRANSIT AT REST IN CORONARY PATIENTS. I. Mena, H. Bishop, T. Nelson, L.R. Bennett. LAC Harbor-UCLA Medical Center, Los Angeles, CA.

Conventional techniques at rest are insensitive for detection of coronary disease. We analyse the usefulness of Cardiac Transit Index (CTI) at rest. After an antecubital intravenous bolus injection of 15 mc Tc-99m pertechnetate, its passage is detected in the RAO projection. Right atrium (RA), left ventricle (LV), and ascending aorta (AA) time/activity curves are generated with a minicomputer. The Δt is 0.5 secs. LV and AA curves are deconvolved with the RA curve, thus correcting these curves for bolus shape. The LV and AA downslopes are gamma fitted, normalized and the areas under the downslopes are calculated and expressed as a ratio, LV/AA = CTI. The same data is reformated and left ventricular ejection fraction (EF) and segmental wall motion (SWM) are determined. In 25 normal individuals, at rest, the CTI was 1.79±0.3 ($\bar{x}$±SD) denoting a slower washout for the left ventricle than for the aorta. In 37 patients with myocardial infarction and abnormal LV SWM and EF, the CTI is 1.36±0.24 $p<0.001$. In 14 patients with coronary artery disease by angiography and normal rest SWM and EF the CTI was 1.34±.2 not different from the latter group and $p<0.001$ vs normal. The sensitivity of the CTI is 0.78 and the specificity is 0.95. An 8% of studies were not processable. Long transit time fractions of cardiac flow are responsible for the excessive counts detected in the downslope of the cardiac curve as compared to the AA curve. These fractions include LV turbulent flow and coronary circulation. In coronary patients counts during the washout phase of the LV are reduced relative to the washout of the aorta, thus shifting the index towards unity. The CTI is a sensitive parameter for the identification at rest of coronary patients with normal left ventriculograms.

10:30 a.m.-12:30 p.m. Room 210

CLINICAL SCIENCE

RADIATION EFFECTS SYMPOSIUM

EFFECT ON BREAST AND SKIN. T. Webster, Massachusetts General Hospital, Boston, MA.

EFFECTS ON THYROID. H. N. Wellman, Indiana University Medical Center, Indianapolis, IN.

EFFECTS ON HEMATOPOIETIC SYSTEM. A. B. Brill, Vanderbilt University, Nashville, TN.

EFFECTS ON LUNG AND GENETIC EFFECTS. T. Radford, University of Pittsburgh, School of Public Health, Pittsburgh, PA.

SUMMARY AND CONCLUSIONS. A. Hillberg, National Academy of Sciences, Washington, DC.

10:30 a.m.-12:30 p.m. Room 201

RADIOPHARMACEUTICAL CHEMISTRY

RECEPTOR BINDING RADIOTRACERS

Chairman: Michael D. Loberg
Co-Chairman: Buck A. Rhodes

A SYNTHESIS OF CARRIER FREE FLUORINE-18 LABELED AROMATIC COMPOUNDS AND ITS APPLICATION TO THE PREPARATION OF THE FLUORINE-18 LABELED NEUROLEPTIC HALOPERIDOL. T.J. Tewson and M.J. Welch. Department of Radiology, Washington University School of Medicine, St. Louis, MO.

There is considerable interest in the mapping and evaluation of neuroreceptors by the use of positron emission tomography but most literature syntheses will not provide compounds with the specific activities of $>10^3$ curies/mmole required. The p-fluorobutyrophenones such as haloperidol and spiroperidol are obvious candidates for labeling with fluorine-18 but current methods of preparation provide low specific activity material. Decomposition of aromatic diazonium compounds in a dipolar aprotic solvent and a non-nucleophilic acid may give electron deficient aromatic cations and if these are generated in the presence of carrier free fluorine-18 hydrogen fluoride they should combine to give the arylfluoride. Piperidyl triazines are stable, easily purified compounds, soluble in organic solvents in the absence of acid. Treatment with acid generates the diazonium salt and piperidine free of water and oxides of nitrogen which are common contaminants of conventional diazotization procedures. Refluxing phenyl and p-tolyl triazines in tetrahydrofuran containing methane sulphonic acid and carrier free fluorine-18 hydrogen fluoride gives the fluoroaromatic compounds in approximately 50% yield in a four minute reaction time. The reaction was then applied to 2-N-piperidyl-p-diaza-4-[4-(p-chlorophenyl)-4-hydroxypiperidyl] butryophenone in refluxing 1,2-dimethoxyethane to give a 22% yield of carrier free fluorine-18 haloperidol in a four minute reaction time. This type of reaction should also be applicable to the labeling of spiroperidol , a neuroleptic with a higher receptor binding affinity than haloperidol.

HALOGENATED ESTROGEN ANALOGS AS POTENTIAL BREAST TUMOR IMAGING AGENTS. J. A. Katzenellenbogen, D. F. Heiman, R. Goswami, K. J. Allison, K. E. Carlson, and D. W. Payne. Department of Chemistry, University of Illinois, Urbana, IL

Three series of halogenated estrogens analogs have been prepared as potential breast tumor imaging agents: α-alkyl-α'-iodostilbestrols (I), side-chain halohexestrols (II), and ring halogenated hexestrols (III). We have measured the estrogen receptor binding affinity (RAC) of these compounds and measured (or estimated) their non-specific binding (to albumin, NSB). The ratio RAC/NSB, called the "merit factor" (MF), can be used to predict the uptake selectivity of these analogs (MF for estradiol is 100 by definition). In series I, MF depends critically on the nature of R (MF = 30 when R = i-Pr); in series II, MF increases as the size of the halogen decreases (MF = 120 when R = F); in series III, MF is high for some of the fluoro-analogs. Tissue uptake studies done in rats with some of the analogs in tritium-labeled form show that uptake selectivity parallels MF.

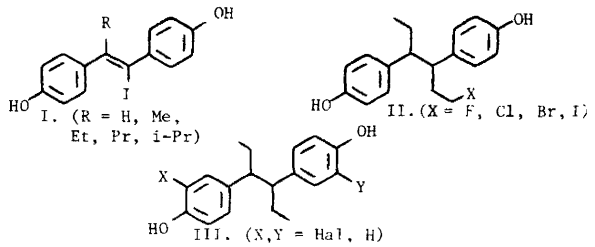

RADIOLABELLED ACETYLCHOLINESTERASE INHIBITORS AS POSSIBLE MYOCARDIAL IMAGING AGENTS. R.F. Dannals, H.D. Burns, L.G. Marzilli, T.E. Dannals, T.C. Trageser and H.N. Wagner. The Johns Hopkins University and Medical Institutions, Baltimore, MD.

Quaternary ammonium salts of pharmacological interest are generally believed to induce their principal response by altering some normal physiological action of acetylcholine, the substrate of acetylcholinesterase (AChE). AChE activity in mammalian organs is widespread and varied. In some species, particularly high AChE activities have been found in heart tissues.

We have prepared an iodinated derivative of a known AChE inhibitor, phenyltrimethylammonium iodide, for possible use in myocardial imaging. 4-iodophenyltrimethylammonium acetate (I-PTMA) was prepared by two methods: a. isotopic exchange and exhaustive methylation of 4-iodoaniline, b. chloramine-T iodination of N,N-dimethylaniline, followed by quaternization with methyl iodide. I-PTMA was characterized by IR, PMR, element analyses and TLC.

Biodistribution studies in albino ICR mice and in rabbits showed a significant accumulation of I-PTMA in the heart, with heart to blood ratios (time) in mice of 7:1 (1 min), 7:1 (5 min), 6:1 (10 min), 5:1 (30 min) and 2:1 (60 min). Initial uptake in the heart was greater than 30% of the injected dose/gram. Ten percent of the injected activity was excreted via the kidneys during the first 5 minutes. Less than half of the injected activity was retained in mice after 120 minutes.

It is concluded that I-PTMA could potentially be a useful agent for myocardial imaging. I-123 could be easily substituted for the longer-lived isotopes to make a viable imaging agent.

RECEPTOR BINDING RADIOPHARMACEUTICALS AS AN ALTERNATIVE TO THALLIUM FOR MYOCARDIAL IMAGING: METHYLQUINUCLIDINYL BENZILATE (MQNB). W. Alter, III, M. Grissom, J. Hill, F. Vieras, W. Eckelman, J. Phillips. Armed Forces Radiobiology Research Institute, Bethesda, MD, and George Washington University, D.C..

This study was undertaken to evaluate the use of receptor binding radiopharmaceuticals as myocardial imaging

agents. For imaging, high heart/blood (H/B) and heart/lung (H/L) ratios are desirable. A muscarinic cholinergic antagonist, (H-3) methylquinuclidinyl benzilate (MQNB), was found to have a high affinity (K_a = 5.7 X $10^9 M^{-1}$) for muscarinic receptors in guinea pig ventricular muscle. Dogs (N=5) under chloralose anesthesia were selected for the study of myocardial uptake and distribution of MQNB and to compare these results with those for simultaneously injected thallium-201 (Tl). H/B ratios for the two agents were comparable (MQNB = 44.0 ± 7.4; Tl = 37.8 ± 10.4) whereas the H/L ratio was greater for MQNB (16.4 ± 3.9) than for Tl (5.7 ± 2.3). The region perfused by the left anterior descending coronary artery was rendered ischemic for two hours by ligation (N=3) of this vessel, resulting in a marked reduction in uptake of both agents. Minimum values were measured in tissue obtained from the apical portion of the left ventricle where MQNB was 39.2 ± 11.4% and Tl was 35.2 ± 13.2% of those values measured in normally perfused myocardium. There was a high correlation ($r = 0.84$; $p < 0.001$) between the uptakes of the two agents within the entire ischemic region. This indicates that MQNB is similar to Tl in it's ability to discriminate between normal and ischemic (or infarcted) tissue. It is concluded that MQNB might prove to be an excellent agent for myocardial imaging when labelled with a gamma-emitting radionuclide.

F-18-2-DEOXY-2-FLUORO-D-MANNOSE: BIOLOGICAL BEHAVIOR COMPARED WITH 2-DEOXY-2-FLUORO-D-GLUCOSE. G.D. Robinson, Jr., M.E. Phelps and S.C. Huang. UCLA School of Medicine, Los Angeles, CA.

F-18 labeled 2-deoxy-2-fluoro-D-glucose (FDG) can be used to assess regional glucose utilization in humans in vivo. Steric considerations suggest that 2-deoxy-2-fluoro-D-mannose (FDM), which is produced during FDG syntheses, may have a biological behavior analogous to that of FDG. In vitro enzymatic studies verify that FDM is a substrate for phosphorylation by hexokinase.

F-18 labeled O-acetylated precursors of FDG and FDM were produced by reaction between F-18-fluorine and triacetyl glucal in "Freon 11" solution at -80°C. The compounds were separated using silica gel column chromatography and labeled FDG and FDM were obtained by subsequent acid hydrolysis. TLC analyses verified that FDG and FDM had radiochemical purities greater than 90%.

The biological behaviors of FDG and FDM were compared in rats by tissue sampling at 5, 15, 30 and 60 and 120 min post IV injection. Brain and heart uptakes, with renal excretion of the label, were noted for both compounds. Using 5 rats for each compound at each time interval, the tissue dynamics were indistinguishable. The behaviors of FDG and FDM were compared following IV injection in humans using the ECAT system with kinetic analysis of brain uptakes using a three compartment model. The tomographic brain images were similar for both compounds as were rates and amounts of brain uptake. Calculated rate constants for intercompartmental transport of FDM were approximately twice those for FDG. The results suggest that FDM may be a suitable tracer for glucose utilization studies.

A TRANSFERRIN BINDING MACROMOLECULAR COMPONENT OF EMT-6 SARCOMA (BALB/C MICE). S.M. Larson, S. Grunbaum, J.S. Rasey, N.J. Nelson, D.R. Allen, G.D. Harp, and D.L. Williams. VA Medical Center and University Hospital, Seattle, WA.

Transferrin plays an important role in the uptake of Ga-67 citrate and Fe-59 citrate by experimental mouse tumors growing in long-term tissue culture. In a previous report, we presented kinetic evidence for a high affinity cellular transferrin receptor associated with living cells of the EMT-6 sarcoma, a transplantable mouse tumor, with in-vivo and in-vitro growth forms (JNM 19:715,78). We attempted to isolate a transferrin binding macromolecule from EMT-6 sarcoma. Studies were performed using approximately 10^9 cells (in-vitro growth) or about 1 g of solid subcutaneous tumors (in-vivo growth). Teric acid extracts of the tumor tissue were prepared and incubated with: 1) I-125 labelled human transferrin (10 μCi/μg), or 2) I-125 labelled human transferrin and 2.5 mg/ml human transferrin. Gel chromatography on Sephacryl S-200 SF and Sepharose CL 6B revealed that high specific activity I-125 transferrin bound predominantly to high molecular weight components of approximately 250,000 mol wt. In the presence of 2.5 mg/ml transferrin, the I-125 transferrin was displaced and migrated at the mol wt appropriate for transferrin (~80,000). Both in-vitro and in-vivo grown EMT-6 cells showed the same pattern of binding to a high molecular weight component. We conclude that both in-vivo and in-vitro grown EMT-6 sarcoma contain considerable quantities of transferrin binding macromolecules. This macromolecule has an approximate molecular weight of 250,000 and is liberated from the stroma of the cells after treatment with teric acid, suggesting that the molecule contains both polar and non-polar functional groups.

TRANSFERRIN RECEPTORS IN NORMAL AND VIRUS-TRANSFORMED CELLS IN CULTURE. J.A. Fernandez-Pol, D. Klos, K. Baer and R.M. Donati. VA Medical Center and St. Louis University, St. Louis, MO.

The transferrin (Tr) receptors of normal rat kidney (NRK) and simian virus 40-transformed NRK (SV-NRK) cells have been studied. Cultured cells (0.25 to 5 x 10^5) grown in 60-mm petri dishes were washed at 37°C twice with serum-free Dulbecco's modified Eagle's medium and two times with the same medium containing no Fe. The binding assay was performed using I-125-Tr (150,000 cpm) in 1.5 ml of Fe free medium supplemented with 0.2% bovine serum albumin (treated with Bio-Rad Chelex-100 to remove iron) at 37°C. At set intervals, the amount of I-125-Tr bound to the cells was determined. Unbound I-125-Tr was removed and the cells were washed at 4°C four times with Dulbecco's phosphate buffered saline. The radioactivity of the cells was determined as described (Biochem Biophys Res Commun 78:136, 1977). When cultures of NRK cells were exposed to I-125-Tr maximal binding of I-125-Tr was reached after 30-40 min incubation at 37°C. Additional incubation led to approximately 20% reduction below maximum. In contrast, maximal binding of I-125-Tr to SV-NRK cells was reached after 60 min of incubation at 37°C, and further incubation with I-125-Tr did not significantly reduce the cell bound radioactivity. In both NRK and SV-NRK cells the uptake of I-125-Tr was inversely proportional to cell density and no relationship to changes in cell size was found. The results indicate that the number of available Tr receptors per cell decreases as cell density increases. The difference between the kinetics of I-125-Tr binding to NRK and SV-NRK cells may be due to changes in cell membrane properties induced by viral transformation. (Supported by VA 657/2620-01).

STUDIES OF THE MECHANISM OF GALLIUM-67 UPTAKE BY TUMOR, ABSCESS AND NORMAL TISSUES. R.L. Hayes, J.J. Rafter and B.L. Byrd, Medical and Health Sciences Division, Oak Ridge Associated Universities (ORAU), Oak Ridge, TN.

We have previously proposed that the initial biodistribution of Ga-67 involves its entry into tumor and normal tissue by different routes. Support for this contention was obtained by experimental alterations of serum iron binding capacity (Proc. SE Ch. SNM Meeting, Birmingham, AL.). We have now compared the uptake of Ga-67 in a hepatoma and an experimental abscess in the rat.

An increase in unsaturated iron binding capacity (UBIC) was produced by inducing anemia. Blockage of Ga-67 binding to plasma proteins was produced by I.V. administration of scandium. As previously observed, an increase in UBIC resulted in a significant decrease in tumor uptake while normal tissue uptake increased. Ga-67 uptake in the experimental abscess also decreased significantly. With scandium administration, a significant decrease in normal tissue uptake of Ga-67 occurred without alterations in either tumor or abscess uptakes.

These results suggest that the apparent initial entry of Ga-67 into tumor and inflammatory lesions is similar and different from that that occurs with normal tissues. It may be, however, that, although a primary factor controlling tumor and abscess uptake is the degree of Ga-67's binding to plasma protein, different routes are involved,

i.e., "free" Ga-67 labels leukocytes and these migrate to inflammatory processes while a direct permeation of tumor cell membranes occurs. (ORAU operates under Contract No. EY-76-C-05-0033 with the U.S. Dept. of Energy. This work was supported by NCI, DHEW, Grant No. CA-11858.)

IgG and IgE ANTI-INSULIN ANTIBODY FLUCTUATIONS IN DIABETICS UNDERGOING DESENSITIZATION THERAPY FOR INSULIN ALLERGY. R.G. Hamilton and N.F. Adkinson, Jr., The Johns Hopkins School of Medicine, Baltimore, MD.

Immunopathological reactions occur in 5-10% of insulin-dependent diabetics. Clinically, the most important of these reactions are systemic allergic reactions mediated by IgE anti-insulin antibodies (Abs) and insulin resistance resulting from high IgG anti-insulin Ab titres. We have developed a solid phase radioassay (SPRIA) which permits the quantitation of human insulin-specific IgG and IgE Ab levels using a single solid phase reagent and two I-125 labeled detection proteins (Protein A and Rabbit anti-human IgE). These radioassays have been applied to the study of Ab fluctuations in two insulin-dependent diabetics undergoing desensitization therapy (D.T.) to porcine insulin after manifesting recurrent urticarial reactions related to insulin therapy. Patient I exhibited a marked increase in IgE and IgG Abs by 13 days post D.T., rising to maximum by 2.5 months. IgG Ab levels declined slowly during the next 12.5 months while IgE Abs declined to one-fifth of original baseline levels. This pattern suggests initial immune stimulation followed by differential loss of IgE Ab. Patient II, however, exhibited only modest decline (25%) in IgE Abs by 7.5 months after initial D.T. during which period, IgG fell by 65%. This immunological pattern is consistent with the induction of partial immunological tolerance affecting both IgG and IgE Abs. These two Ab patterns suggest the immune responses to D.T. are variable and complex. These initial studies illustrate the use of SPRIA technology in studying two classes of human Abs using a single solid phase reagent under conditions which minimize the effect of large quantities of IgG (ug/ml) on detection of relatively small quantities of IgE (ng/ml).

10:30 a.m.-12:00 p.m. Exhibit Hall

MIXED POSTER SESSION II

BONE/ONCOLOGY

Chairman: Frederic H. Gerber
Co-Chairman: Schyler V. Hilts

INCREASED UPTAKE IN NONJOINT BONE IN RHEUMATOID ARTHRITIS. K. Rosenspire, M. Blau, A.C. Kennedy, F.A. Green and J. Steinbach. State University of New York at Buffalo, Buffalo, NY.

We have investigated the uptake of Tc-99m bone scanning agents in joints and bones of normal and arthritic patients. Gamma camera-computer images were made in a series of 40 male patients (20 with classical rheumatoid arthritis (RA) and 20 controls). Knees, hands, forearms and thighs were studied. Uptake was measured as counts per unit area normalized for body weight and dose.

We have previously reported quantitative data on increased Tc-99m pyrophosphate uptake in RA joints. An unexpected finding was increased uptake in the midshaft of the radius and ulna in patients with RA. Patients with highly active disease were found to have 41% higher midshaft uptake than controls.

A similar increase in nonjoint bone was measured in rabbits with experimental arthritis. There was a 44% increase in uptake of the midshaft proximal to an inflammed joint compared with the midshaft uptake on the control side.

The mechanism of increased uptake in nonjoint bone in RA is not clear. These increases in midshaft bone adjacent to an inflammed joint might be due to increased blood flow to the limb or to osteoporotic changes of varying extents. Juxta-articular osteoporosis is commonly found with RA and osteoporosis from disuse of the limb or even a more systemic effect may be involved. Bone turnover from any source would lead to increased uptake in the involved bone. We are presently carrying out total body retention studies with Tc-99m MDP to determine whether there is increased bone turnover in RA patients.

LOCAL DISTRIBUTION OF Tc-99m PYROPHOSPHATE AND Tc-99m PERTECHNETATE IN NORMAL AND ARTHRITIC RABBIT JOINTS. K. Rosenspire, M. Blau and F.A. Green. State University of New York at Buffalo, Buffalo, NY.

We have measured the distribution of Tc-99m pyrophosphate and Tc-99m pertechnetate in the tissues of normal and arthritic joints of rabbits.

Experimental arthritis was induced in mature New Zealand white rabbits by sensitization to ovalbumin (in complete adjuvant) followed by an intra-articular injection of this antigen into one knee joint. The contralateral joint which served as a control was injected with saline.

Two weeks after the intra-articular injection, rabbits were injected I.V. with either 1 mCi Tc-99m pyrophosphate or 2 mCi Tc-99m pertechnetate. Imaging and joint dissection were done at 2 hrs for pyrophosphate and at 20 min for TcO_4^-.

Images of rabbits injected with pertechnetate showed a 42% increase in uptake in the inflammed joint while the pyrophosphate injected rabbits had a 56% increase in uptake compared to the control side.

The knee joints of rabbits were dissected to determine which tissues accounted for the increased uptake.

		% Dose/gram ± S.D.	
		Pertechnetate	Pyrophosphate
Bone:	Inflammed	0.029±0.006	0.085±0.018
	Control	0.021±0.004	0.053±0.009
Soft Tissue: *	Inflammed	0.051±0.019	0.017±0.014
	Control	0.034±0.017	0.010±0.007

*includes patella, menisci, tendons, ligaments, marrow, synovium, synovial fluid and fat pad

With both agents inflammed joints showed increased uptake over normal joints for all tissues. With pertechnetate the major uptake is in soft tissues, but with pyrophosphate, bone uptake accounts for most of the localization.

TECHNETIUM-99m ANTIMONY COLLOID BONE MARROW IMAGING WITHIN 24 HOURS OF SUBCAPITAL FRACTURE TO ASSESS VASCULARITY OF THE FEMORAL HEAD. *J.H. Turner, A.A. Martindale, and Q.P.W. Olsthoorn. Fremantle Hospital, Western Australia.*

Subcapital femoral neck fracture often compromises the blood supply to the head of femur and in the acute stage viability cannot be determined by X-rays. Tc-99m antimony colloid bone marrow (BM) imaging within 24 hours of subcapital fracture is currently being evaluated in preoperative assessment of blood supply of the femoral head.

In an experimental study avascularity of the right femoral head was produced in 12 rabbits by subcapital osteotomy. These femoral heads were pinned with a fine Kirschner wire and the BM imaged with Tc-99m antimony colloid within 24 hours of surgery. No activity was observed in the right femoral head in any of the 12 rabbits. Preoperative images and images of femoral heads pinned without fracture of the femoral neck in an additional 3 rabbits were normal. X-ray abnormalities did not become apparent in the avascular femoral heads for 3 weeks. Morphological abnormalities were first seen in femoral head BM cells 3 days after loss of blood supply but RNA synthesis in such cells in the rabbit has been shown to cease within 12 hours and this early impairment of cell function was demonstrated by Tc-99m antimony colloid imaging. Tc-99m antimony colloid was compared Tc-99m sulphur colloid BM imaging under standard conditions in 4 rabbits and the uniform superiority of Tc-99m antimony colloid was attributed to preferential BM uptake of the smaller colloidal particles.

Evaluation of preoperative femoral head BM imaging after subcapital fracture requires further follow up but satisfactory images have been obtained with Tc-99m antimony colloid in the 15 patients studied to date.

BONE IMAGES AFTER PARATHYROIDECTOMY (PRT): Wilfrido M. Sy, Albert J. Smith, Ramon S. Lao, The Brooklyn Hospital, Brooklyn, New York.

Five adults who had been on dialysis for 4 to 7 years showed marked parathyroid hyperplasia on subtotal PRT. All were on dialysis for at least 3 yrs before surgery. 99mTc-SnPYP serial scans consisted of 5:1 ant and post views and scintigraphs of selected areas using a WFV camera were obtained. One patient was studied for 28 mos, three for 12-14 mos, and one for 7 mos after PRT. Absolute cts and ID/sq/cm/min were obtained in selected areas in two patients.

Decreased activity was observed in calvarium, mandible, hands, metaphyses of large bones, patella and sometimes ribs, occurring usually 12 mos after PRT. In the first four mos, minimal or no change was usually seen. In one patient who was imaged for 28 mos, the pre- and latest post-PRT images showed marked difference in activity and absolute area cts. But scan changes lagged behind the dramatic disappearance of pruritus and bone pain. These were present in all before PRT. In x-ray evident sclerosis decreased activity was more discernible on scan despite lack of associated x-ray changes. Although there was definite symmetric decrement in bone activity, residual abnormality persisted. This paralleled the alkaline phosphatase which stayed abnormally high despite initial sharp drop.

From these data we conclude that scan activity change reflecting probably bone morbidity changes occur after PRT, but complete reversal was not achieved even after 28 months.

INCREASED SPECIFICITY OF VERTEBRAL BONE SCANS. S. DeLuca, K.M. McKusick, F. Wisneltery, H.W. Strauss. Massachusetts General Hospital, Boston, Massachusetts.

Patterns of 99m Tc MDP distribution in diseased vertebra were classified and correlated with x-ray and clinical data in 98 adult patients to determine the increased specificity of bone scanning. Bone images were obtained 2 hours following IV infection of 20 millicuries of Tc-99 MDP using a whole body imaging device and 500 K spot images were taken with an Anger camera equipped with a parallel hole collimator. Four patterns were recognized: 1. entire vertebra diffused; 2. transverse band activity through the body; 3. lateral activity in the body (pedicular); and 4. asymmetric activity lateral to the body. (Scanning results are shown below).

	PATTERNS			
	1	2	3	4
DJD	7	2		20
TRAUMA		21		
METASTATIC		13	2	1
OSTEOMYELITIS			1	

The presence of lateral eccentric activity outside the vertebra indicates degenerative disease, whereas, lateral (pedicular) vertebral activity is not uncommonly associated with metastasis. Transverse band-like activity is not specific for vertebral collapse, but occurs occasionally in the presence of metastatic disease as well as osteopenia and degenerative disease.

THE PRESENT STATE OF INTERNAL RADIATION THERAPY WITH INTRA-ARTERIAL YTTRIUM-90 RESIN SPHERES. E.D.Grady. Georgia Institute of Technology, Atlanta, GA.

One hundred twenty patients have been treated by the author and his associates using intra-arterial Yttrium-90 particles too large to pass through the capillaries. The liver has been shown to be the organ most suitable for this method. It now appears that using an improved product and improved methods of administration with better patient selection this is the simplest and best method available for treating inoperable and localized liver cancer, either primary or metastatic. Sixteen of the last twenty-six cases treated have had good objective regression of cancer, improvement of symptoms and prolongation of life. The treatment is relatively simple and associated with few side effects. The material is being produced for experimental use at the Nuclear Research Center of Georgia Institute of Technology and is distributed through the Medical Research Foundation.

THE USE OF ISOTOPE ANGIOGRAPHY TO ASSESS THE BLOOD SUPPLY OF REIMPLANTED DIGITS. A.Z. Rudavsky, B. Strauch, A. Daniller and C.M. Moss. North Central Bronx Hospital and The Albert Einstein College of Medicine, Bronx, NY.

This study was undertaken to determine the usefulness of isotope angiography for the evaluation of perfusion of reimplanted digits.

Isotope angiography was performed by obtaining serial images of the reimplanted digits and associated hand following bolus injection of technetium-99m pertechnetate into a contralateral antecubital vein. Static images of the affected digits and hand were obtained five minutes after completion of the dynamic study. Ten patients who underwent reimplantation of one or more digits following traumatic amputation were studied by this technique. Isotope angiography demonstrated direct arterial perfusion and/or collateral blood supply in each case.

Isotope angiography appears to be a useful procedure for evaluation of the blood supply to reimplanted digits. It is concluded that the ultimate survival of reimplanted digits is not dependent on continued patency of the digital artery anastamosis.

UPTAKE OF BONE-SEEKING RADIONUCLIDES BY MALIGNANT SOFT-TISSUE TUMORS. L.D. Samuels, Hadassah University Hospital, Jerusalem, Israel.

Uptake of bone-seeking radionuclides in soft tissue malignant tumors was first shown with Sr-87m by Samuels and others. This series has been extended by a study of the significance of uptake of Tc-99m phosphate complexes in an extended series of patients with a variety of tumors.

In a large series of patients, both children and adults, usually with clinical suspicion of malignant tumors, bone scans were performed, most recently entirely with Tc-99m MDP. Unusual soft tissue uptake was noted, and these 40 scans where possible and by followup surgery and pathological confirmation of diagnosis.

Although the mechanism for the increased uptake appears more-related to disturbed calcium balance in tumors than to altered blood flow, no definite explanation has yet been made of the phenomenon. Examples will be shown of uptake of bone-seeking isotopes in malignant tumors of the mediastinum, pelvis, abdomen, breast, thorax and muscle, and comparisons to Ga-67 scans made.

Judicious use of bone-seeking radionuclides to localize soft-tissue malignancies, both primary and secondary, is encouraged.

ANALYSIS OF DIFFUSE GALLIUM LUNG UPTAKE. A. Kubo, Y. Takagi, Y. Ando and S. Hashimoto. Keio University, School of Medicine, Tokyo, Japan.

Ga-67 scan was performed on 3224 patients with various diseases in Keio University and it's branch hospitals, from Dec. 1973 to May 1978. One hundred and ninety-three (6.0%) showed bilateral diffuse lung uptake of Ga-67. We graded ++ when the accumulation of Ga-67 over the lung was as high as or higher than that over the liver, + when the accumulation over the lung was lower than that over the liver, and ± when there was slight diffuse accumula-

tion of Ga-67 seen in the lung. Among the 193 cases, 39 showed extremely high Ga-67 lung uptake of grade ++. The factors causing diffuse Ga-67 lung uptake were investigated in these 39 cases.

Most of these 39 cases had various malignant diseases as a primary disease(11 of malignant lymphoma, 10 of lung ca, 2 of breast ca, 2 of colon ca and 6 of other ca). About one third of these 39 cases showed no significant abnormal findings on the chest x-ray. Of the 32 cases of malignant diseases, 25 were given a great amount of anticancerous drugs before Ga-67 scan. Eleven cases in which some bacteria or true fungi were observed by sputum culture, were the most likely to be "opportunistic infection" associated with decreased immunity. Eighteen cases in which no bacteria or true fungi were observed, all received various kinds of anticancerous drugs. Of these 18 cases, most cases were considered compatible with "drug-induced pneumonitis" except 3 of diffuse lung metastases and 1 of bilateral pleural effusion.

Ga-67 scan seems to be useful for a early detection of pulmonary infection or drug-induced pneumonitis associated with any malignant diseases being treated.

INTRA-ARTERIAL HEPATIC INFUSION OF Tc-99m-MAA: A PREDICTIVE TEST OF CHEMOTHERAPEUTIC RESPONSE OF LIVER TUMORS. W.D.Kaplan, W.D.Ensminger, E.H.Smith, C.J.D'Orsi, D.C. Levin. Department of Radiology, Joint Program in Nuclear Medicine, Harvard Medical School, Sidney Farber Cancer Institute, Boston, MA.

Hepatic metastases carry a grave prognosis with a median survival of less than 2½ months reported. Hepatic artery infusion of chemotherapeutic agents has produced tumor regression in patients in whom systemic therapy with the same agent had been unsuccessful.

Based on our earlier experiences showing that hepatic artery infusion of Tc-99m-sulfur colloid (SC) was a better indication of drug distribution than contrast angiography, we have utilized the perfusion patterns from arterial infusions of Tc-99m-macroaggregated albumin (MAA) to predict the response to chemotherapy.

Twenty patients with baseline IV Tc-99m-SC liver scans for liver tumors were studied. Following placement of hepatic catheters, 4.0mCi of Tc-99m-MAA (in 0.2ml) was infused by a mechanical pump at flow rates of 10-21ml/hr. Anterior 500,000 count perfusion images were obtained.

Prediction of chemotherapeutic response was based upon Tc-99m-MAA perfusion of focal hepatic defects. Prediction of no drug response was made if focal defects showed no perfusion or extrahepatic collections of radioaggregates were seen. Response to therapy was equated with a decrease in focal defect size, hepatic size, or both.

Seventeen of 20 patients were correctly identified. Two patients who did not respond despite tumor uptake had unexpected arterial thrombosis and a change in catheter position. This technique has the potential for directing catheter placement, precisely defining drug flow rates, and predicting responders to intra-arterial therapy.

TUMORAL CALCINOSIS: SCINTIGRAPHIC STUDIES OF AN AFFECTED FAMILY. S. Balachandran, Y. Abbud, M. J. Prince and A. B. Chausmer. University of Texas Medical Branch, Galveston, TX.

Tumoral Calcinosis is a rare pattern of ectopic calcification characterized by large, nodular, periarticular deposits of amorphous calcium phosphate. The disease has its onset in childhood and is associated with normocalcemia, hyperphosphatemia, and a familial distribution. A large family in which 7 of 13 siblings had demonstrable clinical, radiologic, and pathologic findings of tumoral calcinosis was evaluated. The purposes were to compare the efficacy of bone scintiscans with serum phosphorus levels in detecting subclinical disease early in asymptomatic siblings and to assess therapeutic results in affected family members following initiation of phosphate depletion therapy. History, physical exam, serum calcium, serum phosphorus, and bone scintiscans were performed in 12 of 13 siblings. All the affected siblings had markedly elevated serum phosphorus levels and abnormal bone scintiscans, while the unaffected siblings had normal serum phosphorus levels and normal bone scintiscans. All the siblings, affected and unaffected, were normocalcemic. After initiation of phosphate depletion therapy, gross changes in the appearance of some of the lesions were detected on bone scintiscans, while the serum phosphorus levels remained significantly elevated and unchanged. These conclude that bone scintiscans are no more sensitive than serum phosphorus levels in detecting subclinical disease in asymptomatic siblings. However, they are very helpful in assessing the extent of the disease and changes following therapeutic intervention.

HEMOPOIETIC (Fe-52) VS RETICULOENDOTHELIAL (Tc-99m-S) MARROW DISTRIBUTION. E. Fordham, A. Ali, G. Rayudu, W. Knospe. Rush-Presbyterian-St. Luke's Medical Center, Chicago, Il. P. Richards, T. Ku. Brookhaven Natl. Lab., Upton, N.Y.

38 patients underwent marrow imaging ½ hour after IV administration of 10 mCi Tc-99m-S colloid, and 4 to 12 hours after IV administration of 0.5 mCi Fe-52-citrate. RE scans were evaluated for degree of central marrow activity, peripheral marrow expansion, hepatomegaly and splenomegaly. Fe-52 scans in the same patients were evaluated for degree of central marrow activity, peripheral marrow expansion and uptake in liver, spleen and other extramedullary foci.

37 of the 38 studies demonstrated exactly matching central and peripheral marrow distribution patterns. Included were 9 polycythemias, 9 myelofibroses, 6 chronic granulocyticleukemias (2 myelofibrotic), 3 essential thrombocytoses, 1 lymphoproliferative disorder, 1 multiple myeloma (post radiation), 3 lymphomas (2 post radiation), 1 malignant histiocytosis, 2 sickle cell anemias and 2 hypoplastic anemias.

Only 1 of the 38 showed dissimilar marrow distribution. A case of aplastic anemia had marked central and peripheral RE marrow activity; Fe-52 uptake was limited to the liver.

In these disorders there was no correlation between the presence and degree of hepatic and/or splenic enlargement and the presence and degree of Fe-52 uptake. Certain trends were apparent, however; splenomegaly without Fe-52 uptake was the rule in otherwise uncomplicated polycythemia. On the other hand, splenic erythropoiesis was quite common in myelofibrosis, particularly with increasing central marrow failure. Hepatic Fe-52 uptake was common in chronic granulocytic leukemia (splenic uptake to lesser degree), often without significant organomegaly.

THE VALUE OF BONE SCANNING IN THE EARLY RECOGNITION OF DELIBERATE CHILD ABUSE. G.N. Sfakianakis, G.M. Haase, V.N. Ortiz, and T.S. Morse. Children's Hospital, Columbus, OH.

Subtle fractures may be missed or inadequately delineated on initial bone x-rays taken to diagnose the battered child syndrome. Radionuclide bone imaging was evaluated as a screening method to facilitate recognition of child abuse.

Forty four children suspected of having been battered underwent bone imaging at the time of initial presentation for treatment of trauma or burns. High resolution collimator gamma-camera polaroid imaging was performed 4 hr after 200 μCi/Kg Tc-99m-Diphosphonate iv injection. Twenty eight children had negative scans; they never showed x-ray evidence of skeletal injury although 10 were found to have been abused. In 16 children bone imaging demonstrated focal hyperactivity compatible with fractures: three abused children had unifocal lesions due to fractures as shown by concurrent radiographs; six(4 abused) had more lesions on the scan than fractures showed by radiographs; in the remaining 7 children with positive scans simultaneous roentgenograms showed no fractures but later x-ray studies in 5 showed sclerosis or periosteal new bone formation. Six of these 7 children were found to be victims of abuse. Disparities between scan and x-rays were in the ribs(8 patients), long bones(9 patients) and mandible(1 patient). Although not all scan lesions were proven to be fractures, reinterpretation of x-rays(2 patients), followup x-rays(5 patients)and review of previous radiographs with fractures(1 patient)did reveal evidence of fractures. Skull fractures were missed(2 patients)by scans.

Bone scans can demonstrate occult skeletal lesions in suspected abuse cases at the initial medical encounter so that the cycle of progressive injury can be interrupted and the child removed from the offending environment.

10:30 a.m.-12:30 p.m. Room 206

IN VITRO RADIOASSAY

HEPATOBILIARY DISEASE

Chairman: Fuad S. Ashkar
Co-Chairman: Marie Perlstein

HEPATOBILIARY DISEASE IN PERSPECTIVE. Fuad S. Ashkar, Jackson Memorial Hospital, Miami, FL.

RADIOASSAY (RIA) FOR ANTIBODY TO HEPATITIS B CORE ANTIGEN (HB_cAb) F. Ashkar, F. Block, M. Hourani, and A. Serafini, Nuclear Medicine, University of Miami School of Medicine, Jackson Memorial Hospital, Miami, Florida.

RIA for antibody to hepatitis B core antigen determination is based upon the principle of competitive binding for hepatitis B core antigen (HB_cAg) coated beads, by 125 I-labeled antibody to HB_cAb and HB_cAb present in patient serum or recalcified plasma.

Our study was designed to establish the efficacy of RIA detection of HB_cAb, compared with previous detection methods. Three groups were evaluated: 1. A known panel of 40 experimental and control specimens, with variable antibody levels; 2. Samples from 941 blood donors randomly selected without regard to age or sex; 3. Specimens from 447 admissions to Jackson Memorial Hospital, Miami, Florida. Results of the panel showed the mean values from the data did not differ significantly from known standards values. Sensitivity: specimens at the greatest dilution (1:128) still exceed the percent neutralization of the negative serum. Specificity: in samples containing HB_sAg or HB_sAb, in addition to HB_cAb, their presence did not interfere with the assay for HB_cAb. Accuracy: less than 2% variability from expected values was present. Examination of data from healthy blood donors revealed 8.3% positive for HB_cAb, with corresponding HB_sAb positive in 8.3% of samples. Random hospital admissions demonstrated HB_cAb 27% positively in patients, with 23% HB_sAb positive, and 2% HB_sAg positive.

Radioassay for HB_cAb is a specific, sensitive, accurate method of detecting patients exposed to hepatitis B virus, that are acutely ill or chronic carriers; high titers are indicative of persistently viral replication.

FATTY ACID METABOLISM AND DRUG SUSCEPTIBILITY OF M. TUBERCULOSIS. E.E. Camargo, and H.N. Wagner, Jr. The Johns Hopkins Medical Institutions, Baltimore, MD.

We previously reported that radiometric measurement of differential oxidation of (1-C-14) fatty acid by mycobacteria could provide a basis for differentiation of species of these organisms. We have now investigated the relationship between fatty acid metabolism and drug resistance. Two similar strains of M. tuberculosis, H37Rv (susceptible to all drugs, S) and H37Rv (resistant to isoniazid, R) were compared. Both strains were suspended in 1 ml of 7H9 medium with 1 uCi of one of the fatty acids, from acetate to stearic, dissolved in alcohol or in catalase-bovine serum albumin (BSA). The C-14 carbon dioxide production was measured radiometrically. No significant difference between S and R was observed in the oxidation rates of lauric, myristic and palmitic in catalase-BSA. However, R showed significantly ($p<.001$) higher oxidation rates of octanoic, palmitic and stearic in alcohol. For M. avium serotype 1, resistant to all drugs, the oxidation rates for octanoic, palmitic and stearic were even higher. A comparison of the ability of these 3 organisms to produce niacin both in 7H9 and 7H11 (with .1% aspartic) media was then made. Filtrates of the media that supported growth of the organisms were assayed by the L. plantarum radiometric microbiologic method. The amounts of niacin produced by S increased from 1.15 $\times 10^{-4}$ pg/bacteria/day in 7H9 to 3.3×10^{-4} pg/bacteria/day in 7H11. The R strain, however, produced less niacin than S in both media: $.54\times10^{-4}$ pg/bacteria/day and 2.0×10^{-4} pg/bacteria/day, respectively, in 7H9 and 7H11. The extremely resistant species M. avium produced no niacin.

Our results suggest that drug resistance of M. tuberculosis is associated with an increased rate of oxidation of long chain fatty acids and reduced production of niacin.

PHYSIOLOGY AND METABOLISM OF BILE ACIDS. Laurence M. Demers, The M.S. Hershey Medical Center, Hershey, PA.

RADIOASSAY OF BILE ACIDS IN NORMALS AND HEPATOBILIARY DYSFUNCTION. Fuad S. Ashkar, M. Hourani, F. Block, and A. Serafini, Nuclear Medicine, University of Miami, School of Medicine, Jackson Memorial Hospital, Miami, Florida.

Radioassay (RIA) measurement of the bile acids Cholyglycine (CG) and Sulfolithocholylglycine (SLCG) has given the physician an extra tool to evaluate patients with hepatobiliary dysfunction. Bile acids are steriods derived from cholesterol in the liver and their blood level is the single most sensitive and specific indicator of liver disease.

CG and SLCG Radioassay test system is stabilized to extract the antigen bile acids from the protein. Following the antigen antibody complex formation, it is precipitated by polyethylene glycol, and centrifuged to separate the bound from the free portions. 38 patients consisting of normals, patients with liver disease, gall bladder disease, biliary obstructions and pancreatic disease were studied with liver function tests, hepato biliary scans and CG and SLCG blood levels.

The normal values for CG & SLCG is 0-60.0 and 0-80.0 ug/100 ml, in the fasting state. In 18 patients with gall bladder disease the range was 10-300 for SLCG and 10-780 for CG. In 10 pts. with liver disease and no evidence of cholecystitis and/or lithiasis the levels were 140-1650 for SLCG and 29-3200 for CG. In 3 pts. with a picture of biliary obstruction SLCG was 105-900 & CG, 740-2200, patients with pancreatitis and normals the range was 14-160 & 10-100 (some of these patients were not in fasting states). Radioassay of CG & SLCG in addition to being helpful in the diagnosis of liver disease can also play an important role in the management of people with biliary tract disease.

A RADIOMETRIC ASSAY FOR ALL ACTIVE FORMS OF VITAMIN B-6 IN BIOLOGICAL MATERIAL. T.R. Guilarte, and P.A. McIntyre. The Johns Hopkins Medical Institutions, Baltimore, MD.

Currently available methods for determination of vitamin B6 in biological materials are not satisfactory. The ideal method should be simple, sensitive, specific and able to measure all active forms of the vitamin, e.g., pyridoxine, pyridoxal, pyridoxamine, and their respective phosphorylated forms. We have developed a radiometric microbiological method which fulfills these criteria. Kloeckera brevis, a yeast whose growth is dependent on vitamin B6 was selected from among several microorganisms investigated. In the presence of free vitamin B6, the growth of this yeast was found to be proportional to the amount of the vitamin present. In addition, the 3 different forms of the free vitamin stimulated growth equally. The phosphorylated forms could be dephosphorylated before the test by either acid hydrolysis or enzymatic dephosphorylation using a phosphatase without interfering with the assay. In the presence of 1 uCi of (1-C-14)DL-valine the organism produced C-14 carbon dioxide proportional to the amount of the free vitamin B6. The sensitivity of the assay was 1 ng. The biologically inactive human metabolite of vitamin B6, 4-pyridoxic acid, did not stimulate production of C-14 carbon dioxide from valine. Thus the method is simple, sensitive, specific and responds equally to the 3 active free forms of the vitamin. It can be used for the measurement of vitamin B6 in biological fluids and foods.

2:00 p.m.-3:30 p.m. Room 210

CLINICAL SCIENCE

ENDOCRINE

Chairman: John E. Freitas
Co-Chairman: Marguerite T. Hays

COST EFFECTIVENESS OF ADRENAL IMAGING IN CUSHING'S SYNDROME. J.E. Freitas*, M.D. Gross, D.P. Swanson, and W.H. Beierwaltes. *William Beaumont Hospital, Royal Oak, MI. and University of Michigan Medical Center, Ann Arbor, MI.

Retrospective analysis of the medical records of 46 consecutive patients with Cushing's syndrome was performed to determine if routine adrenal imaging would reduce the total cost of their diagnostic evaluations. One patient did not have a confirmed final diagnosis and was excluded from further analysis. The remaining 45 previously untreated patients underwent adrenal imaging and an inpatient evaluation between 5/75 and 2/79. All patients received 1-2 mCi of I-131-iodomethyl-norcholesterol (NP-59) intravenously and were imaged with a gamma camera within 2-8 days post-injection. All patients were correctly categorized into 4 imaging patterns: I) Symmetric bilateral visualization - 26 with Cushing's disease, 3 with ectopic ACTH syndrome, II) Marked asymmetric visualization - 4 with adenomatous hyperplasia, III) Unilateral visualization - 7 with Cushing's adenoma, 2 with adrenal carcinoma, and IV) Bilateral non-visualization - 3 with adrenal carcinoma.

The average cost of the total diagnostic evaluation per patient without the scan versus with the scan (scan cost included) is shown below:

	all patients	scan patterns I	II	III	IV
without scan	$1381	$775	$2540	$2490	$2390
scan utilized	$ 940	$976	$ 750	$ 750	$1425

Since routine NP-59 adrenal imaging in Cushing's syndrome leads to a 32% cost reduction in the evaluation of the average patient, all patients with suspected Cushing's syndrome should undergo adrenal imaging prior to an inpatient evaluation.

DEMONSTRATION OF STEROID-PRODUCING GONADAL TUMORS BY EXTERNAL SCANNING WITH 6β-131-I-IODOMETHYL-19-NORCHOLEST-5(10)-EN-3β-OL, (NP-59). H. W. Wahner, P. C. Carpenter, R. M. Salassa, and D. S. Duick. Mayo Clinic and Mayo Foundation, Rochester, MN.

Benign adrenal cortical tumors and, occasionally, carcinomas have been successfully imaged with NP-59 in the past. This report concerns the successful imaging with NP-59 of (1) bilateral testicular Leydig's cell tumors producing both testosterone and cortisone in a 23-year-old male with Nelson's syndrome and bilateral enlarged testis and (2) a virilizing ovarian Leydig's cell tumor in a 58-year-old female, which was not detectable by CT or ultrasound. Both cases had surgical removal of the tumor. To define normal gonadal uptake, 87 adrenal scans performed in patients with suspected adrenal disease were reviewed for evidence of uptake in the gonadal region, and testicular uptake was measured in two patients with adrenocortical, but no evidence for gonadal, disease.

No discernable isotope accumulation was noted in the region of ovaries or testis in patients scanned for adrenal disease between 1 and 7 days after NP-59. Testicular uptake in two patients was 0.008 and 0.005% of the dose at 72 hours, about ten times less than in normal adrenal glands. Uptake decreased from a maximum at 24 hours, suggesting that blood background significantly contributed to this uptake. Uptake at 72 hours in the testis of the index patient was 0.17% (left) and 0.11% (right) and in the ovary of the other patient was 0.16%, well within the range of uptake seen in adrenal glands.

NP-59 can be used for the detection of certain gonadal neoplasias even when CT and ultrasound do not indicate a mass. The study thus may be helpful to identify a site for exploratory surgery.

ERRONEOUS NEGATIVE ADRENAL IMAGING WITH 131-I-6-BETA IODOMETHYL 19 NORCHOLESTEROL (131-I CHOL). L. Gordon, R.K. Mayfield, J.H. Levine, M.F. Lopes-Virella, J. Sagel, M.G. Buse. Medical University of South Carolina, Charleston, S. C.

Adrenal scanning with 131-I Chol is a new advance in the preoperative localization of tumors causing Cushing's syndrome. The primary source of adrenal cholesterol for steroidogenesis is a circulating lipoprotein pool. Adrenal adenomas concentrate the isotope, producing unilateral scan, whereas carcinomas almost never bind sufficient label to allow visualization. We report another cause for non-visualization of adrenals. A woman with suspected pituitary-dependent Cushing's disease was injected with 2 mCi 131-I Chol. No adrenal uptake or imaging occurred during 8 days of observation. The patient also had diabetes and severe hyperlipidemia-Cholesterol (Chol) 992 mg/dl, triglycerides (T.G.)6464 mg/dl. Lipoprotein electrophoresis revealed >90% of the total lipid to be chylomicra and VLDL. Fractionation of the patient's lipoprotein revealed 90% of the 131-I Chol to be bound to the chylomicra and VLDL with only 3% each bound to LDL and HDL. The patient was treated rigorously with diet, insulin and Clofibrate. After 1 month of therapy, Chol was 209, T.G. 255. Lipoprotein electrophoresis now revealed no chylomicra, 46% VLDL, 15% HDL, 38% LDL. One hour after repeat injection with 131-I Chol 35% of the isotope bound to VLDL, 34% to LDL and 18% to HDL. After 4 days the distribution was VLDL 29%, LDL 40%, HDL 26%. Both adrenal glands were visualized. Uptake was 0.8% on the right and 1% on the left. Conclusions: 1. Adrenal carcinoma is not the only cause of negative adrenal scans. 2. Abnormalities of circulating lipoproteins may affect adrenal uptake and imaging after injection of 131-I Chol. 3.Plasma lipids should be measured prior to adrenal scanning.

BONE MASS CHANGE WITH CALCITONIN THERAPY IN OSTEOPOROSIS, AS ASSESSED BY TOTAL BODY ACTIVATION ANALYSIS. C.H. Chesnut III, D.J. Baylink, W.B. Nelp, University Hospital, Seattle, Wa. and VA Hospital, Tacoma, Wa.

50 postmenopausal osteoporotic (PM-OP) females age 50-80 are participating in a 2 yr. controlled study of the effect of calcitonin (CT) in PM-OP; treated group (TG, n=26) receives 100 MRC units of synthetic salmon CT, 1200 mgm Ca CO_3 and 400 units vit. D2 daily, and control group (CG, n=24) receives only $CaCO_3$ and D2 in above dosage.

After 18 months of study participation, total body calcium by neutron activation analysis increased 2.24% ± .78 ($\bar{x}$ ± SEM) in TG and decreased 2.15% ± .89 CG. Intergroup differences and changes from baseline were significant ($p < .001$). Total urinary hydroxyproline (U-HP) decreased 4.45% ± in TG and increased 21.5% ± 12.63 in CG from baseline; non-dialyzable U-HP increased 22.19% ± 21.23 in TG and decreased 18.81% ± 17.04 in CG. Such changes were significant ($p < .02$) both between groups and from baseline. iPTH (n-terminal assay) increased, and serum PO_4 decreased, significantly ($p < .001$) in TG. No change in baseline was noted in TG in serum Ca or alkaline phosphatase, or in the urinary Ca/creatinine ratio. CT antibody (AB) increased significantly in 18/26 of TG; no correlation of AB level to other evaluated parameters was however noted. In TG no new spinal compression fractures were noted; clinical symptoms were subjectively improved. Preliminary iliac crest bone biopsy results in TG (n=5) revealed a decrease ($p < .001$) in % resorbing surface and an increase ($p < .05$) in % forming surface.

These preliminary data indicate that CT prevents bone mass loss, and increases bone mass above pre-treatment values, perhaps by decreasing bone resorption and slightly increasing bone formation (U-HP and bone biopsy data).

BONE MASS CHANGE WITH STANOZOLOL THERAPY IN OSTEOPOROSIS, AS ASSESSED BY TOTAL BODY ACTIVATION ANALYSIS. C.H. Chesnut III, D.J. Baylink, W.B. Nelp, University Hospital, Seattle, Wa., and VA Hospital, Tacoma, Wa.

43 postmenopausal osteoporotic (PM-OP) females age 50-80 are participating in a 2 yr. controlled double blind study of effects of the anabolic steroid stanozolol in PM-OP; treated group (TG) receives stanozolol 6 mgm po qd 3/4 weeks, and control group (CG) receives placebo on a similar

schedule. Both groups ingest 1000 mgm of dietary Ca qd.

Initial data assessment in 30 patients (15 TG, 15 CG) completing the study revealed total body calcium by neutron activation analysis to increase 4.43% ± 1.14 ($\bar{x}$ ± SEM) in TG and .37% ± 1.18 in CG. Intergroup differences, and change from baseline in TG, were significant ($p<.001$). Drug effect persisted throughout the 24 mo. period. Total urinary hydroxyproline (U-HP) decreased 3.34% ± 14.14 in TG and increased 36.90% ± 18.17 in CG from baseline; non-dialyzable U-HP increased 7.18% ± 10.92 in TG and decreased 6.58% ± 9.23 in CG. Such changes were significant between groups ($p<.001$) and from baseline ($p<.02$). iPTH (n-terminal assay) and urinary Ca/creatinine (U-Ca) decreased ($p<.001$) in TG, and serum Ca increased ($p<.001$) in TG with no significant change in CG in these parameters. Preliminary iliac crest bone biopsy results in TG (n=6) revealed a significant ($p<.001$) 70.71% ± 9.6 decrease in % resorbing surface over the 2 yr. study period. In TG no new spinal compression fractures were noted, and clinical symptoms were subjectively improved.

These preliminary data indicate a definite beneficial effect of stanozolol in increasing bone mass above pre-treatment levels; this beneficial effect could be explained by a primary (1°) decrease in U-Ca, or by a combined 1° decrease in both U-Ca and bone resorption.

EFFECT OF GROWTH HORMONE (GH) OR THYROXINE (T-4) THERAPY ON THE METAPHYSEAL UPTAKE OF Tc-99m-METHYLENE DIPHOSPHONATE IN GH OR T-4 DEFICIENT CHILDREN. W.C. Klingensmith III, G.J. Klingensmith, S. Tollefsen. U. of Colorado Medical Center, Denver, CO.

Children with short stature secondary to GH or T-4 deficiency often benefit from replacement therapy. However, in the case of GH, the hormone is scarce, must be administered intramuscularly three times per week, and usually one cannot determine a significant increase in linear growth velocity until four months after initiation of therapy. We postulated that quantification of the metaphyseal uptake of Tc-99m-methylene diphosphonate (TcMDP) might provide a more sensitive indicator of response to therapy. Nine children (8 GH deficient and 1 T-4 deficient) were studied before and periodically after initiation of therapy. One tenth the usual dose of TcMDP was injected and two hours later one anterior ten minute digital image of the knees and femurs was recorded using a medium sensitivity collimator. For each femur, regions of interest were placed on the distal femoral metaphysis and mid femoral shaft, and the metaphysis (cts/pixel) to shaft (cts/pixel) ratio was determined. None of five GH deficient patients who were studied after up to 34 days of GH showed a significant change from baseline. Three of five patients who had follow-up studies beyond 34 days showed significant increases in metaphyseal uptake: two GH deficient children had 75% increases after 35 and 68 days of GH therapy, and one T-4 deficient child had a 160% increase after 48 days of therapy. This early experience suggests that metaphyseal uptake of TcMDP may be useful in monitoring the results of hormonal therapy and may also be useful in some diagnostic problems.

SIGNIFICANCE OF NON-PALPABLE "COLD" SCINTIGRAPHIC THYROID DEFECTS IN PATIENTS FOLLOWING CHILDHOOD NECK RADIATION. M.D.Okerlund, J.Sommers, T. Sakmar, M.Galante, T. Hunt, and O. Clark. University of California, San Francisco, CA.

540 consecutive patients with remote past history of neck radiation were evaluated, including pinhole gamma camera photographs (150,000 counts) with Tc-99m pertechnetate. 31 had nonpalpable "cold" defects. In 18 of these the nonpalpable lesion was in a gland with a larger palpable lesion, and was solitary in 13. The two groups were then compared to determine the possible significance of a nonpalpable radiation-induced cold lesion as a first versus second diagnostic entity.

	Second lesion	Solitary lesion
Thyroiditis	2(11%)	5(38%)
Adenoma	7(39%)	5(38%)
Carcinoma	6(33%)	2(15%)
Involutional nodule	3(17%)	1(8%)

All such defects were found to be solid at surgery, and the pathologic results indicate (1)A radiation-induced nonpalpable nodule is much more likely to be malignant if it is the second lesion in the gland than if solitary (2) Multinodularity is not necessarily a sign of benignity after radiation (3)The commonest cause of nonpalpable solitary "cold" lesions is thyroiditis, followed by adenona, and only then by malignancy. Additionally only 2 malignancies (with both groups pooled)which were nonpalpable were associated with invasion or extraglandular spread. All results seem to mitigate against radical or aggressive therapy of solitary nonpalpable radiation-induced lesions, particularly if associated with other evidence of Hashimoto's thyroiditis such as irregular labelling, hypothyroidism, or positive antibody tests.

HISTOPATHOLOGY OF THYROID LESIONS THAT CAUSED DISCREPANT FINDINGS BETWEEN Tc-99m SCAN AND I-123 SCAN. U. Y. Ryo, P. Vaidya, A. Schneider, and S. M. Pinsky. Michael Reese Hospital and Medical Center, Chicago, IL.

Through a series of studies on comparison of I-123 and Tc-99m as thyroid imaging agent for past 4 years, we have experienced 40 cases with discrepant findings between Tc-99m and I-123 scans. Detailed histopathological findings of the thyroids were available for correlation with the scan findings in 12 of the 40 cases. In all but one case, Tc-99m scan was obtained before the I-123 scan and interval between the 2 scans ranged 2-43 days (mean: 8 days).

In 7 of the 12 cases, hot or warm lesion with Tc-99m became cold or cool with I-123; lesions were adenomatous nodule in 4, colloid nodule in 2, and thyroiditis in 1 case. In 2 cases with adenomatous nodule, there were microscopic foci of carcinoma in the adenoma. There was extrathyroidal uptake seen on Tc-99m scan but not seen on I-123 scan in 3 cases; the lesions were metastatic follicular Ca in 2, and the lesion was a pendulous colloid nodule with adenomatous foci in 1 case. A hot lesion seen only on Tc-99m scan and not seen on I-123 scan was a colloid adenoma with degenerative changes and a warm lesion seen only on I-123 scan was a small adenomatous nodule containing microscopic foci of Ca. Though, carcinomas were present in 3 cases the microscopic foci were not attributable to be the cause of the discrepant scan findings.

Contrary to series of reports, our results indicate that benign thyroid lesions are more likely cause of discrepant finding between Tc-99m scan and I-123 scan. A true extrathyroidal uptake on Tc-99m scan may indicate high probability of metastatic follicular carcinoma.

THALLIUM CHLORIDE-201 (T1C1-201)THYROIDAL UPTAKE AND ITS CONTROL BY TSH. M.L.Maayan, E.M.Volpert, E.J.Fine, E.M.Lopez, J.Eisenberg, N.A.Solomon and A.Kyriakakos, V.A.Med.Ctr. and SUNY, Brooklyn, NY

Patients injected with T1C1-201 for myocardial scanning present good thyroidal visualization. Serial determinations in mice injected with T1C1-201 indicated its concentration in kidney>thyroid >heart>liver>skeletal muscle. This was not relatable to blood flow alone since the biological half life($T_{1/2}$)in serum(2½')is much shorter than the thyroidal(53-55 hr)in human subjects and experimental animals. Moreover,the T1C1-201 1 hr Thyroid /Serum Concentration Ratio(T/S)was comparable to that of I-131 and Tc-99m, indicating presence of a gradient for T1C1-201 also. Increase of endogenous TSH induced by PTU led to a significant rise in the T/S for Tc-99m, I-131 and T1C1-201,while TSH inhibition with L-thyroxine led to a decrease in the T/S for Tc-99m and T1C1-201. In vitro the Thyroid/Medium Concentration Ratio (T/M) of Tc-99m and T1C1-201 was decreased after a 20'incubation in presence of ouabain, an inhibitor of the Na,K, sensitive ATP-ase.However, perchlorate given in vitro or in vivo failed to diminish the T1C1-201 T/M and T/S ratios or to affect its $T_{1/2}$ in human subjects,while T/M was depressed by KC1 substitution for NaCl in the medium. Conclusions: a.T1C1-

201 is concentrated in the thyroid by a process of active transport which is TSH dependent. b. Its inhibition by K but not by perchlorate suggests sites with different polarities within the active transport system or a second active transport system, ATP-ase and TSH dependent.

2:00 p.m.-3:30 p.m. Room 211

CLINICAL APPLICATIONS

GASTROENTEROLOGY/PEDIATRICS

Chairman: John A. Gantz
Co-Chairman: Judith E. Ho

LIVER SCAN PATTERNS IN PARTIAL BUDD-CHIARI SYNDROME. P.R. Bradley-Moore and J.L. Doppman. NIH., Bethesda, Md. 20015.

We describe two less well known liver scan patterns of the Partial Budd-Chiari syndrome.

Well known are "classical" upper posterior central prominence due to caudate hypertrophy, hepatomegaly with or without tracer inhomogeneity, the normal pattern, the cirrhosis pattern, the pattern of multiple secondaries, normal sized or small liver with diminished or almost no uptake, and left lobe rounded with excess marrow uptake. These portray the complete syndrome.

The Partial Budd-Chiari syndrome, less well known, is caused by thrombosis of some but not all of the hepatic veins, and thus may give segmental loss at any site.

Two cases, presenting with hepatomegaly and ascites, had multiple Tc-99m Sulfur Colloid scans, one series showing upper posterior central tracer deficit with rapid change in subsequent months then slow return to normal, the other patient showing permanent loss of the left lobe only. Hepatic venography diagnosed Partial Budd-Chiari syndrome.

We conclude the Partial Budd-Chiari liver scan is best recognised by; segmental or subsegmental tracer deficit; rapidity of segmental change; return towards normal.

SERENDIPITY IN TECHNETIUM-99m DIMETHYL IMINODIACETIC ACID (HIDA) CHOLESCINTIGRAPHY. H. S. Weissmann, M. S. Frank and L. M. Freeman. Montefiore Hospital and Medical Center and Albert Einstein College of Medicine, Bronx, N. Y.

Tc-99m dimethyl iminodiacetic acid (HIDA) cholescintigraphy has proven to be an extremely useful method for evaluating biliary disease. Additionally, we have often discovered interesting and diagnostically significant non-biliary pathology. In many situations, these abnormalities rather than biliary tract disease represented the cause of the patient's pain. These serendipitous findings discovered in over 500 cholescintigraphic studies may be best categorized by one of the four phases of the study in which they presented themselves. These are: I. Blood Pool Phase (0-3 min. post injection) - abnormal perfusion patterns, organomegaly and organ displacement can be evaluated, e.g., cardiovascular abnormalities, such as specific cardiac chamber enlargement, pericardial effusion and aortic aneurysm, ascites and splenomegaly. II. Hepatocyte Phase (approx. 5-20 min. p.i.) - intrahepatic space-occupying processes are readily detectable, e.g., metastatic disease, hepatoma, abscess, hematoma, etc. III. Renal Phase (15% of HIDA is excreted by the kidneys in the first 10-15 min.). Absence of renal activity may indicate kidney failure. Obstructive uropathy, renal mass lesions and renal displacement by extrinsic masses or retroperitoneal hemorrhage have all been noted. IV. Intestinal Phase (from 30 min. on in most patients). Mass lesions are detected by separation or displacement of bowel loops ("photon-deficient" areas). Pancreatic and other retroperitoneal masses and intra-abdominal abscesses, e.g., periappendiceal, have been detected in this fashion. Duodenal stasis or "hold up" have also been an indicator of pancreatic disease. Bowel malrotations represent another abnormality detected in this phase.

SALIVARY GLAND IMAGING. G.S. Freedman, R.A. Knobelman, J.M. Dowaliby, and C.A. LaVallee. Temple Medical Center, New Haven, CT.

Improved gamma camera resolution combined with electonic magnification and improved image formating allows significant improvements in the quality and diagnostic efficacy of salivary gland imaging. The methodology includes a flow study, sequential 5-minute images for 20 minutes then oblique views with magnification in the RAO and LAO positions, then anterior and oblique views after stimulation of the gland with lemon. Twenty patients have been studied by these improved methods during the past year. In addition to the consistent morphological demonstration of the parotid and submandibular gland, the excretory salivary ducts are consistently demonstrated. Pathological entities encountered include: 1. Benign and malignant tumors. 2. Congenital sublingual cyst. 3. Obstructing calculi within the gland and within the ducts. 4. Metastatic disease. 5. Fibrotic changes. In some instances these conditions were also studied by sialography, computerized axial tomography, and ultrasound. Comparison of the relative values of the various imaging modality are presented.

RADIOCOPPER KINETIC STUDIES IN THE DIAGNOSIS OF WILSON'S DISEASE. H. W. Wahner and N. P. Goldstein. Mayo Clinic and Mayo Foundation, Rochester, MN.

The diagnosis of typical Wilson's disease (WD) is made by (1) Kayser-Fleischer rings (KFR), (2) <20.0 mg/dl serum ceruloplasmin, (3) hepatic copper >50 mcg/g dry tissue, and (4) urinary copper >100 mcg/24 hrs. However, 5% of WD patients have normal ceruloplasmin. Several liver diseases may show KFR and high liver and urine copper. Drugs may alter urinary copper levels. 64-Cu kinetic studies were performed to evaluate their diagnostic usefulness in difficult diagnostic cases.

Studies (intravenous 64-Cu) were performed in 15 control subjects, 19 symptomatic WD, 6 asymptomatic WD, 7 obligatory WD heterozygotes, 6 primary biliary cirrhosis (PBC), and 3 with WD and normal ceruloplasmin. Urinary and fecal 64-Cu excretion readily separated the control subjects and WD patients (both symptomatic and asymptomatic). However, there was overlap of the WD and PBC patients. These two groups had high urinary and/or low fecal excretion of 64-Cu. The study of total plasma 64-Cu, and more specifically incorporation in ceruloplasmin, always identified WD (symptomatic or asymptomatic) since this was the only group that failed to show incorporation of 64-Cu in ceruloplasmin. Prior treatment with penicillamine or administration of penicillamine during the study did not alter the absence of 64-Cu incorporation into ceruloplasmin, although the urinary and/or fecal excretion of 64-Cu were altered. Study of the ceruloplasmin incorporation for 72 hours after intravenous injection of 800-1000 µCi of 64-Cu chloride without the necessity of measuring urinary and fecal 64-Cu excretion is a reliable and practical test for the diagnosis of WD, both typical and atypical in presentation.

COMBINED DYNAMIC VENOGRAPHY, AORTOGRAPHY AND STATIC MULTI-ORGAN IMAGING IN THE PREOPERATIVE DIFFERENTIAL DIAGNOSIS OF ABDOMINAL TUMORS IN CHILDREN. L.D. Samuels and N. Ramu, Hadassah University Hospital, Jerusalem, Israel.

This study was undertaken to develop an improved method for preoperative differential diagnosis of pediatric abdominal tumors with non-invasive nuclear medical techniques.

Tc-99m TC, 1-3mCi, is injected via foot or leg vein and inferior venacavagram (IVC) acquired on serial frames of a

multiimager, followed by static liver-spleen imaging.Tc-99m DTPA or glucoheptonate, 3-10mCi, are then injected via arm or jugular vein and abdominal aortography also acquired on multi-imager for 30-90",followed by static imaging of combined liver-spleen-kidneys. Finally, static brain scans are obtained as part of metastatic workup, without additional radionuclide administration. In some cases Tc-99m MDP is substituted for DTPA for aortography and renal imaging, followed by static skeletal imaging after 2-3 hours.

I (LDS) have previously described nuclear medicine methods for static multi-organ imaging of abdominal tumors in children, allowing more-prompt and specific surgical intervention. The present technique provides much more information, replaces the roentgenographic IVC and angiography in selected cases and provides specific preoperative differential diagnosis in over 90% of our series of cases.

The technique will be illustrated for the common neoplasms Wilms' tumor and adrenal neuroblastoma as well as less-frequent abdominal lymphomas, hepatoma and renal cyst and hematoma.

Since the entire sequence of procedures may be completed within one hour without advance preparation of the child, prompt and more-specific surgical treatment is facilitated, with expected improved morbidity and long-term survival.

HEPATOBILIARY SCINTIGRAPHY WITH TC-99m PIPIDA IN INFANTS AND CHILDREN. M. Majd, R. P. Altman and R.C. Reba. Children's Hospital National Medical Center, Washington,DC.

Twenty-two Tc-99m PIPIDA biliary scans were obtained in 16 patients ranging in age from 11 days to 5 years. Twelve examinations were performed in 9 neonates with persistent jaundice. One was done in an infant krown to have alpha-1 antitrypsin deficiency. The other 9 studies were performed in 7 patients having previous Kasai portoenterostomy for biliary atresia. In the group of jaundiced neonates there were 3 cases of biliary atresia, 4 with presumed hepatitis and 2 with cholestasis due to prolonged hyperalimentation. All 3 patients with biliary atresia showed an obstructive pattern with no demonstrable excretion into the intestinal tract. A repeat examination in one of them after administration of phenobarbital showed no change in the scan pattern. In 4 patients with presumed neonatal hepatitis, one showed obstructive pattern similar to that of biliary atresia. The other 3 had normal scans. One of the 2 patients with prolonged hyperalimentation initially showed minimal excretion of radionuclide, but a repeat scan after administration of phenobarbital was normal. The initial scan in the other case showed no demonstrable excretion, but a repeat scan one month later was normal. The studies in the patients after Kasai portoenterostomy showed excretion of radionuclide except in one case with cirrhosis. In another case a bile cyst was demonstrated. The results of this study suggest that (1) Tc-99m PIPIDA hepatobiliary scintigraphy is useful in differential diagnosis of biliary atresia from other causes of neonatal jaundice, (2) pretreatment with phenobarbital reduces the number of false positive scans, and (3) it is useful in follow-up evaluation of Kasai portoenterostomy for patency of the anastomosis and detection of the complications.

THE RADIONUCLIDE DETECTION OF GASTROESOPHAGEAL REFLUX AND ASPIRATION IN CHILDREN. S. Heyman, J. A. Kirkpatrick, H. S. Winter, and S. Treves. Harvard Medical School and Children's Hospital Medical Center, Boston, MA

Gastroesophageal reflux is associated with several complications. Recurrent pulmonary infections are presumably due to the aspiration of gastric contents. Radiographic studies have been relatively insensitive, while pH monitoring and manometry cannot detect aspiration. A radionuclide (RN) method was developed to provide prolonged monitoring, utilizing a milk-Tc-99m sulfur colloid mixture (dose 1 mCi). Animal and laboratory studies confirmed the stability of the radiopharmaceutical.

Sequential images of the stomach and thorax are recorded on the computer at 1 minute intervals for 1 hour in the anterior projection. No maneuvers are employed to facillitate reflux. Further images are obtained at 2 and 24 hours. Time activity curves are obtained from the stomach, esophagus, and abnormal foci. Together with enhanced computer images, these reveal the presence and frequency of reflux, the presence of aspiration and the gastric emptying rate. Phantom studies showed that volumes of 0.025 ml could be detected.

To date, 124 RN studies have been performed, 61 being positive for reflux. Aspiration occurred in 5. Fifty-four patients had barium studies (Ba) within one week of the RN studies. Both were positive in 8 (14.8%) and both negative in 26 (48.2%). Reflux was present in the RN study alone in 16 (29.6%) and in the Ba study only in 4 (7.4%). Thus, the Ba study was positive in 22.2% and the RN study in 44.4%, reflecting the greater sensitivity. Aspiration occurred in 2 RN studies, but none of the Ba studies. The study is physiological, easy to perform, and merits further evaluation.

RADIONUCLIDE EVALUATION OF GASTROESOPHAGEAL REFLUX IN CHILDREN. J.J. Conway, S.C. Weiss, S.R. Luck, and R.I. Goldstein. The Children's Memorial Hospital, Chicago, IL.

Gastroesophageal reflux appears related to respiratory disorders in children. Patients with asthma, chronic lung disease of unknown origin, sleep apnea and sudden infant death syndrome have an increased incidence of gastroesophageal reflux.

The incidence of gastroesophageal reflux varies significantly between institutions and is probably related to the aggressiveness of the radiologist in seeking the diagnosis. Malmud's technique of radionuclide diagnosis has been adapted to children and is indeed a more sensitive modality.

A total of 36 radionuclide and x-ray studies were compared. 27 of 30 or 90% were positive with the radionuclide technique and only 10 of 30 or 33% were positive with the x-ray technique. Most of the radionuclide studies were performed without abdominal pressure in a supine position after instilling the radionuclide into the stomach via a nasogastric tube. Computer analysis from regions of interest over the esophagus area was the most sensitive means of detecting reflux. Of interest, two episodes of apnea occurred in two children when reflux was not present.

If gastroesophageal reflux is sought, the more physiologic approach offered by the radionuclide technique is supported by its significantly greater sensitivity.

2:00 p.m.-3:30 p.m. Room 201

RADIOPHARMACEUTICAL CHEMISTRY POSTER SESSION II

Chairman: Frank P. Castronovo
Co-Chairman: Howard J. Glenn

A NEW LIPOSOME TYPE WITH IMPROVED DISTRIBUTION FOR IMAGING D. Hnatowich, B. Clancy, S. Kulprathipanja and T. O'Connell University of Massachusetts Medical Center, Worcester, Ma. and Massachusetts Institute of Technology, Cambridge, Ma.

Previous studies have consistantly reported preferential uptake of liposomes in the liver and spleen: a major disadvantage in imaging applications. However, biodistributions may be influenced by lipid composition; an attractive feature of liposomes still to be exploited. We are investigating several new liposome types with different charge to improve biodistribution for imaging. A measure of liposome charge is obtained by ion exchange; on AG 1 anion exchange columns, 84% of neutral, 39% of half-negative and 28% of conventional negative liposomes (lecithin,

dicetyl phosphate, cholesterol) are eluted under specific conditions. A new liposome type was prepared by replacing lecithin (DPPC) with cardiolipin (CL), a compound with a double negative charge at neutral pH. These liposomes showed 10% elution under identical column conditions, confirming their expected high negative charge. DPPL and CL liposomes, labeled with Ga-67 oxine, were administered IV to mice to obtain distribution at 2 hrs. The mean results for two preparations of each liposome type are listed below in percent injected dose per gram: each datum is the average of 10 animals.

	BLOOD	LIVER	SPLEEN	LUNG	KIDNEY	HEART	MUSCLE	BONE
DDPC	7.8	22.8	83.3	7.6	4.2	2.2	0.9	6.3
CL	3.2	6.0	4.7	2.8	1.9	2.0	2.0	8.7

These results show that accumulation of activity in certain tissues may be significantly altered with cardiolipin liposomes possessing high negative charges over that of conventional negative liposomes. The decreased accumulation in liver and spleen provides a decidedly improved biodistribution for imaging. This work supported in part by BRS Grant RR05712-07.

STUDIES ON THE BINDING OF A CHEMOTACTIC FACTOR, N-FORMYL-SELENOMETHIONINE-METHIONINE TO RABBIT NEUTROPHILS. Pavanaram K. Sripada, Richard P. Spencer, Grace Vitkauskas, Elmer L. Becker. University of Connecticut Health Center, Farmington, CT.

Certain N-formyl-peptides elicit chemotaxis, phagocytosis and lysosomal enzyme release by binding to a receptor on rabbit neutrophils. We synthesized the peptide N-formyl-selenomethionine-methionine (NFS) and compared its ability to elicit the above neutrophil responses with the S analog. Both cold and labeled (Se-75) selenomethionine were formylated in acetic anhydride and formic acid under nitrogen. After purification by TLC, the formyl derivative was condensed with the methyl ester of L-methionine to form the dipeptide; the ester was hydrolyzed to yield the free acid to study its biological activity and binding to rabbit neutrophils. This was done by using neutrophils obtained from the peritoneal cavity. The NFS elicited the expected biological responses of lysomal enzyme release and chemotaxis (although dipeptides are known to be less active than tripeptides). NFS also appears to bind to the same receptors as the other N-formyl-peptides. The S and Se compounds likely bind to the same sites. It was shown that the N-formyl-Se-75 compound had specific binding to neutrophils and competed with N-formyl-nor-leucine-leucine-phenylalanine. NFS, by virtue of its Se-75 label, may permit a study of the neutrophil membrane.

AN IMAGING METHOD FOR THE COMPETITIVE BINDING ASSESSMENT OF BETA RECEPTOR OCCUPANCY. H.W. Strauss, C. Homcy, and S. Kopiwoda. Massachusetts General Hospital, Boston, MA.

Hydroxybenzolpindolol (HBP) is a beta receptor blocker that can be iodinated without loss of its beta receptor binding interaction. We have investigated the biodistribution of 125-I-HBP in mice and determined its alterations after administration of propranolol (PROP). Biodistribution was determined in groups of six mice in 5, 15, 30 and 60 and 90 minutes. Although concentration was seen in all the organs, the liver has the highest concentration (20.4% dose/organ ± 2.3 SE) and the organ with the greatest change after propranolol was the lung (3.2% ± 0.4 to 1.8 ± .2% after 1 mg/kg PROP P<.001). To determine if this alteration in 125-I-HBP content in the lungs could be used as an index of beta receptor occupancy, studies were performed in four anesthetized rabbits, who received 100uCi of I-HBP intravenously. Following administration, the lung concentration of 125-I-HBP decreased only by 10% over a 30 minute interval of observation. In subsequent studies following the initial administration of 100uCi of 125-I-HBP, baseline images were recorded and sequential 200ug doses of PROP were administered with images recorded 1 minute after each dose. Quantification of lung activity revealed a loss of I-HBP activity at each dose up to a total PROP dose of 1200ug.

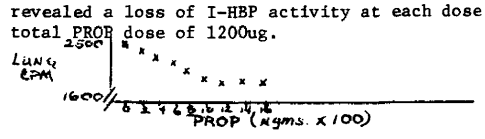

These studies suggest that I-HBP pulmonary imaging may be a useful means of determining the adequacy of beta receptor blockade.

ADRENAL MEDULLA IMAGING WITH I-131-ρ-IODOBENZYLGUANIDINE. J.L. Wu, D.M. Wieland, L.E. Brown, D.P. Swanson, and W.H. Beierwaltes. University of Michigan Hospital, Ann Arbor, MI.

The development of an adrenal (A.) medullary imaging agent has been actively pursued over the past decade. We herein report the tissue distribution in dogs of radiolabeled ortho and para isomers of the neuron blocking agent, iodobenzylguanidine (I), and the successful imaging of dog and primate A. medullae with the I-131 labeled para isomer.

The compounds were synthesized by radioiodide exchange in refluxing water. Radiochemical yields were 60-80%; specific activity 0.6-0.8 mCi/mg. Dogs were injected intravenously with 100 μCi of the I-125-compounds and sacrificed at various time intervals from 0.5 to 192 hours. Samples of 17 different tissues were excised and their radioactivity content determined. For imaging, dogs and rhesus monkeys were injected with 0.25-1.0 mCi of I-131-compound and posterior images obtained at intervals up to 6 days post injection using a standard gamma camera interfaced to a minicomputer.

The para-I showed higher affinity for the dog adrenal medulla, giving an uptake of 14.7% kg dose/gm at 72 hour with A. medulla-to-nontarget concentration ratios of 90, 600, 650 and 1300 for A. cortex, liver, kidney and blood respectively.

Distinct visualization of the A. medullae of three dogs were obtained starting at 2 days. Similar results were obtained in rhesus monkeys. The I-123-para isomer is undergoing preliminary human evaluation as a potential A. medulla, pheochromocytoma, and neuroblastoma imaging agent.

(ABSTRACT WITHDRAWN)

DEVELOPMENT OF A GENERATOR FOR IONIC GALLIUM-68. R.D. Neirinckx and M.A. Davis. Department of Radiology, Harvard Medical School, Boston, MA.

Two types of chromatographic generators that deliver ionic gallium-68 have been developed which could have prac-

tical commercial application. Both systems are based on organic adsorbents. Simple neutralization of their eluates suffices to make the product injectable or ready for further chemical manipulation.

In one system Ga-68 is eluted with dilute hydrofluoric acid (HF) from a strongly basic anion-exchange resin, Bio-Rad AG1-X8, onto which Ge-68 is strongly adsorbed. The distribution coefficients for germanium and gallium were measured as a function of the HF concentration. Up to 600 collections of Ga-68 have been made from experimental generators. The Ge-68 breakthrough is less than 10^{-3} percent, while Ga-68 yields are higher than 95 percent.

An alternative system is based on a chelate resin, which was synthesized by copolymerization of formaldehyde and pyrogallol. Very high distribution coefficients of germanium between this resin and dilute hydrochloric acid were obtained while gallium is only weakly adsorbed. Up to 600 collections of Ga-68 have been made from experimental generators, with Ge-68 breakthrough levels lower than 10^{-3} percent. Gallium-68 yields vary between 60 and 90 percent. These generators offer significant advantages for the synthesis of organ and disease specific Ga-68-radiopharmaceuticals compared to the currently available commercial generator which produces Ga-68 complexed with EDTA.

THE DESIGN AND TESTING OF AN AUTOMATED Ge-68/Ga-68 SOLVENT EXTRACTION GENERATOR. G.J. Ehrhardt, R. Head, L. Djordjevic, and M.J. Welch. Department of Radiology, Washington University School of Medicine, St. Louis, MO.

Gallium-68 is an ideal radionuclide for positron tomography because of its convenient 68 minute half life and its availability in a form readily converted to radiopharmaceuticals of interest from 280 day Ge-68 in the Ge-68/Ga-68 oxine solvent extraction generator. To enhance the practical usefulness of this generator system, we have designed, built, and tested an automated Ge-68/Ga-68 oxine solvent extraction generator. Considered in this design were the needs for routine simplicity of operation and the elimination of the possibility of operator errors in the solvent extraction procedure. Unfortunately, the design of the Tc99m MEK solvent extractor was not applicable due to our use of solvents heavier than water.

The solvent extractor employs two sequential separatory funnels, solenoid valves, and stirring motors, one for the initial extraction and the second for an aqueous backwash to guard against carry-over of Ge-68. Phase separation is achieved via golf-tee shaped hollow teflon buoys which float at the water/methylene chloride interface and intercept a photoelectric beam which controls its respective solenoid valve. The extractor is operated by a pre-programmed solid state electronics package.

The yield of Ga-68 oxine is 55%, with .001% Ge-68 breakthrough. By comparison, Ga-68 EDTA column generators exhibit yields of approximately 45% and Ge-68 breakthrough of .004%.

A LARGE SCALE EXTRACTION PROCEDURE FOR THE PURIFICATION OF A GA-67 BINDING GLYCOPROTEIN. D.H. Brown, J. E. Carlton, J. J. Rafter, and R.L. Hayes, Medical and Health Sciences Division, Oak Ridge Associated Universities (ORAU), Oak Ridge, TN.

A scaled up method has been developed for obtaining a 45,000 MW Ga-67-binding glycoprotein (GBGP) that occurs in minute amounts in Morris 5123C rat hepatomas. The amino acid composition, N-terminal amino acid residue, % nitrogen, and nonamino carbohydrate content of this molecule has been reported (Cancer Res. 38:4440-4444, 1978). Milligram quantities of the components are needed to complete its characterization and to determine its function and possible use in tumor detection. Our present technique permits us to process up to 20 grams of tumor in a 24-hr cycle. From the following procedure a preparation of the GBGP is obtained that contains 3 minor contaminants as determined by reverse phase HPLC and electrophoresis: The steps include high-speed centrifugation of the tumor homogenate in 0.25 M sucrose followed by extraction of the pellet for 1 hr in ice water. After centrifugation of the extract and concentration of the supernatant by ultrafiltration, the retentate is applied to a 600 ml DEAE Sephacel column. The GBGP is recovered in a symmetrical peak at 0.06 M NaCl from a 2 liter 0-0.1 M NaCl gradient in 0.01 M Tris pH 7.0. Since chromatography and electrophoresis of extracts of other tumor types yield products of a similar character, it is assumed the procedure reported here will provide a methodology applicable for the purification of this compound from other types of tissue. (ORAU operates under Contract No. EY-76-C-05-0033 with the U.S. Dept. of Energy. This work was supported by NCI, DHEW, Grant No. CA-11858.)

GENERATOR PRODUCTION OF MANGANESE-52m FOR POSITRON TOMOGRAPHY.* T.H. Ku, P. Richards, L.G. Stang, and T. Prach. Brookhaven National Laboratory, Upton, NY.

A generator system has been developed to produce the short-lived positron-emitter manganese-52m (21.1 m, 192.5% annihilation gammas). The generator column consists of 0.6 ml of AG 1X8 anion exchange resin on which the parent nuclide, 8.3 h iron-52, is absorbed as the chloride complex. Manganese or nickel targets are irradiated with medium-energy protons at the BLIP (Brookhaven Linac Isotope Producer) to prepare clinically useful quantities of high specific activity Fe-52. The total yields achievable are 120 mCi with a Mn target and several hundred millicuries with a Ni target. Fe-52 from a Mn target is purer (0.7% Fe-55 and no Fe-59 versus 2.0% Fe-55 and 0.17% Fe-59). However, when used in a generator, these impurities present no problem to the radionuclidic quality of Mn-52m since they are retained on the column. Carrier-free Mn-52m is eluted from the generator by passage of 2 ml 8N HCl with a yield greater than 90%. The eluate is evaporated to dryness and taken up in the desired buffer ready for use. The entire elution operation takes less than 10 minutes. No Fe-52 breakthrough has been detected. The generator is being evaluated at Brookhaven for regional myocardial perfusion using the PETT III tomographic instrument. Preliminary studies in a dog infarct model have shown promising results.

*Work done under Contract EY-76-C-02-0016 U.S.D.O.E.

EVALUATION OF RU-HIDA AS A POTENTIAL AGENT FOR DELAYED STUDIES OF THE BILIARY TRACT. E.R. Schachner, C. Gil, H. L. Atkins, P. Som, S.C. Srivastava, D.F. Sacker, and P. Richards. Brookhaven National Laboratory, Upton, NY.

Failure of early diagnosis of biliary atresia in children results in the development of cirrhosis and thereby death. Commonly used hepatobiliary agents are not ideal for follow-up studies because of their unfavorable physical properties or short half life. The excellent physical properties of Ru-97 (Energy 216 Kev., γ 86%, $T_{\frac{1}{2}}$ 2.9 d.) fulfill these criteria. Therefore, Ru-HIDA is being investigated as a potential hepatobiliary agent that would allow an improved diagnosis of the disease. For convenience, biodistribution studies were done with Ru-103-HIDA ($T_{\frac{1}{2}}$ 39.4 d.). Blood clearance in dogs with Tc-99m-PIPIDA and Ru-103-HIDA showed similar clearance rates ($T_{\frac{1}{2}} \simeq$ 2 min. for both). However, in rats the excretion of Ru-103-HIDA from the liver was slightly slower than Tc-99m-PIPIDA (3.42 $\pm$ 0.42 %/organ and 0.61 $\pm$ 0.06 %/organ for Ru-103-HIDA and Tc-99m-PIPIDA respectively, 2 hr. after injection). Images performed in rabbits and dogs with Ru-97-HIDA showed early uptake in liver and gallbladder, and slow excretion in the gastrointestinal tract. Studies were also performed in a rat model with biliary obstruction and the results showed a very high concentration in liver and kidneys compared to the normal (0.65 $\pm$ 0.05 %/g. vs. 0.20 $\pm$ 0.03 %/g. in liver and 2.20 $\pm$ 0.27 %/g. vs. 0.40 $\pm$ 0.10 %/g. in kidneys). These findings suggest that Ru-97-HIDA would be useful for performing delayed (e.g. 1-3 days) studies of the biliary tract.

THE USE OF AFFINITY CHROMATOGRAPHY TO DETERMINE SERUM PROTEIN-RADIOPHARMACEUTICAL INTERACTIONS. A.D. Nunn. The Upstate Medical Center, Syracuse, New York.

An HSA affinity adsorbent has been used as a model to study serum protein binding of some radiopharmaceuticals.

The affinity matrix was prepared from HSA and CNBr Sephadex using published procedures and packed into a column 17 x 0.7 cm diameter. The eluant was 0.05M tris, 0.1M NaCl buffer, pH 7.4 at 0.6 ml per minute. Aliquots of the renal agents I-131 hippuran and Tc-99m acetylcysteine were loaded onto the column and radioactivity in the eluate determined using an on-line detector or by counting collected fractions.

A clean separation of I-131 iodide contaminant in the hippuran was achieved in 30'. The level of contamination agreed with that found by paper chromatography. Elution of the hippuran (after the iodide) was, as expected, concentration dependent in the range 2.5-500 µg, with a symmetrical elution curve.

Elution curves of the Tc-99m were complex. A small component due to free Tc-99m was identified. Two other bands, both peaking earlier than hippuran but tailing badly were also seen. Apart from the tail the Tc-99m was eluted earlier than phenol red, which is known to bind extensively to serum proteins but has a high renal extraction efficiency. It thus appears that the lower than hippuran renal extraction efficiency of Tc-99m acetylcysteine is due to its known distribution in the extravascular space as a result of its low protein binding, possibly coupled with a lower affinity for the renal transport mechanism than hippuran. Preliminary results with Tc-99m DMS confirm that this is strongly bound to the albumin-eluting later than the phenol red.

RADIOBROMINATED STEROID ANALOGUES AS POTENTIAL AGENTS FOR PROSTATIC IMAGING. R.V. Pozderac, P.A. Weinhold, R.E. Counsell, A. Castonguay, W.H. Klausmeier, R.W.S. Skinner, V.A. Medical Center and the Dept. of Pharmacology, University of Michigan Ann Arbor, Mich.

A clinically useful prostatic imaging agent is not currently available. This report addresses data concerning a radiobrominated androgen and outlines an approach for the design and development of such an agent.

One hundred forty steroid analogues were evaluated for their receptor binding characteristics by an in vitro competitive binding assay, in which 5α-androstan-17β-ol-3-one-(H-3) (DHT-H-3) and the non-labeled steroid were incubated with minced rat prostate.

A series of brominated analogues were synthesized and evaluated by the above assay. Brominated analogues were selected not only for synthetic considerations, but also because such analogues would allow for the incorporation of Br-77, a radionuclide with suitable gamma emission characteristics for imaging. Several brominated analogues were found to inhibit the binding of DHT-H-3 (85 to 90%) in the subcellular fractions of the cytosol and purified nuclei of the rat prostate both in vitro and in vivo.

2-Bromo-17β-hydroxy-5α-androst-1-en-3-one was selected for further studies because of the availability of rapid and high yielding synthetic methodology.

In vitro data utilizing rat prostate minces indicated this steroid, labeled with Br-82, remained intact during transport across the plasma membranes, binds to soluble protein receptors and is retained in the nuclei. Very little metabolism or debromination (<5.0%) has been detected.

In vivo studies, which will include imaging procedures, using this compound labeled with Br-77, are in progress.

RECEPTOR-BINDING RADIOPHARMACEUTICALS AS AN ALTERNATIVE TO THALLIUM FOR MYOCARDIAL IMAGING: DIHYDROALPRENOLOL. W. A. Alter, III, M. Grissom, J. Hill, F. Vieras, W. Eckelman, J. Phillips. Armed Forces Radiobiology Research Institute, Bethesda, MD and George Washington University, D.C.

This study was undertaken to investigate the use of receptor-binding radiopharmaceuticals as myocardial imaging agents. For imaging, it is desirable to have high heart/blood (H/B) and heart/lung ratios as well as homogeneous distribution throughout the myocardium. A B-adrenergic antagonist (H-3) dihydroalprenolol (DHA) was found to have a relatively high affinity (Ka = 1.2 x $10^8 M^{-1}$) for rat ventricular muscle. Chloralose-anesthetized dogs (N=4) were chosen for the study of myocardial uptake and distribution of DHA and to compare these results with those for simultaneously injected thallium-201 (Tl). Both the H/B and H/L ratios were higher for Tl (32.6 + 10.0 and 7.9 + 3.6, respectively) than for DHA (4.2 + 1.1 and 0.34 + 0.08, respectively). Myocardium perfused by the left anterior descending coronary artery was rendered ischemic for two hours by ligation (N=3) of this vessel, resulting in a marked reduction in uptakes of both agents. Minimum values were measured in tissues obtained from the apical portion of the left ventricle where DHA was 35.2 + 12.3% and Tl was 34.7+13.6% of those values measured in normally perfused myocardium. There was a significant correlation (r = 0.84, p 0.001) between the values of these two agents within the entire ischemic region. This indicates that DHA is similar to Tl in its ability to discriminate between normal and ischemic (or infarcted) tissue. Despite this good correlation, DHA does not have sufficient high myocardial selectivity (relative to lung and blood) to be attractive as a parent structure for a gamma-labeled myocardial imaging agent.

PREPARATION OF CARRIER-FREE Br-77- AND Br-75-2-BROMO-α-ERGOCRYPTINE (BROMOCRIPTINE). C.C. Huang and A.M. Friedman, Argonne National Laboratory, Argonne, IL, R. Dinerstein and H. Kulmala, The University of Chicago, Chicago, IL.

2-Bromo-α-ergocryptine has been found to be an agonist for dopamine receptor, and is used for the treatment of humoral disorders and Parkinson's disease. In order to study the mechanism of action of the drug with the receptor and the specific localization of the dopamine receptor in the brain, a high specific activity of the labeled drug is essential so as to reduce any significant non-specific binding. Previous preparation with Br-82 by Markey et al. was too low a specific activity for this purpose.

Carrier-free Br-77 for the bromination was produced according to the method of Nunn et al. Synthesis of Br-77-bromocriptine was achieved by reaction of α-ergocryptine (3 mg) with Br-77-Br_2 (400 µCi) for 30 min at room temperature. The solution was washed with a mixture of 0.5 N NH_4OH and 0.5% $Na_2S_2O_3$. After removal of the solvent, the product was separated from the unreacted starting materials by preparative TLC (silica gel, 1:1 acetone-CCl_4). Part of the silica gel containing the product was scraped off and eluted with acetone. This carrier-free product (10 µCi) was identified by TLC and radiochromatogram. Br-75 was produced by As-75(He-3,3n)Br-75 reaction. The Br-75-labeled product was prepared in 25% yield in the similar fashion as described above. The results indicate that it is also feasible to prepare millicurie quantities of the product with either of the isotopes.

Intraperitoneal injection of the Br-77-labeled compound into a rat showed that 30 min after injection, 2-6% dose · g body wt./g organ wt. was present in various parts of the brain; whereas 38% was still retained in the blood.

A SIMPLIFIED METHOD OF SELECTIVE SPLEEN SCANNING WITH 99m-Tc-LABELED ERYTHROCYTES: CLINICAL APPLICATIONS. R.R. Armas, M.L. Thakur, A. Gottschalk. Yale University School of Medicine, New Haven, CT.

We have developed a simple technique for spleen scanning with erythrocytes that requires neither a special RBC labeling kit nor RBC washing. Initially, intravenous "cold" pyrophosphate is administered to the patient followed by withdrawal of a blood sample 30 minutes later. Pertechnetate is added to the sample which is then incubated at 49° for 35 minutes and reinjected. Selective splenic imaging may begin one to two hours later.

We have studied several patients with this technique and found it useful in a number of conditions: (1) Evaluating possible "pseudodefects" caused by overlap between the left lobe of the liver and the spleen on colloid scanning; (2) Delineating splenic injuries not optimally visualized on colloid scan; (3) Detecting splenosis in previous splenectomized patients; and (4) Defining the spleen in any patient in whom a splenic lesion is suspected when the colloid scan is equivocal.

The technique requires no special laboratory skills and uses only materials readily available in any nuclear medicine facility.

This work supported in part by DOE Contract EY-76-S-02-4078

EFFECTS OF PRETREATMENT REGIMENS ON THE OSSEOUS UPTAKE OF Na P-32 AND P-32 PYROPHOSPHATE. R.E. O'Mara, V.B. Chanamolu and G.A. Wilson. University of Rochester Medical Center, Rochester, NY

Testosterone (TET) or parathormone (PTH) have been used as pretreatment regimens before administering P-32 to patients with widespread osseous neoplastic disease. This usually necessitates hospitalization. We evaluated the change in uptake of P-32 in various chemical combinations in normal rabbits who were divided into 3 groups: control (no pre-treatment), PTH, and TET (pretreatment). All rabbits received the medications determined on a weight basis and were then injected with sodium phosphate or P-32 labeled PPi utilizing 6 equal I.V. injections every other day over a 12-day period (standard treatment plan). Groups of 3 were sacrificed following the 1st, 3rd and last injections. Tissue samples obtained from blood, urine, bone, bone marrow, muscle and liver were weighed and counted in a standard well counter. Autoradiographic specimens were made and calibrated for bone uptake. No significant differences were seen at any study period between the control, PTH or TET groups. Likewise, no significant differences were seen between the sodium phosphate or PPi with the average osseous uptake after the last injection being 30,970 cpm/g and 31,733 cpm/g respectively. No significant differences were noted in the autoradiographic specimens.

As a result, we feel that this lack of difference in a normal animal model casts doubt on the use of pretreatment regimens for patients receiving P-32 therapy for osseous neoplastic disease. Cessation of these regimens will result in considerable cost saving. We favor the utilization of PPi over sodium phosphate since this results in less radiation dose to non-osseous soft tissues due to its more rapid clearance.

EVALUATION AND APPLICATION OF ALUMINA COLUMN RB-82 GENERATORS. Y. Yano, T.F. Budinger, H.A. O'Brien, Jr.*, and P.M. Grant* Donner and Los Alamos*Scientific Laboratories, University of California, CA.

Rubidium-82 ($T_{½}$ 75 sec) is the daughter of Sr-82 ($T_{½}$ 25 d) and can be obtained by ion exchange using columns of alumina, Bio Rex 70 or Chelex 100. This study evaluates the potentials of an alumina column. Strontium-82/85 was obtained by spallation with medium energy protons at LAMPF and loaded on the three types of columns with no added carrier. Breakthrough of Sr-82/85 and yield of Rb-82 were determined as a function of column volume, NaCl concentration, flow rate and total volume of eluant. With up to 4 ml of 2% NaCl solution at pH 8-9, the breakthrough of Sr-82/85 for each 20 ml elution was 10^{-6}-10^{-5} from alumina and 10^{-6}-10^{-4} from Chelex 100 and Bio Rex 70. A 2.5 times faster flow rate increased the breakthrough of Sr-82/85 by 38% from alumina. A second and third alumina column were loaded with 22 mCi Sr-82 and 51 mCi Sr-82 respectively for myocardial blood flow imaging studies in animal and human subjects using the 280 crystal positron ring detector. Breakthroughs of Sr-82/85 were between 10^{-6} and 10^{-5} for 2.8 l of eluant volume put through the column in 140 elutions over a two mo period. An improved table top Rb-82 generator using solenoid valves and 12.7 cm of lead shielding was used in these studies.

A minimum volume of 1 cc of alumina was required to maintain a < 10^{-5} Sr-82/85 breakthrough and a concentration of 2% NaCl was necessary to obtain Rb-82 yields of 60%.

The alumina column Rb-82 generator maintained a lower breakthrough of Sr-82 than Bio Rex 70 or Chelex 100 under the conditions of this study. The Rb-82 generator provided 20-40 mCi of Rb-82 as often as every 5-10 min with < 10^{-5} breakthrough of Sr-82/85.

ACCEPTANCE TESTING OF THALLIUM-201
K.T. Study, K. Breslow, and B.A. Rhodes, University of New Mexico, Alb. NM

Studies were undertaken to develop quantitative assays for determination of carrier Tl(I) in Thallium-201 preparations, as well as chromatographic techniques for evaluation of radiochemical purity. Radiochemical purity is evaluated by use of an ion exchange chromatography paper developed in 4M KCl. Results show that Tl(I) exhibits an Rf of 0.7-0.8 while Tl(III) results in an Rf of 0.1-0.15. Chromatographic results correlate well with electrophoretic results. Other systems utilizing silica gel chromatography were also evaluated.

Studies were performed to determine ug quantities of carrier thallium in available Tl-201 products. The Rhodamine-B test, a fluorometric technique, was found to conform to Beer's law for concentrations from 0.1-2.0 ug Tl/ml.. The intensity of fluorescence emitted by Rhodamine B (which is directly proportional to the amount of Tl) is measured by visual comparisons of the intensity of fluorescence given off by the samples and standard solutions of TlCl. The simplest and most accurate means of quantitating carrier thallium was found to be by the use of a spectrofluorometric technique. TlCl emits a characteristic native fluorescence when dissolved in water or saline. The sample, or a dilution of the sample is transferred to a cuvette and excited with a wavelength of 222 nm. The emission wavelength of 385 nm. is then measured with a photomultiplier photometer. A log-log plot of the relative fluorescent intensities generated from solutions of known TlCl concentration demonstrates a linear output from concentrations ranging from 1 ug/ml. to 20 ug/ml. Unknown samples of Tl-201 are compared to the standard plot and the concentration of Tl(I) is determined.

NEW RADIOPHARMACEUTICALS FOR ASSESSMENT OF HEPATIC AND G.I. FUNCTION. G.S. Boyd and M.V. Merrick. University of Edinburgh, Scotland, U.K.

A gamma labelled compound behaving in vivo like natural bile acids would have many clinical uses. We have studied four acids labelled with Se75, a) 23 selena 3α,7α, chenodesoxycholic, b) 22 selena cholic, c) 23 selena 25 homodesoxycholic, d) 23 selena 25 homocholic, e) the glycine conjugate of b), (f,g) the taurine conjugates of b) & d) and h) the "bile acid" fraction of the bile from rabbits given 19 methylselenomethyl cholesterol.

A mixture of one of the test compounds with C14 cholic acid was delivered into the duodenum of rats with total biliary fistulae immediately before recovery from anaesthetic. Consecutive total bile aliquots were collected for 45 or 60 minute periods for 24 hours. In separate experiments d), f) and g) were administered intravenously.

With the exception of a) there was a very close correspondence between the C14 and Se75 content of the bile samples, indicating that the rates of absorption and excretion of all the analogues is very close to that of the natural compound. The ratio of the ratio of C14 to Se75 in the total recoved bile to that in the mixture administered orally is shown in the table.

Compound	a)	b)	c)	d)	e)	f)	g)	h)
Measured C14/Se75	45.9	3.29	2.61	0.85	1.97	1.24	1.23	3.08
Administered C14/Se75	± 27	±0.38	±0.67	±0.02	±0.39	±0.04	±0.08	±0.33

We conclude that d), f) & g) most closely resemble cholic acid.

Further studies and initial clinical trials are in progress.

RADIOLABELED RUTHENIUM COMPOUNDS AS POTENTIAL TUMOR-LOCALIZING AGENTS.* S.C. Srivastava, P. Richards, G.E. Meinken, S.G. Pande, P. Som, and H.L. Atkins, Brookhaven National Laboratory, Upton, NY; S.M. Larson, Z. Grunbaum, and J.S. Rasey, VA Hospital, Seattle WA.

The excellent physical properties of Ru-97 ($t_{½}$ 2.9 d, 216 keV γ 86%), the high chemical reactivity of Ru, the potential antitumor activity of several Ru coordination compounds, and the BLIP production of Ru-97, provide a unique combination for the application of this isotope in nuclear oncology. A number of labeled compounds (initially using Ru-103) were synthesized, characterized, and evalu-

ated in normal and tumor-bearing animals (EMT-6 sarcoma Balb/c mice; squamous cell carcinoma rats; Greene melanoma hamsters). These included ionic Ru, a number of hydrophilic and lipophilic chelates, and various ammine compounds with Ru in II, III, and IV oxidation states. Results in the EMT-6 sarcoma mice were as follows. At 24-96 hr, tumor uptake (% dose per g) of a number of compounds (1.7-6.8) is close to that of Ga-67 citrate (3.5-7.1) as well as tumor-to-blood (T/B) and tumor-to-muscle (T/M) ratios. The tumor concentration index (TCI) defined as the ratio of % dose per g in tumor to % dose per g remaining in whole body for seven most active compounds at 24-96 hr (1.33-2.68) is comparable to or better than that of Ga-67 citrate (1.45-1.81). Ru-oxine 7-carboxylic acid acetate (TCI max 72 hr 2.68; T/B 2.4; T/M 7.2) and cis-dichlorotetraammineruthenium(III) chloride (TCI max 96 hr 2.0; T/B 4.4; T/M 4.2) look particularly promising when compared to Ga-67 citrate (TCI max 24 hr 1.81; T/B 4.2; T/M 13.4). Efforts are underway to maximize tumor uptake and reduce blood and normal tissue uptake using various approaches. Results to date demonstrate considerable promise for several Ru-labeled agents.

DOSIMETRY OF AUTOLOGOUS BABOON PLATELETS LABELED WITH IN-111 OXINE. C.E. HOTTE, J.J. VECCHIONE, C.B. LEDIG, C.R. VALERI, A.D. CALLOW AND P.C. KAHN. Tufts-New England Medical Center and the Naval Blood Research Laboratory, Boston, MA

The internal radiation dosimetry of autologous platelets labeled with In-111 oxine was investigated in the baboon. In 10 studies performed in 5 adult male baboons, platelet concentrates isolated from 400 ml of ACD anticoagulated blood were washed free of plasma, resuspended in saline, incubated with 1 mCi of In-111 oxine at 37°C for 30 minutes, washed and resuspended in platelet-poor-plasma, and autotransfused. Platelet isolation and labeling was performed in plastic bags used routinely in blood banks. Quantitation of In-111 platelet distribution was accomplished using computer analysis of gamma camera images obtained at 2 hrs, 48 hrs, and 6 days after injection. Blood activity was determined from samples drawn at each imaging time.

The initial recovery of platelet associated In-111 activity was about 80%. Platelet lifespan was linear and about 5 days. Significant In-111 platelet activity expressed as percent of injected dose was initially present only in the spleen(10.3%) and liver (13.2%). Activity in blood decreased to soft tissue levels by 6 days while spleen and liver activity increased and remained high over the same time period (13.2% and 19.4% respectively at 6 days). No activity was seen in excreta over the 6 day period. Using the MIRD technique, the total average radiation dose (D)was found to be 1.63 rads to liver; 6.86 rads to spleen; 0.24 rads to gonads and 0.39 rads to total body per 0.5 mCi of In-111 injected. Since the circulation of baboon and human platelets are similar, radiation dosimetry in man after transfusion of In-111 platelets will probably be comparable to that in the baboon although this remains to be demonstrated.

RADIOLABELLED PLATELETS: DIFFICULTIES ENCOUNTERED IN THEIR RECOVERY AND SEPARATION. D.C. Buffkin, B. Chang, M.M. Webber, and R.C. Verma. UCLA, School of Medicine, Los Angeles, California.

Recently, much attention has been directed toward improving the efficiency of radiolabelling platelets. Many problems have been overcome and platelets are being reported as potential scanning agents in the detection of emboli, atherosclerosis, and some malignancies. Our attention has now turned to the problem of recovering, isolating and counting the re-infused labelled platelets. Reported whole blood counting techniques assume the label is uniquely bound to the platelets, without verification.

Three methods for the separation of labelled platelets were assessed: 1) Harker's "double spin" method (low speed →PRP at high speed→pellet); 2) sedimentation at 1 G for 40 minutes (supernatant is counted); and 3) single low spin method (decant PRP and count). Resuspension of the pellet in method 1 in saline as well as PPP was also evaluated.

Our results showed a wide range with respect to the number of platelets in a blood sample which were isolated and available for counting: 1) the double spin method, using the IEC centrifuge (Universal Model) yielded 37-88% of the platelets; results with the Sorvall GLC-1 centrifuge ranged from 9-43%; 2) the sedimentation technique yielded 5-21%; and, 3) the single spin method yielded 69-96% of the platelets. In the double spin method, greater recovery was found by resuspending the pellet in PPP.

Therefore, it would appear that the single, low spin method of platelet separation yields the greatest amount of radiolabelled platelets from any given blood sample. This may allow a more definitive elaboration of the biologic half-life of labelled platelets, based upon accurate numbers rather than assumption.

3:45 p.m.-5:00 p.m. Room 210

CLINICAL SCIENCE

GASTROENTEROLOGY II

Chairman: John McAfee
Co-Chairman: James W. Ryan

DYNAMIC ESOPHAGEAL SCINTIGRAPHY: CHOLINERGIC EFFECTS ON CLEARANCE AND TRANSIT. R.S.Fisher, L.S.Malmud, F.A.Stelzer, K.Phaosawasdi, R.D.Tolin, J.Reilley and G.Applegate. Temple University Hospital, Philadelphia, PA

The purpose of this study was to measure the effects of a cholinergic drug (bethanechol) on esophageal function using the technique of dynamic esophageal scintigraphy and to relate any changes in esophageal transit and clearance to primary and secondary contractions. Primary contractions were induced by deglutition of a 15 ml bolus of 150 uCi Tc-99m sulfur colloid in water. Secondary contractions were measured using a similar bolus of activity instilled into the mid-esophagus. Fifteen patients with symptomatic gastroesophageal reflux and 10 normal subjects were studied before and following bethanechol or (its antagonist) atropine administration. Atropine decreased the amplitude and duration of primary and secondary contractions and the number of post-deglutition contractions in normals. Propagation velocities were unchanged. Esophageal transit of a swallowed bolus was prolonged, and clearance of an instilled liquid bolus was delayed. Bethanechol increased the amplitude and duration of primary and secondary contractions in normals and patients with reflux, but did not alter the incidence of post-deglutition contractions. Propagation velocities were decreased significantly. Bethanechol improved esophageal transit and clearance in patients with symptomatic esophageal reflux. We conclude that esophageal scintigraphy is a sensitive technique for evaluating esophageal transit and clearance and may be employed to demonstrate the efficacy of bethanechol, a therapeutic modality, in the management of esophageal transit disorders in patients with symptomatic reflux esophagitis.

CLINICAL ROLE OF 99m-Tc-DIETHYL-IDA SCINTIGRAPHY IN JAUNDICED PATIENTS. S. Pauwels, L. Piret, A. Schoutens, G. Vandermoten and C. Beckers. Dept. Nuclear Medicine, Univ. of Louvain and Brussels, Belgium.

99m-Tc-N-α(2,6 diethylacetanilide)-iminodiacetic acid (99m-Tc-diethyl-IDA) is actually the most interesting radiopharmaceutical for hepatobiliary function study. The aims of this work were to establish in jaundiced patients whether 99m-Tc-diethyl-IDA scintigraphic studies allowed to distinguish between obstructive and hepatocellular jaundice. 76 jaundiced patients with documented hepatobiliary damage and serum total bilirubin up to 35mg/dl were investigated, including 41 patients with obstruction jaundice and 35 with hepatocellular damage. Anterior views of the abdo-

men were obtained after 5,10,15,20,30,60 min; if necessary, late pictures until the 24th hr were added. The results were classified according to previously described scintigraphic criteria(1). Full agreement with the final clinical diagnosis was obtained in 97% of hepatocellular jaundice and in 83% of obstructive jaundice. A correct discrimination between hepatocellular and obstructive jaundice was possible in 91% of the cases. When serum bilirubin raised above 20mg/dl, the demonstration of an obstructive damage was never possible. In 18 obstructive jaundiced patients, both ultrasonography and 99m-Tc-diethyl-IDA were performed. In conclusion, each procedure taken alone, allowed to demonstrate the obstructive cause of the jaundice in 72% of the cases. Taken together, these 2 procedures allowed a correct diagnosis in 89% of the cases. In cases of unsatisfactory ultrasound methodology, diethyl-IDA remains a reliable method to demonstrate the obstructive cause of the jaundice.

(1) PAUWELS S, STEELS M, PIRET L, et al. J Nucl Med 19 : 783-788, 1978.

SIMPLIFIED CCK/CHOLESCINTIGRAPHY IN ACUTE ABDOMINAL DISEASE. E.A. Eikman, J.W. Williams, J.D. Zander, J.C. Wheeler, T.A. Okulski. University of South Florida and James A. Haley VA Medical Center, Tampa, Fl.

We have simplified the initially described cholescintigraphic procedure for assessing cystic duct patency. Adults receive 40 Ivy dog u cholecystokinin (CCK), followed in 30 min. by 150 uCi I-131 rose bengal (RB) or, lately, 2-15 mCi Tc-99m HIDA. Images are recorded at 60-90 min., and at up to 12-48 hours (using I-131 RB) if excretion is slow.

We studied 67 patients. The test showed gallbladder radioactivity - thereby excluding cystic duct obstruction - in 48 patients. Seventeen of these had chronic cholecystitis, the others a variety of other diseases.

Thirteen patients with acute cholecystitis showed a positive test: excretion of radioactivity into the bowel, without gallbladder activity. In two patients with probable earlier acute cholecystitis, resolved cystic duct obstruction accompanied improvement.

In 6 jaundiced patients radioactivity did not appear in the bowel, precluding interpretation. Our total experience with I-131 RB indicates that excretion is usually adequate if bilirubin is 10 mg/dl, and occasionally adequate at higher levels. A single false positive interpretation in this series was associated with bilirubin of 31 mg/dl.

The simplified CCK/cholecystintigraphic procedure provided reliable assessment of cystic duct patency in patients with acute abdominal pain.

EVALUATION OF THE POST-OPERATIVE PATIENT WITH Tc-99m DIMETHYL IMINODIACETIC ACID (HIDA) CHOLESCINTIGRAPHY. H. S. Weissmann, M. S. Frank and L. M. Freeman. Montefiore Hospital and Medical Center and Albert Einstein College of Medicine, Bronx, N. Y.

Tc-99m HIDA cholescintigraphy is a useful procedure for evaluating the post-operative patient. It can accurately demonstrate the caliber and functional patency of biliary-enteric anastomoses and of the common bile duct (CBD) in post-cholecystectomy patients.

Twenty patients who had biliary-enteric bypass surgery of all types, e.g., choledochoduodenostomy, were studied. It visualized the presence of a bile leak and demonstrated its extent and course. In addition, it defined the preferential route of bile flow to be via the anastomosis which the other available nonphysiologic, retrograde procedures could not determine. Serial studies were useful in documenting resolution. It was able to document biliary patency in all other cases including one where the primary disorder was sclerosing cholangitis.

Thirty-five post-cholecystectomy patients were studied for recurrent pain or jaundice. Ultrasound was able to demonstrate the presence of a dilated CBD but this was a non-diagnostic finding in many, in view of their previous CBD explorations. HIDA could accurately visualize the dilated CBD, and in addition, define the rate of bile flow indicating the presence or absence of a functional obstruction. Cholescintigraphy successfully visualized a cystic duct remnant in two subsequently confirmed cases. Thus, HIDA may be a useful screening procedure in post-cholecystectomy patients.

COMPUTER ANALYSIS OF HEPATOBILIARY STUDIES IN THE DIAGNOSIS OF LIVER DISEASE. J.S. Arnold, W.E. Barnes, N. Khedkar, M. Nelson. VA Medical Center, Hines, IL and Loyola University, Stritch School of Medicine, Maywood, IL USA

Hepatic extraction efficiency, regurgitation, and biliary excretion are parameters of liver function which are known to be important for differential diagnosis of hepatobiliary disease. A compartmental model and computerized analytical procedure have been developed for deriving these parameters from kinetic data collected in the course of clinical hepatobiliary visualization studies using Tc-99m-pyridoxylideneglutamate (PG). The technique differs from previous kinetic analyses in that activity in liver and bile are monitored directly and corrected for blood and body wall background. Sequential digital images are collected for 50 min. with a LFOV Anger camera positioned over heart, liver, gall bladder, and intestine. At the conclusion of the study anterior and posterior images of the liver and intestine are recorded to measure the percent administered dose present in the liver and bile compartments. Count data are corrected for blood and body wall background by a method previously reported. Kinetic analysis is performed using a compartmental model in which activity is transferred from blood to liver, from liver back to blood (regurgitation), and from liver to bile (excretion). In 10 patients studied, a marked increase in regurgitation was noted in cirrhotic and alcoholic hepatitis cases, as well as a normal or elevated blood flow. In biliary obstructive disease there was a marked decrease in blood to liver transfer, probably due to reduced blood clearance. The characteristic differences in kinetic parameters of hepatic function found for different disease states suggest that this technique may be useful in differentiating between surgical and non-surgical jaundice.

PHARMACOKINETICS OF [C-14]-AMINOPYRINE BREATH TEST IN PATIENTS WITH LIVER DISEASE. Y. Tarcan, B.A. Faraj, Vernon M. Camp, Rauf Sarper, W. Fajman, James B. Cantrell and J. Galambos. Departments of Radiology (Division of Nuclear Medicine) and Medicine, Emory University, Atlanta, GA.

Several studies have demonstrated the impairment of hepatic drug metabolism in hepatocellular diseases (Wilkinson and Schenker, Drug. Metab. Rev. 4: 139, 1975; Hepner and Vesell, Ann. Intern Med. 83: 632, 1975). Using an animal model, Lauterburg and Bircher (Gastroenterology 65: A-32/556, 1973) showed that assessment of the exhalation rate of C-14-CO_2 following i.v. administration of C-14-aminopyrine (C-14-Apy) yielded quantitative information on the hepatic demethylation of this compound which responded to experimentally induced pathologic changes in the liver. In this investigation we set out to measure the rate of Apy demethylation by breath analysis in normal subjects (n=10) and patients with liver disease (n=48). Subjects were given an oral dose of [C-14]-Apy (1.5 µci, sp. act. 12.2 mci/mmol; Amersham/Searle) and breath samples were collected at determined intervals over a period of 6 hrs. The percentage of administered C-14 excreted in C-14-CO_2 in 2 hrs was 15 $\pm$ 3.1 (SD)% in control subjects and significantly less ($p<0.01$) in patients with cirrhosis (4.1 $\pm$ 1.6) and hepatitis (5.04 $\pm$ 3.7). Furthermore, pharmacokinetic analysis of the data revealed a significant change in the average biological $t_{\frac{1}{2}}$ and the disappearance rate constant (k) of C-14-CO_2 from breath in cirrhotics ($t_{\frac{1}{2}}$ = 300 min; k= 2.6 x 10^{-3} min^{-1}) as compared to control subjects ($t_{\frac{1}{2}}$ = 150 min; k= 6.0 x 10^{-3} min^{-1}). The data suggest that Apy breath test is a simple and noninvasive procedure for the evaluation of the microsomal function of the liver.

CLINICAL COMPAPISON OF Tc-99m-DIETHYL-IDA AND Tc-99m-PIPIDA FOR EVALUATION OF THE HEPATOBILIARY SYSTEM. W.C. Klingensmith III, A.R. Fritzberg, V. Spitzer, and L.J. Koep. U. of Colorado Medical Center, Denver, CO.

A direct clinical comparison of Tc-99m-diethyl-iminodiacetic acid (Tc-99m-diethyl-IDA) and Tc-99m-paraisopropyl iminodiacetic acid (Tc-99m-PIPIDA) was made by performing paired studies in 15 patients with a wide range of hepatobiliary function. Ten patients had liver transplants, three had chronic active hepatitis, one had chronic active hepatitis and cholangiocarcinoma, and one had sclerosing cholangitis. The average time between studies was 1-2 days with a maximum of 3 days. Anterior and right lateral images were routinely acquired at 5, 10, 15, 30, 45, and 60 minutes; if intestinal activity was not present at 60 minutes imaging was continued until intestinal activity appeared or until 24 hours. In addition, cumulative three hour urine collections were made in 12 patients injected with Tc-99m-PIPIDA and I-131 rose bengal.

Tc-99m-diethyl-IDA was superior to Tc-99m-PIPIDA in demonstrating: 1) the liver parenchyma, 2) the hepatic ducts, and 3) small bowel activity early after injection. The percent of injected dose excreted in the urine in three hours increased significantly with increasing total serum bilirubin levels for Tc-99m-PIPIDA ($p < 0.05$), but there was no change in I-131 rose bengal renal excretion with increasing bilirubin levels. Urinary excretion of Tc-99m-PIPIDA as a function of total serum bilirubin was not significantly different from Tc-99m-diethyl-IDA as determined in a previous study. In conclusion, Tc-99m-diethyl-IDA is superior to Tc-99m-PIPIDA for imaging the hepatobiliary system.

03:45 p.m.-5:00 p.m. Room 300/301

CLINICAL SCIENCE

CARDIOVASCULAR VI

Chairman: Eli Botvinick
Co-Chairman: Robert Slutsky

COMPARATIVE SENSITIVITY AND SPECIFICITY OF EXERCISE RADIONUCLIDE VENTRICULOGRAPHY AND REST-EXERCISE THALLIUM IMAGING IN THE DETECTION OF CORONARY ARTERY DISEASE. J.H. Caldwell, J.L. Ritchie, G.W. Hamilton, and J.W. Kennedy. Veterans Administration Medical Center, Seattle, WA.

Supine rest-exercise radionuclide ejection fraction (EF) measurements and rest-exercise thallium myocardial imaging (Tl) were performed in 52 patients having coronary angiography to determine the relative sensitivity and specificity of each test. Maximal heart rate (HR), systolic blood pressure (SBP), pressure-rate product (PxR/100), ST depression (ST+), and limiting symptoms were compared to determine if differences existed between the types of exercise. Rest and exercise Tl myocardial images were acquired in a standard manner. EF measurements were made on LAO equilibrium cardiac blood pool images acquired every 2 min during exercise to symptom limited maximum. Eleven patients with no stenosis ≥50% were considered normal (Nl) and 41 pts had coronary artery disease (CAD). Rest-exercise Tl images were normal in all 11 Nl pts and 6 pts with CAD and were abnormal in 35 with CAD. An abnormal rest-ex EF (failure to ↑ by 0.05 EF units or a ↓ in EF) occurred in 5 of 11 Nl pts and in 38 of 41 pts with CAD. The sensitivity was 85% for Tl and 93% for rest-ex EF (p=.06), whereas the specificity was 100% for Tl and 54% for rest-ex EF (p=.02). The two tests combined detected all pts. In the pts with CAD, the results of the hemodynamic studies were

	HR	SBP	PxR/100	angina*	DOE*	ST+*
treadmill-Tl	122±20	141±30	172±49	21	9	17
supine-EF	104±19	164±24	173±50	16	15	16

We conclude that exercise EF measurements are at least as sensitive, but less specific than, Tl in detecting CAD. Left ventricular stress, ST sensitivity, and limiting symptoms are equivalent for the two types of exercise.
*(Number of patients)

CORRELATION OF REST AND EXERCISE RADIONUCLIDE ANGIOCARDIOGRAPHIC VENTRICULAR FUNCTION WITH THE NUMBER OF SIGNIFICANTLY STENOSED VESSELS IN 230 PATIENTS WITH CORONARY ARTERY DISEASE. P. McEwan, G.E. Newman, J. Portwood, S. Port, M.T. Upton, F. Cobb, R.H. Jones, Duke Medical Center, Durham, NC

This study was undertaken to explore the relation between left ventricular function (LVF) at rest (R) and exercise (Ex) and the number (#) of stenosed vessels (V). Initial transit angiocardiograms (RNA) were performed upright at R and during Ex on a bicycle ergometer on 230 patients (pts). All pts underwent cardiac catheterization for symptomatic coronary disease. Results of mean R and Ex RNA ejection fraction in % (EF), left ventricular end-diastolic volume in mls (EDV) and Ex induced wall motion (WM) abnormalities are tabulated. The pts were grouped by the # of diseased V at catheterization and by R normal (NL) or abnormal (AB) LVF.

#V	LVF	#Pts	R EF	Ex EF	R EDV	Ex EDV	%ΔEDV	Ex WM AB
0	NL	28	65± 8	70±11	111±24	135±43	18%	0
1	NL	30	66± 9	65±12	107±29	145±43	26%	25%
1	AB	20	43±10	48±13	158±60	174±62	9%	30%
2	NL	36	66± 7	65±11	116±26	154±50	25%	39%
2	AB	28	41±10	45±14	172±59	201±68	14%	36%
3	NL	46	65± 7	54±14	124±38	172±51	28%	63%
3	AB	42	35±12	35±12	224±97	253±80	11%	45%

Twenty-eight pts had NL coronaries and NL LVF at catheterization and served as controls. In pts with AB R LVF there was a variation in response to Ex, but a pattern of decreasing EF and increasing EDV was seen at R as the # of V stenosed increased. However, in pts with NL LVF at R, the magnitude of the fall in EF and the incidence of Ex induced WM abnormalities increased progressively with the # of diseased vessels.

THE RELATION OF GLOBAL LEFT VENTRICULAR FUNCTION WITH EXERCISE TO THALLIUM-201 EXERCISE SCINTIGRAMS. H.D. Kirshenbaum, R.D. Okada, F.G. Kushner, H. Gewirtz, H.W. Strauss, C.A. Boucher, and G.M. Pohost. Massachusetts General Hospital, Boston, Massachusetts.

Transient (TD) or persistent defects (PD) on 201-Tl exercise images are thought to be related to ischemia or scar respectively. In order to assess the relationship between a defect and its redistribution pattern, and left ventricular function, exercise 201-Tl and multigated cardiac blood pool scanning (MBPS) were performed in 61 patients (pts) who underwent elective cardiac catheterization for evaluation of chest pain syndromes - 50 pts had coronary artery disease (CAD) and 11 did not. Propranolol therapy was present in 34 pts with CAD and four pts without CAD. Initially, pts underwent maximal or symptom-limited graded supine exercise using a bicycle ergometer. Electrocardiographic ischemia developed in 20 (40%) pts with CAD. At peak stress, 201-Tl was given and serial images recorded over a two hour interval. Then, rest and EX MBPS were performed using Tc-99m. Changes in left ventricular ejection fraction (LVEF) with exercise on MBPS were as follows:

Thallium	#Pts	Rest LVEF(±SEM)	EX LVEF(±SEM)	p
TD	16	.65 ± .02	.58 ± .03	<.01
PD	7	.58 ± .08	.59 ± .08	NS
TD + PD	20	.60 ± .03	.56 ± .03	NS
Negative (CAD)	7	.65 ± .04	.72 ± .06	NS
Negative(No CAD)	10	.67 ± .03	.73 ± .03	NS
Negative (All)	17	.66 ± .03	.73 ± .03	<.05

Thus, pts with exclusively TD on exercise 201-Tl images have more acute ischemic functional compromise of their LV than do pts with only PD. The combination of TD + PD on the same scan appears to lie between these two extremes. LVEF improves with exercise in pts with negative 201-Tl scintigrams.

SENSITIVITY OF EXERCISE RADIONUCLIDE VENTRICULOGRAPHY IN CORONARY ARTERY DISEASE DETECTION: IMPORTANCE OF ADEQUATE EXERCISE. T.J. Brady, J.H. Thrall, K. Lo, J. Clare, W.L. Rogers, and B. Pitt. University of Michigan Medical Center Ann Arbor, MI.

Exercise radionuclide ventriculography (ERV) using equilibrium gated blood pool imaging has been shown to be a sensitive (SEN) indicator of coronary artery disease

(CAD). To determine if the level of exercise (EX) effects this SEN, the supine bicycle exercise data from 110 patients (PTS) with suspected CAD was evaluated. The EX's were graded as adequate (AD) if PTS developed (1) angina or (2) ST segment depression > 1 mm during EX or if they (3) achieved a pressure rate product (PRP) > 250. (PRP = heart rate times systolic blood pressure/100). The EX's were graded as inadequate (INAD) for PTS failing to attain any one of these three criteria.

Angiographic CAD (≥ 70% stenosis) was present in 86 PTS of whom 80 had an abnormal ERV for a SEN of 93%. In 24 PTS with normal coronary arteries the ERV was normal in 22 PTS for a specificity of 92%. In both cases of false positive ERV, the patients had regional wall motion abnormalities during EX radionuclide and EX contrast ventriculography.

In the 86 PTS with CAD, 71 PTS achieved AD EX of whom 70 had abnormal ERV for a SEN of 99%. In 15 PTS who failed to achieve AD EX the ERV was abnormal in 10 for a SEN of 66%. The universal reason for INAD EX was leg fatigue. In the 5 false negative patients with INAD EX, the mean ejection fraction increased .12 during exercise.

It is concluded that some patients with CAD may have normal ventricular response at INAD EX levels. To attain a high degree of sensitivity requires AD EX during ERV.

QUANTITATIVE ASSESSMENT OF FRACTIONAL MYOCARDIAL UPTAKE OF Tl-201: CHANGES BY EXERCISE LOADING IN CORONARY ARTERY DISEASE. Y. Yonekura, Y. Ishii, K. Torizuka, K. Yamamoto, T. Mukai, K. Kadota, H. Kambara, and C. Kawai. Kyoto Univ., Kyoto, Japan.

Fractional myocardial uptake of Tl-201 was measured for the quantitative assessment of the extent of response in coronary artery disease (CAD). 10 normals (N) and 22 CAD, 9 of which has less than 70% stenosis (CAD I) and 13 of which has more than 70% stenosis (CAD II) in the proximal portion of coronary arteries, were studied at rest and with exercise loading by bicycle ergometer. After intravenous injection of Tl-201, its rapid transport process were recorded during the initial 5 minutes by a scintillation camera. Total injected dosage (A) were obtained from the counts during the initial passage through the heart and lung, and myocardial uptake (B) were counted with the same geometry from the subsequent accumulation within myocardial region. The fractional myocardial uptake (B/A) is assumed to be proportional to fractional myocardial blood flow to cardiac output (MBF/CO) according to the indicator fractionation principle.

Change rate of MBF/CO on the exercise loading (ΔMBF/CO) were significantly less in CAD I (1.33 ± 0.16) and CAD II (1.05 ± 0.19) than in N (1.75 ± 0.11). MBF/CO increased proportionally to the increment of double product (HR x BP) by exercise in N, whereas it didn't in CAD. Sensitivity of this method was superior to the stress ECG (77%) and the stress myocardial perfusion imaging (MPI) (77%), not only in CAD I (100%) but also in CAD II (89%). This result indicated that this type of global assessment of the myocardial reserve capacity is valuable in addition to the simple stress MPI.

APPARENT WORSENING OF THALLIUM-201 MYOCARDIAL DEFECTS DURING REDISTRIBUTION - WHAT DOES IT MEAN? D. Tanasescu, D. Berman, H. Staniloff, M. Brachman, L. Ramanna, and A. Waxman. Cedars-Sinai Medical Center, Los Angeles, Calif.

Although decrease in the relative thallium-201 (Tl) activity in delayed images compared to stress images has occasionally been noted, its clinical significance is unknown. The present study correlates the apparent worsening pattern with the results of coronary arteriography in 5 pts. Stress and redistribution myocardial scans were obtained in the anterior, 45° left anterior oblique (LAO) and 70° LAO views. Regional Tl uptake was assessed with a 5 point scoring system (0=normal, 2=definitely abnormal, 4=no uptake). The results are shown below:

Pt.	Loc.	Stress	Redistribution	Coronary Angiography
1	Apex	1	2	LAD 75* Cx50 RCA 99
2	Apex	1	2	LAD 75 Cx95 RCA 75
	Inf	1	2	
3	Inf	0	2	LAD 100 Cx75 RCA 100
4	Inf	1	2-3	LAD 95 Cx100 RCA 75
5	Apex	0-1	2	NCA

Loc=location; Inf=inferior; LAD=left anterior descending; Cx=circumflex; RCA=right coronary artery; NCA=normal coronary arteriograms. Number = % stenosis, * = diagonal branch only.

In all of the CAD pts, the region of apparent worsening corresponded to the region supplied by the vessel with the least severe stenosis. This apparent worsening pattern may represent a higher rate of washout from a given segment than from the adjacent segments, possibly related to increased relative regional blood flow. The apparent worsening during redistribution appears to have different diagnostic implications from the pattern of stress abnormality, and may signify the area with the highest rather than the lowest perfusion.

VARIABLE TIME TO REDISTRIBUTION IN TL-201 EXERCISE MYOCARDIAL SCINTIGRAPHY: INVERSE RELATIONSHIP TO DEGREE OF CORONARY STENOSIS. D. Berman, J. Maddahi, M. Freeman, H. Staniloff, U. Elkayam, Y. Charuzi, D. Tanasescu, M. Brachman, H.J.C. Swan, J. Forrester, and A. Waxman. Cedars-Sinai Medical Center, Los Angeles, California.

We have observed that the time to redistribution of Tl-201 (Tl) is variable. To investigate the relationship between degree of coronary artery (CA) stenosis (sten) and the rate of redistribution (R) of Tl, serial myocardial scintigrams were obtained 5 min, <1 hr, 3-6 hr, and 12-24 hr after maximal treadmill exercise (Ex) in 31 pts undergoing coronary angiography (angio). The degree of sten in CA supply of each of 60 abnormal segments was determined from angio. Tl defects were classified by the time to return to normal. Of 60, 59 Tl defects were associated with >50% sten of the corresponding CA. In 12/60 time to R was rapid (<1 hr): these 12 segments were associated with mild to moderate CA sten (8-50% and 4-75%). In 16/60 time to R was 3-6 hr: associated CA lesions were moderate to severe (8-75% and 8-90%). Importantly, in 12/60 defects, time to R was prolonged(12-24 hrs). In all 12, associated CA lesions were severe (5-90% and 7-100% with collaterals). The remaining 20/60 showed no R. Of the CA supplying these 20 regions, 14 had total occlusion, 4 had subtotal occlusion, 1 had 50% lesion and 1 had <50% narrowing. In conclusion; 1) the rate of redistribution appears to be inversely related to degree of CA sten; 2) Redistribution may be very rapid in pts with mild to moderate CA lesions; therefore, Tl imaging must begin immediately after exercise for maximal sensitivity. 3) Redistribution may be slow in pts with severe CA sten, and thus very delayed redistribution imaging helps avoid the false diagnosis of myocardial infarction.

AUTHOR/LECTURER INDEX

C

D

E

F

G

H

I

J

K

S

T

SCIENTIFIC EXHIBITS

All Scientific Exhibits to be presented at the 26th Annual Meeting of the Society are listed below by the title and author. Submitted Exhibits are listed alphabetically by last name of first author and Teaching Exhibits by subject categories. All exhibits will be on display in the Exhibit Hall, Georgia World Congress Center. For full abstracts, exhibit numbers and locations, and times for viewing and Scientific Rounds, please consult the Exhibit Program for the meeting.

SUBMITTED EXHIBITS

COMPARISON OF LEFT VENTRICULAR WALL MOTION DETECTED BY MULTIPLE GATED ACQUISITION OF THALLIUM-201 PERFUSION MYOCARDIAL SCAN AND Tc-99m LABELED RED BLOOD CELLS CARDIAC BLOOD POOL. H.M. Abdel-Dayem and E.V. Leslie, Erie County Medical Center, Buffalo, NY.

A RETROSPECTIVE ANALYSIS OF RENAL ABNORMALITIES DETECTED ON BONE SCANS. K.J. Adams, L.R. Witherspoon, and S.E. Shuler, Ochsner Medical Institutions, New Orleans, LA.

RELATIVE SHUNT FLOW DETERMINATION IN CORONARY ARTERY FISTULAS AS AN AID TO DECISION MAKING FOR SURGICAL CORRECTION. M.H. Adatepe, F.R. Begg, O.M. Powell, G.J. Magovern, Allegheny General Hospital, Pittsburgh, PA.

DECISION MAKING AND BAYESIAN ANALYSIS AS DEMONSTRATED BY A CLINICAL QUESTIONNAIRE. H. Agress, Jr., Hackensack Hospital, Hackensack, NJ.

COMPUTER ANALYSIS OF HEPATOBILIARY STUDIES IN THE DIAGNOSIS OF LIVER DISEASE. J.S. Arnold, W.E. Barnes, N. Khedkar, and M. Nelson, VA Medical Center, Hines, IL and Loyola University, Stritch School of Medicine, Maywood, IL.

AUTOMATED ROC CURVES. A.B. Ashare, Wright State University, Dayton, OH.

RADIOASSAY OF BILE ACIDS IN NORMAL AND HEPATOBILIARY DYSFUNCTION. F.S. Ashkar, M. Hourani, F. Block, and A. Serafini, University of Miami, School of Medicine, Jackson Memorial Hospital, Miami, FL.

PERITONEO-VENOUS SHUNT PATENCY TEST. M.A. Bartheld and D.J. Zbrzeznj, University of Texas Medical Branch, Galveston, TX.

Tc-99m HYDROXYDIPHOSPHONATES: THE ROLE OF THE HYDROXY GROUP UPON OSSEOUS AND NON-OSSEOUS UPTAKE IN THE CANINE MODEL. J.A. Bevan, A.J. Tofe, M.D. Francis, B.L. Barnett, and J.J. Benedict, The Procter & Gamble Company, Miami Valley Laboratories, Cincinnati, OH.

MANIFESTATIONS OF SICKLE CELL DISEASE IN RADIONUCLIDE IMAGING. J.J. Chan, and H.M. Park, Indiana University Medical Center, Indianapolis, IN.

A COMPARISON OF FOUR MOBILE CAMERAS IN ONE INSTITUTION: QUANTITATED PERFORMANCE PARAMETERS AT Tc-99m AND Tl-201 ENERGIES. D. Chapman, K. Newcomer, and A. Waxman, Cedars-Sinai Medical Center, Los Angeles, CA.

VENTILATION AND CLEARANCE OF THE SINUSES AND MIDDLE EARS UTILIZING XENON-133. J.H. Christie, R.C. Robinson, F.R. Kirchner, D.F. Preston, and A.V. Wegst, University of Kansas Medical Center, Kansas City, KS.

POST-OPERATIVE CHOLESCINTIGRAPHY OF THE BILIARY ATRESIA PATIENT USING Tc-99m PIPIDA. D.J. Coldcleugh, J. H. Miller, and F. Sinatra. Childrens Hospital of Los Angeles, Los Angeles, CA.

AUTORADIOGRAPHY OF MACRO-CRYOMICROTOME SECTIONS USING ROUTINE MATERIALS AND METHODS. B.Y. Croft, and J.A. Wakefield, University of Virginia, Charlottesville, VA.

TRANSMISSION PHANTOM FOR LARGE SCALE COMPARISON OF IMAGING SYSTEM PERFORMANCE. F.H. DeLand, G.H. Simmons, and N.E. Herrera, VA and University of Kentucky Medical Centers, Lexington, KY., and Danbury Hospital, Danbury, CT.

FACTORS INFLUENCING THE PERFORMANCE OF NUCLEAR MEDICINE COMPUTER SYSTEMS. J. J. Erickson, R.R. Price, J.A. Patton, J.P. Jones, F.D. Rollo, and A.B. Brill, Vanderbilt Medical Center, Nashville, TN.

EFFECT OF IMAGE SIZE ON LESION DETECTABILITY IN NUCLEAR MEDICINE. W.A. Fajman, R. Sarper, P. Sprawls, J. Witcowski, and Y.A. Tarcan, Emory University, Atlanta, GA.

PARENCHYMAL PHASE HEPATOBILIARY IMAGING: A COMPARISON OF Tc-SULFUR COLLOID AND Tc-PIPIDA. J.L. Floyd and F.L. Weiland, Wilford Hall USAF Medical Center, San Antonio, TX.

MULTIPLE ENDOCRINE NEOPLASIA, TYPE IIa (MEN IIa) SYNDROME: ROLE OF FAMILY SCREENING. J.E. Freitas, M.D. Gross, J.C. Sisson, and A.A. Al-Saadi. William Beaumont Hospital, Royal Oak, MI., and University of Michigan Medical Center, Ann Arbor, MI.

CHOLESCINTIGRAPHY WITH Tc-99m PIPIDA. A.P. Frost, R.E. Henry, M.J. Daly, and F.C. Park, VA Medical Center and University of Arizona, Tucson, AZ.

PEDIATRIC SCROTAL IMAGING. M.J. Gelfand, P.J. Williams, and D.X. Horn, Radioisotope Laboratory, University of Cincinnati, and Children's Hospital, Cincinnati, OH.

THE INS AND OUTS OF XENON. D.L. George and B.F. Felinski, The Cooper Medical Center, Camden, NJ.

A HAND SHIELD FOR USE WHEN LOADING SYRINGES WITH RADIOACTIVE MATERIALS FROM MULTIDOSE VIALS. R.V. Gilliam, B.M. Galkin, R. Boon, and C.H. Park, Thomas Jefferson University Hospital, Philadelphia, PA.

AUTOMATION AND OPERATOR INDEPENDENT DATA PROCESSING OF CARDIAC STUDIES. M.L. Goris, H.D. Fawcett, (Stanford), D.Pavel (University of Chicago), M. Yester (University of Alabama), J. Jengo (UC Los Angeles), T. Nelson, and P.A. Briandet (Informatek States), Atlanta, GA.

LOW CONTRAST DETECTABILITY - THE $1.50 PHANTOM. M.M. Graham, T.K. Lewellen, University of Washington, Seattle, WA.

TRANSMISSION COMPUTED TOMOGRAPHIC FINDINGS AFTER EXPERIMENTALLY-PRODUCED ACUTE PULMONARY ARTERIAL OCCLUSION IN THE DOG. Z.D. Grossman, G.M. Gagne, A. Zens, F.D. Thomas, C.C. Chamberlain, A. Singh, W.N. Cohen, and E.R. Heitzman, The Upstate Medical Center, Syracuse, NY.

COMPARISON OF RV FUNCTION EVALUATION BY GATED FIRST-PASS, EQUILIBRIUM GATED, AND LIST-MODE FIRST-PASS RADIONUCLIDE VENTRICULOGRAPHY. R.B. Grove, J.A. Harolds, T. A. Powers, R.W. Pederson, and R.D. Bowen, VA Medical Center, Nashville, TN.

INCREASED EFFICIENCY AND RELIABILITY OF ABDOMINAL SONOGRAPHY BASED ON DIRECT MEASUREMENTS FROM RADIONUCLIDE LIVER AND GALLIUM SCANS. R.B. Grove, M.L. Weinstein, R.L. Martin, T.A. Powers, and R.D. Bowen, VA Medical Center, Nashville, TN.

RADIONUCLIDE MEASUREMENT OF ABSOLUTE DIFFERENTIAL GFR. R.B. Grove, T.A. Powers, R.D. Bowen, J.M. Plunkett, S. Kadir, J.A. Harolds, and W.J. Stone, VA Medical Center, Nashville, TN.

EVALUATION OF BONE VIABILITY BY UTILIZING BONE SCANNING TECHNIQUES. W.T. Harris, and J.J. Prather, St. Vincent Infirmary, Little Rock, AR.

NUCLEAR MEDICINE IN THE INTENSIVE CARE UNIT: TECHNOLOGICAL CONSIDERATIONS. P. Hogendoorn, S. Gaines, R. Vandierendonk, and T.D. Cradduck, Victoria Hospital, London, Ontario, Canada.

NUCLEAR CARDIOLOGY - WHAT SHOULD BE ORDERED? G.L. Jackson, F.W. Gutierrez, F. Kinney, E. Lim, H.F. Moffitt, G.R. Muller, and A.J. Reeves, Harrisburg Hospital, Harrisburg, PA.

INTERPRETATION OF "COLD" AREAS IN RADIO-

NUCLIDE BONE IMAGES. J.R. Jinkins, W.A. Fajman, Y.A. Tarcan, and H.H. Lo, Emory University, Atlanta, GA.

A GENERAL PURPOSE RADIOASSAY PROGRAM FOR OBTAINING THE BEST FIT IN CONSTRUCTING THE RADIOASSAY STANDARD CURVE. S.R. Kiser, H.G. Lehmann, and R.J. Lull, Letterman Army Medical Center, San Francisco, CA.

NUCLEAR MEDICINE CASE OF THE WEEK. A MEDICAL STAFF EDUCATION PROJECT. B. Kovaleski, K. Vanags, M. Schreyer, W. Bohlman, T. Stanton, G. Alvarez, and J.A. Franco, O'Connor Hospital, San Jose, CA.

A SIMPLE, INEXPENSIVE COMPUTER GATE FOR EJECTION FRACTION STUDIES. D.A. Krueger, G.J. Szabados, and R.H. Heck, St. Joseph Hospital, Denver, CO.

IMPROVED TECHNETIUM-99m HEPARIN FOR THE SCINTIGRAPHIC DETECTION OF EXPERIMENTAL MYOCARDIAL INFARCTS. P.V. Kulkarni, R.W. Parkey, L.M. Buja, J.E. Wilson, F.J. Bonte, and J.T. Willerson, University of Texas Health Science Center, Dallas, TX.

A COMPARISON OF TECHNIQUES TO MEASURE COUNT RATE PERFORMANCE OF GAMMA CAMERAS. T.K. Lewellen, R. Murano, and D.L. Williams, University of Washington and the VA Hospital, Seattle, WA.

REGIONAL CEREBRAL BLOOD FLOW: TECHNICAL ASPECTS OF THE Xe-133 WASHOUT METHOD. D.C. McCormick, R.R. Hovey-Andersen, D.J. McMillan, M.T. Madsen, and R.E. Polcyn, University of Wisconsin Hospitals, Madison, WI.

INTERVENTION RADIOANGIOCARDIOGRAPHY IN CORONARY ARTERY DISEASE. D. Manyari, L. Melendez, T. Cradduck, and A. Driedger, University of Western Ontario, London, Canada.

GATED CARDIAC EMISSION COMPUTED TOMOGRAPHY. S.C. Mirell, H.S. Hecht, and W.H. Blahd, VA Wadsworth Medical Center, Los Angeles, and University of California, Los Angeles, CA.

MYOCARDIAL PERFUSION EXAMINATION USING THALLIUM-201, MULTIPLE GATED IMAGE ACQUISITION AND BILATERAL COLLIMATOR. J. Muz, S.J. Figiel, and T.M. Kumpuris, Harper-Grace Hospitals, Detroit, MI.

INDICATIONS FOR HEPATOBILIARY IMAGING WITH TECHNETIUM-99m PIPIDA. P.Z. Norwood, L.A. Forstrom, L. Williams, VA Hospital, Minneapolis, MN.

INTERCOMPARISON OF COMMERCIALLY AVAILABLE BONE SEEKING Tc-99m PHOSPHATE/COMPLEX KITS. R.E. O'Mara, V. Chanamolu, G.A. Wilson, and D.A. Weber, University of Rochester Medical Center, Rochester, NY.

TESTING GAMMA-CAMERA PERFORMANCE UNDER CLINICAL CONDITIONS. P. Paras, G.J. Hine, C. Warr, R. Adams, and J.T. Lewis, Bureau of Radiological Health, Food and Drug Administration, Rockville, MD.

CARDIOPULMONARY APPLICATION OF RADIONUCLIDES IN PEDIATRICS. B. Pastakia, L.M. Lieberman, J. Levy, D.S. Moodie and R.E. Polcyn, University of Wisconsin Hospitals, Madison, WI.

TECHNIQUES FOR EVALUATION OF IMAGING DEVICES. J.A. Patton, R.R. Price, J.J. Erickson, A.B. Brill, and F.D. Rollo, Vanderbilt University Medical Center, Nashville, TN.

PORTABLE NUCLEAR CARDIOLOGY: EXPERIENCE WITH COMPUTERIZED GATED BLOOD POOL IMAGING TECHNIQUES AT REST AND EXERCISE ON A COMPLETELY PORTABLE BASIS. M.C. Robertson, S. Feinberg, A. Hileman, A.T. Hornbeck, and R. Rendo, Nuclear Medico Services, Inc., Van Nuys, CA.

STANDARDIZATION OF RADIOLABELED TEST MEALS FOR THE MEASUREMENT OF GASTRIC EMPTYING RATE. R.G. Robinson, A. Hurwitz, W.F. Herrin, J.H. Christie, and D.F. Preston, Kansas University Medical Center, Kansas City, KS.

ADDITIVE COLOR HEART MOTION DISPLAY. K. L. Sandock, University of Missouri and Truman VA Hospital, Columbia, MO.

IMAGING OF THE SPLEEN. A. Shirkhoda, W.H. McCartney, E.V. Staab, and C.A. Mittelstaedt, North Carolina Memorial Hospital, Chapel Hill, NC.

ASSESSMENT OF LEVEEN SHUNT PATENCY WITH TC-99m MACROAGGREGATED ALBUMIN. A. Singh, F.D. Thomas, Z.D. Grossman, and J.G. McAfee, Upstate Medical Center, Syracuse, NY.

A METHOD FOR QUANTITATION OF RELATIVE EXTRACTION EFFICIENCIES TO FACILITATE THE CLINICAL COMPARISON OF HEPATOBILIARY RADIOPHARMACEUTICALS. V.M. Spitzer, A.R. Fritzberg, and W.C. Klingensmith, III, University of Colorado Medical Center, Denver, CO.

NUCLEAR ANATOMY OF DIVERSIONARY CENTRAL NERVOUS SYSTEM SHUNTS IN CHILDREN. J.R. Sty and D.P. Babbitt, Milwaukee Children's Hospital, Milwaukee, WI.

SIGNIFICANCE OF RIB LESIONS IN Tc-99m PYROPHOSPHATE BONE SCAN. L.J. Talarico, H.M. Abdel-Dayem, and E.V. Leslie, Erie County Medical Center, Buffalo, NY.

DOSE TO LIVER AND SPLEEN OF PEDIATRIC PATIENTS UNDERGOING 99mTc-SULFUR COLLOID SCANNING PROCEDURES. S.R. Thomas, R.C. Purdom, J.G. Kereiakes, M.J. Gelfand, H. R. Maxon, and E.L. Saenger, Radioisotope Laboratory, Cincinnati General Hospital, Cincinnati, OH.

GATED REGIONAL SPIROMETRY. J.J. Touya, R.R. Price, J.A. Patton, J. Erickson, J. P. Jones, and F.D. Rollo, Vanderbilt University Medical Center, Nashville, TN.

PRACTICAL NUCLEAR PHARMACY. P. The-Tran and R.D. Wasnich, Pacific Radiopharmacy, Honolulu, HI.

BONE SCANNING IN THE DETECTION OF OCCULT FRACTURES. A. Vasilas, J. Batillas, W.F. Pizzi, and T.M. Gokcebay, Beekman Downtown Hospital, New York, NY.

EFFECTS OF CONTAMINATE RADIOACTIVITY ON RADIOIMMUNOASSAYS. L.R. Witherspoon, S. E. Shuler, M.M. Garcia, and L.A. Zollinger, Ochsner Medical Institutions, New Orleans, LA.

OBLIQUE THYROID IMAGES: USEFUL OR NOT? L.R. Witherspoon, S.E. Shuler, and K.M. Karlin, Ochsner Medical Institutions, New Orleans, LA.

TEACHING EXHIBITS

CARDIOLOGY

INTERCOMPARISON OF 3 SEMIAUTOMATIC METHODS OF DETERMINATION OF LEFT VENTRICULAR EJECTION FRACTION (LVEF): COMPARISON WITH CONTRAST VENTRICULOGRAPHY, J.B. Bingham, K.A. McKusick, E.J. Tarolli, C.A. Boucher, R.D. Okada, G.M. Pohost, and H.W. Strauss. Massachusetts General Hospital, Boston, MA.

NUCLEAR MEDICINE IN THE INTENSIVE CARE UNIT: CLINICAL APPLICATION. A.A. Driedger, W.J. Sibbald, J. Calvin, and T.D. Cradduck, Victoria Hospital, London, Ontario, Canada

RIGHT VENTRICULAR EJECTION FRACTION ASSESSMENT BY RAPID MULTIPLE GATED EQUILIBRIUM SCINTIGRAPHY: DESCRIPTION, VALIDATION, AND APPLICATION OF A NEW TECHNIQUE AT REST AND DURING EXCERCISE. J. Maddahi, D. Berman, D. Matsuoka, H.J. C. Swan, J. Forrester, and A. Waxman, Cedars-Sinai Medical Center, Los Angeles, CA.

PERSISTENTLY POSITIVE Tc-99m STANNOUS PYROPHOSPHATE MYOCARDIAL SCINTIGRAMS: A CLINICOPATHOLOGIC STUDY. R.W. Parkey, L.M. Buja, S.E. Lewis, L.R. Poliner, F. J. Bonte, and J.T. Willerson, University of Texas Health Science Center at Dallas, Dallas, TX.

PEDIATRICS

RADIONUCLIDE CYSTOGRAPHY - A TEN-YEAR EXPERIENCE. J.J. Conway, S. Weiss, L. King, and C. Firlit, The Children's Memorial Hospital, Chicago, IL.

PEDIATRIC NUCLEAR CARDIOLOGY. E. Schultz, D. Gilday, J. Ash, and M. Desouza, The Hospital for Sick Children, Toronto, Ontario.

Tc-99m PERTECHNETATE SCROTAL IMAGING IN PEDIATRICS. G.N. Sfakianakis, and J.P. Smith, Children's Hospital, Columbus, OH.

RENAL ANATOMY AND FUNCTION IN PEDIATRIC NUCLEAR MEDICINE. G.N. Sfakianakis, and E. Sfakianaki, Children's Hospital, Columbus, OH.

RADIOPHARMACY, DOSIMETRY, AND RADIOASSAY

RADIOCHEMICAL PURITY DETERMINATION OF Tc-99m HIDA. P.J. Grady, J. Kuperus, D. Leffew, M. Tubis, and W.H. Blahd, VA Wadsworth and Long Beach Medical Centers, Los Angeles and Long Beach; and University of California, Los Angeles, CA.

TELLURIUM-123m; A NEW RADIONUCLIDE FOR LABELING RADIOPHARMACEUTICALS. R.D. Ice, G.P. Basmadjian, G.R. Parker, S.L. Mills, R.A. Magarian, and A.S. Kirschner, College of Pharmacy, The University of Oklahoma, Oklahoma City, OK.

A METHODOLOGY DESIGNED TO GIVE DETAILED RADIO-BIOKINETIC INFORMATION IN HUMANS. K.A. Lathrop, B.M.W. Tsui, and P.V. Harper, The University of Chicago and The Franklin McLean Memorial Research Institute, Chicago, IL.

FACTORS INFLUENCING BLOOD CLEARANCE OF BONE SCANNING RADIOPHARMACEUTICALS. A REVIEW. A. Owunwanne, R.E. O'Mara, and G.A. Wilson, University of Rochester, Rochester, NY.